The Omental Fat Band as an Immunomodulatory Microenvironment for Ovarian Cancer

Courtney Alicia Cohen

Dissertation submitted t o the faculty of Virginia Polytechnic Institute and State University in partial fulfillment of the requirements for the degree of Doctor of Philosophy

in

Biomedical and Veterinary Sciences

Paul C. Roberts, Chair
Eva Marie Schmelz
William S. Swecker
David R. Bevan
Liwu Li

April 30th, 2013
Blacksburg, VA.

Keywords: omentum, ovarian cancer, metastasis, microenvironment, parity, IL-12

The Omental Fat Band as an Immunomodulatory Microenvironment for Ovarian Cancer

By

Courtney Alicia Cohen

(Abstract)

Cancer research is evolving. Historically concerned with the mechanisms by which malignant cells circumvent cell death signaling and maintain unchecked proliferation, focus has shifted to the complex interactions between the tumor cell and the surrounding microenvironment. Ovarian cancer has one of the highest incidence-to-death ratios of all cancers, and is typically asymptomatic until the later stages, often resulting in metastasis prior to discovery. Naturally occurring phenotypes like lactation and child-bearing (parity) reduce ovarian cancer incidence, but the mechanisms are not understood. As the primary site for ovarian cacner metastasis, and a secondary lymphoid organ capable of mounting potent innate and adaptive immune responses, we believe the omental fat band (OFB) provides a unique opportunity to study complex interactions within the tumor microenvironment. Additionally, we hypothesize that once understood, leukocyte populations within the OFB could be modulated to disrupt the pro-tumorigenic cascade. Using fluorescence-activated cell sorting (FACS) and quantitative realtime PCR (qRT-PCR), we comparatively evaluated the changes in the compositional immune profile of the OFB as a result of parity and cancer. Parous mice were associated with a reduction in macrophages and neutrophils in the OFB, resulting in an inherent “protective state” that was refractory to metastatic cancer cell growth after intraperitoneal implantation. This indicates that the leukocyte populations within the

OFB play an important role in tumor development. Therefore we utilized the potent T_H1-type immunomodulatory cytokine IL-12 in a membrane-bound form to circumvent reported side effects, such as hepatic and renal damage, cardiotoxicity and death. Targeted IL-12 delivery to the OFB resulted in delayed disease development, although not protection from subsequent challenge. This was also associated with a reduction tumor-associated macrophages (TAMs) and neutrophils (TANs) within the OFB. Kinetic studies demonstrated that these changes were induced by a significant reduction in neutrophil and macrophage chemoattractants early on in the pro-tumorigenic cascade (7 days post-implantation). This work demonstrates that the OFB is a functionally plastic tissue that can be harnessed and re-mobilized to display an anti-tumorigenic microenvironment.

Acknowledgements

I am truly thankful for all the wonderful memories and experiences since joining this program. To all those faculty, fellow students and friends that touched my life during my time at Virginia Tech, I am extremely grateful. To my mentors, Dr. Roberts and Dr. Schmelz, thank you for taking me on late in the game, and for your time, guidance and expertise. To my committee, Dr. Bevan, Dr. Swecker and Dr. Li, thank you for all the constructive input, and for your incredible patience. To Dr. Ward Kirner, thank you for making the trip up from Atlanta to serve as my external examiner, for your advice and good humor.

I have had wonderful labmates, both past and present. To Dr. Andrew Herbert, who has always been my example of what a strong scientist should be; your integrity, honesty, and respect have always been the motivation that got me through this program. Your confidence in me gave me confidence in myself; I am incredibly grateful to have gotten the chance to work with you, and I'm honored to call you a friend. To Lynn Heffron, our lab momma, you are a brilliant scientist with extraordinary potential, and I can't wait to see how high you'll rise now that you've been given the chance. You have always been indispensible in the lab, both during animal studies and as a scientific sound board, and I am truly thankful for the extraordinary amount of help and time you have always given me without a second thought. To Amanda Shea, my co-worker, counterpart, and absolute best friend in the world, there is no way I could have gotten through this program without you. You have been a friend, mentor, counselor and cheering squad throughout this process, and I can only hope that I've been the same for you. I can't wait to watch you turn the world of science policy on its head, there's no one I'd trust more to take on the job than you! To Dr. Angela Anderson, your constant positive attitude and dedication to your students has been an inspiration over the years, and I'm thankful for all the advice and support. To all the other lab members I have been fortunate to work with, Dr Neeraj Singh, Matthew Kurnick, Julie Karfakis, Elizabeth Strawn, Dr Tila Khan, Amanda Gasser, Joey Mazzei, Dr Binu Velayudhan, and so many others; you have all been a part of getting me to where I am today with your support, guidance, laughter and love. I have been fortunate to work with so many amazing people.

Thank you to my family, who has never been anything but encouraging; I am very lucky to have such an incredible support system. To my parents, who have been extraordinarily patient and shown an amazing amount of faith, thank you for always believing in me. To my big brother Jim and sister-in-law Michele, thank you for always giving me the confidence to be myself, to be strong, and for showing me how to face my problems with humor and determination. To my little sisters Tessa and Sarah, thank you for always seeing me in the best possible light, for believing in me, and for being such a blast (even if we are stuck at the beach in a monsoon). To my brother-in-law Mario, you have always astounded me with your incredible work ethic, fun-loving nature and compassion; thank you for being a part of our lives, and for taking such good care of my little sister. To my Aunt Pam, thank you for making such a long trip to watch me defend, for igniting my love of reading, and for our 'adventures' when I was a kid. Thank you to my grandfather, Dr. Stanley Cohen, who was such an incredible role model, motivator and friend. You taught me the importance of hard work, critical thinking and a wide appreciation for all the wonder in the world. I wish you could have been here to see me accomplish this goal, thank you for always believing in me. To my wonderful grandmother Leanore Cohen, thank you for all your support and guidance, you have always shown me how to face obstacles with grace and a strong will, and I admire those qualities in you very much. To my grandparents Alice and Jim Childs, thank you for your love and for always being so proud of my every little accomplishment.

To all the awesome and incredible friends I have made in the last 5 years, I could write pages describing all the little ways that you have improved my life, learning and experiences here. To Andy and Karlie Herbert, Amanda Shea, Josh Nicholson, Anne and Bill Hyman, Josh and Heather Graham, Neeraj Singh, Ashish Ranjan, Brent Sanford, Clifton Cassidy, Jeff and Stacia Alexander, Lauren Thomas, Gade Kimsawatde, Vrushali Chavan, Andrew Fulton, Jason Ridley, Angela Anderson, Tim and Kara Hudson, Megan Duvall, Matthew and Lauren Moskitis, Brian Gehring, Brian Lauby, Jen Morrison, Stephen Lindamood and all the other wonderful people that I've had the honor of knowing, you have all been a cherished part of my life, and I thank you for that.

I reserve the biggest thank you for my wonderful boyfriend James. From the moment I met you, my life changed for the better. You have always believed in me without doubt, you've been my biggest fan and supporter, and an incomparable force of good and kindness in my life. I have nothing but admiration for your integrity, strength and compassion, and I'm incredibly grateful for all your support, especially in the last few months. I could never have gotten through this without you; you believed in me, so I couldn't fail. I love you, and I will be grateful for the rest of my life.

Attributions

Several colleagues aided in the writing and research behind the chapters presented as part of this dissertation. A brief description of their contributions is included here.

Chapter 3. Intra-abdominal Fat Depots Represent Distinct Immunomodulatory Microenvironments: A Murine Model.

Chapter 3 was accepted in PlosOne.

Shea, A.A. is a member of the Schmelz lab in the Human Nutrition, Food and Exercise (HNFE) department at VT. As co-author of this paper, she aided in the design and performance of the experiments, collection and analysis of data, generation of figures, interpretation of data and the writing of this paper.

Heffron, C.L. is a member of the Roberts lab in the Biomedical Sciences and Pathobiology (DBSP) department at VT. As a co-author of this paper, she aided in experimental planning, animal work and sample collection and processing.

Schmelz, E.M. is the Principal Investigator of the Schmelz lab in the HNFE department at VT. As a co-author of this paper, she aided in the design of these experiments, the interpretation of data and the writing of this paper, and provided editorial comments; she was co-principal investigator for one of the grants supporting this research.

Roberts, P.C. is the Principal Investigator of the Roberts lab in the DBSP department at VT. As a co-author of this paper, he aided in the design of these experiments, the interpretation of data and the writing of this paper, and provided editorial comments; he was co-principal investigator for one of the grants supporting this research.

Chapter 4. Parity-Associated Protection Against Ovarian Cancer Metastasis in the Omental Fat Band.

Chapter 4 was submitted to Cancer Research and Prevention. All attributions are the same as above.

Chapter 5. IL-12 Immunomodulation Reduces Peritoneal Outgrowth of Ovarian Cancer Cells.

Chapter 5 is in preparation for Cancer Immunology Research. All attributions are the same as above.

TABLE OF CONTENTS

Table of Figures

Table of Tables

Table of Abbreviations

ACT: adoptive cellular therapies
APCs: antigen presenting cells
BMI: body mass index
ConA: concavalin A
CTAs: cancer-testis antigen
DCs: dendritic cells
DIO: diet-induced obesity
EOC: epithelial ovarian cancer
EMT: epithelial-to-mesenchymal transition
FBS: fetal bovine serum
FDCs: follicular dendritic cells
FFL: firefly luciferase
FFLs: MOSE-L FFL-expressing cells
FFL/IL-12s: MOSE-L, FFL- and mbIL-12-expressing cells
GM-CSF: granulocytic/monocytic colony stimulating factor
HEV: high endothelial venules
HF: high fat
IDCs: interdigitating dendritic cells
IGF: insulin growth factor
IL-#: interleukin-#
iNOS: inducible nitric oxide synthase
i.p.: intraperitoneal
IUCAC: institutional animal care and usage committee
i.v.: intravenous
LF: low fat
mAbs: monoclonal antibodies
Mad-CAM: mucousal addressin
mbIL-12: membrane-bound IL-12
MCSF: monocytic colony stimulating factor
MDSCs: myeloid-derived suppressor cells
MHC: major histocompatibility complex
MMP: matrix metalloproteinase
MOSE: mouse ovarian surface epithelium
NK: natural killer
NKT: natural killer T cells
NSAIDs: non-steroidal anti-inflammatory drugs
OFB: omental fat band
PBS: phosphate buffered saline
PC: peritoneal cavity
PD-L1: programmed death ligand
PNAd: peripheral lymph node addressin
RBCs: red blood cells
ROS: reactive oxygen species
TADCs: tumor-associated DCs
TAM: tumor-associated macrophage
T_C: cytotoxic T cells
TCR: T cell receptor
TGFβ: tumor growth factor beta
T_H: helper T cells
TILs: tumor-infiltrating T cells
TLR: toll-like receptor
TME: tumor microenvironment
TNFα: tumor necrosis factor alpha
Treg: regulatory T cells
VEGF: vascular endothelial growth factor

CHAPTER 1. Literature Review

OVARIAN CANCER

The remarkable diversity of neoplastic cells as they transform towards a malignant phenotype has been well documented. Weinberg et al describe the ten hallmarks of tumor pathogenesis, which catalog the capabilities tumor cells develop in order to survive and progress. Currently, these hallmarks of cancer include **i)** resisting cell death, **ii)** sustaining proliferative signaling, **iii)** inducing angiogenesis, **iv)** enabling replicative immortality, **v)** activating invasion and metastasis, **vi)** evading growth suppression, **vii)** avoiding immune destruction, **viii)** tumor-promoting inflammation, **ix)** genome instability and mutation, and **x)** deregulating cellular energetics[1]. Ovarian cancer is the most deadly gynecological malignancy and ranked fourth in cancer-related fatalities among women in the Western world[2]. In 2012, there were roughly 22,280 new cases of ovarian cancer diagnosed in the United States, and 15,500 deaths. The 5-year survival rate is only 44%, and has improved by just 6% in the past 40 years, despite research and development[2]. In 2012, an estimated 138 million dollars will be spent by the NIH in ovarian cancer research alone[3]. Ovarian cancer has one of the highest death-to-incidence ratios in the US, and most deaths are attributed to relapse [4, 5]. Multimodal therapy with surgery and chemotherapy may initiate complete remission, but chemo-resistant disease recurs in most patients, and the prognosis is dismal[6].

The high mortality rate of ovarian cancer is primarily due to a lack of early detection tools. In addition, ovarian cancer is largely asymptomatic until the more advanced stages, when the disease has metastasized throughout the peritoneal cavity (PC)[7, 8]. However, in the small percentage of cases that are caught early (usually due to accidental discovery during another procedure), the 5 year survival rate is >90%. Therefore, novel strategies are urgently needed to improve early detection and treatment outcomes, as well as an improved understanding of disease pathogenesis from its inception.

Ovarian cancer is an extremely heterogeneous disease, usually developing from the surface epithelium of the ovary. Epithelial ovarian cancer (EOC) is further subclassified into four major categories based on histology: **i)** serous are the most common, resembling normal epithelial cells, **ii)**

endometrioid, which derive from the endometrium, **iii)** mucinous, which derive from the cervical glands, and i**v)** clear cell, which derive from the vaginal rests. Of all EOCs, Serous tumors represent 80-85% of total cases, while endometrioid make up 10%, mucinous less than 3%, and clear cell 5%[9, 10]. Serous tumors can be even further categorized as low-grade (Type I) or high-grade (Type II), and all of the above subtypes have differing genetic and protein alterations and molecular pathogeneses[11, 12, 13]. High-grade malignancies tend to be fast growing and chemo-sensitive while low-grade tumors tend to grow more slowly and be less sensitive to chemotherapy[12]. Despite distinct differences in response to conventional chemotherapeutics between subtypes, the *organ* of origin (and not the tumor histology) still determines the treatment regimen. Indeed, while ~70% of tumors of serous histology show clinical response to drugs, only ~15% of clear cell tumors are responsive[14]. This is another example of the importance of the incredible heterogeneity of ovarian cancer, highlighting the need for a more thorough understanding of the disease.

Ovarian cancer is unique in that as the epithelium transforms into a more malignant phenotype, it becomes *more* differentiated, instead of less[15]. Acquisition of invasiveness is accompanied by the loss of epithelial features, and the gain of a more mesenchymal phenotype, called the epithelial-to-mesenchymal transition (EMT). This more invasive phenotype is driven by a combination of downregulated E-cadherin and E-cadherin promoter activity, as well as increased levels of β-catenin, Snail and other mesenchymal markers[16]. Hereditary mutations are only responsible for about 10% of ovarian malignancies, and usually involve BRCA1 or BRCA2. The remaining ~90% of cases are termed 'sporadic' EOC. The *incessant ovulation hypothesis* was put forth by Fathalla in 1971, and suggests that with every ovulatory cycle, ovarian surface epithelial cells acquire stress injuries. Continual repair and the necessary release of cytokines, chemokines, and matrix remodeling enzymes, as well as recruitment of activated immune cells result in a recurring inflammatory and oxidative state thought to predispose ovarian epithelial cells to transformation[17, 18, 19, 20]. Use of oral contraceptives that inhibit ovulation, multiparity (giving birth repeatedly) and the length of lactation negatively correlate with the development of EOC, supporting this hypothesis[21, 22, 23, 24, 25]. However, progesterone-only contraceptives, which do *not* inhibit ovulation also

reduce the risk of EOC development. For this reason the *gonadotropin hypothesis* was described, in which exposure to gonadotropin hormones stimulates EOC proliferation.[26]

In a study to determine potential early tumorigenic changes in the ovarian surface epithelium, comparative molecular and morphological analyses of early tumors and normal tissue indicated that EOCs originate from precursor lesions within ovarian inclusion cysts[27]. However, recent evidence supports a paradigm shift, in which high-grade serous ovarian cancers, as well as endometrioid and clear cell cancers actually originate from the fallopian tube epithelium[28, 29]. The *oxido-reductive fallopian tube epithelial damage hypothesis* postulates that iron-induced oxidative stress derived from retrograde menstruation provides the inflammatory conditions required to encourage the development of EOC at this site.

Whether or not it is responsible for the *initiation* of neoplastic growth, inflammation is certainly an important factor in cancer progression. Of the total global cancer burden, about 15% is ascribed to chronic infection, of which inflammation is a major component[30]. There is also increased cancer risk as a result of inflammation due to chemical and physical agents and autoimmune reactions[31, 32]. Pelvic inflammatory disease has also been associated with an increased risk of ovarian cancer[33]. Many inflammatory cytokines and chemokines (ie: TNFα, IL-1β, IL-6) are inducible by hypoxia, which is a common physiological state within tumor tissue[34]. These inflammatory cytokines can then stimulate the production of VEGF, an important angiogenic factor, making the signaling environment cyclic and tumor-sustaining[35]. TNFα is a diverse signaling molecule; it can induce angiogenic factors or destroy blood vessels, stimulate fibroblast growth or induce programmed cell death in diseased cells[36, 37]. TNFα also regulates MMP9, an important factor in the degradation of extracellular matrix components thus initiating tissue invasion within the ovarian tumor microenvironment. TNFα, IL-1β, IL-6 and MCSF have all been detected in human EOC tumor microenvironments, as well as in the microenvironments of other cancers[36, 38]. Further, TNFα mRNA in human EOC is positively correlated with tumor grade[38]. Signaling is thought to occur in both a paracrine and an autocrine manner due to the existence of the p75 receptor in tumor-associated leukocytes and the p55 receptor found on both tumor cells and stromal cells[38]. In animal

studies, mice that did not have the TNFα gene were resistant to the development of skin cancer, and the overexpression of TNFα increases the invasive phenotype in some cancer cell lines.[39, 40] Similarly, mice that were IL-1β deficient were resistant to metastasis, and IL-6-deficient mice were resistant to the development of an inflammation-induced cancer model[39, 41]. Clearly these inflammatory mediators play an important role in cancer pathogenesis.

In order for tumor cells to receive the requisite oxygen and nutrients for survival and proliferation, they must be within 100 μm of a capillary[42]. Thus, angiogenesis is another important regulating factor in EOC growth and metastasis, and signaling can occur in both an autocrine and paracrine manner. High levels of vascularization within the host tissue have thus been correlated with aggressiveness of tumor growth, and tumor cells have even been shown to migrate to the nearest microvessel and begin dividing from there[43, 44, 45, 46, 47]. Vascular endothelial growth factor (VEGF)-A is the main regulator of angiogenesis, and has been correlated with poor prognosis clinical trials[48]. VEGF is in fact a vascular permeability factor, meaning that it can lead to persistent extravasation of fibrin and fibronectin, along with a continuous generation of extracellular matrix[49]. VEGF signaling and angiogenesis promotion play an important role in the progression and prognosis of EOC[48, 50]. Conversely, VEGF also exerts an immunosuppressive effect in cancer models, being correlated with low levels of IL-12, inhibition of dendritic cell (DC) maturation, low numbers of natural killer T (NKT) cells and the upregulation of regulatory T cells (Tregs)[51, 52, 53].

Ovarian cancer is unique in that cells do not need to go through the process of extravasating and intravasating through various tissues to metastasize. Instead, tumor cells can simply slough off of the primary tumor and become free-floating within the PC. The natural flow of the peritoneal fluid then disseminates these cells throughout the PC, where they begin to develop pro-tumorigenic niches at alternative sites[54, 55]. While a primary tumor may shed a large number of metastatic cells every day, only a limited number of these cells will survive. This is largely dependent on their ability to acquire traits that promote survival, as well as their ability to *induce changes* in the target tissue that provide a pro-tumorigenic microenvironment[44, 56, 57]. The tumor microenvironment (TME) is a complex system

consisting of tumor cells, inflammatory cells, stromal cells and matrix components. Although genetic alterations within the tumor cells are important, stromal constituents in the microenvironment also play a crucial role in tumor development. In EOC patients that undergo surgical debulking of tumors, the omental fat band (OFB) is typically removed as a preventative measure because it is a well-known site of cancer cell seeding and outgrowth, making it a TME of crucial importance[54, 55, 58, 59, 60, 61].

THE TUMOR MICROENVIRONMENT

The tumor microenvironment (TME) is a complex signaling milieu composed of epithelial cells, fibroblasts, mast cells and immune cells, as well as the tumor cells themselves[62, 63]. Tumor cells are able to hijack resident and recruited normal cells to serve as contributing members of the TME; this constant crosstalk supports tumor initiation and progression in a variety of ways. These accessory cells have had a demonstrable effect on sustaining tumor cell proliferative signaling, resisting cell death, evading growth suppressors, inducing angiogenesis, activating invasion and metastasis, reprogramming metabolism and evading immune destruction –in other words, the aforementioned hallmark characteristics of cancer. (Figure 1)TME dynamics include neoplastic cells that are constantly proliferating, a vascular network of endothelial cells that promotes neoangiogenesis, and the extracellular matrix scaffolding produced by fibroblasts. Additionally, immune cell components that propagate an immunosuppressive phenotype, preventing tumor cell recognition and clearance[64, 65]. Tumor development is completely dependent on the TME, making it important to understand the constantly shifting pathophysiology of the system as a whole, instead of focusing on specific "key" signaling events or cell-to-cell interactions in an attempt to modulate it in a therapeutic manner[66]. Extensive and sometimes redundant signaling networks exist between the tumor cells, immune cells and the tumor stroma; thus it is important to understand these interactions as a constantly shifting whole.

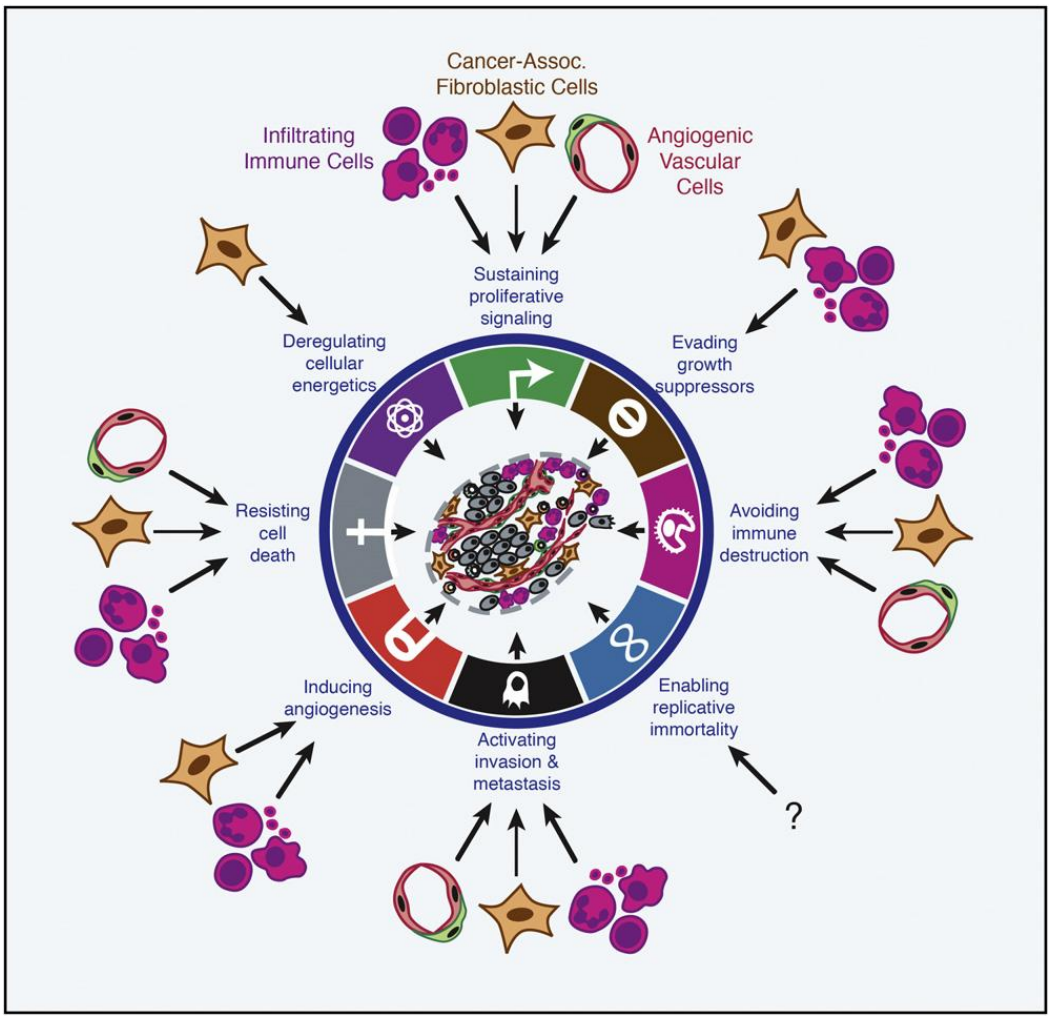

Figure 1.1 The effects of the tumor microenvironmental on the Hallmarks of cancer[66]. **Reproduced from Cancer Cell, March 2012, Vol 21, No. 3, Pages 309-322 with permission from Elsevier Publishing.

Within the TME, neoplastic cells are able to hijack signaling pathways that are critical for normal homeostasis of the immune system to evade host immune responses, thus maintaining tolerance[67, 68]. One of the most widely researched cell types in the tumor microenvironment is the tumor-associated macrophage (TAM). Macrophages are an incredibly plastic immune population, and can alter their activation status or phenotype as a result of various signaling cues[69]. Macrophage subsets are structured to mimic the T cell categories: pro-inflammatory (M1s) and anti-inflammatory, or alternatively activated (M2s), with further subdivisions also based on functionality[65]. M1s are polarized by TLR2/4 ligands and IFNγ, and mediate innate immunity; they secrete pro-inflammatory cytokines to promote T_H1 responses

via antigen presentation, have high expression of FcγRs, and are capable of cell destruction[70, 71]. M2s are polarized as a result of IL-4 and/or IL-13 signaling (M2as), immune complexes (M2bs) or IL-10 (M2cs)[72, 73, 74]. Further, M2s are responsible for the secretion of anti-inflammatory cytokines (IL-10), and T_H2-promoting chemokines (CCL17, CCL22), and thus are involved in immunoregulation, promotion of angiogenesis and tissue remodeling, all of which can be useful in tumor progression.

Due to their re-education within the TME, TAMs are considered pro-tumorigenic and M2-like[74, 75, 76]. They secrete a host of factors that support tumor growth and development, and are found distributed throughout the tumor mass[33]. These pro-tumorigenic signals include angiogenic factors (VEGF), matrix destruction factors (MMP1, -2, -7, -9, and -14), immunosuppressive signals (IL-10, CCL22 and TGFβ) to decrease reactive oxygen species released by tumoricidal macrophages, as well as to recruit regulatory T cells (Tregs) that will then dampen cytotoxic T cell (T_C) responses[69, 76, 77, 78, 79, 80, 81, 82]. They also secrete factors that promote tumor growth, such as CCL2, CCL5, CXCL9, CXCL10 and CXCL16[70]. Several chemokines are responsible for recruitment of blood monocytic precursors to different areas of the TME prior to differentiation, including CCL2, CCL5, CCL7, CXCL8, and CXCL12[83]. Tumor cells can also secrete various colony-stimulating factors that prolong the survival of existing TAMs[84]. Finally, TAMs show a downregulation of CCR2, which is hypothesized to support the retention of TAMs in the TME.[85]

In early carcinogenesis, macrophages are typically more M1-like, and it is not until the later stages that M2-like TAMs are prevalent[86]. Thus, it seems that in the pro-tumorigenic niche, a re-education of macrophages from an M1 to an M2-like phenotype occurs in a dynamic fashion. This process is dependent on a wide variety of receptors, signaling pathways, and transcription factors. Briefly, the pathways implicated in the M1-TAM transition include NFκB, TLR-MyD88/TRIF, HIF-1, Notch and various cytokine signaling networks[87, 88, 89, 90, 91, 92, 93, 94, 95, 96]. Wong et al has also recently proposed that B cells play a role in the differentiation of TAMs in the tumor microenvironment, via IL-10 secretion[97]. Cancer cell induction of TAM over-expression of IRAK-M, an immunosuppressive transcription factor that negatively regulates TLR signaling is mediated by TGFβ and has also been implicated in the evasion

of host immune surveillance[98, 99, 100]. Not surprisingly, in several human cancer models, high TAM incidence correlates with poor prognosis[76, 78, 101, 102].

Dendritic cells (DCs) also play a crucial role in the maintenance of immunological tolerance, as well as in the activation of antigen-specific immunity, and thus provide a link between innate and adaptive immunity[33]. Tumor-associated DCs (TADCs) typically have an immature phenotype and are unable to stimulate T cells[103]. Structurally, immature TADCs are usually found throughout the tumor mass, while mature DCs are confined to the peritumoral region[104]. Mature TADCs also express T cell inhibitory programmed death ligand 1 (PD-L1) which promotes T cell anergy or apoptosis when engaged to its receptor, PD-1 on T cells[105, 106]. The disruption of this suppressive pathway through the blockade of PD-L1 enhanced DC-mediated T cell activation, boosting efficacy of adoptive T cell immunotherapy against EOC has been evaluated with some success[106]. Higher PD-L1 expression has been negatively correlated with patient survival[107].

Myeloid-derived suppressor cells (MDSCs) are also a crucial player in the immunosuppression of the TME, responsible for antagonizing tumor immunosurveillance[78, 108, 109]. This population is described as a phenotypically heterogeneous mixture of myeloid cells at different states of maturation. They have been identified as a major component of several cancer types in animal models, as well as in a clinical setting, and are shown to accumulate as tumors progress[110, 111, 112]. Additionally, MDSCs are able to dampen T cell IFNγ production, disrupt TCR antigen recognition, and overproduce reactive oxygen species (ROS)[113, 114, 115]. Murine MDSCs are identified by their cell surface expression of CD11b, Ly6G and Ly6C, and can be further characterized as monocytic ($CD11b^{+}Ly6G^{+}Ly6C^{hi}$) or granulocytic ($CD11b^{+}Ly6G^{+}Ly6C^{lo}$)[116]. In a breast cancer model, MDSCs were found to accumulate in the blood, bone marrow, and secondary lymphoid organs, as well as in the tumors themselves as the cancer progressed[117, 118, 119, 120]. MDSCs have also been shown to correlate with poor prognoses in pancreatic, esophageal, hepatocellular, and colorectal cancers[111]. In the TME, they mediate suppression of endogenous T cells via secretion of IL-10, producing a T_H2-type T cell response, and through the inhibition of macrophage pro-inflammatory IL-12 secretion[121, 122].

In ovarian cancer patients, the presence of tumor-infiltrating T cells (TILs) is correlated with a positive prognosis after surgery and chemotherapy[123]. Conversely, increased numbers of immunosuppressive $CD4^+CD25^+$ Tregs are correlated with decreased susceptibility to chemotherapy and thus reduced survival[82]. Further, the ratio of TILs:Tregs within the primary tumor significantly correlates with patient survival.[82] In advanced ovarian cancer patients, the reduced presence of $CD3^+CD56^+$ NKT cells was correlated with increased VEGF in the ascites fluid, platinum resistance and poor prognosis[50, 51]. Further, it has been shown that the formation of ascites in late stage ovarian cancer may be inhibited by CD1-mediated NK cell activation[107]. Taken together this data indicates a significant role of different T cell subtypes in EOC progression, providing justification for the development of therapeutics that target these cells within the tumor microenvironment.

As mentioned, Tregs are another significant player in this signaling network, and are either recruited by tumor cells or polarized from endogenous TILs via tumor cell production of IL-10 and TGFβ[124]. Tregs then suppress effector T cells via either direct contact or through their own secretion of inhibitory IL-10 and TGFβ[125]. Tregs have also been shown to markedly downregulate the activity of both NK cells and B cells[126, 127]. Several strategies have been implemented to attempt to circumvent the suppressive TME or render it more conducive to effector T cell function, proliferation and persistence. One such example is the administration of lymphodepleting chemotherapies, such as cyclophosphamide or fludarabine which may eradicate Tregs within the TME and generate a more favorable signaling milieu for the development of effector T cells through enhanced levels of IL-2 IL-7, IL-12 and IL-15[128, 129, 130, 131, 132, 133]. Additionally, inhibitory ligands, or infusion of pro-inflammatory IL-12 have been utilized in hostile tumor microenvironment modulation to target the deactivation of Tregs and encourage effector T cell function[134, 135, 136].

Upregulated humoral immunity also plays a role in the pro-tumorigenic microenvironment[137]. This is partly attributed to an increase in T_H2 cells with concomitant IL-4 and IL-10 signaling, a pattern also associated with inflammatory conditions that are associated with an increased risk of cancer development[138, 139, 140, 141, 142]. B cell hyperactivity has been targeted in adult acute lymphoblastic leukemia,

non-Hodgkin's lymphoma and advanced colon cancer via an anti-CD20 chimeric monoclonal antibody (Rituximab) with varying degrees of success[143, 144, 145]. The involvement of pathogenic B cells in the tumor microenvironment is not surprising, given the suppressive nature of many humoral- and T_H2-associated cytokines [146]. For instance, IL-10 stimulates angiogenesis, and IL-13 promotes survival of neoplastic cells while suppressing cell-mediated immunity[147, 148]. In a B cell-deficient mouse model, resistance to a variety of histologically diverse syngeneic tumors was associated with enhanced T_H1 cytokines and protective cytotoxic T lymphocyte (CTL) responses[149]. B cell depletion also showed increased efficacy in a vaccine against a melanoma line, again associated with increased cell-mediated immunity.[150] Additionally, immunoglobulins (Ig) released by B cells play a role in the pro-tumorigenic microenvironment[150, 151]. The incidence of tumor-associated antigens is actually a poor prognostic indicator in a number of cases[152]. It is hypothesized that increased Ig levels in the microenvironment result in the accumulation of immune complexes (ICs), and that these Ig-ICs promote pro-tumorigenic inflammatory responses[153, 154]. High circulating IC levels are also correlated with poor prognosis in a number of cancers, and have long been associated with the initiation of inflammatory cascades and tissue destruction in autoimmune disorders, although the underlying mechanism is not completely understood[146, 155, 156]. This pro-inflammatory cascade is thought to involve receptors for the Fc portion of IgG, which plays a central role in regulating immune responses following interaction with ICs[155]. Thus, FcyRI and FcyRIII mediate immune cell activation via an intracellular tyrosine-based activating motif (ITAM) which triggers oxidative bursts, antibody-dependant cell-mediated cytotoxicity (ADCC) by NK cells and degranulation by mast cells[155]. Alternatively, FcyRII inhibits inflammatory responses through engagement of immune tyrosine-based inhibitory motifs (ITTIMs). Further, ICs activate the complement cascade, resulting in formation of lytic factors and potent inducers of leukocyte recruitment[157]. Therefore, prolonged humoral activity promotes the tumor microenvironment both directly and indirectly as another component in this complex signaling milieu. As we have described, there are several redundant mechanisms by which EOC is able to polarize the tumor microenvironment, creating an

immunosuppressive, pro-tumorigenic niche. The *flux* of these processes needs to be understood as a complex, interacting, dynamic system in order to develop effective therapies.

CANCER THERAPEUTICS

General cytotoxic therapies such as chemotherapy and radiation after cytoreductive surgery are the standard of care for EOC patients. Chemotherapy regimens generally include intraperitoneal (i.p.) administration of a combination of paclitaxel (a microtubule, and thus growth inhibitor) and platinum-based agents (carboplatin, cisplatin). Roughly 70% of new patients respond favorably to this primary treatment[158]. Unfortunately, a further 70% of these remission patients eventually relapse, with the resultant disease being chemoresistant[159, 160]. Patients who experience progressive disease within 6 months of platinum-based therapy (as well as those who do not respond to therapy while on first-line platinum treatment) are considered platinum refractory/resistant[161]. Ovarian cancer is an incredibly heterogenous and aggressive disease, and the current treatment strategy is evolving to incorporate a multi-modal approach, in which platinum-based cytotoxic therapies are combined with inhibitors against metabolism (gemcitabine), angiogenesis (Bevacizumab -VEGFR) or commonly disregulated growth factors (Panitumumab-EGFR,) in an effort to disrupt multiple pro-tumorigenic mechanims. In the case of platinum-resistant disease, doxorubicin or topotecan (topoisomerase inhibitors) are used as a second-line chemotherapeutic[161, 162]. However, the 5-year survival rate remains extremely low, and personalized medicine is in its infancy, highlighting a need for improved treatment modalities.

The tumor microenvironment is an incredibly dynamic signaling milieu, with constant cell-cell signaling interactions that foster tumor progression. Increasing attention has been given to the addition of biologically active signaling molecules as adjuvant therapy in the treatment of various cancer models and the prevention of metastatic disease. Among these are granulocyte/macrophage-colony-stimulating factor (GM-CSF), IFNs, and IL-2. GM-CSF regulates the proliferation, differentiation and function of mature myeloid cells and thus has been used to try to induce macrophage tumoricidal activity in vivo[163, 164, 165, 166, 167, 168]. In one study, i.p. administration increased the number of macrophages contained within rat OFB

milky spots (although not those free-floating in the PC), as well as improving the cytotoxicity of those macrophages against a colon cancer cell line[165]. Further, GM-CSF can be safely administered i.p. in a clinical context in order to target disseminating gastrointestinal and gynecological cancers [169]. In combination with IFNγ and carboplatin, GM-CSF has shown promise in Phase II clinical trials against platinum-sensitive EOC[170]. Several additional studies have been published evaluating the role of IFNs as either a first-line therapy or as a maintenance strategy, although not all resulted in protection (or provided positive responses)[171, 172, 173, 174]. In particular, IFNγ has been shown to reverse the immunosuppressive properties of macrophages, suggesting the efficacy of local administration to tumor microenvironments[174]. In a study by Curiel et al, a fusion toxin called ONTAK consisting of IL-2 fused genetically to the enzymatically active and translocating domains of diphtheria toxin was shown to deplete functional Tregs, and led to improved prognosis in a clinical setting[175]. Clearly, there are a wide variety of immunomodulatory cytokines that could aid in disruption of the TME and tumor regression, if properly utilized.

Another growing area of cancer treatment has been the application of anti-tumor mAb (monoclonal antibody) therapies.[176] The mechanisms of action are diverse and include inducing apoptosis or Fc-dependant recruitment of complement components or innate immune effector cells to promote tumor destruction, as well directly blocking specific functional targets, such as tumor growth factors[177, 178, 179]. Oregovomab is an anti-CA125 (a common tumor-associated antigen) mAb which has already reached Phase III clinical trials[180]. The most challenging hurdle in the use of anti-tumor antigens has been the weakly immunogenic nature of these markers due to immune recognition as "self". Cancer-testis antigens (CTAs) have become a very popular anti-tumor target due their high immunogenicity and restricted expression in normal tissue[181]. In a healthy host, CTAs are only expressed in testicular tissue and due to the blood-testis barrier these antigens are protected from exposure to the immune system[182]. In this manner, CTA-specific T cells are not removed from the immune repertoire during negative selection, and high-affinity CTA-reactive precursor T cells remain to be utilized in tumor immunotherapy[183]. CTAs are

found to be expressed in hematological malignancies, and are correlated with poor prognosis[184, 185, 186]. Some of the commonly discussed CTA targets include MAGE-A, MAGE C1, and NY-ESO-1[187, 188]. In normal cells, most CpG dinucleotides at gene promoter regions are unmethylated while other CpG islands in other areas of the genome are methylated, preventing transcription[189] Decreased levels of overall genomic methylation are found early in the pathogenesis of most cancers, and are responsible for the aberrant expression of CTAs[190, 191]. Clinically, the use of anti-tumor antigens has met with limited success due to the inherent heterogenous expression among individual patients, as well as the potent aforementioned immunosuppressive microenvironment[192].[192]

Attempts have also been made to alter the TME using antibodies that target pro-tumorigenic cytokines within the signaling milieu. In a breast cancer model, use of Met-CCL5, an agonist of CCR1 and CCR5, significantly reduced macrophage infiltration to the tumor site, and slowed tumor growth. CCR1 and CCR5 are expressed on circulating leukocytes, and aid in migration to the tumor site as a result of CCL5 secreted by the mammary cells[193]. In humans, a mAb against CCL2, and an inhibiting mAb against CCR2 are currently under clinical evaluation[194, 195]. Bevacizumab, an anti-VEGF monoclonal antibody, has been effective in clinical studies of platinum-resistant disease[196, 197, 198]. Much emphasis has also been focused on FcγR expression in patients recently due to the discovery that those with high-affinity polymorphisms of FcγRIIa and FcγRIIIa had increased recurrence-free survival[199, 200, 201].

Despite the common conception that TAMs are pro-tumorigenic, in clinical settings macrophage engagement of FcyRs is a crucial component in the efficacy of mAb-mediated tumor suppression[202, 203, 204, 205, 206, 207], again indicative of macrophage plasticity given the signaling milieu. A recent study determined that TAMs in the presence of anti-tumor mAbs retain tumoricidal properties, and depletion of TAMs actually *reduced* mAb-mediated tumor suppression[208]. DeNardo et al have shown that depleting microenvironmental IL-4 in a 3D culture system using an anti-IL-4 mAb reduced the invasive phenotype of mammary epithelial cells in the presence of $CD4^+$ T cells and TAMs[209]. While the depletion of NK cells and neutrophils had no effect, the depletion of macrophages blocked the anti-tumor effects of an

anti-CD40 treatment[205]. In a human pancreatic cancer model, anti-CD40 mAb was shown to reverse the immunosuppressive cytokine profile of TAMs[210]. Zolendronic acid has also been shown to inhibit tumor progression, at last partly due to the inhibition of macrophage migration, proliferation and secretion of MMP9. It has also been shown to reverse the M2-like polarization of TAMs by increasing iNOS expression, while simultaneously downregulating IL-10 and VEGF[211, 212]. In fact, targeting TAMs and other tumor-associated leukocytes has not only been shown to induce a tumoricidal effect, but also to restore the efficacy of radiotherapy, anti-angiogenic therapy and chemotherapy treatments[213, 214, 215].

Despite the overwhelming amount of research dedicated to cancer, relatively little has been done to understand the effects of multiple, concurrent interactions on the tumor microenvironment, although this more closely resembles the physiological TME as a complex signaling milieu with pathway redundancies. Paclitaxel has been hypothesized to have a positive effect by directly downregulating Tregs, and the nucleoside analog gemcitabine was shown to reduce the number of myeloid suppressor T cells without altering effector T and NK cell populations. However, when gemcitabine was administered in combination with oxaliplatin, IL-2 and GM-CSF, it also suppresses Tregs[216, 217, 218]. This synergistic effect highlights the need for an improved understanding of the dynamic TME as tumors progress, in order to more appropriately tailor and bolster cancer therapeutics.

As described, immunotherapy, or the practice of re-training the patients' own immune system in an anti-tumorigenic fashion, represents a promising avenue of cancer treatment. This strategy has been utilized in a variety of ways, from the cytokine and mAb treatments described above, to cancer vaccinations targeting the induction of a tumor-specific T cell response. Cancer vaccination as a broad term refers to both immunoprevention and immunotherapy, and may provide the key to inducing a potent response by encouraging the development of immune memory[219, 220]. These treatment strategies are potentially less toxic than conventional chemo- and radiotherapy, and may be especially useful in older or otherwise frail cancer patients, as well as those in advanced stages or experiencing relapse[221, 222]. Vaccination strategies against breast cancer have already been developed and demonstrate an induction of

tumor-specific $CD4^+$ and $CD8^+$ T cell responses. Unfortunately these have met with limited success due to the low immunogenicity[223, 224, 225]. Adoptive cellular therapies (ACT), in which an immunogenic tumor-associated antigen has been targeted have also been employed, as described above. One strategy to overcome the low frequency of tumor-specific T cells is to reprogram immune cells *ex vivo* before reintroduction to the host. Using a combination of ACT followed by differentiation-inducing interleukins, it is possible to selectively activate and expand tumor-primed T cells, NK cells and NKT cells, potentially providing long-lived protection against relapse in a clinical setting.[222, 226, 227]

IL-12 IMMUNOMODULATION

The utilization of the patient's own immune system to eradicate EOC has become a popular strategy in recent years. These immune-based therapies are an attractive option due to the highly immunogenic nature of ovarian tumors[228]. The major hurdles to overcome in order for this type of therapy to be effective include the identification of the appropriate tumor-specific antigen, the generation of sufficient immune response, and overcoming immune inhibition by the TME[229]. While the generation of tumor antigen-specific T cells for EOC therapy is important, we have previously discussed the ability of the TME to suppress the immune system through a variety of secreted factors and signals, protecting the tumor cells from eradication. Obviously the pro-tumorigenic niche as a whole needs to be repolarized to render immunotherapies more effective. Several cytokines have been utilized in an effort to counteract the immunosuppressive tumor microenvironment. One of the most effective, and yet most fraught with side effects is IL-12, demonstrating a need for a more targeted, elegant administration strategy.

IL-12 is a heterodimeric cytokine that has potent T_H1-type immunostimulatory effects on T_H cells, T_C cells, and NK cells. IL-12 has a molecular mass of 70 kDa, and is composed of subunits of 40 and 35 kDa each[230]. The p40 chain is homologous to the IL-6 cytokine receptor, while the p35 subunit is homologous to IL-6 and GM-CSF, although neither subunit appears to be biologically active on its own[231, 232]. Receptors for IL-12 (IL-12R) can be found on resting and activated NK cells, and activated $CD4^+$ and $CD8^+$ T cells, as well as B cells, macrophages and DCs[233, 234, 235]. Signaling through IL-12

induces rapid tyrosine phosphorylation of mitogen activated protein (MAP) kinases in activated T cells, as well as of Janus (JAK) kinases in activated T cells and NK cells, and Stat3 and Stat 4 (signal transducers and transcription factors) in $CD4^+$ T cells. As a potent immunomodulator, IL-12 upregulates the expression of MHC class I and II molecules, and possesses anti-angiogenic properties[236, 237, 238, 239, 240]. The major source of IL-12 production is APCs, which in turn induces IFNγ secretion by normal lymphocytes[241, 242, 243, 244]. Several cytokines, including TNFα, IL-1β, IL-2 and IL-15 can act synergistically with IL-12 to stimulate IFNγ secretion[245, 246, 247, 248]. Following an innate immune response, IL-12 and IFNγ production can support the differentiation of activated $CD4^+$ and $CD8^+$ T cells into effectors of cell-mediated immunity[249]. Activation of T and NK cells via IL-12 also stimulates the production of TNFα, IL-3, GM-CSF, MCSF, and IL-8[235, 250, 251]. Co-administration with IL-2, IL-15, IL-21, IL-8, or GM-CSF has a synergistic effect, increasing the levels of pro-inflammatory cytokines induced[252]. However, IL-12 does not support the proliferation of resting T or NK cells, only those that have been previously activated[252]. Conversely, IL-12 does further stimulate the cytolytic activity of antigen-specific $CD8^+$ T cells and NK cells, increasing production of cytolytic effector molecules perforin and serine esterases and enhances the adhesion of NK cells to target cells[250, 253, 254, 255]. The synergistic activity of this cytokine further highlights the need for an improved understanding of microenvironmental signaling as a system.

A variety of animal models and clinical trials have illustrated that IL-12 is a powerful anti-tumorigenic therapeutic[256, 257, 258, 259, 260]. The administration of IL-12 into tumor-bearing mice can delay, reduce and even completely inhibit tumor development. Intra-tumoral IL-12 injection elicited potent anti-tumor activities, mediated by NK cell cytotoxic activity[261]. In 1994, Phase I clinical trials began at the New England Medical Center, Dana-Farber Cancer Institute, Indiana University Medical Center and the Pittsburgh Cancer Institute. This trial used a bolus i.v. injection of recombinant human IL-12, administered to patients with advanced stage solid tumors.[262] This treatment was associated with significant immunomodulatory effects, but unfortunately IL-12 –related toxicosis had to be monitored closely, as systemic administration is associated with side effects. High levels of circulating IL-12 were

associated with several undesirable problems, including fever, fatigue, nausea, headache, allergy, immunosuppression, systemic mastocytosis, severe hepatic and renal dysfunction, cardiotoxicity and death.[263, 264, 265]In order to abrogate tumor growth while avoiding any systemic administration-related toxicity, tumor cells and accessory cells have been engineered to express IL-12 in several animal models[266, 267]. Importantly, induction of IL-12 directly in tumor cells did not affect the cells' ability to proliferate in vitro, but inhibited their ability to grow in immunocompetent mice[268, 269]. Using IL-12 as an adjuvant therapy may prove appropriate for treatment of cancer recurrence, if targeted delivery systems can be improved.

One such strategy is to induce membrane-bound expression of IL-12 (mbIL-12) on cancer cells as a targeted anti-tumor vaccine. Membrane-bound cytokines increase the immunogenicity of tumor cells, and stimulate antitumor immunity more effectively[270, 271, 272, 273, 274, 275, 276, 277]. Numerous strategies have been developed to compensate for the missing stimulatory signals present in the TME. Indeed, tumor cells expressing membrane-bound TNFα, GM-CSF, IL-2, IL-4, IL-12 and IFNγ have all been utilized[278, 279, 280, 281, 282, 283, 284]. Additionally, some have even created vaccines that express multiple cytokines, chemokines and/or costimulatory molecules simultaneously on tumor cells in an attempt to increase the efficacy of these vaccines via a combinatorial approach[285]. Importantly, mbIL-12 maintains its biological activity, proving comparable to that of the secreted form[286]. Additionally, mbIL-12$^+$ tumor cells are able to stimulate ConA-activated splenocytes to proliferate, induce CD8$^+$ T cells to express CD69 and IFNγ without additional involvement of APCs, and have overall reduced tumorigenicity[287]. A tumor cell vaccine expressing both IL-12 and IL-2 was shown to have a synergistic effect in both subcutaneous and intravenous tumor models[280]. While Lim et al found potent activation of effector T cells using this mbIL-12 model, Nagarajan et al reported no such activation[288]. This may be a result of differing anchoring strategies, the former having used a TNFα (Type II transmembrane) protein, the latter having used a GPI anchor system. Depending on the tumor model, different immune cells, including CD8$^+$ T cells, CD4$^+$ T cells, NK cells and/or NKT cells appear to be responsible for the efficacy of mbIL-12 treatment[289, 290, 291, 292]. Even more striking, mbIL-12 was shown to be stable, with minimal free-floating IL-12 (and thus

minimal undesirable side effects) found in the circulation following administration despite potent antitumor activities[293]. Therefore, mbIL-12 shows a lot of potential as a strategy to repolarize the TME in an anti-tumorigenic manner due to its potent immunomodulatory properties, and the inherent safety of a more targeted approach.

THE OMENTAL FAT BAND (OFB)

The omental fat band (OFB) is a vascularized fatty tissue contained between mesothelial sheets within the PC that runs along the underside of the stomach to the pancreas, and extends like a curtain down to the spleen. It contains distinct aggregates of leukocytes, termed "milky spots" due to the opaque color, organization and identity of these immune cells, and were first described and named by Ranvier in 1876 in rabbit OFBs[294]. Despite the highly organized structure within the milky spots themselves, the distribution throughout the OFB, size of individual milky spots and number of cells per milky spot is highly variable[295]. Milky spots contain high endothelial venules (HEVs) that facilitate immune cell entry and egress from the bloodstream via expression of peripheral lymph node addressin (PNAd) and mucosal addressin (Mad-CAM1)[296]. Milky spots are hypothesized to be the mode of entry of B1 cells from the bloodstream into the PC, although not the sole mode of B2-B cell transport[296, 297]. The OFB has powerful antimicrobial properties, and has been named by some as a secondary lymphoid organ due to its role in immunosurveillance within the peritoneal cavity. In an immunocompetent host, circulating lymphocytes travel through specialized structures called secondary lymphoid organs to be presented antigen. These secondary, or peripheral, lymphoid organs have a precise architecture with distinct regions enriched for B and T cells. Interdigitating and follicular dendritic cells (IDCs, FDCs) are the prototypical APCs associated with peripheral lymphoid organs, responsible for the development of antigen-specific responses. In a study by Rangel-Moreno et al, lymphotoxin-alpha deficient mice ($LTa^{-/-}$), which lack lymph nodes and Peyer's patches, were splenectomized and reconstituted with wild-type bone marrow. Antigens were found to collect at milky spots of these otherwise secondary lymphoid organ-deficient mice after injection into the PC, resulting in antigen-specific antibody development and T cell proliferation, supporting the claim that the omentum can serve as a secondary lymphoid organ. In fact,

flow from the PC to milky spots allows entry of both antigens and leukocytes; locally activated lymphocytes, as well as mature lymphocytes from elsewhere were shown to recirculate through the OFB as part of a general surveillance route in search of antigen[298]. In a study of inflammation, macrophages and neutrophils were also shown to follow the milky spot route from circulation into the peritoneal cavity[299]. This passage between milky spots and the omental surface is believed to occur as a result of fenestrations in the mesothelial single-cell layer[300]. These fenestrations are not found in the mesothelial layer elsewhere on the OFB[295]. The label of 'secondary lymphoid organ' remains somewhat controversial however, because the overall milky spot architecture is unique. B cell clusters have been readily identified, but they do not appear to contain centrally located $CD35^{+}CD21^{+}$ CXCL13-producing FDCs. CXCL13 is chemotactic for B cells, and thus is an important aspect of typical lymphoid organ follicular structure. There is CXCL13 expression co-localized with CD11b (monocyte lineage) and FDCM1 (FDCs) staining, but it occurs on the outside of B cell clusters within milky spots. Further, FDCM1 staining does not colocalize with other known FDC markers, raising the possibility of a unique follicular cell phenotype. Milky spot formation is not incumbent upon lymphoid tissue inducer cells, as are lymph nodes and Peyer's patches, and thus follow a distinct developmental program that requires CXCL13-producing macrophages and stromal cells[298]. As well as being the site for leukocyte entry and egress through the omentum, milky spots have also been hypothesized to be a region of B1-B cell development and self-renewal and macrophage maturation[43, 297, 301, 302].

The OFB is of particular importance to EOC because it is a well known spot for metastatic seeding and outgrowth. In fact, the OFB is typically removed by surgeons as a preventative measure during tumor debulking because it is such a successful TME. Cancer cell seeding to the OFB has been shown to cause a rapid influx of immature macrophages into milky spots, an overall increase in leukocyte number in individual milky spots, as well as the formation of new milky spots in areas of tumor cell seeding. (Increases in milky spot number and size have also been shown in an intraperitoneal inflammation model)[303]. Decades ago it was determined that an omentectomy would reduce the ability for cancer cells to seed after peritoneal injection[58]. Despite the increase in immune cells, milky spots are

unable to prevent or reverse tumor cell growth, and the OFB is rapidly overrun. Indeed, in one study the adherence of tumor cells to milky spots was so tight that repeated aggressive lavage was not sufficient to detach them within minutes of i.p. injection. This observation provides further support for the practice of removing the OFB in all clinical patients in danger of PC malignancy[59]. Macrophages harvested from the OFB retain tumoricidal ability ex vivo, indicating that there must be some polarizing event occurring in the TME that prevents this activity[61, 295]. After an initial influx of immature macrophages to milky spots as a result of peritoneal stimulation with tumor cells, one study showed no changes in the percentage of macrophage subpopulations, nor in the organization of these, indicating that the ability of cancer cells to polarize the microenvironment in an immunosuppressive manner is fairly rapid[59].

The fetal omentum has recently been shown to be an important site for B1 B cell development from hematopoietic progenitors, and may even play a role in the homeostasis of this cell population in adults[304]. B1 cells are specialized B cells that are thought to be more "innate-like", and are the predominant B cell population in the peritoneal and pleural cavities. They are also distinguished from the common circulating B cell population (B2 cells) due to their role in natural low-affinity IgM antibody production, which is crucial in providing early protection from a variety of pathogens[305, 306]. Thus, they are thought to bridge the gap between infection and activation of the adaptive immune system which involves clonal expansion and differentiation of conventional B2 and T cells, and requires several days to undergo full activation and differentiation[307, 308]. Further, they can maintain themselves by self-replenishment or self renewal[43]. B1 cells can be distinguished based on their surface markers, expressing high levels of IgM, and low levels of IgD, CD23 and B220. Peritoneal B1 cells also express CD11b, and can be further subdivided into B1a cells, which are $CD5^{+}$, and B1b cells, which are $CD5^{lo/-}$. B1 cells express autoantigen receptors, as well as antigen receptors that bind conserved epitopes on common pathogens[305]. One such example is the T15 idiotype which binds phosphorylcholine, a common component of the cell surface of some bacteria[309]. B cell homing to 'conventional' secondary lymphoid structures is controlled by CXCL13 production of follicular non-hematopoietic stromal cells and

macrophages, and indeed B1 cell homing to the OFB as well as the PC is CXCL13/CXCR5 signaling-dependent[297].

The OFB has potent angiogenic properties; in a recent study, milky spots contained hypoxic regions that produce high levels of VEGF and other pro-angiogenic chemokines, hypothesized to account for the complex lymphatic and capillary networks within omental tissue[294, 304]. Omental vessels in milky spot regions from naïve mice were shown to be constitutively angiogenic, or constantly signaling for the development of new blood vessels, supporting the hypothesis that this phenotype would promote the rapid influx of immune cells in the event of a PC infection[57]. This organ has been used surgically to facilitate wound healing in reconstructive procedures or to close large surgical incisions due to its angiogenic and immunological properties, as well as its large size[300, 310, 311]. Mesothelial cells lining the OFB further propagate pro-angiogenic signaling by secreting VEGF-A in response to hypoxic conditions or TGFβ signlaing[57, 312].

Despite its immunological properties, the OFB is often removed in the case of ovarian cancer patients as a preventative measure because it is a known preferential site of cancer cell seeding and outgrowth. This leaves women more susceptible to subsequent infections. Despite the apparent immune function of milky spots, cancer cells can bind to aggregates and continue their metastatic growth program[58, 59, 165, 313]. In mice, the omentum supports tumor cell proliferation and morphological changes within hours of i.p. injection. Indeed, cancer cells were detected in the OFB at milky spots as early as *five minutes* post- i.p. injection[59]. $VCAM^{+}$ mesothelial cells that cover milky spots have been shown to be the major producers of VEGF-A in the OFB, although adipocytes were not evaluated due to the method of immune and mesothelial cell segregation, and may also contribute[57]. While the existing vasculature in the OFB promotes initial tumor survival, metastatic growth requires the formation of new blood vessels from formerly quiescent ones; a process termed the "angiogenic switch". Gerber et al postulate that this inherent pro-angiogenic phenotype may contribute to the ease with which EOC converts the OFB into a pro-tumorigenic microenvironment[57]. *In summary, the OFB is the primary site of EOC metastasis, possesses potent angiogenic properties, and normally functions as a secondary lymphoid organ,*

important in immunosurveillance of the PC. It is an excellent example of the inherent complexity of TMEs, possessing a dynamic and complex signaling network that is hijacked by ovarian cancer cells to create a pro-tumorigenic niche. Therefore, it is crucial that we understand the cascade of events that polarizes the OFB from an effective line of host defense to an incredibly successful TME in a stepwise, dynamic fashion if we are to create more effective therapies.

IMMUNOSENESCENCE

One of the difficulties of cancer immunology research is the incredible heterogeneity of results between different cancer models and in clinical oncology[314]. It has been suggested that there is a co-evolution of tumors and host immunity, and that the dynamics of this co-evolution are reflected in the variable data[314]. In other words, tumor cells may have co-existed with immune defense systems for an extended period of time, resulting in the selection of tumor variants no longer recognized by anti-tumor specific T cells ("immunoediting"), as well as chronic antigen exposure, resulting in T cell exhaustion or anergy. These processes are susceptible to modulation by altering the cytokine milieu, as well as by altering expression of T cell receptors[315]. This would be especially pertinent in aged individuals who are experiencing age-associated immune alterations, or "immunosenescence".

The majority of cancer cases occur in patients over the age of 65. It has been reported that certain immunotherapeutic regimens that have proven effective in younger animal models were rendered ineffective when administered to an older subset[316, 317]. As discussed previously, while a variety of anti-tumor antigens have been reported and tested, these immunotherapies are largely ineffective[318, 319]. This could be attributed to the mostly late-stage phenotype of clinical patients, which may be experiencing T cell exhaustion as a result of chronic co-habitation with tumor cells[314]. Additionally, there is a well-documented correlation between aging and the incidence and prevalence of cancer[320, 321, 322, 323]. Further, it was recently demonstrated that aging is accompanied by a low-grade inflammatory state (also thought to be a pro-tumorigenic factor) due to impaired regulation of the immune response[324, 325, 326]. This phenomenon has actually been termed "inflamm-aging" [327]. It is hypothesized that chronic antigenic load

as a result of a lifetime of antigenic experiences reduces the number of "virgin" (non-antigen experienced) T cells, filling the immunological space with expanded clones of memory and effector T cells expressing a senescent phenotype (progressively shortening telomeres and reduced replicative capacity). The chronic antigenic load (bacteria, virus, fungi, toxins and mutated cells) continuously activates the innate immune system, resulting in a progressive increase of inflammatory cytokines and markers, a chronic inflammatory state, favoring the onset of typical age-related diseases such as atherosclerosis, osteoporosis and cancer[322].

The actual mechanism behind immunosenescence is not well understood, but there are presently hypothesized to be three contributing factors: **i)** thymic involution with development, **ii)** intrinsic changes due to cell membrane damage leading to altered signaling, and **iii)** chronic antigenic stimulation throughout a lifetime [328, 329, 330]. Thus, the relative ineffectiveness of immunotherapies in the clinical setting so far may be a result of immunosenescence of the majority of patients treated, limiting the reported success of these therapeutic methods[221, 331]. *This is particularly pertinent in EOC, a disease that affects primarily post-menopausal women.*

PARITY

The incidence of ovarian cancer is reduced due to a variety of factors including oral contraceptive use, lactation and parity[332]. The risk of ovarian cancer is decreased by up to 50% in women who give birth prior to 20 years of age, and this rate increases progressively with each additional pregnancy[333]. This pattern has been demonstrated across a variety of ethnic groups and geographic locations, denying the possibility of socioeconomic effects or environmental factors.[24] However, little work has been done to determine the underlying molecular mechanisms that affect parity-related ovarian cancer protection.

Parity also provides protection against breast cancer, and scientists have attempted to define a molecular signature related to modulation of the mammary microenvironment. However, focus has been given to hormone and growth factor interactions. D'Cruz et al. used microarray analysis to attempt to identify a "parity signature" that would be indicative of a protective microenvironment in the mammary

gland against breast cancer[334]. They generated a list of 40+ genes that were parity-associated, indicating a general increase in epithelial differentiation, immune regulation and the TGFβ signaling pathway, and concomitant decrease in epithelial proliferation. *This parity trend was conserved in mice, rats and humans, validating the use of rodents as a model for this research*[334, 335]. Additionally, tumor suppressor p53 is upregulated in parous mammary tissue, as compared to nulliparous tissue, again indicating a tumor-resistant microenvironment[336]. There are currently several hypotheses regarding the protective effects of parity. The first three suggest that cells are rendered less susceptible to oncogenic stimuli as a result of changes in i) epithelial growth factor availability; ii) hormone balance; iii) or a terminal differentiation of a specific subpopulation of cells; and the last that iv) involution following pregnancy eliminates pre-malignant cells[332]. We submit that the resident immune populations within the relevant immune microenvironment must also play a role in this protective environment.

Despite the number of studies that have isolated "key" signaling events, or "crucial" cell types involved in the pathogenesis of EOC (among others), and despite the amount of money that has been spent in the last four decades on EOC research, there is still a huge disconnect between efficacy in vitro, in preclinical animal trials, and clinical results. Since the 1970s, the 5 year survival rate in EOC patients has only improved by 6%, and the rate of drug-resistant recurrence is still high. We hypothesize that this discrepancy is due in part to the lack of knowledge of specific TME signaling networks as a SYSTEM, a network of complex interactions that must be understood and dealt with as a WHOLE, instead of attempting to break it down into the simplicity of the in vitro arena. The redundant pathways that exist within the TME illustrate the futility of targeting one cell type or signaling molecule as the miracle cure of EOC. Additionally, common clinical variables such as patient immunosenescence could have an overwhelming impact on an otherwise successful therapeutic regimen, while parity-associated changes could be defined and harnessed to identify a successful tumor suppressive state. Therefore, it is clear that these factors must also be understood in the context of the tumor microenvironment as a whole. ***Here, we aim to i) characterize the PC and OFB as complex signaling microenvironments ii) to determine the cascade of events that allow EOC to redirect immune populations and immune signaling pathways to***

create a pro-tumorigenic niche in nulliparous and parous models, and iii) to elucidate the stepwise microenvironmental changes induced via a commonly used membrane-bound immunomodulatory molecule as an immunotherapeutic.

REFERENCES

1. Hanahan D, Weinberg RA. Hallmarks of cancer: the next generation. *Cell* 2011, 144(5): 646-674.
2. Siegel R, Naishadham D, Jemal A. Cancer statistics, 2012. *CA: a cancer journal for clinicians* 2012, 62(1): 10-29.
3. Siegel R, DeSantis C, Virgo K, Stein K, Mariotto A, Smith T*, et al.* Cancer treatment and survivorship statistics, 2012. *CA: a cancer journal for clinicians* 2012, 62(4): 220-241.
4. Li GT. [Effect of evidence-based medicine on the decision of chemotherapy for epithelial ovarian cancer]. *Zhonghua fu chan ke za zhi* 2012, 47(8): 582-586.
5. Benson JR, Jatoi I, Keisch M, Esteva FJ, Makris A, Jordan VC. Early breast cancer. *Lancet* 2009, 373(9673): 1463-1479.
6. Chu CS, Kim SH, June CH, Coukos G. Immunotherapy opportunities in ovarian cancer. *Expert review of anticancer therapy* 2008, 8(2): 243-257.
7. Saad AF, Hu W, Sood AK. Microenvironment and pathogenesis of epithelial ovarian cancer. *Hormones & cancer* 2010, 1(6): 277-290.
8. Stone RL, Sood AK, Coleman RL. Collateral damage: toxic effects of targeted antiangiogenic therapies in ovarian cancer. *The lancet oncology* 2010, 11(5): 465-475.
9. Kaku T, Ogawa S, Kawano Y, Ohishi Y, Kobayashi H, Hirakawa T*, et al.* Histological classification of ovarian cancer. *Medical electron microscopy : official journal of the Clinical Electron Microscopy Society of Japan* 2003, 36(1): 9-17.
10. Soslow RA. Histologic subtypes of ovarian carcinoma: an overview. *International journal of gynecological pathology : official journal of the International Society of Gynecological Pathologists* 2008, 27(2): 161-174.
11. Romero I, Bast RC, Jr. Minireview: human ovarian cancer: biology, current management, and paths to personalizing therapy. *Endocrinology* 2012, 153(4): 1593-1602.
12. Shih Ie M, Kurman RJ. Ovarian tumorigenesis: a proposed model based on morphological and molecular genetic analysis. *The American journal of pathology* 2004, 164(5): 1511-1518.
13. Mok SC, Bell DA, Knapp RC, Fishbaugh PM, Welch WR, Muto MG*, et al.* Mutation of K-ras protooncogene in human ovarian epithelial tumors of borderline malignancy. *Cancer research* 1993, 53(7): 1489-1492.
14. Sugiyama T, Kamura T, Kigawa J, Terakawa N, Kikuchi Y, Kita T*, et al.* Clinical characteristics of clear cell carcinoma of the ovary: a distinct histologic type with poor prognosis and resistance to platinum-based chemotherapy. *Cancer* 2000, 88(11): 2584-2589.
15. Naora H. Developmental patterning in the wrong context: the paradox of epithelial ovarian cancers. *Cell cycle* 2005, 4(8): 1033-1035.
16. Bagnato A, Rosano L. Epithelial-mesenchymal transition in ovarian cancer progression: a crucial role for the endothelin axis. *Cells, tissues, organs* 2007, 185(1-3): 85-94.
17. Landen CN, Jr., Mathur SP, Richardson MS, Creasman WT. Expression of cyclooxygenase-2 in cervical, endometrial, and ovarian malignancies. *American journal of obstetrics and gynecology* 2003, 188(5): 1174-1176.
18. Maccio A, Mantovani G, Turnu E, Artini P, Contu G, Volpe A. Preovulatory human follicular fluid in vitro inhibits interleukin (IL)-1 alpha, IL-2, and production and expression of p55 chain IL-2 receptor of lymphomonocytes. *Fertility and sterility* 1994, 62(2): 327-332.
19. Fathalla MF. Incessant ovulation--a factor in ovarian neoplasia? *Lancet* 1971, 2(7716): 163.
20. Ness RB, Cottreau C. Possible role of ovarian epithelial inflammation in ovarian cancer. *Journal of the National Cancer Institute* 1999, 91(17): 1459-1467.

21. **Whittemore AS, Balise RR, Pharoah PD, Dicioccio RA, Oakley-Girvan I, Ramus SJ*, et al.* Oral contraceptive use and ovarian cancer risk among carriers of BRCA1 or BRCA2 mutations. *British journal of cancer* 2004, 91(11): 1911-1915.**
22. **Risch HA, Marrett LD, Howe GR. Parity, contraception, infertility, and the risk of epithelial ovarian cancer. *American journal of epidemiology* 1994, 140(7): 585-597.**
23. **Riman T, Dickman PW, Nilsson S, Correia N, Nordlinder H, Magnusson CM*, et al.* Risk factors for invasive epithelial ovarian cancer: results from a Swedish case-control study. *American journal of epidemiology* 2002, 156(4): 363-373.**
24. **Gwinn ML, Lee NC, Rhodes PH, Layde PM, Rubin GL. Pregnancy, breast feeding, and oral contraceptives and the risk of epithelial ovarian cancer. *Journal of clinical epidemiology* 1990, 43(6): 559-568.**
25. **Nasca PC, Greenwald P, Chorost S, Richart R, Caputo T. An epidemiologic case-control study of ovarian cancer and reproductive factors. *American journal of epidemiology* 1984, 119(5): 705-713.**
26. **Choi KC, Kang SK, Tai CJ, Auersperg N, Leung PC. Follicle-stimulating hormone activates mitogen-activated protein kinase in preneoplastic and neoplastic ovarian surface epithelial cells. *The Journal of clinical endocrinology and metabolism* 2002, 87(5): 2245-2253.**
27. **Pothuri B, Leitao MM, Levine DA, Viale A, Olshen AB, Arroyo C*, et al.* Genetic analysis of the early natural history of epithelial ovarian carcinoma. *PloS one* 2010, 5(4): e10358.**
28. **Maccio A, Madeddu C. Inflammation and ovarian cancer. *Cytokine* 2012, 58(2): 133-147.**
29. **Li J, Fadare O, Xiang L, Kong B, Zheng W. Ovarian serous carcinoma: recent concepts on its origin and carcinogenesis. *Journal of hematology & oncology* 2012, 5: 8.**
30. **Parkin DM, Pisani P, Ferlay J. Global cancer statistics. *CA: a cancer journal for clinicians* 1999, 49(1): 33-64, 31.**
31. **Gulumian M. The role of oxidative stress in diseases caused by mineral dusts and fibres: current status and future of prophylaxis and treatment. *Molecular and cellular biochemistry* 1999, 196(1-2): 69-77.**
32. **Ekbom A, Helmick C, Zack M, Adami HO. Ulcerative colitis and colorectal cancer. A population-based study. *The New England journal of medicine* 1990, 323(18): 1228-1233.**
33. **Balkwill F, Mantovani A. Inflammation and cancer: back to Virchow? *Lancet* 2001, 357(9255): 539-545.**
34. **Koong AC, Denko NC, Hudson KM, Schindler C, Swiersz L, Koch C*, et al.* Candidate genes for the hypoxic tumor phenotype. *Cancer research* 2000, 60(4): 883-887.**
35. **Leek RD, Landers RJ, Harris AL, Lewis CE. Necrosis correlates with high vascular density and focal macrophage infiltration in invasive carcinoma of the breast. *British journal of cancer* 1999, 79(5-6): 991-995.**
36. **Kollias G, Douni E, Kassiotis G, Kontoyiannis D. The function of tumour necrosis factor and receptors in models of multi-organ inflammation, rheumatoid arthritis, multiple sclerosis and inflammatory bowel disease. *Annals of the rheumatic diseases* 1999, 58 Suppl 1: I32-39.**
37. **Lejeune F, Lienard D, Eggermont A. Regional administration of recombinant tumour necrosis factor-alpha in cancer, with special reference to melanoma. *BioDrugs : clinical immunotherapeutics, biopharmaceuticals and gene therapy* 1998, 9(3): 211-218.**
38. **Naylor MS, Stamp GW, Foulkes WD, Eccles D, Balkwill FR. Tumor necrosis factor and its receptors in human ovarian cancer. Potential role in disease progression. *The Journal of clinical investigation* 1993, 91(5): 2194-2206.**
39. **Vidal-Vanaclocha F, Fantuzzi G, Mendoza L, Fuentes AM, Anasagasti MJ, Martin J*, et al.* IL-18 regulates IL-1beta-dependent hepatic melanoma metastasis via vascular cell adhesion**

molecule-1. *Proceedings of the National Academy of Sciences of the United States of America* 2000, 97(2): 734-739.
40. Malik ST, Griffin DB, Naylor MS, Fiers W, Oliff A, Balkwill FR. The complex effects of recombinant tumour necrosis factor-alpha (rhTNF-alpha) in human ovarian cancer xenograft models. *Progress in clinical and biological research* 1990, 349: 393-403.
41. Tricot G. New insights into role of microenvironment in multiple myeloma. *Lancet* 2000, 355(9200): 248-250.
42. Folkman J. Angiogenesis in cancer, vascular, rheumatoid and other disease. *Nature medicine* 1995, 1(1): 27-31.
43. Kirsch M, Schackert G, Black PM. Metastasis and angiogenesis. *Cancer treatment and research* 2004, 117: 285-304.
44. Zetter BR. Angiogenesis and tumor metastasis. *Annual review of medicine* 1998, 49: 407-424.
45. Ellis LM, Fidler IJ. Angiogenesis and metastasis. *European journal of cancer* 1996, 32A(14): 2451-2460.
46. Li CY, Shan S, Cao Y, Dewhirst MW. Role of incipient angiogenesis in cancer metastasis. *Cancer metastasis reviews* 2000, 19(1-2): 7-11.
47. Leenders WP, Kusters B, de Waal RM. Vessel co-option: how tumors obtain blood supply in the absence of sprouting angiogenesis. *Endothelium : journal of endothelial cell research* 2002, 9(2): 83-87.
48. Cooper BC, Ritchie JM, Broghammer CL, Coffin J, Sorosky JI, Buller RE*, et al.* Preoperative serum vascular endothelial growth factor levels: significance in ovarian cancer. *Clinical cancer research : an official journal of the American Association for Cancer Research* 2002, 8(10): 3193-3197.
49. Balkwill FR. The chemokine system and cancer. *The Journal of pathology* 2012, 226(2): 148-157.
50. Bamias A, Koutsoukou V, Terpos E, Tsiatas ML, Liakos C, Tsitsilonis O*, et al.* Correlation of NK T-like CD3+CD56+ cells and CD4+CD25+(hi) regulatory T cells with VEGF and TNFalpha in ascites from advanced ovarian cancer: Association with platinum resistance and prognosis in patients receiving first-line, platinum-based chemotherapy. *Gynecologic oncology* 2008, 108(2): 421-427.
51. Papamichail M, Perez SA, Gritzapis AD, Baxevanis CN. Natural killer lymphocytes: biology, development, and function. *Cancer immunology, immunotherapy : CII* 2004, 53(3): 176-186.
52. Ohm JE, Gabrilovich DI, Sempowski GD, Kisseleva E, Parman KS, Nadaf S*, et al.* VEGF inhibits T-cell development and may contribute to tumor-induced immune suppression. *Blood* 2003, 101(12): 4878-4886.
53. Lissoni P, Malugani F, Bonfanti A, Bucovec R, Secondino S, Brivio F*, et al.* Abnormally enhanced blood concentrations of vascular endothelial growth factor (VEGF) in metastatic cancer patients and their relation to circulating dendritic cells, IL-12 and endothelin-1. *Journal of biological regulators and homeostatic agents* 2001, 15(2): 140-144.
54. Healy JC, Reznek RH. The peritoneum, mesenteries and omenta: normal anatomy and pathological processes. *European radiology* 1998, 8(6): 886-900.
55. Sheth S, Horton KM, Garland MR, Fishman EK. Mesenteric neoplasms: CT appearances of primary and secondary tumors and differential diagnosis. *Radiographics : a review publication of the Radiological Society of North America, Inc* 2003, 23(2): 457-473; quiz 535-456.
56. Folkman J. Role of angiogenesis in tumor growth and metastasis. *Seminars in oncology* 2002, 29(6 Suppl 16): 15-18.
57. Gerber SA, Rybalko VY, Bigelow CE, Lugade AA, Foster TH, Frelinger JG*, et al.* Preferential attachment of peritoneal tumor metastases to omental immune aggregates and possible role

of a unique vascular microenvironment in metastatic survival and growth. *The American journal of pathology* 2006, 169(5): 1739-1752.
58. Lawrance RJ, Loizidou M, Cooper AJ, Alexander P, Taylor I. Importance of the omentum in the development of intra-abdominal metastases. *The British journal of surgery* 1991, 78(1): 117-119.
59. Krist LF, Kerremans M, Broekhuis-Fluitsma DM, Eestermans IL, Meyer S, Beelen RH. Milky spots in the greater omentum are predominant sites of local tumour cell proliferation and accumulation in the peritoneal cavity. *Cancer immunology, immunotherapy : CII* 1998, 47(4): 205-212.
60. Hagiwara A, Takahashi T, Sawai K, Taniguchi H, Shimotsuma M, Okano S*, et al.* Milky spots as the implantation site for malignant cells in peritoneal dissemination in mice. *Cancer research* 1993, 53(3): 687-692.
61. Dullens HF, Rademakers LH, Doffemont M, Van Veen PT, Bulder R, Den Otter W. Involvement of the omental lymphoid organ in the induction of peritoneal immunity against tumor cells. *Invasion & metastasis* 1993, 13(5): 267-276.
62. Coussens LM, Werb Z. Inflammation and cancer. *Nature* 2002, 420(6917): 860-867.
63. Allavena P, Garlanda C, Borrello MG, Sica A, Mantovani A. Pathways connecting inflammation and cancer. *Current opinion in genetics & development* 2008, 18(1): 3-10.
64. Kenny PA, Lee GY, Bissell MJ. Targeting the tumor microenvironment. *Frontiers in bioscience : a journal and virtual library* 2007, 12: 3468-3474.
65. Schmieder A, Michel J, Schonhaar K, Goerdt S, Schledzewski K. Differentiation and gene expression profile of tumor-associated macrophages. *Seminars in cancer biology* 2012, 22(4): 289-297.
66. Hanahan D, Coussens LM. Accessories to the crime: functions of cells recruited to the tumor microenvironment. *Cancer cell* 2012, 21(3): 309-322.
67. Elgert KD, Alleva DG, Mullins DW. Tumor-induced immune dysfunction: the macrophage connection. *Journal of leukocyte biology* 1998, 64(3): 275-290.
68. Pardoll D. Does the immune system see tumors as foreign or self? *Annual review of immunology* 2003, 21: 807-839.
69. Murray PJ, Wynn TA. Obstacles and opportunities for understanding macrophage polarization. *Journal of leukocyte biology* 2011, 89(4): 557-563.
70. Biswas SK, Mantovani A. Macrophage plasticity and interaction with lymphocyte subsets: cancer as a paradigm. *Nature immunology* 2010, 11(10): 889-896.
71. Ojalvo LS, King W, Cox D, Pollard JW. High-density gene expression analysis of tumor-associated macrophages from mouse mammary tumors. *The American journal of pathology* 2009, 174(3): 1048-1064.
72. Doyle AG, Herbein G, Montaner LJ, Minty AJ, Caput D, Ferrara P*, et al.* Interleukin-13 alters the activation state of murine macrophages in vitro: comparison with interleukin-4 and interferon-gamma. *European journal of immunology* 1994, 24(6): 1441-1445.
73. Gordon S, Martinez FO. Alternative activation of macrophages: mechanism and functions. *Immunity* 2010, 32(5): 593-604.
74. Sica A, Schioppa T, Mantovani A, Allavena P. Tumour-associated macrophages are a distinct M2 polarised population promoting tumour progression: potential targets of anti-cancer therapy. *European journal of cancer* 2006, 42(6): 717-727.
75. Mantovani A, Sozzani S, Locati M, Allavena P, Sica A. Macrophage polarization: tumor-associated macrophages as a paradigm for polarized M2 mononuclear phagocytes. *Trends in immunology* 2002, 23(11): 549-555.

76. **Qian X, Zhang J, Liu J. Tumor-secreted PGE2 inhibits CCL5 production in activated macrophages through cAMP/PKA signaling pathway. *The Journal of biological chemistry* 2011, 286(3): 2111-2120.**
77. **Hagemann T, Wilson J, Burke F, Kulbe H, Li NF, Pluddemann A*, et al.* Ovarian cancer cells polarize macrophages toward a tumor-associated phenotype. *J Immunol* 2006, 176(8): 5023-5032.**
78. **Bingle L, Brown NJ, Lewis CE. The role of tumour-associated macrophages in tumour progression: implications for new anticancer therapies. *The Journal of pathology* 2002, 196(3): 254-265.**
79. **Bonde AK, Tischler V, Kumar S, Soltermann A, Schwendener RA. Intratumoral macrophages contribute to epithelial-mesenchymal transition in solid tumors. *BMC cancer* 2012, 12: 35.**
80. **Bogdan C, Stenger S, Rollinghoff M, Solbach W. Cytokine interactions in experimental cutaneous leishmaniasis. Interleukin 4 synergizes with interferon-gamma to activate murine macrophages for killing of Leishmania major amastigotes. *European journal of immunology* 1991, 21(2): 327-333.**
81. **Gazzinelli RT, Oswald IP, James SL, Sher A. IL-10 inhibits parasite killing and nitrogen oxide production by IFN-gamma-activated macrophages. *J Immunol* 1992, 148(6): 1792-1796.**
82. **Curiel TJ, Coukos G, Zou L, Alvarez X, Cheng P, Mottram P*, et al.* Specific recruitment of regulatory T cells in ovarian carcinoma fosters immune privilege and predicts reduced survival. *Nature medicine* 2004, 10(9): 942-949.**
83. **Mantovani A, Sica A, Sozzani S, Allavena P, Vecchi A, Locati M. The chemokine system in diverse forms of macrophage activation and polarization. *Trends in immunology* 2004, 25(12): 677-686.**
84. **Mantovani A, Bottazzi B, Colotta F, Sozzani S, Ruco L. The origin and function of tumor-associated macrophages. *Immunology today* 1992, 13(7): 265-270.**
85. **Venkatakrishnan G, Salgia R, Groopman JE. Chemokine receptors CXCR-1/2 activate mitogen-activated protein kinase via the epidermal growth factor receptor in ovarian cancer cells. *The Journal of biological chemistry* 2000, 275(10): 6868-6875.**
86. **Wang B, Li Q, Qin L, Zhao S, Wang J, Chen X. Transition of tumor-associated macrophages from MHC class II(hi) to MHC class II(low) mediates tumor progression in mice. *BMC immunology* 2011, 12: 43.**
87. **Hagemann T, Wilson J, Kulbe H, Li NF, Leinster DA, Charles K*, et al.* Macrophages induce invasiveness of epithelial cancer cells via NF-kappa B and JNK. *J Immunol* 2005, 175(2): 1197-1205.**
88. **Chen GH, Olszewski MA, McDonald RA, Wells JC, Paine R, 3rd, Huffnagle GB*, et al.* Role of granulocyte macrophage colony-stimulating factor in host defense against pulmonary Cryptococcus neoformans infection during murine allergic bronchopulmonary mycosis. *The American journal of pathology* 2007, 170(3): 1028-1040.**
89. **Banerjee S, Halder K, Bose A, Bhattacharya P, Gupta G, Karmahapatra S*, et al.* TLR signaling-mediated differential histone modification at IL-10 and IL-12 promoter region leads to functional impairments in tumor-associated macrophages. *Carcinogenesis* 2011, 32(12): 1789-1797.**
90. **Rius J, Guma M, Schachtrup C, Akassoglou K, Zinkernagel AS, Nizet V*, et al.* NF-kappaB links innate immunity to the hypoxic response through transcriptional regulation of HIF-1alpha. *Nature* 2008, 453(7196): 807-811.**
91. **Werno C, Menrad H, Weigert A, Dehne N, Goerdt S, Schledzewski K*, et al.* Knockout of HIF-1alpha in tumor-associated macrophages enhances M2 polarization and attenuates their pro-angiogenic responses. *Carcinogenesis* 2010, 31(10): 1863-1872.**

92. White DE, Kurpios NA, Zuo D, Hassell JA, Blaess S, Mueller U*, et al.* Targeted disruption of beta1-integrin in a transgenic mouse model of human breast cancer reveals an essential role in mammary tumor induction. *Cancer cell* 2004, 6(2): 159-170.
93. Pello OM, De Pizzol M, Mirolo M, Soucek L, Zammataro L, Amabile A*, et al.* Role of c-MYC in alternative activation of human macrophages and tumor-associated macrophage biology. *Blood* 2012, 119(2): 411-421.
94. Wang N, Gates KL, Trejo H, Favoreto S, Jr., Schleimer RP, Sznajder JI*, et al.* Elevated CO2 selectively inhibits interleukin-6 and tumor necrosis factor expression and decreases phagocytosis in the macrophage. *FASEB journal : official publication of the Federation of American Societies for Experimental Biology* 2010, 24(7): 2178-2190.
95. Kopan R, Ilagan MX. The canonical Notch signaling pathway: unfolding the activation mechanism. *Cell* 2009, 137(2): 216-233.
96. Sanchez-Martin L, Estecha A, Samaniego R, Sanchez-Ramon S, Vega MA, Sanchez-Mateos P. The chemokine CXCL12 regulates monocyte-macrophage differentiation and RUNX3 expression. *Blood* 2011, 117(1): 88-97.
97. Wong SC, Puaux AL, Chittezhath M, Shalova I, Kajiji TS, Wang X*, et al.* Macrophage polarization to a unique phenotype driven by B cells. *European journal of immunology* 2010, 40(8): 2296-2307.
98. del Fresno C, Otero K, Gomez-Garcia L, Gonzalez-Leon MC, Soler-Ranger L, Fuentes-Prior P*, et al.* Tumor cells deactivate human monocytes by up-regulating IL-1 receptor associated kinase-M expression via CD44 and TLR4. *J Immunol* 2005, 174(5): 3032-3040.
99. Deng JC, Cheng G, Newstead MW, Zeng X, Kobayashi K, Flavell RA*, et al.* Sepsis-induced suppression of lung innate immunity is mediated by IRAK-M. *The Journal of clinical investigation* 2006, 116(9): 2532-2542.
100. Standiford TJ, Kuick R, Bhan U, Chen J, Newstead M, Keshamouni VG. TGF-beta-induced IRAK-M expression in tumor-associated macrophages regulates lung tumor growth. *Oncogene* 2011, 30(21): 2475-2484.
101. Pollard JW. Tumour-educated macrophages promote tumour progression and metastasis. *Nature reviews Cancer* 2004, 4(1): 71-78.
102. Shiao SL, Ganesan AP, Rugo HS, Coussens LM. Immune microenvironments in solid tumors: new targets for therapy. *Genes & development* 2011, 25(24): 2559-2572.
103. Allavena P, Sica A, Vecchi A, Locati M, Sozzani S, Mantovani A. The chemokine receptor switch paradigm and dendritic cell migration: its significance in tumor tissues. *Immunological reviews* 2000, 177: 141-149.
104. Sica A, Porta C, Morlacchi S, Banfi S, Strauss L, Rimoldi M*, et al.* Origin and Functions of Tumor-Associated Myeloid Cells (TAMCs). *Cancer microenvironment : official journal of the International Cancer Microenvironment Society* 2012, 5(2): 133-149.
105. Dong R, Cwynarski K, Entwistle A, Marelli-Berg F, Dazzi F, Simpson E*, et al.* Dendritic cells from CML patients have altered actin organization, reduced antigen processing, and impaired migration. *Blood* 2003, 101(9): 3560-3567.
106. Curiel TJ, Wei S, Dong H, Alvarez X, Cheng P, Mottram P*, et al.* Blockade of B7-H1 improves myeloid dendritic cell-mediated antitumor immunity. *Nature medicine* 2003, 9(5): 562-567.
107. Hamanishi J, Mandai M, Iwasaki M, Okazaki T, Tanaka Y, Yamaguchi K*, et al.* Programmed cell death 1 ligand 1 and tumor-infiltrating CD8+ T lymphocytes are prognostic factors of human ovarian cancer. *Proceedings of the National Academy of Sciences of the United States of America* 2007, 104(9): 3360-3365.
108. Diaz-Montero CM, Salem ML, Nishimura MI, Garrett-Mayer E, Cole DJ, Montero AJ. Increased circulating myeloid-derived suppressor cells correlate with clinical cancer stage, metastatic

tumor burden, and doxorubicin-cyclophosphamide chemotherapy. *Cancer immunology, immunotherapy : CII* 2009, 58(1): 49-59.

109. Mundy-Bosse BL, Lesinski GB, Jaime-Ramirez AC, Benninger K, Khan M, Kuppusamy P*, et al.* Myeloid-derived suppressor cell inhibition of the IFN response in tumor-bearing mice. *Cancer research* 2011, 71(15): 5101-5110.

110. Filipazzi P, Huber V, Rivoltini L. Phenotype, function and clinical implications of myeloid-derived suppressor cells in cancer patients. *Cancer immunology, immunotherapy : CII* 2012, 61(2): 255-263.

111. Ohki S, Shibata M, Gonda K, Machida T, Shimura T, Nakamura I*, et al.* Circulating myeloid-derived suppressor cells are increased and correlate to immune suppression, inflammation and hypoproteinemia in patients with cancer. *Oncology reports* 2012, 28(2): 453-458.

112. Nagaraj S, Collazo M, Corzo CA, Youn JI, Ortiz M, Quiceno D*, et al.* Regulatory myeloid suppressor cells in health and disease. *Cancer research* 2009, 69(19): 7503-7506.

113. Terabe M, Matsui S, Park JM, Mamura M, Noben-Trauth N, Donaldson DD*, et al.* Transforming growth factor-beta production and myeloid cells are an effector mechanism through which CD1d-restricted T cells block cytotoxic T lymphocyte-mediated tumor immunosurveillance: abrogation prevents tumor recurrence. *The Journal of experimental medicine* 2003, 198(11): 1741-1752.

114. Kusmartsev S, Nefedova Y, Yoder D, Gabrilovich DI. Antigen-specific inhibition of CD8+ T cell response by immature myeloid cells in cancer is mediated by reactive oxygen species. *J Immunol* 2004, 172(2): 989-999.

115. Corzo CA, Cotter MJ, Cheng P, Cheng F, Kusmartsev S, Sotomayor E*, et al.* Mechanism regulating reactive oxygen species in tumor-induced myeloid-derived suppressor cells. *J Immunol* 2009, 182(9): 5693-5701.

116. Youn JI, Nagaraj S, Collazo M, Gabrilovich DI. Subsets of myeloid-derived suppressor cells in tumor-bearing mice. *J Immunol* 2008, 181(8): 5791-5802.

117. Habibi M, Kmieciak M, Graham L, Morales JK, Bear HD, Manjili MH. Radiofrequency thermal ablation of breast tumors combined with intralesional administration of IL-7 and IL-15 augments anti-tumor immune responses and inhibits tumor development and metastasis. *Breast cancer research and treatment* 2009, 114(3): 423-431.

118. Liu Y, Lai L, Chen Q, Song Y, Xu S, Ma F*, et al.* MicroRNA-494 is required for the accumulation and functions of tumor-expanded myeloid-derived suppressor cells via targeting of PTEN. *J Immunol* 2012, 188(11): 5500-5510.

119. Kaufman B, Wu Y, Amonkar MM, Sherrill B, Bachelot T, Salazar V*, et al.* Impact of lapatinib monotherapy on QOL and pain symptoms in patients with HER2+ relapsed or refractory inflammatory breast cancer. *Current medical research and opinion* 2010, 26(5): 1065-1073.

120. Meyer C, Sevko A, Ramacher M, Bazhin AV, Falk CS, Osen W*, et al.* Chronic inflammation promotes myeloid-derived suppressor cell activation blocking antitumor immunity in transgenic mouse melanoma model. *Proceedings of the National Academy of Sciences of the United States of America* 2011, 108(41): 17111-17116.

121. Bunt SK, Clements VK, Hanson EM, Sinha P, Ostrand-Rosenberg S. Inflammation enhances myeloid-derived suppressor cell cross-talk by signaling through Toll-like receptor 4. *Journal of leukocyte biology* 2009, 85(6): 996-1004.

122. Ozao-Choy J, Ma G, Kao J, Wang GX, Meseck M, Sung M*, et al.* The novel role of tyrosine kinase inhibitor in the reversal of immune suppression and modulation of tumor microenvironment for immune-based cancer therapies. *Cancer research* 2009, 69(6): 2514-2522.

123. Raspollini MR, Castiglione F, Garbini F, Villanucci A, Amunni G, Baroni G*, et al.* Correlation of epidermal growth factor receptor expression with tumor microdensity vessels and with vascular endothelial growth factor expression in ovarian carcinoma. *International journal of surgical pathology* 2005, 13(2): 135-142.

124. Li X, Ye F, Chen H, Lu W, Wan X, Xie X. Human ovarian carcinoma cells generate CD4(+)CD25(+) regulatory T cells from peripheral CD4(+)CD25(-) T cells through secreting TGF-beta. *Cancer letters* 2007, 253(1): 144-153.

125. Bluestone JA, Abbas AK. Natural versus adaptive regulatory T cells. *Nature reviews Immunology* 2003, 3(3): 253-257.

126. Ghiringhelli F, Menard C, Martin F, Zitvogel L. The role of regulatory T cells in the control of natural killer cells: relevance during tumor progression. *Immunological reviews* 2006, 214: 229-238.

127. Lim HW, Hillsamer P, Banham AH, Kim CH. Cutting edge: direct suppression of B cells by CD4+ CD25+ regulatory T cells. *J Immunol* 2005, 175(7): 4180-4183.

128. Muranski P, Boni A, Wrzesinski C, Citrin DE, Rosenberg SA, Childs R*, et al.* Increased intensity lymphodepletion and adoptive immunotherapy--how far can we go? *Nature clinical practice Oncology* 2006, 3(12): 668-681.

129. Bracci L, Moschella F, Sestili P, La Sorsa V, Valentini M, Canini I*, et al.* Cyclophosphamide enhances the antitumor efficacy of adoptively transferred immune cells through the induction of cytokine expression, B-cell and T-cell homeostatic proliferation, and specific tumor infiltration. *Clinical cancer research : an official journal of the American Association for Cancer Research* 2007, 13(2 Pt 1): 644-653.

130. Dudley ME, Yang JC, Sherry R, Hughes MS, Royal R, Kammula U*, et al.* Adoptive cell therapy for patients with metastatic melanoma: evaluation of intensive myeloablative chemoradiation preparative regimens. *Journal of clinical oncology : official journal of the American Society of Clinical Oncology* 2008, 26(32): 5233-5239.

131. Wallen H, Thompson JA, Reilly JZ, Rodmyre RM, Cao J, Yee C. Fludarabine modulates immune response and extends in vivo survival of adoptively transferred CD8 T cells in patients with metastatic melanoma. *PloS one* 2009, 4(3): e4749.

132. Mueller CS, Reichrath J. Histology of melanoma and nonmelanoma skin cancer. *Advances in experimental medicine and biology* 2008, 624: 215-226.

133. Wrzesinski C, Paulos CM, Kaiser A, Muranski P, Palmer DC, Gattinoni L*, et al.* Increased intensity lymphodepletion enhances tumor treatment efficacy of adoptively transferred tumor-specific T cells. *Journal of immunotherapy* 2010, 33(1): 1-7.

134. Zhang M, Yao Z, Dubois S, Ju W, Muller JR, Waldmann TA. Interleukin-15 combined with an anti-CD40 antibody provides enhanced therapeutic efficacy for murine models of colon cancer. *Proceedings of the National Academy of Sciences of the United States of America* 2009, 106(18): 7513-7518.

135. Cocco C, Pistoia V, Airoldi I. New perspectives for melanoma immunotherapy: role of IL-12. *Current molecular medicine* 2009, 9(4): 459-469.

136. Weiss JM, Back TC, Scarzello AJ, Subleski JJ, Hall VL, Stauffer JK*, et al.* Successful immunotherapy with IL-2/anti-CD40 induces the chemokine-mediated mitigation of an immunosuppressive tumor microenvironment. *Proceedings of the National Academy of Sciences of the United States of America* 2009, 106(46): 19455-19460.

137. Dalgleish AG, O'Byrne KJ. Chronic immune activation and inflammation in the pathogenesis of AIDS and cancer. *Advances in cancer research* 2002, 84: 231-276.

138. Agarwal A, Verma S, Burra U, Murthy NS, Mohanty NK, Saxena S. Flow cytometric analysis of Th1 and Th2 cytokines in PBMCs as a parameter of immunological dysfunction in patients of

superficial transitional cell carcinoma of bladder. *Cancer immunology, immunotherapy : CII* 2006, 55(6): 734-743.

139. Kanazawa M, Yoshihara K, Abe H, Iwadate M, Watanabe K, Suzuki S*, et al.* Effects of PSK on T and dendritic cells differentiation in gastric or colorectal cancer patients. *Anticancer research* 2005, 25(1B): 443-449.

140. Brandtzaeg P, Carlsen HS, Halstensen TS. The B-cell system in inflammatory bowel disease. *Advances in experimental medicine and biology* 2006, 579: 149-167.

141. Ilavska S, Jahnova E, Tulinska J, Horvathova M, Dusinska M, Wsolova L*, et al.* Immunological monitoring in workers occupationally exposed to asbestos. *Toxicology* 2005, 206(2): 299-308.

142. Moons LM, Kusters JG, Bultman E, Kuipers EJ, van Dekken H, Tra WM*, et al.* Barrett's oesophagus is characterized by a predominantly humoral inflammatory response. *The Journal of pathology* 2005, 207(3): 269-276.

143. Silverman GJ. Therapeutic B cell depletion and regeneration in rheumatoid arthritis: emerging patterns and paradigms. *Arthritis and rheumatism* 2006, 54(8): 2356-2367.

144. Gokbuget N, Hoelzer D. Novel antibody-based therapy for acute lymphoblastic leukaemia. *Best practice & research Clinical haematology* 2006, 19(4): 701-713.

145. Barbera-Guillem E, Nelson MB, Barr B, Nyhus JK, May KF, Jr., Feng L*, et al.* B lymphocyte pathology in human colorectal cancer. Experimental and clinical therapeutic effects of partial B cell depletion. *Cancer immunology, immunotherapy : CII* 2000, 48(10): 541-549.

146. Tan TT, Coussens LM. Humoral immunity, inflammation and cancer. *Current opinion in immunology* 2007, 19(2): 209-216.

147. Sakamoto T, Saito H, Tatebe S, Tsujitani S, Ozaki M, Ito H*, et al.* Interleukin-10 expression significantly correlates with minor CD8+ T-cell infiltration and high microvessel density in patients with gastric cancer. *International journal of cancer Journal international du cancer* 2006, 118(8): 1909-1914.

148. Rose-John S, Scheller J, Elson G, Jones SA. Interleukin-6 biology is coordinated by membrane-bound and soluble receptors: role in inflammation and cancer. *Journal of leukocyte biology* 2006, 80(2): 227-236.

149. Shah S, Divekar AA, Hilchey SP, Cho HM, Newman CL, Shin SU*, et al.* Increased rejection of primary tumors in mice lacking B cells: inhibition of anti-tumor CTL and TH1 cytokine responses by B cells. *International journal of cancer Journal international du cancer* 2005, 117(4): 574-586.

150. Perricone MA, Smith KA, Claussen KA, Plog MS, Hempel DM, Roberts BL*, et al.* Enhanced efficacy of melanoma vaccines in the absence of B lymphocytes. *Journal of immunotherapy* 2004, 27(4): 273-281.

151. Schreiber H, Wu TH, Nachman J, Rowley DA. Immunological enhancement of primary tumor development and its prevention. *Seminars in cancer biology* 2000, 10(5): 351-357.

152. Gumus E, Erdamar S, Demirel G, Horasanli K, Kendirci M, Miroglu C. Association of positive serum anti-p53 antibodies with poor prognosis in bladder cancer patients. *International journal of urology : official journal of the Japanese Urological Association* 2004, 11(12): 1070-1077.

153. de Visser KE, Eichten A, Coussens LM. Paradoxical roles of the immune system during cancer development. *Nature reviews Cancer* 2006, 6(1): 24-37.

154. Barbera-Guillem E, May KF, Jr., Nyhus JK, Nelson MB. Promotion of tumor invasion by cooperation of granulocytes and macrophages activated by anti-tumor antibodies. *Neoplasia* 1999, 1(5): 453-460.

155. Takai T. Fc receptors and their role in immune regulation and autoimmunity. *Journal of clinical immunology* 2005, 25(1): 1-18.

156. Schmidt RE, Gessner JE. Fc receptors and their interaction with complement in autoimmunity. *Immunology letters* 2005, 100(1): 56-67.
157. Barrington R, Zhang M, Fischer M, Carroll MC. The role of complement in inflammation and adaptive immunity. *Immunological reviews* 2001, 180: 5-15.
158. Armstrong DK, Bundy B, Wenzel L, Huang HQ, Baergen R, Lele S*, et al.* Intraperitoneal cisplatin and paclitaxel in ovarian cancer. *The New England journal of medicine* 2006, 354(1): 34-43.
159. Ozols RF, Bundy BN, Greer BE, Fowler JM, Clarke-Pearson D, Burger RA*, et al.* Phase III trial of carboplatin and paclitaxel compared with cisplatin and paclitaxel in patients with optimally resected stage III ovarian cancer: a Gynecologic Oncology Group study. *Journal of clinical oncology : official journal of the American Society of Clinical Oncology* 2003, 21(17): 3194-3200.
160. Markman M, Webster K, Zanotti K, Rohl J, Belinson J. Use of tamoxifen in asymptomatic patients with recurrent small-volume ovarian cancer. *Gynecologic oncology* 2004, 93(2): 390-393.
161. Steffensen KD, Waldstrom M, Pallisgard N, Lund B, Bergfeldt K, Wihl J*, et al.* Panitumumab and Pegylated Liposomal Doxorubicin in Platinum-Resistant Epithelial Ovarian Cancer With KRAS Wild-Type: The PaLiDo Study, a Phase II Nonrandomized Multicenter Study. *International journal of gynecological cancer : official journal of the International Gynecological Cancer Society* 2012.
162. Garcia AA, Hirte H, Fleming G, Yang D, Tsao-Wei DD, Roman L*, et al.* Phase II clinical trial of bevacizumab and low-dose metronomic oral cyclophosphamide in recurrent ovarian cancer: a trial of the California, Chicago, and Princess Margaret Hospital phase II consortia. *Journal of clinical oncology : official journal of the American Society of Clinical Oncology* 2008, 26(1): 76-82.
163. Metcalf D, Nicola NA. Direct proliferative actions of stem cell factor on murine bone marrow cells in vitro: effects of combination with colony-stimulating factors. *Proceedings of the National Academy of Sciences of the United States of America* 1991, 88(14): 6239-6243.
164. Metcalf D. The role of the colony-stimulating factors in resistance to acute infections. *Immunology and cell biology* 1987, 65 (Pt 1): 35-43.
165. Koenen HJ, Smit MJ, Simmelink MM, Schuurman B, Beelen RH, Meijer S. Effect of intraperitoneal administration of granulocyte/macrophage-colony-stimulating factor in rats on omental milky-spot composition and tumoricidal activity in vivo and in vitro. *Cancer immunology, immunotherapy : CII* 1996, 42(5): 310-316.
166. Chachoua A, Oratz R, Hoogmoed R, Caron D, Peace D, Liebes L*, et al.* Monocyte activation following systemic administration of granulocyte-macrophage colony-stimulating factor. *Journal of immunotherapy with emphasis on tumor immunology : official journal of the Society for Biological Therapy* 1994, 15(3): 217-224.
167. Grabstein KH, Urdal DL, Tushinski RJ, Mochizuki DY, Price VL, Cantrell MA*, et al.* Induction of macrophage tumoricidal activity by granulocyte-macrophage colony-stimulating factor. *Science* 1986, 232(4749): 506-508.
168. Hill AD, Redmond HP, Austin OM, Grace PA, Bouchier-Hayes D. Granulocyte-macrophage colony-stimulating factor inhibits tumour growth. *The British journal of surgery* 1993, 80(12): 1543-1546.
169. Toner GC, Gabrilove JL, Gordon M, Crown J, Jakubowski AA, Meisenberg B*, et al.* Phase I trial of intravenous and intraperitoneal administration of granulocyte-macrophage colony-stimulating factor. *Journal of immunotherapy with emphasis on tumor immunology : official journal of the Society for Biological Therapy* 1994, 15(1): 59-66.

170. Schmeler KM, Vadhan-Raj S, Ramirez PT, Apte SM, Cohen L, Bassett RL*, et al.* A phase II study of GM-CSF and rIFN-gamma1b plus carboplatin for the treatment of recurrent, platinum-sensitive ovarian, fallopian tube and primary peritoneal cancer. *Gynecologic oncology* 2009, 113(2): 210-215.

171. Windbichler GH, Hausmaninger H, Stummvoll W, Graf AH, Kainz C, Lahodny J*, et al.* Interferon-gamma in the first-line therapy of ovarian cancer: a randomized phase III trial. *British journal of cancer* 2000, 82(6): 1138-1144.

172. Hall GD, Brown JM, Coleman RE, Stead M, Metcalf KS, Peel KR*, et al.* Maintenance treatment with interferon for advanced ovarian cancer: results of the Northern and Yorkshire gynaecology group randomised phase III study. *British journal of cancer* 2004, 91(4): 621-626.

173. Ribas A, Butterfield LH, Glaspy JA, Economou JS. Current developments in cancer vaccines and cellular immunotherapy. *Journal of clinical oncology : official journal of the American Society of Clinical Oncology* 2003, 21(12): 2415-2432.

174. Schuurhuis DH, van Montfoort N, Ioan-Facsinay A, Jiawan R, Camps M, Nouta J*, et al.* Immune complex-loaded dendritic cells are superior to soluble immune complexes as antitumor vaccine. *J Immunol* 2006, 176(8): 4573-4580.

175. Curiel DT, Zhu ZB. Combining chemotherapy with virotherapy: a novel treatment strategy for malignant pleural mesothelioma. *Cancer biology & therapy* 2006, 5(2): 236-237.

176. Reichert JM. Metrics for antibody therapeutics development. *mAbs* 2010, 2(6): 695-700.

177. Overdijk MB, Verploegen S, van den Brakel JH, Lammerts van Bueren JJ, Vink T, van de Winkel JG*, et al.* Epidermal growth factor receptor (EGFR) antibody-induced antibody-dependent cellular cytotoxicity plays a prominent role in inhibiting tumorigenesis, even of tumor cells insensitive to EGFR signaling inhibition. *J Immunol* 2011, 187(6): 3383-3390.

178. Weiner LM, Surana R, Wang S. Monoclonal antibodies: versatile platforms for cancer immunotherapy. *Nature reviews Immunology* 2010, 10(5): 317-327.

179. Sharkey RM. Radioimmunotherapy against the tumor vasculature: A new target? *Journal of nuclear medicine : official publication, Society of Nuclear Medicine* 2006, 47(7): 1070-1074.

180. Berek JS, Taylor PT, Gordon A, Cunningham MJ, Finkler N, Orr J, Jr.*, et al.* Randomized, placebo-controlled study of oregovomab for consolidation of clinical remission in patients with advanced ovarian cancer. *Journal of clinical oncology : official journal of the American Society of Clinical Oncology* 2004, 22(17): 3507-3516.

181. Fiszer D, Kurpisz M. Major histocompatibility complex expression on human, male germ cells: a review. *American journal of reproductive immunology* 1998, 40(3): 172-176.

182. Westbrook VA, Schoppee PD, Diekman AB, Klotz KL, Allietta M, Hogan KT*, et al.* Genomic organization, incidence, and localization of the SPAN-x family of cancer-testis antigens in melanoma tumors and cell lines. *Clinical cancer research : an official journal of the American Association for Cancer Research* 2004, 10(1 Pt 1): 101-112.

183. Anwer K, Barnes MN, Fewell J, Lewis DH, Alvarez RD. Phase-I clinical trial of IL-12 plasmid/lipopolymer complexes for the treatment of recurrent ovarian cancer. *Gene therapy* 2010, 17(3): 360-369.

184. Tureci O, Sahin U, Zwick C, Koslowski M, Seitz G, Pfreundschuh M. Identification of a meiosis-specific protein as a member of the class of cancer/testis antigens. *Proceedings of the National Academy of Sciences of the United States of America* 1998, 95(9): 5211-5216.

185. Lim ST, Hee SW, Quek R, Lim LC, Yap SP, Loong EL*, et al.* Comparative analysis of extra-nodal NK/T-cell lymphoma and peripheral T-cell lymphoma: significant differences in clinical characteristics and prognosis. *European journal of haematology* 2008, 80(1): 55-60.

186. van Baren N, Brasseur F, Godelaine D, Hames G, Ferrant A, Lehmann F*, et al.* Genes encoding tumor-specific antigens are expressed in human myeloma cells. *Blood* 1999, 94(4): 1156-1164.

187. Jungbluth AA, Ely S, DiLiberto M, Niesvizky R, Williamson B, Frosina D*, et al.* The cancer-testis antigens CT7 (MAGE-C1) and MAGE-A3/6 are commonly expressed in multiple myeloma and correlate with plasma-cell proliferation. *Blood* 2005, 106(1): 167-174.

188. van Rhee F, Szmania SM, Zhan F, Gupta SK, Pomtree M, Lin P*, et al.* NY-ESO-1 is highly expressed in poor-prognosis multiple myeloma and induces spontaneous humoral and cellular immune responses. *Blood* 2005, 105(10): 3939-3944.

189. Sproul D, Kitchen RR, Nestor CE, Dixon JM, Sims AH, Harrison DJ*, et al.* Tissue of origin determines cancer-associated CpG island promoter hypermethylation patterns. *Genome biology* 2012, 13(10): R84.

190. Gama-Sosa MA, Slagel VA, Trewyn RW, Oxenhandler R, Kuo KC, Gehrke CW*, et al.* The 5-methylcytosine content of DNA from human tumors. *Nucleic acids research* 1983, 11(19): 6883-6894.

191. Christman JK, Sheikhnejad G, Dizik M, Abileah S, Wainfan E. Reversibility of changes in nucleic acid methylation and gene expression induced in rat liver by severe dietary methyl deficiency. *Carcinogenesis* 1993, 14(4): 551-557.

192. Linn YC, Yong HX, Niam M, Lim TJ, Chu S, Choong A*, et al.* A phase I/II clinical trial of autologous cytokine-induced killer cells as adjuvant immunotherapy for acute and chronic myeloid leukemia in clinical remission. *Cytotherapy* 2012, 14(7): 851-859.

193. Robinson SC, Scott KA, Wilson JL, Thompson RG, Proudfoot AE, Balkwill FR. A chemokine receptor antagonist inhibits experimental breast tumor growth. *Cancer research* 2003, 63(23): 8360-8365.

194. Loberg RD, Ying C, Craig M, Day LL, Sargent E, Neeley C*, et al.* Targeting CCL2 with systemic delivery of neutralizing antibodies induces prostate cancer tumor regression in vivo. *Cancer research* 2007, 67(19): 9417-9424.

195. Vergunst CE, Gerlag DM, Lopatinskaya L, Klareskog L, Smith MD, van den Bosch F*, et al.* Modulation of CCR2 in rheumatoid arthritis: a double-blind, randomized, placebo-controlled clinical trial. *Arthritis and rheumatism* 2008, 58(7): 1931-1939.

196. Monk BJ, Han E, Josephs-Cowan CA, Pugmire G, Burger RA. Salvage bevacizumab (rhuMAB VEGF)-based therapy after multiple prior cytotoxic regimens in advanced refractory epithelial ovarian cancer. *Gynecologic oncology* 2006, 102(2): 140-144.

197. Burger M, Thiounn N, Denzinger S, Kondas J, Benoit G, Chapado MS*, et al.* The application of adjuvant autologous antravesical macrophage cell therapy vs. BCG in non-muscle invasive bladder cancer: a multicenter, randomized trial. *Journal of translational medicine* 2010, 8: 54.

198. Burger RA, Sill MW, Monk BJ, Greer BE, Sorosky JI. Phase II trial of bevacizumab in persistent or recurrent epithelial ovarian cancer or primary peritoneal cancer: a Gynecologic Oncology Group Study. *Journal of clinical oncology : official journal of the American Society of Clinical Oncology* 2007, 25(33): 5165-5171.

199. Bibeau F, Lopez-Crapez E, Di Fiore F, Thezenas S, Ychou M, Blanchard F*, et al.* Impact of Fc{gamma}RIIa-Fc{gamma}RIIIa polymorphisms and KRAS mutations on the clinical outcome of patients with metastatic colorectal cancer treated with cetuximab plus irinotecan. *Journal of clinical oncology : official journal of the American Society of Clinical Oncology* 2009, 27(7): 1122-1129.

200. Cartron G, Dacheux L, Salles G, Solal-Celigny P, Bardos P, Colombat P*, et al.* Therapeutic activity of humanized anti-CD20 monoclonal antibody and polymorphism in IgG Fc receptor FcgammaRIIIa gene. *Blood* 2002, 99(3): 754-758.

201. Musolino A, Naldi N, Bortesi B, Pezzuolo D, Capelletti M, Missale G*, et al.* Immunoglobulin G fragment C receptor polymorphisms and clinical efficacy of trastuzumab-based therapy in

patients with HER-2/neu-positive metastatic breast cancer. *Journal of clinical oncology : official journal of the American Society of Clinical Oncology* 2008, 26(11): 1789-1796.

202. Horikawa M, Iinuma H, Inoue T, Ogawa E, Fukushima R. Clinical significance of intraperitoneal CD44 mRNA levels of magnetically separated CD45-negative EpCAM-positive cells for peritoneal recurrence and prognosis in stage II and III gastric cancer patients. *Oncology reports* 2011, 25(5): 1413-1420.

203. McEarchern JA, Oflazoglu E, Francisco L, McDonagh CF, Gordon KA, Stone I*, et al.* Engineered anti-CD70 antibody with multiple effector functions exhibits in vitro and in vivo antitumor activities. *Blood* 2007, 109(3): 1185-1192.

204. Oflazoglu E, Stone IJ, Gordon KA, Grewal IS, van Rooijen N, Law CL*, et al.* Macrophages contribute to the antitumor activity of the anti-CD30 antibody SGN-30. *Blood* 2007, 110(13): 4370-4372.

205. Oflazoglu E, Stone IJ, Brown L, Gordon KA, van Rooijen N, Jonas M*, et al.* Macrophages and Fc-receptor interactions contribute to the antitumour activities of the anti-CD40 antibody SGN-40. *British journal of cancer* 2009, 100(1): 113-117.

206. Minard-Colin V, Xiu Y, Poe JC, Horikawa M, Magro CM, Hamaguchi Y*, et al.* Lymphoma depletion during CD20 immunotherapy in mice is mediated by macrophage FcgammaRI, FcgammaRIII, and FcgammaRIV. *Blood* 2008, 112(4): 1205-1213.

207. Clynes RA, Towers TL, Presta LG, Ravetch JV. Inhibitory Fc receptors modulate in vivo cytotoxicity against tumor targets. *Nature medicine* 2000, 6(4): 443-446.

208. Grugan KD, McCabe FL, Kinder M, Greenplate AR, Harman BC, Ekert JE*, et al.* Tumor-Associated Macrophages Promote Invasion while Retaining Fc-Dependent Anti-Tumor Function. *J Immunol* 2012.

209. DeNardo DG, Barreto JB, Andreu P, Vasquez L, Tawfik D, Kolhatkar N*, et al.* CD4(+) T cells regulate pulmonary metastasis of mammary carcinomas by enhancing protumor properties of macrophages. *Cancer cell* 2009, 16(2): 91-102.

210. Beatty GL, Chiorean EG, Fishman MP, Saboury B, Teitelbaum UR, Sun W*, et al.* CD40 agonists alter tumor stroma and show efficacy against pancreatic carcinoma in mice and humans. *Science* 2011, 331(6024): 1612-1616.

211. Rogers TL, Holen I. Tumour macrophages as potential targets of bisphosphonates. *Journal of translational medicine* 2011, 9: 177.

212. Coscia M, Quaglino E, Iezzi M, Curcio C, Pantaleoni F, Riganti C*, et al.* Zoledronic acid repolarizes tumour-associated macrophages and inhibits mammary carcinogenesis by targeting the mevalonate pathway. *Journal of cellular and molecular medicine* 2010, 14(12): 2803-2815.

213. Chi KH, Wang YS, Kao SJ. Improving radioresponse through modification of the tumor immunological microenvironment. *Cancer biotherapy & radiopharmaceuticals* 2012, 27(1): 6-11.

214. Crawford Y, Ferrara N. Tumor and stromal pathways mediating refractoriness/resistance to anti-angiogenic therapies. *Trends in pharmacological sciences* 2009, 30(12): 624-630.

215. Farinha P, Masoudi H, Skinnider BF, Shumansky K, Spinelli JJ, Gill K*, et al.* Analysis of multiple biomarkers shows that lymphoma-associated macrophage (LAM) content is an independent predictor of survival in follicular lymphoma (FL). *Blood* 2005, 106(6): 2169-2174.

216. Emens LA, Reilly RT, Jaffee EM. Cancer vaccines in combination with multimodality therapy. *Cancer treatment and research* 2005, 123: 227-245.

217. Suzuki E, Kapoor V, Jassar AS, Kaiser LR, Albelda SM. Gemcitabine selectively eliminates splenic Gr-1+/CD11b+ myeloid suppressor cells in tumor-bearing animals and enhances

antitumor immune activity. ***Clinical cancer research : an official journal of the American Association for Cancer Research*** **2005, 11(18): 6713-6721.**

218. Correale P, Cusi MG, Tsang KY, Del Vecchio MT, Marsili S, Placa ML*, et al.* Chemo-immunotherapy of metastatic colorectal carcinoma with gemcitabine plus FOLFOX 4 followed by subcutaneous granulocyte macrophage colony-stimulating factor and interleukin-2 induces strong immunologic and antitumor activity in metastatic colon cancer patients. ***Journal of clinical oncology : official journal of the American Society of Clinical Oncology*** **2005, 23(35): 8950-8958.**

219. Cavallo F, Signorelli P, Giovarelli M, Musiani P, Modesti A, Brunda MJ*, et al.* Antitumor efficacy of adenocarcinoma cells engineered to produce interleukin 12 (IL-12) or other cytokines compared with exogenous IL-12. ***Journal of the National Cancer Institute*** **1997, 89(14): 1049-1058.**

220. Finn OJ. Cancer vaccines: between the idea and the reality. ***Nature reviews Immunology*** **2003, 3(8): 630-641.**

221. Provinciali M. Immunosenescence and cancer vaccines. ***Cancer immunology, immunotherapy : CII*** **2009, 58(12): 1959-1967.**

222. Payne KK, Toor AA, Wang XY, Manjili MH. Immunotherapy of cancer: reprogramming tumor-immune crosstalk. ***Clinical & developmental immunology*** **2012, 2012: 760965.**

223. Curigliano G, Spitaleri G, Pietri E, Rescigno M, de Braud F, Cardillo A*, et al.* Breast cancer vaccines: a clinical reality or fairy tale? ***Annals of oncology : official journal of the European Society for Medical Oncology / ESMO*** **2006, 17(5): 750-762.**

224. Zhou J, Zhong Y. Breast cancer immunotherapy. ***Cellular & molecular immunology*** **2004, 1(4): 247-255.**

225. Ladjemi MZ, Jacot W, Chardes T, Pelegrin A, Navarro-Teulon I. Anti-HER2 vaccines: new prospects for breast cancer therapy. ***Cancer immunology, immunotherapy : CII*** **2010, 59(9): 1295-1312.**

226. Chatila T, Wong R, Young M, Miller R, Terhorst C, Geha RS. An immunodeficiency characterized by defective signal transduction in T lymphocytes. ***The New England journal of medicine*** **1989, 320(11): 696-702.**

227. Kazanietz MG, Bustelo XR, Barbacid M, Kolch W, Mischak H, Wong G*, et al.* Zinc finger domains and phorbol ester pharmacophore. Analysis of binding to mutated form of protein kinase C zeta and the vav and c-raf proto-oncogene products. ***The Journal of biological chemistry*** **1994, 269(15): 11590-11594.**

228. Chekmasova AA, Brentjens RJ. Adoptive T cell immunotherapy strategies for the treatment of patients with ovarian cancer. ***Discovery medicine*** **2010, 9(44): 62-70.**

229. Coukos G, Conejo-Garcia JR, Roden RB, Wu TC. Immunotherapy for gynaecological malignancies. ***Expert opinion on biological therapy*** **2005, 5(9): 1193-1210.**

230. Kobayashi M, Fitz L, Ryan M, Hewick RM, Clark SC, Chan S*, et al.* Identification and purification of natural killer cell stimulatory factor (NKSF), a cytokine with multiple biologic effects on human lymphocytes. ***The Journal of experimental medicine*** **1989, 170(3): 827-845.**

231. Schoenhaut DS, Chua AO, Wolitzky AG, Quinn PM, Dwyer CM, McComas W*, et al.* Cloning and expression of murine IL-12. ***J Immunol*** **1992, 148(11): 3433-3440.**

232. Merberg DM, Wolf SF, Clark SC. Sequence similarity between NKSF and the IL-6/G-CSF family. ***Immunology today*** **1992, 13(2): 77-78.**

233. Desai BB, Quinn PM, Wolitzky AG, Mongini PK, Chizzonite R, Gately MK. IL-12 receptor. II. Distribution and regulation of receptor expression. ***J Immunol*** **1992, 148(10): 3125-3132.**

234. Chizzonite R, Truitt T, Desai BB, Nunes P, Podlaski FJ, Stern AS*, et al.* IL-12 receptor. I. Characterization of the receptor on phytohemagglutinin-activated human lymphoblasts. *J Immunol* 1992, 148(10): 3117-3124.
235. Naume B, Gately MK, Desai BB, Sundan A, Espevik T. Synergistic effects of interleukin 4 and interleukin 12 on NK cell proliferation. *Cytokine* 1993, 5(1): 38-46.
236. Pignata C, Sanghera JS, Cossette L, Pelech SL, Ritz J. Interleukin-12 induces tyrosine phosphorylation and activation of 44-kD mitogen-activated protein kinase in human T cells. *Blood* 1994, 83(1): 184-190.
237. Ihle JN, Witthuhn BA, Quelle FW, Yamamoto K, Silvennoinen O. Signaling through the hematopoietic cytokine receptors. *Annual review of immunology* 1995, 13: 369-398.
238. Bacon CM, McVicar DW, Ortaldo JR, Rees RC, O'Shea JJ, Johnston JA. Interleukin 12 (IL-12) induces tyrosine phosphorylation of JAK2 and TYK2: differential use of Janus family tyrosine kinases by IL-2 and IL-12. *The Journal of experimental medicine* 1995, 181(1): 399-404.
239. Jacobson NG, Szabo SJ, Guler ML, Gorham JD, Murphy KM. Regulation of interleukin-12 signal transduction during T helper phenotype development. *Research in immunology* 1995, 146(7-8): 446-456.
240. Szabo SJ, Jacobson NG, Dighe AS, Gubler U, Murphy KM. Developmental commitment to the Th2 lineage by extinction of IL-12 signaling. *Immunity* 1995, 2(6): 665-675.
241. D'Andrea A, Rengaraju M, Valiante NM, Chehimi J, Kubin M, Aste M*, et al.* Production of natural killer cell stimulatory factor (interleukin 12) by peripheral blood mononuclear cells. *The Journal of experimental medicine* 1992, 176(5): 1387-1398.
242. Macatonia SE, Hosken NA, Litton M, Vieira P, Hsieh CS, Culpepper JA*, et al.* Dendritic cells produce IL-12 and direct the development of Th1 cells from naive CD4+ T cells. *J Immunol* 1995, 154(10): 5071-5079.
243. Chan SH, Perussia B, Gupta JW, Kobayashi M, Pospisil M, Young HA*, et al.* Induction of interferon gamma production by natural killer cell stimulatory factor: characterization of the responder cells and synergy with other inducers. *The Journal of experimental medicine* 1991, 173(4): 869-879.
244. Chan SH, Kobayashi M, Santoli D, Perussia B, Trinchieri G. Mechanisms of IFN-gamma induction by natural killer cell stimulatory factor (NKSF/IL-12). Role of transcription and mRNA stability in the synergistic interaction between NKSF and IL-2. *J Immunol* 1992, 148(1): 92-98.
245. Carson WE, Ross ME, Baiocchi RA, Marien MJ, Boiani N, Grabstein K*, et al.* Endogenous production of interleukin 15 by activated human monocytes is critical for optimal production of interferon-gamma by natural killer cells in vitro. *The Journal of clinical investigation* 1995, 96(6): 2578-2582.
246. Gazzinelli RT, Hieny S, Wynn TA, Wolf S, Sher A. Interleukin 12 is required for the T-lymphocyte-independent induction of interferon gamma by an intracellular parasite and induces resistance in T-cell-deficient hosts. *Proceedings of the National Academy of Sciences of the United States of America* 1993, 90(13): 6115-6119.
247. Tripp CS, Wolf SF, Unanue ER. Interleukin 12 and tumor necrosis factor alpha are costimulators of interferon gamma production by natural killer cells in severe combined immunodeficiency mice with listeriosis, and interleukin 10 is a physiologic antagonist. *Proceedings of the National Academy of Sciences of the United States of America* 1993, 90(8): 3725-3729.
248. Wu CY, Demeure C, Kiniwa M, Gately M, Delespesse G. IL-12 induces the production of IFN-gamma by neonatal human CD4 T cells. *J Immunol* 1993, 151(4): 1938-1949.
249. Scott P. IL-12: initiation cytokine for cell-mediated immunity. *Science* 1993, 260(5107): 496-497.

250. **Naume B, Gately M, Espevik T. A comparative study of IL-12 (cytotoxic lymphocyte maturation factor)-, IL-2-, and IL-7-induced effects on immunomagnetically purified CD56+ NK cells. *J Immunol* 1992, 148(8): 2429-2436.**
251. **Aste-Amezaga M, D'Andrea A, Kubin M, Trinchieri G. Cooperation of natural killer cell stimulatory factor/interleukin-12 with other stimuli in the induction of cytokines and cytotoxic cell-associated molecules in human T and NK cells. *Cellular immunology* 1994, 156(2): 480-492.**
252. **Weiss JM, Subleski JJ, Wigginton JM, Wiltrout RH. Immunotherapy of cancer by IL-12-based cytokine combinations. *Expert opinion on biological therapy* 2007, 7(11): 1705-1721.**
253. **Gately MK, Gubler U, Brunda MJ, Nadeau RR, Anderson TD, Lipman JM*, et al.* Interleukin-12: a cytokine with therapeutic potential in oncology and infectious diseases. *Therapeutic immunology* 1994, 1(3): 187-196.**
254. **Robertson MJ, Ritz J. Interleukin 12: Basic Biology and Potential Applications in Cancer Treatment. *The oncologist* 1996, 1(1 & 2): 88-97.**
255. **Salcedo TW, Azzoni L, Wolf SF, Perussia B. Modulation of perforin and granzyme messenger RNA expression in human natural killer cells. *J Immunol* 1993, 151(5): 2511-2520.**
256. **Zou JJ, Schoenhaut DS, Carvajal DM, Warrier RR, Presky DH, Gately MK*, et al.* Structure-function analysis of the p35 subunit of mouse interleukin 12. *The Journal of biological chemistry* 1995, 270(11): 5864-5871.**
257. **Noguchi Y, Richards EC, Chen YT, Old LJ. Influence of interleukin 12 on p53 peptide vaccination against established Meth A sarcoma. *Proceedings of the National Academy of Sciences of the United States of America* 1995, 92(6): 2219-2223.**
258. **Zeh HJ, 3rd, Hurd S, Storkus WJ, Lotze MT. Interleukin-12 promotes the proliferation and cytolytic maturation of immune effectors: implications for the immunotherapy of cancer. *Journal of immunotherapy with emphasis on tumor immunology : official journal of the Society for Biological Therapy* 1993, 14(2): 155-161.**
259. **Andrews JV, Schoof DD, Bertagnolli MM, Peoples GE, Goedegebuure PS, Eberlein TJ. Immunomodulatory effects of interleukin-12 on human tumor-infiltrating lymphocytes. *Journal of immunotherapy with emphasis on tumor immunology : official journal of the Society for Biological Therapy* 1993, 14(1): 1-10.**
260. **Bigda J, Mysliwska J, Dziadziuszko R, Bigda J, Mysliwski A, Hellmann A. Interleukin 12 augments natural killer-cell mediated cytotoxicity in hairy cell leukemia. *Leukemia & lymphoma* 1993, 10(1-2): 121-125.**
261. **Ferlazzo G, Pack M, Thomas D, Paludan C, Schmid D, Strowig T*, et al.* Distinct roles of IL-12 and IL-15 in human natural killer cell activation by dendritic cells from secondary lymphoid organs. *Proceedings of the National Academy of Sciences of the United States of America* 2004, 101(47): 16606-16611.**
262. **Atkins MB, Redman B, Mier J, Gollob J, Weber J, Sosman J*, et al.* A phase I study of CNI-1493, an inhibitor of cytokine release, in combination with high-dose interleukin-2 in patients with renal cancer and melanoma. *Clinical cancer research : an official journal of the American Association for Cancer Research* 2001, 7(3): 486-492.**
263. **Chakrabarti R, Chang Y, Song K, Prud'homme GJ. Plasmids encoding membrane-bound IL-4 or IL-12 strongly costimulate DNA vaccination against carcinoembryonic antigen (CEA). *Vaccine* 2004, 22(9-10): 1199-1205.**
264. **Car BD, Eng VM, Lipman JM, Anderson TD. The toxicology of interleukin-12: a review. *Toxicologic pathology* 1999, 27(1): 58-63.**

265. Leonard JP, Sherman ML, Fisher GL, Buchanan LJ, Larsen G, Atkins MB*, et al.* Effects of single-dose interleukin-12 exposure on interleukin-12-associated toxicity and interferon-gamma production. *Blood* 1997, 90(7): 2541-2548.
266. Zitvogel L, Lotze MT. Role of interleukin-12 (IL12) as an anti-tumour agent: experimental biology and clinical application. *Research in immunology* 1995, 146(7-8): 628-638.
267. Pappo I, Tahara H, Robbins PD, Gately MK, Wolf SF, Barnea A*, et al.* Administration of systemic or local interleukin-2 enhances the anti-tumor effects of interleukin-12 gene therapy. *The Journal of surgical research* 1995, 58(2): 218-226.
268. Tahara H, Lotze MT. Antitumor effects of interleukin-12 (IL-12): applications for the immunotherapy and gene therapy of cancer. *Gene therapy* 1995, 2(2): 96-106.
269. Meko JB, Yim JH, Tsung K, Norton JA. High cytokine production and effective antitumor activity of a recombinant vaccinia virus encoding murine interleukin 12. *Cancer research* 1995, 55(21): 4765-4770.
270. Zhang S, Wang Q. Factors determining the formation and release of bioactive IL-12: regulatory mechanisms for IL-12p70 synthesis and inhibition. *Biochemical and biophysical research communications* 2008, 372(4): 509-512.
271. Ling P, Gately MK, Gubler U, Stern AS, Lin P, Hollfelder K*, et al.* Human IL-12 p40 homodimer binds to the IL-12 receptor but does not mediate biologic activity. *J Immunol* 1995, 154(1): 116-127.
272. Heinzel FP, Hujer AM, Ahmed FN, Rerko RM. In vivo production and function of IL-12 p40 homodimers. *J Immunol* 1997, 158(9): 4381-4388.
273. Gillessen S, Carvajal D, Ling P, Podlaski FJ, Stremlo DL, Familletti PC*, et al.* Mouse interleukin-12 (IL-12) p40 homodimer: a potent IL-12 antagonist. *European journal of immunology* 1995, 25(1): 200-206.
274. Mattner F, Fischer S, Guckes S, Jin S, Kaulen H, Schmitt E*, et al.* The interleukin-12 subunit p40 specifically inhibits effects of the interleukin-12 heterodimer. *European journal of immunology* 1993, 23(9): 2202-2208.
275. Jana M, Pahan K. IL-12 p40 homodimer, but not IL-12 p70, induces the expression of IL-16 in microglia and macrophages. *Molecular immunology* 2009, 46(5): 773-783.
276. Cooper AM, Khader SA. IL-12p40: an inherently agonistic cytokine. *Trends in immunology* 2007, 28(1): 33-38.
277. Khader SA, Partida-Sanchez S, Bell G, Jelley-Gibbs DM, Swain S, Pearl JE*, et al.* Interleukin 12p40 is required for dendritic cell migration and T cell priming after Mycobacterium tuberculosis infection. *The Journal of experimental medicine* 2006, 203(7): 1805-1815.
278. Marr RA, Addison CL, Snider D, Muller WJ, Gauldie J, Graham FL. Tumour immunotherapy using an adenoviral vector expressing a membrane-bound mutant of murine TNF alpha. *Gene therapy* 1997, 4(11): 1181-1188.
279. Soo Hoo W, Lundeen KA, Kohrumel JR, Pham NL, Brostoff SW, Bartholomew RM*, et al.* Tumor cell surface expression of granulocyte-macrophage colony-stimulating factor elicits antitumor immunity and protects from tumor challenge in the P815 mouse mastocytoma tumor model. *J Immunol* 1999, 162(12): 7343-7349.
280. Ji J, Li J, Holmes LM, Burgin KE, Yu X, Wagner TE*, et al.* Synergistic anti-tumor effect of glycosylphosphatidylinositol-anchored IL-2 and IL-12. *The journal of gene medicine* 2004, 6(7): 777-785.
281. Ji J, Li J, Holmes LM, Burgin KE, Yu X, Wagner TE*, et al.* Glycoinositol phospholipid-anchored interleukin 2 but not secreted interleukin 2 inhibits melanoma tumor growth in mice. *Molecular cancer therapeutics* 2002, 1(12): 1019-1024.

282. Chang MR, Lee WH, Choi JW, Park SO, Paik SG, Kim YS. Antitumor immunity induced by tumor cells engineered to express a membrane-bound form of IL-2. *Experimental & molecular medicine* 2005, 37(3): 240-249.
283. Choi KS, Song EK, Yim CY. Cytokines secreted by IL-2-activated lymphocytes induce endogenous nitric oxide synthesis and apoptosis in macrophages. *Journal of leukocyte biology* 2008, 83(6): 1440-1450.
284. Cimino AM, Palaniswami P, Kim AC, Selvaraj P. Cancer vaccine development: protein transfer of membrane-anchored cytokines and immunostimulatory molecules. *Immunologic research* 2004, 29(1-3): 231-240.
285. Tuve S, Chen BM, Liu Y, Cheng TL, Toure P, Sow PS*, et al.* Combination of tumor site-located CTL-associated antigen-4 blockade and systemic regulatory T-cell depletion induces tumor-destructive immune responses. *Cancer research* 2007, 67(12): 5929-5939.
286. Kim YS. Tumor Therapy Applying Membrane-bound Form of Cytokines. *Immune network* 2009, 9(5): 158-168.
287. Lim HY, Ju HY, Chung HY, Kim YS. Antitumor effects of a tumor cell vaccine expressing a membrane-bound form of the IL-12 p35 subunit. *Cancer biology & therapy* 2010, 10(4): 336-343.
288. Nagarajan S, Selvaraj P. Glycolipid-anchored IL-12 expressed on tumor cell surface induces antitumor immune response. *Cancer research* 2002, 62(10): 2869-2874.
289. Takeda K, Seki S, Ogasawara K, Anzai R, Hashimoto W, Sugiura K*, et al.* Liver NK1.1+ CD4+ alpha beta T cells activated by IL-12 as a major effector in inhibition of experimental tumor metastasis. *J Immunol* 1996, 156(9): 3366-3373.
290. Cui J, Shin T, Kawano T, Sato H, Kondo E, Toura I*, et al.* Requirement for Valpha14 NKT cells in IL-12-mediated rejection of tumors. *Science* 1997, 278(5343): 1623-1626.
291. Egilmez NK, Jong YS, Sabel MS, Jacob JS, Mathiowitz E, Bankert RB. In situ tumor vaccination with interleukin-12-encapsulated biodegradable microspheres: induction of tumor regression and potent antitumor immunity. *Cancer research* 2000, 60(14): 3832-3837.
292. Elzaouk L, Moelling K, Pavlovic J. Anti-tumor activity of mesenchymal stem cells producing IL-12 in a mouse melanoma model. *Experimental dermatology* 2006, 15(11): 865-874.
293. Pan WY, Lo CH, Chen CC, Wu PY, Roffler SR, Shyue SK*, et al.* Cancer immunotherapy using a membrane-bound interleukin-12 with B7-1 transmembrane and cytoplasmic domains. *Molecular therapy : the journal of the American Society of Gene Therapy* 2012, 20(5): 927-937.
294. Mebius RE. Lymphoid organs for peritoneal cavity immune response: milky spots. *Immunity* 2009, 30(5): 670-672.
295. Krist LF, Eestermans IL, Steenbergen JJ, Hoefsmit EC, Cuesta MA, Meyer S*, et al.* Cellular composition of milky spots in the human greater omentum: an immunochemical and ultrastructural study. *The Anatomical record* 1995, 241(2): 163-174.
296. Berberich S, Dahne S, Schippers A, Peters T, Muller W, Kremmer E*, et al.* Differential molecular and anatomical basis for B cell migration into the peritoneal cavity and omental milky spots. *J Immunol* 2008, 180(4): 2196-2203.
297. Ansel KM, Harris RB, Cyster JG. CXCL13 is required for B1 cell homing, natural antibody production, and body cavity immunity. *Immunity* 2002, 16(1): 67-76.
298. Rangel-Moreno J, Moyron-Quiroz JE, Carragher DM, Kusser K, Hartson L, Moquin A*, et al.* Omental milky spots develop in the absence of lymphoid tissue-inducer cells and support B and T cell responses to peritoneal antigens. *Immunity* 2009, 30(5): 731-743.
299. Doherty NS, Griffiths RJ, Hakkinen JP, Scampoli DN, Milici AJ. Post-capillary venules in the "milky spots" of the greater omentum are the major site of plasma protein and leukocyte

extravasation in rodent models of peritonitis. *Inflammation research : official journal of the European Histamine Research Society [et al]* 1995, 44(4): 169-177.

300. Williams R, White H. The greater omentum: its applicability to cancer surgery and cancer therapy. *Current problems in surgery* 1986, 23(11): 789-865.

301. Beelen RH, Fluitsma DM, Hoefsmit EC. The cellular composition of omentum milky spots and the ultrastructure of milky spot macrophages and reticulum cells. *Journal of the Reticuloendothelial Society* 1980, 28(6): 585-599.

302. Wijffels JF, Hendrickx RJ, Steenbergen JJ, Eestermans IL, Beelen RH. Milky spots in the mouse omentum may play an important role in the origin of peritoneal macrophages. *Research in immunology* 1992, 143(4): 401-409.

303. Mandache E, Moldoveanu E, Negoescu A. Lymphatic follicle-like structures in the stimulated omental milky spots. *Morphologie et embryologie* 1987, 33(4): 285-289.

304. Gray KS, Collins CM, Speck SH. Characterization of omental immune aggregates during establishment of a latent gammaherpesvirus infection. *PloS one* 2012, 7(8): e43196.

305. Hardy CL, Godfrey DI, Scollay R. The effect of antigen stimulation on the migration of mature T cells from the peripheral lymphoid tissues to the thymus. *Developmental immunology* 2001, 8(2): 123-131.

306. Martin A, Scharff MD. Immunology. Antibody alterations. *Nature* 2001, 412(6850): 870-871.

307. Hayakawa S, Uchida T, Mekada E, Moynihan MR, Okada Y. Monoclonal antibody against diphtheria toxin. Effect on toxin binding and entry into cells. *The Journal of biological chemistry* 1983, 258(7): 4311-4317.

308. Montecino-Rodriguez E, Dorshkind K. New perspectives in B-1 B cell development and function. *Trends in immunology* 2006, 27(9): 428-433.

309. Benedict CL, Kearney JF. Increased junctional diversity in fetal B cells results in a loss of protective anti-phosphorylcholine antibodies in adult mice. *Immunity* 1999, 10(5): 607-617.

310. Goldsmith HS, Steward E. Vascularization of brain and spinal cord by intact omentum. *Applied neurophysiology* 1984, 47(1-2): 57-61.

311. Das SK. The size of the human omentum and methods of lengthening it for transplantation. *British journal of plastic surgery* 1976, 29(2): 170-144.

312. Mohammed KA, Nasreen N, Hardwick J, Logie CS, Patterson CE, Antony VB. Bacterial induction of pleural mesothelial monolayer barrier dysfunction. *American journal of physiology Lung cellular and molecular physiology* 2001, 281(1): L119-125.

313. Shimotsuma M, Shields JW, Simpson-Morgan MW, Sakuyama A, Shirasu M, Hagiwara A*, et al.* Morpho-physiological function and role of omental milky spots as omentum-associated lymphoid tissue (OALT) in the peritoneal cavity. *Lymphology* 1993, 26(2): 90-101.

314. Pawelec G. Hallmarks of human "immunosenescence": adaptation or dysregulation? *Immunity & ageing : I & A* 2012, 9(1): 15.

315. Blank C, Mackensen A. Contribution of the PD-L1/PD-1 pathway to T-cell exhaustion: an update on implications for chronic infections and tumor evasion. *Cancer immunology, immunotherapy : CII* 2007, 56(5): 739-745.

316. Pawelec G, Solana R. Immunosenescence. *Immunology today* 1997, 18(11): 514-516.

317. Derhovanessian E, Solana R, Larbi A, Pawelec G. Immunity, ageing and cancer. *Immunity & ageing : I & A* 2008, 5: 11.

318. McNeel DG, Dunphy EJ, Davies JG, Frye TP, Johnson LE, Staab MJ*, et al.* Safety and immunological efficacy of a DNA vaccine encoding prostatic acid phosphatase in patients with stage D0 prostate cancer. *Journal of clinical oncology : official journal of the American Society of Clinical Oncology* 2009, 27(25): 4047-4054.

319. Asemissen AM, Brossart P. Vaccination strategies in patients with renal cell carcinoma. *Cancer immunology, immunotherapy : CII* 2009, 58(7): 1169-1174.
320. Anisimov VN, Sikora E, Pawelec G. Relationships between cancer and aging: a multilevel approach. *Biogerontology* 2009, 10(4): 323-338.
321. Franceschi S, La Vecchia C. Cancer epidemiology in the elderly. *Critical reviews in oncology/hematology* 2001, 39(3): 219-226.
322. Burkle A, Caselli G, Franceschi C, Mariani E, Sansoni P, Santoni A*, et al.* Pathophysiology of ageing, longevity and age related diseases. *Immunity & ageing : I & A* 2007, 4: 4.
323. Pawelec G, Solana R. Are cancer and ageing different sides of the same coin? Conference on Cancer and Ageing. *EMBO reports* 2008, 9(3): 234-238.
324. Miki C, Kusunoki M, Inoue Y, Uchida K, Mohri Y, Buckels JA*, et al.* Remodeling of the immunoinflammatory network system in elderly cancer patients: implications of inflamm-aging and tumor-specific hyperinflammation. *Surgery today* 2008, 38(10): 873-878.
325. Vasto S, Carruba G, Lio D, Colonna-Romano G, Di Bona D, Candore G*, et al.* Inflammation, ageing and cancer. *Mechanisms of ageing and development* 2009, 130(1-2): 40-45.
326. Fulop T, Kotb R, Fortin CF, Pawelec G, de Angelis F, Larbi A. Potential role of immunosenescence in cancer development. *Annals of the New York Academy of Sciences* 2010, 1197: 158-165.
327. Salvioli S, Capri M, Valensin S, Tieri P, Monti D, Ottaviani E*, et al.* Inflamm-aging, cytokines and aging: state of the art, new hypotheses on the role of mitochondria and new perspectives from systems biology. *Current pharmaceutical design* 2006, 12(24): 3161-3171.
328. Mitchell WA, Meng I, Nicholson SA, Aspinall R. Thymic output, ageing and zinc. *Biogerontology* 2006, 7(5-6): 461-470.
329. Larbi A, Dupuis G, Khalil A, Douziech N, Fortin C, Fulop T, Jr. Differential role of lipid rafts in the functions of CD4+ and CD8+ human T lymphocytes with aging. *Cellular signalling* 2006, 18(7): 1017-1030.
330. Pawelec G, Lustgarten J, Ruby C, Gravekamp C. Impact of aging on cancer immunity and immunotherapy. *Cancer immunology, immunotherapy : CII* 2009, 58(12): 1907-1908.
331. Provinciali M, Smorlesi A. Immunoprevention and immunotherapy of cancer in ageing. *Cancer immunology, immunotherapy : CII* 2005, 54(2): 93-106.
332. Blakely CM, Stoddard AJ, Belka GK, Dugan KD, Notarfrancesco KL, Moody SE*, et al.* Hormone-induced protection against mammary tumorigenesis is conserved in multiple rat strains and identifies a core gene expression signature induced by pregnancy. *Cancer research* 2006, 66(12): 6421-6431.
333. Layde PM, Webster LA, Baughman AL, Wingo PA, Rubin GL, Ory HW. The independent associations of parity, age at first full term pregnancy, and duration of breastfeeding with the risk of breast cancer. Cancer and Steroid Hormone Study Group. *Journal of clinical epidemiology* 1989, 42(10): 963-973.
334. D'Cruz CM, Moody SE, Master SR, Hartman JL, Keiper EA, Imielinski MB*, et al.* Persistent parity-induced changes in growth factors, TGF-beta3, and differentiation in the rodent mammary gland. *Molecular endocrinology* 2002, 16(9): 2034-2051.
335. Tsubura A, Uehara N, Matsuoka Y, Yoshizawa K, Yuri T. Estrogen and progesterone treatment mimicking pregnancy for protection from breast cancer. *In vivo* 2008, 22(2): 191-201.
336. Medina D, Kittrell FS. p53 function is required for hormone-mediated protection of mouse mammary tumorigenesis. *Cancer research* 2003, 63(19): 6140-6143.

CHAPTER 2. Specific Aims

Specific Aim 1: Comparatively define the immune microenvironment of the omental fat band (OFB) and the peritoneal serous fluid (PSF) in the homeostatic state.

Rationale: The OFB plays a crucial role in the immunosurveillance of the PC through its function as a secondary lymphoid organ. Further, it is a well-established site of EOC cell seeding and outgrowth following metastasis throughout the PC. The OFB is thought to provide the PC with many of its immune subsets, including B1 cells and some of the free peritoneal macrophages. It is a unique immunological microenvironment. However, its immune profile has not been fully characterized and compared with the PSF that it filters. The PC has long been used as the site for immunizations and metastasis studies due to the ease of injections and the induction of potent immune responses.[1] The cellular composition of the PC is very different from that of organs typically studied to evaluate immune responses, namely the peripheral blood, spleen and lymph nodes. The OFB is a visceral fat depot, a subset of white adipose tissue that is involved in a variety of diseases and metabolic disorders, including cardiovascular disease, insulin dysergulation and certain cancers. Visceral fat depots are thought to act as reservoirs for recruitable leukocyte and progenitor populations that aid in the progression of disease pathogenesis. Currently, intra-abdominal fat depots are used interchangeably when evaluating the role of visceral fat in various diseases. **It is important to understand the *pre-existing* compositional immune profile of these microenvironments within the PC, and how shifting population ratios in the homeostatic state may affect the efficacy of immunotherapies targeted against EOC progression.**

Working Hypothesis: The OFB will contain a resident immune population consistent with its status as a secondary lymphoid organ. Thus, we expect a significant population of B cells, including B1s, as well as T cells, macrophages and monocytes, as previously reported. The peritoneal serous fluid will portray an immune population more indicative of a circulating defense system, with a large proportion of B1 cells, negligible T cells and circulating macrophage populations, as previously reported. The immune compositional profile of the OFB will be a distinct immunomodulatory microenvironment when compared to alternative intra-abdominal fat pads, consistent with its immunoregulatory phenotype, and should be evaluated independently in the context of physiologically and pathologically relevant conditions.

Alternatives: It is possible that all intra-abdominal fat depots will display similar immune compositional profiles, and can be used interchangeably, as has been common practice in the literature. If so, alternative intra-abdominal fat depots should be evaluated following ovarian cancer dissemination to evaluate their role in metastatic growth.

Specific Aim 2. Evaluate the parity-mediated changes in the OFB immune microenvironment in the homeostatic state, and in the tumor microenvironment as a consequence of cancer cell seeding in the PC.

Rationale: EOC is primarily a disease that affects post-menopausal women, and has an extremely high rate of relapse. Parity has been correlated with reduced ovarian cancer incidence, although the molecular mechanisms behind this phenomenon remain unknown. Although various immune cells within OFB milky spots maintain specificity against tumor-associated antigens, or display tumoricidal activities when collected and tested ex vivo, they have become polarized to support a very successful pro-tumorigenic microenvironment through cancer cell initiation of a pro-tumorigenic program. For decades it has been common practice among surgeons to remove the OFB during tumor debulking in an attempt to prevent further EOC metastasis. Due to the asymptomatic nature and late detection of EOC, clinical studies are typically performed when metastasis has already occurred. To determine the molecular mechanisms

behind parity-mediated reduction in ovarian cancer may provide a "protective signature" in this metastatic microenvironment that could be harnessed for the design of cancer therapeutics. **Given the efficiency of tumor cells in providing themselves with a pro-tumorigenic niche, it is important to understand how EOC affects the OFB as a microenvironment, and potentially highlight pro-tumorigenic signaling events that could be targeted and disrupted.**

Subaim 2.1: Determine the age- and parity-related differences in the OFB in the homeostatic state.

Rationale: The success of recently developed immunotherapies targeted against EOC has been somewhat underwhelming in the clinical setting. It has been hypothesized that this may be due to the existence of immunosenescence in the majority of EOC patients, who are post-menopausal. Most immunotherapy studies are performed in young animal models, which may not be the most accurate portrayal of effects in the clinical setting. One study indicated that while three different immunotherapy techniques were effective in providing tumor protection to young mice, these were ineffective in older mice. The three treatment strategies had to be combined to provide any sort of protection. This implies that while immunosenescence is an important factor in the pathogenesis of cancer and must be addressed, it is still possible to reverse or divert pro-tumorigenic signals and induce tumor regression in older patients. Additionally, parous women have a decreased incidence of ovarian and breast cancer development, associated with inherent alterations to mammary tissue in a breast cancer model. This highlights the importance of the pre-metastatic niche in successful tumor development, and indicates a pre-existing microenvironmental profile that is refractory to tumor development. **Therefore, it is crucial to determine the intrinsic age- and parity-related changes in the OFB microenvironment in the homeostatic state in order to define a protective profile that may be harnessed for the development of cancer therapeutics.**

Working Hypothesis: The OFB will display pre-existing age- and parity-specific changes in the immune compositional profile in the homeostatic state.

Alternatives: It is also probable that the mice we chose to use, 12 month old retired breeders, are not yet old enough to be demonstrative of full-blown immunosenescence. However, given the limited availability and high price of older animals, as well as the difficulty in keeping them alive during a long-term study without the development of other ailments, we thought this age group was our most viable option. Additionally, we believe that the 'aged phenotype' is something that develops gradually, so we may be able to use these mature mice to isolate early signaling events in this process.

Subaim 2.2: Determine the changes in the OFB microenvironment after ovarian cancer cell seeding and outgrowth, and the parity-associated changes in tumor development.

Rationale: Ovarian cancer is an aggressive disease that is difficult to treat due to late detection and a high incidence of pre-existing metastasis at the time of treatment. However, epidemiological studies indicate that child-bearing, particularly before the age of 20, provides a significant reduction in the incidence of ovarian cancer. This suggests that it is possible to re-program the pro-tumorigenic niche in a tumor suppressive fashion. The molecular mechanisms behind this phenomenon have not been described, and the impacts on the OFB as the primary site for ovarian cancer metastasis are unknown. **Thus, it is imperative that we evaluate the effects of the "protective parity signature" on tumor growth, as well as its immunomodulatory role on the development of a pro-tumorigenic microenvironment within the OFB.**

Working Hypothesis: Ovarian cancer cell implantation in the peritoneal cavity will result in the development of a pro-tumorigenic niche within the OFB microenvironment, characterized by the influx

and/or polarization of pro-tumorigenic leukocytes. Parity-associated changes to the existing OFB immune microenvironment will provide a niche that is refractory to metastatic growth so that parous mice will have a decreased tumor burden as compared to nulliparous mice, associated with delayed development of the pro-tumorigenic niche previously characterized.

Specific Aim 3. Determine the efficacy of membrane-bound IL-12 immunomodulation following cancer cell seeding and outgrowth in the OFB in a step-wise, kinetic manner.

Rationale: IL-12 has previously been shown to have potent immunostimulatory properties. Briefly, it induces the proliferation and activation of tumor antigen-specific T effector cells, as well as NK cells. In animal and human models it has reduced, and in some cases completely cleared, tumor burden in multiple cancer types. However, clinical trials have been associated with marked toxicity due to the potent inflammatory nature of this cytokine. Thus, a more targeted approach is warranted. Membrane-bound IL-12 has been shown to retain its immunomodulatory properties as compared to the secreted form, inducing CD69 and IFNγ expression in CTLs, and perforin expression in NK cells. The TME is a complex signaling milieu, with a huge variety of pro-tumorigenic populations and signals, all of which have been elucidated in the context of *late stage* disease. However, little is known about the shifting cascade of events that may gradually polarize the TME in this fashion. Moreover, while IL-12 has been tested as a cancer therapeutic in a variety of models, results are again analyzed in the context of late-stage disease, when regulatory and tolerogenic programs are already well underway. **Thus, we propose to induce membrane-bound IL-12 expression in tumor cells and microenvironmental changes in the context of initial metastasis (24 hours post-seeding), early tumor growth (7 days post-seeding) and an established pro-tumorigenic niche (3 weeks post-seeding, which represents end-stage disease in our aggressive ovarian cancer model) in order to study the differences in the overall signaling milieu, and how these changes affect tumor burden.** This evaluation may provide valuable insight into improved treatment opportunities, particularly if combined with improved early detection techniques.

Working Hypothesis: Membrane-bound IL-12 expression will alter the ability of ovarian cancer cells to polarize the microenvironment in a suppressive manner, resulting in increased anti-tumorigenic immune populations like CTLs and M1s, which will slow or halt tumor cell seeding and outgrowth in the OFB. These changes will occur in a step-wise manner, first deactivating tolerogenic immune populations such as Tregs, thus allowing for the influx or re-education of cytotoxic effector cells, such as CTLs and M1s.

Alternatives: Given the widespread assertion that an inflammatory environment propagates a pro-tumorigenic niche, the addition of another potent inflammatory cytokine may have the opposite effect on tumor growth, increasing the growth rate of malignancy. However, given the equally large burden of research describing the immunosuppressive populations present in the tumor microenvironment, and efficacy of IL-12 as a cancer therapeutic, it seems likely that mbIL-12 will have the anticipated result. Additionally, given our repeated assertion that the TME is a complex signaling milieu, and that there are redundant cascades that contribute to the decrease in anti-tumor activity of adaptive and innate effector cells, as well as the increase in regulatory and tolerogenic populations, it is possible that IL-12 treatment will not cause relapse-free disease reduction or clearance. In other words, as it has been postulated that eventual tumor growth is a result of a type of co-evolution of tumor cells alongside tolerogenic immune populations, it is also possible that already seeded tumor cells in the OFB will eventually "evolve" or "learn" (if we really want to anthropomorphize these cells) to circumvent the protection provided by increased IL-12 signaling. In this case, while tumor growth would be slowed, animals would eventually submit to catastrophic tumor burden. However, if this is the case monitoring OFB microenvironmental changes in a kinetic manner may allow us to elucidate the mechanism behind tumor cells overcoming IL-12 treatment, again providing valuable insight into the signaling cascade as a whole, and eventual improvements in treatment regimens. Regardless of the effect on tumor burden, studying the changes in

the signaling microenvironment in its entirety should give us valuable insight into the system as a whole, and its susceptibility to manipulation.

Working Hypothesis: Introduction of ovarian cancer cells into the PC and seeding to the OFB induces stepwise changes to the immune microenvironment that promote a progressively more favorable pro-tumorigenic niche, promoting polarization of TILs to Tregs and circulating monocytes to TAMs.

1. Sorensen EW, Gerber SA, Sedlacek AL, Rybalko VY, Chan WM, Lord EM. Omental immune aggregates and tumor metastasis within the peritoneal cavity. *Immunologic research* 2009, **45**(2-3)**:** 185-194.

CHAPTER 3.

Intra-Abdominal Fat Depots Represent Distinct Immunomodulatory Microenvironments: A Murine Model

Authors: Courtney A. Cohen*[1], Amanda A. Shea*[2], Connie L. Heffron[1], Eva M. Schmelz[2], Paul C. Roberts[1]

*Co-first authors

Affiliations:

1. Department of Biomedical Sciences and Pathobiology, Virginia Polytechnic Institute and State University, Blacksburg, VA, United States

2. Department of Human Nutrition, Foods and Exercise, Virginia Polytechnic Institute and State University, Blacksburg, VA, United States

Full address/email of corresponding author:

Dr. Paul. C. Roberts

Dept. Biomedical Science and Pathobiology

Virginia-Maryland College of Veterinary Medicine, Virginia Tech

Integrated Life Sciences Building

1981 Kraft Drive [0913]

Blacksburg, Va. 24061

Tel: 540-231-7948

Email: pcroberts@vt.edu

**Accepted in PLOSOne

Abstract

White adipose tissue (WAT) is recognized as a diverse endocrine organ involved in energy storage, metabolism, immune function and disease pathogenesis. In contrast to subcutaneous fat, visceral fat (V-WAT) has been associated with numerous diseases and metabolic disorders, indicating specific function related to anatomical location. Although visceral depots are often used interchangeably in V-WAT-associated disease studies, there has been a recent subdivision of V-WAT into "true visceral" and non-visceral intra-abdominal compartments with distinct physiological roles, illustrating a need for depot-specific information. Here, we use FACS analysis to characterize the leukocyte and progenitor populations in the stromal vascular fraction (SVF) from peritoneal serous fluid (PSF), parametrial (pmWAT), retroperitoneal (rpWAT), and omental (omWAT) adipose tissue from seven-month old C57BL/6 female mice (n=10). qRT-PCR was also used to determine individual whole-tissue gene expression profiles. SVF composition displayed significant depot-specific differences between all four microenvironments. PSF SVF contained >99% $CD45^+$ leukocytes, while omWAT contained a smaller percent, but still almost two-fold more leukocytes than pmWAT and rpWAT (75%, 38% and 38% respectively; $p<0.01$). PmWAT was composed primarily of macrophages, whereas rpWAT more closely resembled omWAT, denoted by high levels of B1-B and monocyte populations. Thus, intra-abdominal fat pads represent independent immunomodulatory microenvironments and should be evaluated as distinct entities with unique contributions to physiological and pathological processes.

INTRODUCTION

White adipose tissue (WAT) is the largest endocrine organ in the body, comprising up to 45% of total body composition in obese individuals (BMI≥30). Once thought to be a passive reservoir for excess energy storage, WAT is increasingly recognized for its role in metabolism, immune and endocrine function, thermoregulation, and tissue repair[1]. Its function in both physiological and pathological processes may be influenced by either tissue resident adipocytes or the stromal vascular fraction (SVF), which includes leukocytes, mesenchymal stem cells, adipocyte progenitors, fibroblasts, and endothelial cells[2]. Recent studies indicate functional differences in adipose tissue depots related to anatomical location, specifically between subcutaneous fat (S-WAT) and visceral fat (V-WAT). While expansion of S-WAT is associated with improved insulin sensitivity and decreased risk of type 2 diabetes, V-WAT expansion is linked to an increased risk of cardiovascular disease, glucose dysregulation, hypertension, and certain cancers[3, 4]. Functional and secretory differences between V-WAT and S-WAT include increased lipolysis and expression of inflammatory molecules, and decreased angiogenesis, production of adiponectin and leptin, and responsiveness to insulin[5]. Although V-WAT comprises only about 10% of total body fat, it is strongly correlated with increased morbidity and mortality[5, 6].

Recently, V-WAT has been further classified based on drainage, distinguishing "true" V-WAT depots, e.g. omental and mesenteric fat drained by the portal vein, from intra-abdominal ("non-visceral") depots, drained by the inferior vena cava, including perigonadal (parametrial in females, epididymal in males), retroperitoneal, and perirenal fat[7, 8]. The *portal theory* suggests that exaggerated hepatic delivery of free fatty acids and pro-inflammatory cytokines originating from V-WAT drained by the hepatic portal vein in obese individuals, is responsible for insulin resistance and metabolic deterioration[9]. This has been important in demarcating depots that may be more associated with the development of metabolic syndrome. However, even with this delineation, studies comparing S-WAT and V-WAT are inconsistent in their use of V-WAT. Different fat pads are often used interchangeably although distinct depots are reportedly unique in tissue dynamics (hypertrophic versus

hyperplastic response to excess calories), adipokine release, hormonal responses, vascularization, innervation, and abundance of non-adipocyte components[7, 8]. Due to this diversity, it is possible that individual fat pads play differential roles in the pathogenesis of specific diseases. Thus, it is critical that the inherent differences between intra-abdominal fat depots are properly characterized instead of designating one to represent the contribution of V-WAT as a whole.

Although there is no human counterpart, perigonadal fat is often utilized in murine studies of V-WAT-associated diseases, primarily due to its ease of access and relative abundance[8]. However, the use of this depot as representative of all V-WAT may be not provide a complete picture and makes drawing depot-specific conclusions difficult. A more comprehensive characterization of each depot is warranted. In support of this, one study demonstrated that differences in fat pad composition and functionality endure after transplantation to different anatomical sites, indicating that other factors, such as SVF content, may contribute to functional heterogeneity[10]. While many studies focus on WAT transcriptome, proteome or secretome, limited information exists on the cellular composition of individual depots. Given the metabolic and immunological relevance of V-WAT, there is clearly a need for elucidation of *depot-specific* SVF composition and gene expression profiles in order to provide a more comprehensive understanding of these distinct microenvironments within the peritoneal cavity. Here, we utilized fluorescence-activated cell sorting (FACS) to comparatively characterize the SVF of parametrial WAT (pmWAT), retroperitoneal WAT (rpWAT), omental WAT (omWAT), and the peritoneal serous fluid (PSF), to determine whether they represent unique microenvironments. We also performed qRT-PCR to assess differences in the gene expression profiles. Our results suggest that pmWAT, rpWAT, omWAT, and PSF represent distinct microenvironments with unique cellular composition in the homeostatic state, supporting our hypothesis that distinct fat depots possess inherent properties that may differentially impact disease states.

METHODS AND PROCEDURES

Ethics Statement

Mice were used in accordance with the guidelines of the Virginia Tech (VT) Institutional Animal Care and Usage Committee (IUCAC). Animal work in this study was approved by VT's IACUC (animal protocol # 10-099 HNFE).

Animals

Female C57/BL6 mice (Harlan Laboratories) were housed five per cage in a controlled environment (12 hour light/dark cycle at 21°C) with free access to water and food (18% protein rodent chow, Teklad Diets). Mice were sacrificed at 24 weeks of age (27g average body weight) by CO_2 asphyxiation.

Adipose tissue and peritoneal serous fluid harvest

OmWAT, pmWAT and rpWAT were harvested from each mouse, weighed, and rinsed with calcium- and magnesium-deficient phosphate buffered saline ($PBS^{-/-}$). OmWAT was attached posteriorly to the stomach, connecting to the pancreas, and running down to the anterior of the spleen[11] OmWAT samples were also tested for buoyancy to ensure there was no pancreatic contamination. PmWAT, the largest fat depot, was located directly under the muscle wall on the dorsal side of the abdomen and attached to the uterine horns. RpWAT was the denser fat depot attached dorsally to the peritoneum, directly behind the kidney. Each tissue was then processed for FACS or placed into RNAlater (Qiagen) and stored at -80°C. Resident peritoneal cavity cells were collected via peritoneal lavage with 5ml of $PBS^{-/-}$. The effluent was centrifuged, subjected to erythrocyte lysis (155mM NH_4Cl, 10mM $KHCO_3$, 0.1mM EDTA)[2], and further processed as described below.

Tissue Digestion

SVF from individual fat depots (n=10) were isolated from digested tissue[12, 13] with minor modifications to improve yields. OmWAT was digested in GKN-buffer containing 1.8mg/ml Type IV collagenase, 10% FBS, and 0.1mg/ml DNase. The pmWAT and rpWAT digest buffer included a 1:1 ratio of Krebs-Ringer bicarbonate buffer and collagenase solution (1mg type I collagenase, 10mg BSA, and 2mM $CaCl_2$ in 1ml PBS). Following digest at 37°C for 45 min, cells were passed through a 40µm cell strainer, and erythrocytes were lysed.

FACS Analysis

Cell suspensions were washed in flow buffer (2% BSA in $PBS^{-/-}$), blocked with Fc block (BD Biosciences) for 10 minutes at 4°C, rinsed and subsequently incubated with fluorochrome-labeled antibody combinations (available upon request) for 20 min at 4°C. Fluorochrome-labeled antibodies specific for mouse CD45, CD11b, CD11c, F4/80, Ly6C, MHCII, CD34, CD31, CD4, CD44, CD62L, CD25, CD69, B220, CD19, NK1.1, CD73, Flk-1 and Ly6G were obtained from eBioscience (San Diego, CA). CD105 and Ly6a/e antibodies were obtained from BioLegend (San Diego, CA) and Ly6G, CD3, CD8, CD80, CD117 and MR antibodies were obtained from BD Biosciences (San Jose, CA). Prior to analysis, cells were washed twice and resuspended in $PBS^{-/-}$ with propidium iodide for dead cell exclusion. FACS was performed on a FACSAria (BD Biosciences) and data was analyzed using Flowjo (TreeStar) software.

RNA extraction

WAT was homogenized in Qiazol (Qiagen), and RNA was purified using an RNeasy Lipid Tissue Kit (Qiagen), according to manufacturer's instructions. RNA concentration was determined using a NanoDrop1000 spectrophotometer.

Quantitative real-time PCR

RNA (n=6 per tissue) was subjected to the iScript cDNA synthesis system (Biorad) according to manufacturer's protocol. qRT-PCR was performed with 12.5ng cDNA per sample using gene-specific SYBR Green primers (primer sequences are available upon request) designed with Beacon Design software. SensiMix SYBR and Fluorescein mastermix (Quantace) was used in a 15μL reaction volume. qRT-PCR was performed for 42 cycles at 95°C for 15 sec, 58-60°C for 15 sec, and 72°C for 15 sec, preceded by a 10 min incubation at 95°C on the ABI 7900HT (Applied Biosystems). Melt curves were performed to ensure fidelity of the PCR product. The housekeeping gene was L19 and the ddCt method[14] was used to determine fold differences.

Statistical Analysis

Data was expressed as mean ± standard error of mean (SEM). FACS and qRT-PCR data were analyzed using a one-way ANOVA coupled with a Tukey Post-hoc test in Graphpad Prism. Differences were considered statistically significant at $p<0.05$.

RESULTS

To date, studies investigating the contribution of V-WAT to various diseases have often used intra-abdominal fat pads interchangeably. Considering the reported differences between S-WAT and V-WAT, we believe it is important to determine whether intra-abdominal fat pads are indeed similar with respect to their SVF cellular composition, or represent unique signaling microenvironments that may differentially impact intra-peritoneal processes. Here, we use pmWAT due to its widespread application in murine studies, omWAT due to its classification as a "true" visceral fat and importance in immunological surveillance, and rpWAT due to its characterization as a non-visceral intra-abdominal fat depot with a human counterpart.

Seven-month old female C57/BL6 mice were chosen to match the endpoint of many WAT studies that place young mice on specialized treatment regimens for several weeks or months[8, 15, 16, 17, 18]. This age also allows sufficient fat accumulation for comprehensive FACS analysis of the SVF. Additionally, female mice were utilized because of gender-related differences in adipose accumulation and the importance of omWAT in gynecological diseases, such as ovarian cancer[11, 16].

Fat depot size and cellularity

As expected, pmWAT was the largest fat depot while omWAT represented the smallest (Figure 3.1a). Despite its significantly smaller size, omWAT yielded total numbers of SVF cells similar to pmWAT, whereas rpWAT had a significantly smaller SVF population ($p<0.0001$) (Figure 3.1b). Thus, 20 times more SVF cells *per milligram of tissue* were isolated from omWAT, as compared to pmWAT ($p=0.009$) or rpWAT ($p=0.01$) (Figure 3.1c).

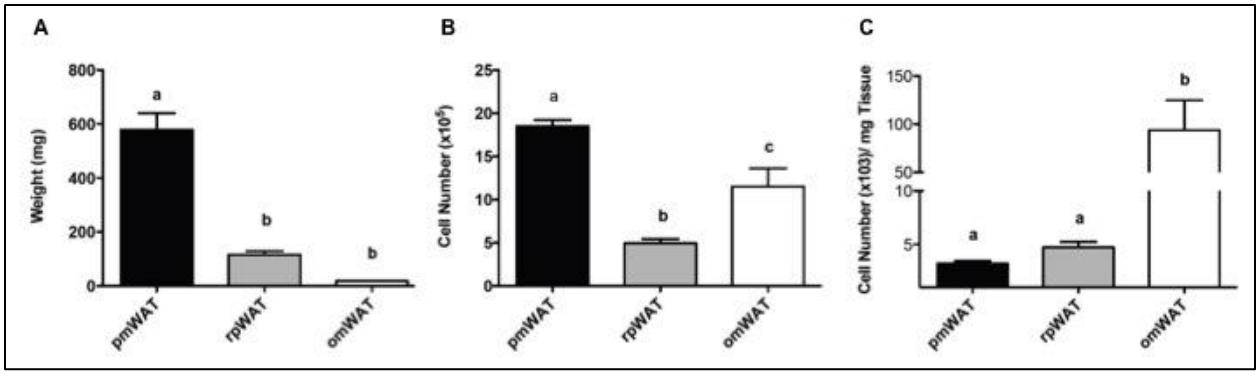

Figure 3.1. Intra-abdominal fat depots display variable stromal vascular fractions. **(a)** Whole tissue weight. **(b)** Total number of SVF cells isolated from the digestion of each tissue. **(c)** Number of SVF cells isolated from the digestion of each milligram (mg) of adipose tissue. pmWAT; parametrial WAT, rpWAT; retroperitoneal WAT, omWAT; omental WAT. [a,b,c] Unlike letters indicate significance, $P < 0.05$.

Fat depot SVF characterization

Individual fat depots were characterized via FACS analysis to identify depot-specific differences. PSF was included as an established immunologically active microenvironment present within the peritoneal cavity[19, 20]. Leukocyte subsets were identified based on well-defined surface markers (Figure 3.2). First, viable cells (identified via propidium iodide exclusion) were separated into $CD45^+$ leukocytes and $CD45^-$ stromal constituents. The $CD45^+$ population was subsequently separated into R1 (lymphocyte) and R2 (monocyte/granulocyte) gates based on forward/side scatter (Figure 3.2a). T-lymphocyte subsets within the $CD3^+$ fraction (R1) were further separated into $CD4^+$ T-helper (T_h) cells, $CD8^+$ T-cytotoxic (T_c) cells, $NK1.1^+$ natural killer T-cells (NKT), or $CD4^-CD8^-$ double-negative (DN) cells (Figure 3.2b). $CD19^+$ B-cells, distributed within both the R1 and R2 gates, were gated into B1 ($B220^{lo/+}CD11b^+$) and B2 ($B220^{lo/+}CD11b^-$) subsets (Figure 3.2c). Monocyte/granulocyte populations (R2) were classified based on CD11b, CD11c and F4/80 staining, followed by analysis of additional surface markers (Ly6C, Ly6G, mannose receptor [MR], CD80, CD69 and CD93) (Figure 3.2d).

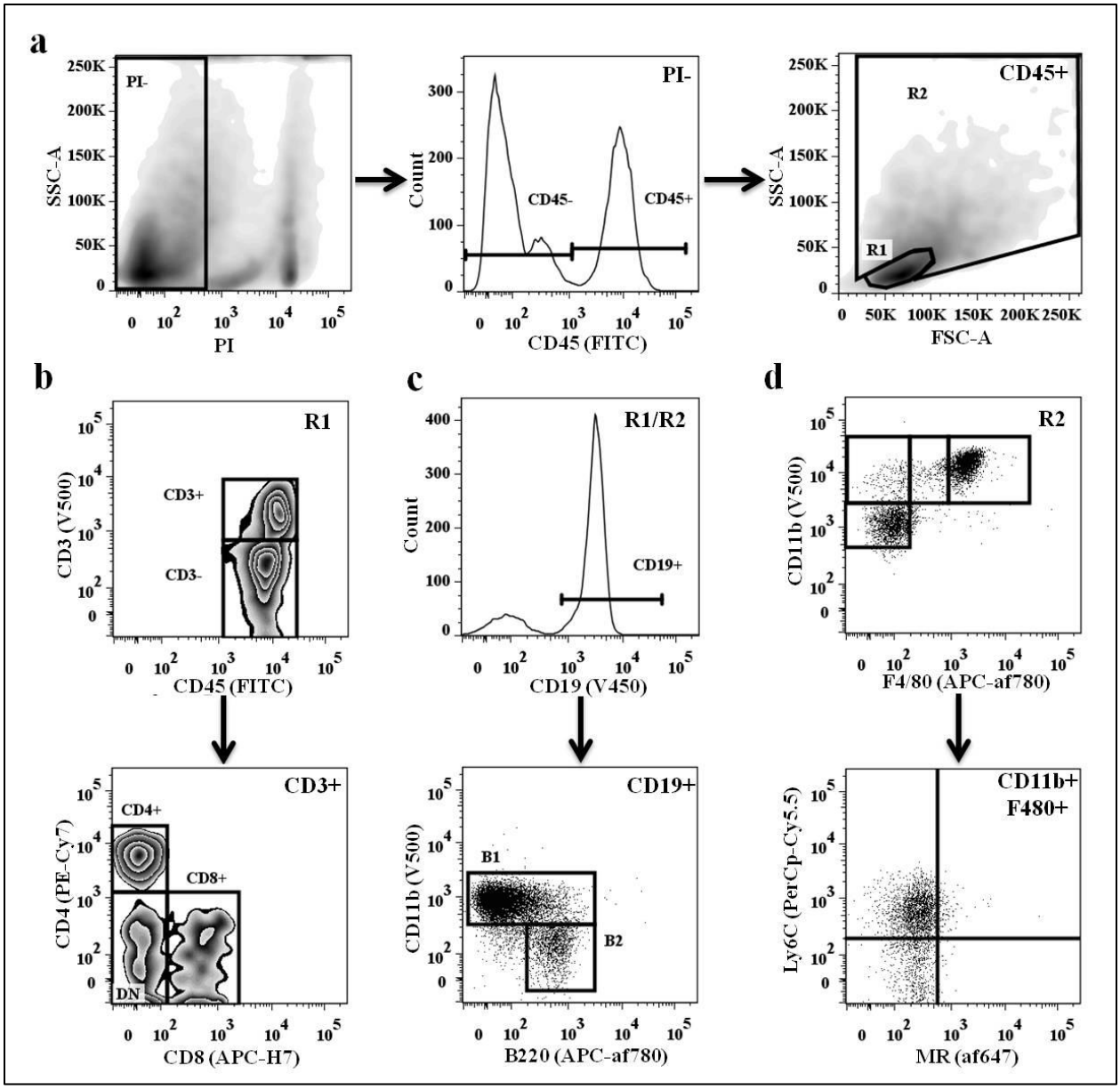

Figure 3.2 FACS analysis gating strategy. **(a)** Digested tissue samples were subjected to PI live/dead cell exclusion, $CD45^+$ leukocytes divided into R1 (lymphocytes) and R2 (mono-, granulocytes) gates based on forward/side scatter followed by doublet exclusion. **(b)** $CD3^+$ T cells from R1 were further subclassified as either $CD4^+$ T_H, $CD8^+$ T_C or DN (double negative). **(c)** $CD19^+$ B cells from R1 and R2 were further subclassified into $CD11b^+$ B1 or $CD11b^-$ B2. **(d)** Monocytic populations from R2 classified based on CD11b, F4/80 and CD11c (not shown) staining, further subdivided based on activation markers.

Markers defining specific populations and distribution of leukocyte subsets within the respective fat pads are detailed in Figure 3.3 and Supplementary Table S3.1. The compositional profiles of individual fat depots were clearly different, supporting the hypothesis that each fat depot is a unique

microenvironment harboring distinct immune cell populations. All three fat depots contained a large $CD45^-$ population within the SVF, whereas the PSF was limited to $CD45^+$ leukocytes (99.1%). Consistent with its role as a secondary lymphoid organ, omWAT contained a twofold higher $CD45^+$ population than pmWAT and rpWAT ($p<0.001$).

Overall Distribution

Of total compartmental leukocytes, pmWAT contained the highest proportion of macrophages (Mθs) (45.2%), with smaller populations of B-cells (12.9%), T-cells (8.2%) and monocyte subsets (2.8%) (Figure 3.3, Supplementary Table S3.1). The immune composition of rpWAT displayed distinct similarities (larger B1- and dendritic cell (DC) and monocyte populations) to omWAT whereas T- and natural killer (NK) cell frequencies (7.3%; 3.5%) more closely matched those of pmWAT, its non-visceral counterpart. OmWAT had proportionally more T-cells (21.5%), DCs (19.1%) and B-cells (35.5%) than pmWAT or rpWAT (Figure 3.3). Confirming previous reports[19], PSF contained a large proportion of B1-cells (38.1%), Mθs (21.0%) and DCs (8.7%), consistent with ongoing immunosurveillance in the peritoneal cavity (Figure 3.3, Supplementary Table 3.1).

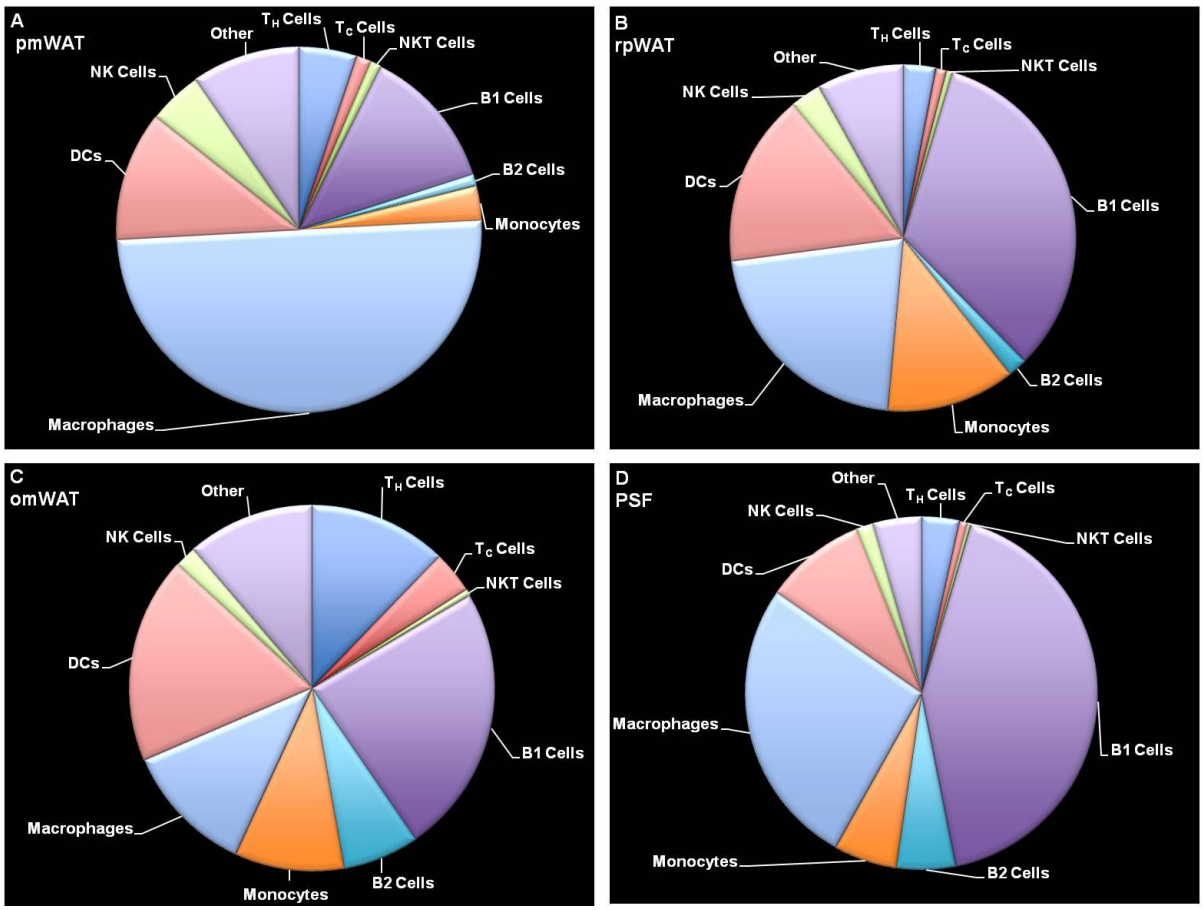

Figure 3.3 Intra-abdominal fat depots display unique leukocyte compositional profiles **(a)** pmWAT, **(b)** rpWAT, **(c)** omWAT, and **(d)** PSF. Subsets defined as described. Macrophages: $CD11b^{+}F480^{lo/+}$; DCs: $CD11c^{+}CD11b^{lo/+}$; NK cells: $CD11b^{+/-}NK1.1^{+}$; T_H cells: $CD3^{+}CD4^{+}$; T_C cells: $CD3^{+}CD8^{+}$; NKT cells: $CD3^{+}NK1.1^{+}$; B1 cells: $CD19^{+}B220^{lo/+}CD11b^{+}$; B2 cells: $CD19^{+}B220^{lo/+}CD11b^{-}$; Monocytes: $CD11b^{lo/+}F480^{-}$; Other: T_{regs} ($CD3^{+}CD4^{+}CD25^{+}$), undetermined T cells ($CD3^{+}CD4^{-}CD8^{-}NK1.1^{-}$), myeloid precursors ($R1,CD3^{-}B220^{-}NK1.1^{-}CD11b^{hi}$), PMNs ($CD11b^{+}Ly6G^{+}Ly6C^{+}$), and PreBoMs ($CD19^{+}CD11b^{hi}B220^{lo}F480^{+}CD93^{+}CD69^{+}$).

Lymphocyte Characterization

OmWAT contained the highest proportion of T-cells, consistent with its role in antigen presentation and development of cell-mediated responses[21]. This corresponds to high expression of *Ccl21*, a chemoattractant important in the homing of T-cells to lymphoid organs. PmWAT and rpWAT had threefold fewer T-cells ($p<0.0001$) than omWAT, although the T_h:T_c ratio in all four microenvironments was 4:1. There were no significant depot-specific differences within the memory ($CD44+/CD62L^{+/-}$) or naïve ($CD44^{-}/CD62L^{+}$) T_h or T_c subsets (data not shown). The proportion of NKT-cells was significantly lower in PSF than all fat depots ($p<0.001$). Interestingly, the majority (>60%) of NK-cells within all four

compartments were $CD94^{hi}$, which has recently been associated with increased proliferation, production of IFNy, and target cell lysis[22]. Further, the $CD27^{hi}$ subset of mature NK (mNK) cells in omWAT was twofold higher ($p<0.001$, data not shown) than the other microenvironments. CD27 expression has been linked to increased responsiveness to chemokines and interactions with DCs, again consistent with the role of omWAT as a major peritoneal immunosurveillance organ[23].

Monocyte/Granulocyte Characterization

Within the R2 gate, four populations based on relative CD11b and F4/80 expression were discernible. Previous reports have described two functionally distinct macrophage subsets within the PSF: the "large peritoneal macrophages" (LPMs), named for their increased forward/side scatter (predominant in the homeostatic state), and "small peritoneal macrophages" (SPMs) which increase in number following LPS stimulation[24]. The largest R2 population present within the PSF was the $CD11b^{+}F4/80^{+}$-LPMs, (61.7%), followed by $CD11b^{+}F4/80^{lo}$-SPMs, and $CD11b^{+}F4/80^{-}$- (I) and $CD11b^{lo}F4/80^{lo}$-monocyte (II) populations present at 8.3%, 3.5%, and 23.5%; respectively (Figure 3.4 a,b).

In contrast, the predominant R2 population in pmWAT was SPMs (77.7%), with minor populations of LPMs (7.0%) and monocytes (I and II) (7.6%; 5.4%). Similarly, in rpWAT the SPM population was predominant (42.4%), with LPMs representing only 5.7% of total cells within the R2 gate. However, the monocytic (I and II) subsets represented a significant proportion (31.7%, and 17.1%; respectively) of the R2 gate. The omWAT R2 composition was also defined by a predominant SPM subset (30.9%), with the LPMs and monocytes (I and II) comprising 3.1%, 27.9%, and 34.6%; respectively.

A CD80/MR expression profile was used to evaluate depot-specific differences in macrophage activation status. SPMs residing within PSF and omWAT expressed CD80, whereas pmWAT and rpWAT SPMs were $CD80^{-}$. MR expression was only noted in SPMs isolated from PSF, omWAT and rpWAT (Figure 3.4c). This further suggests that depot-specific factors inherently contribute to activation or differentiation of their inherent SVF leukocytes.

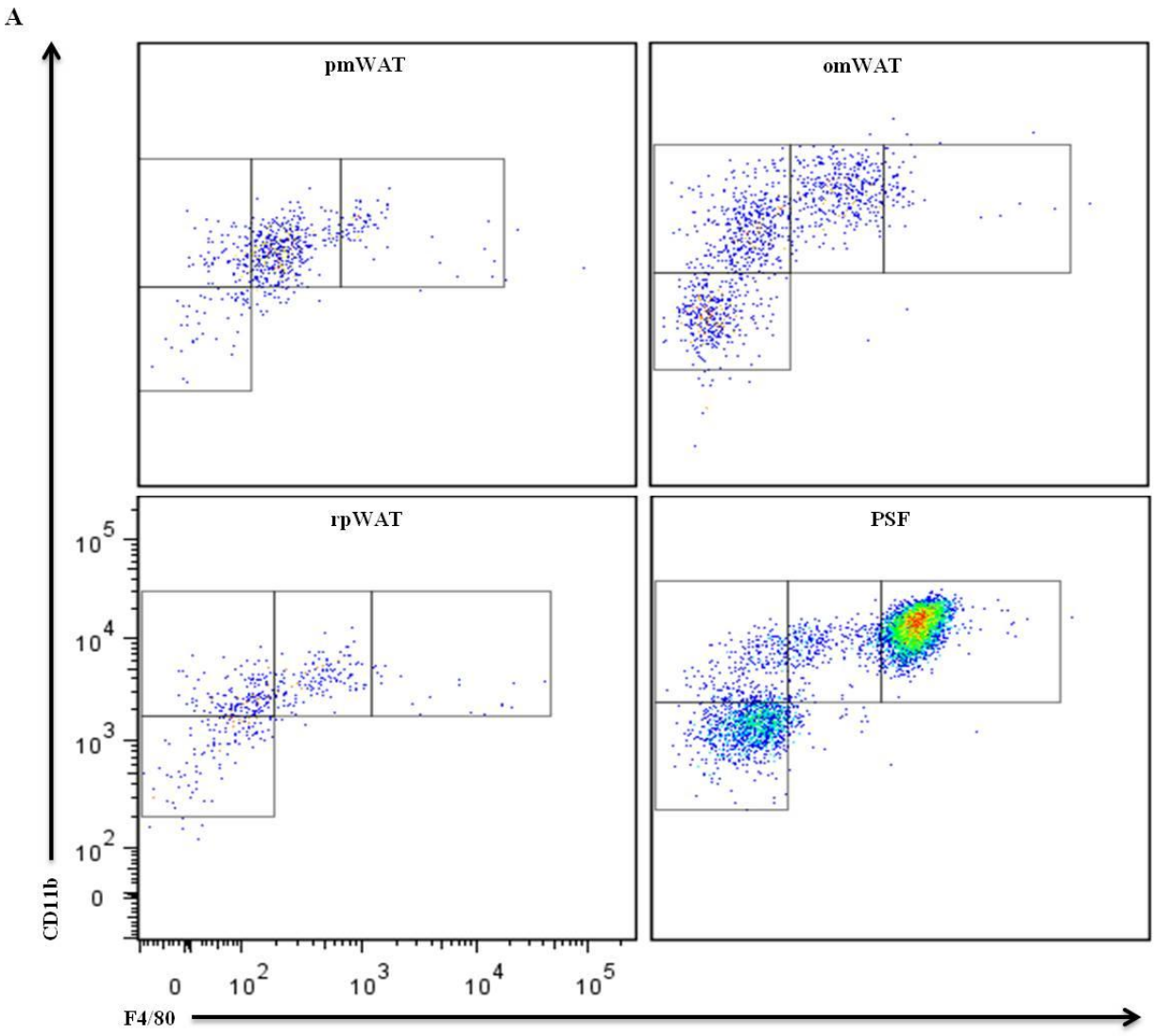

Figure 3.4a. FACS analysis monocytic subset gating strategy. **(a)** pmWAT, **(b)** rpWAT, **(c)** omWAT, **(d)** PSF

B

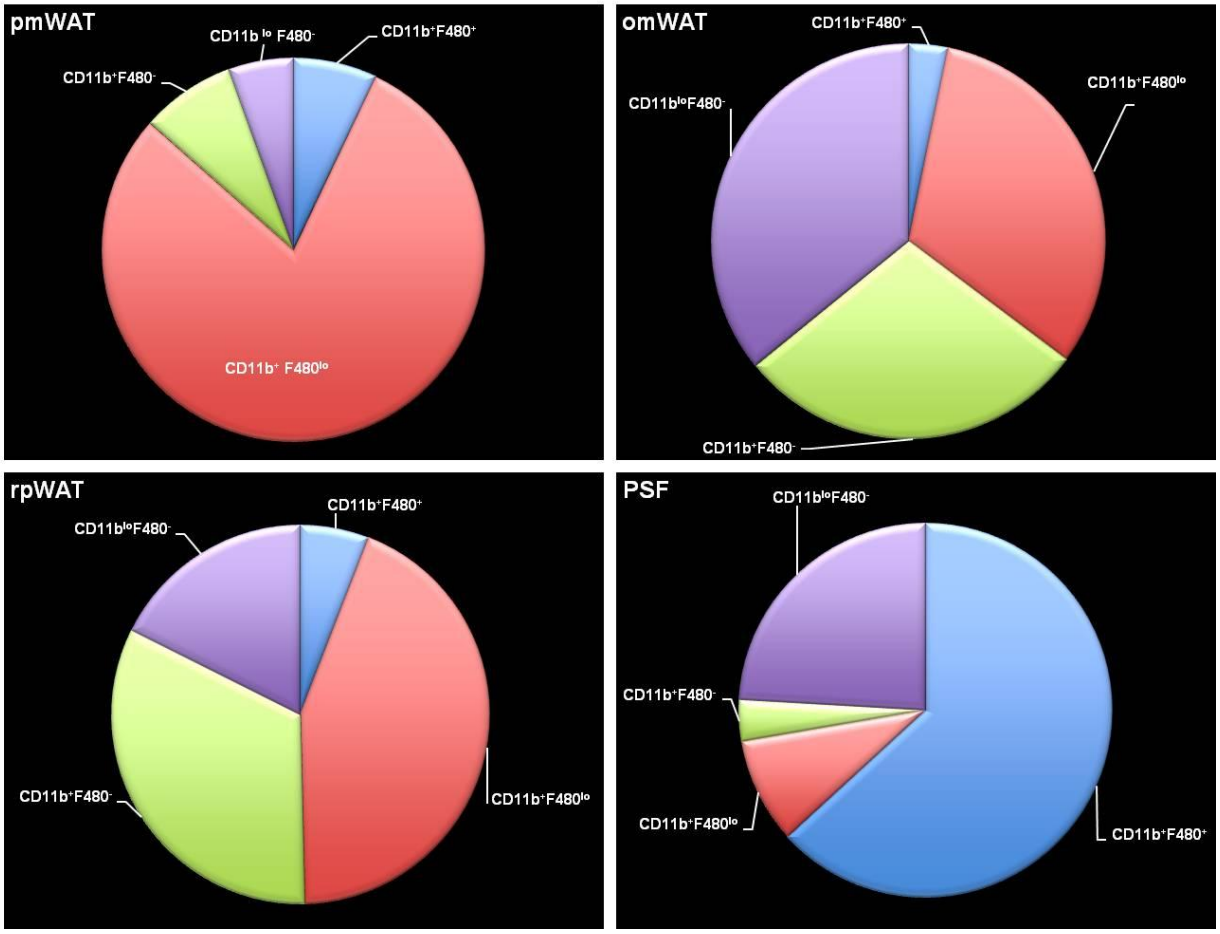

Figure 3.4b. Intra-abdominal fat depots display unique monocytic subset ratios. **(a)** pmWAT, **(b)** rpWAT, **(c)** omWAT, **(d)** PSF

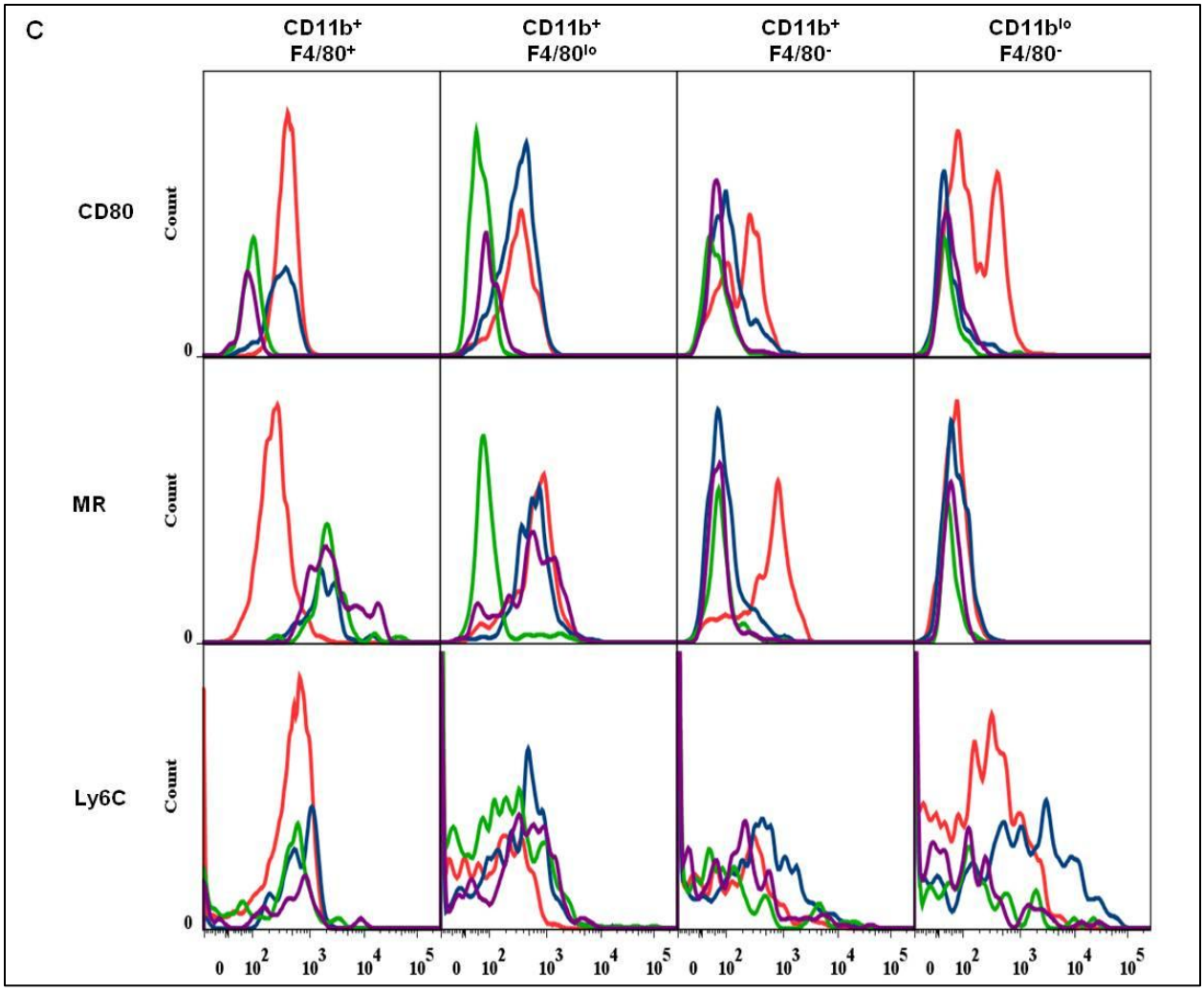

Figure 3.4c. Intra-abdominal fat depot monocytic subsets display depot-specific activation status. **(a)** pmWAT, **(b)** rpWAT, **(c)** omWAT, **(d)** PSF

Key
pmWAT
rpWAT
omWAT
PSF

PreBoMs

During analysis, a small, distinct $CD45^{+}$ cell population (0.7%) was identified within the PSF that was not present in the fat depots. We refer to this subset as "PreBoMs" (pre-B or -macrophages) due to their expression of unique and potentially novel surface markers (Figure 3.5). These cells were $CD19^{+}B220^{lo/+}$, expressed high levels of CD11b and were found within the R2 gate, implying a more

granular phenotype. Additionally, they expressed CD93, a premature B-cell marker, and CD69, an early activation marker. Similar to the age-associated and IL-10-producing B-cells reported recently[25, 26], preBoMs were $CD1d^+$ and $CD5^+$. However, they also expressed F4/80, a mature macrophage marker. We were unable to evaluate CD11c expression within this population to confirm if these cells are one of the aforementioned novel B-cell subtypes, or a new subset residing within the peritoneal cavity. Because of the importance of innate-like B-cell subsets in peritoneal immunosurveillance, it needs to be determined whether this subset plays a role in metabolic disorders and peritoneal diseases.

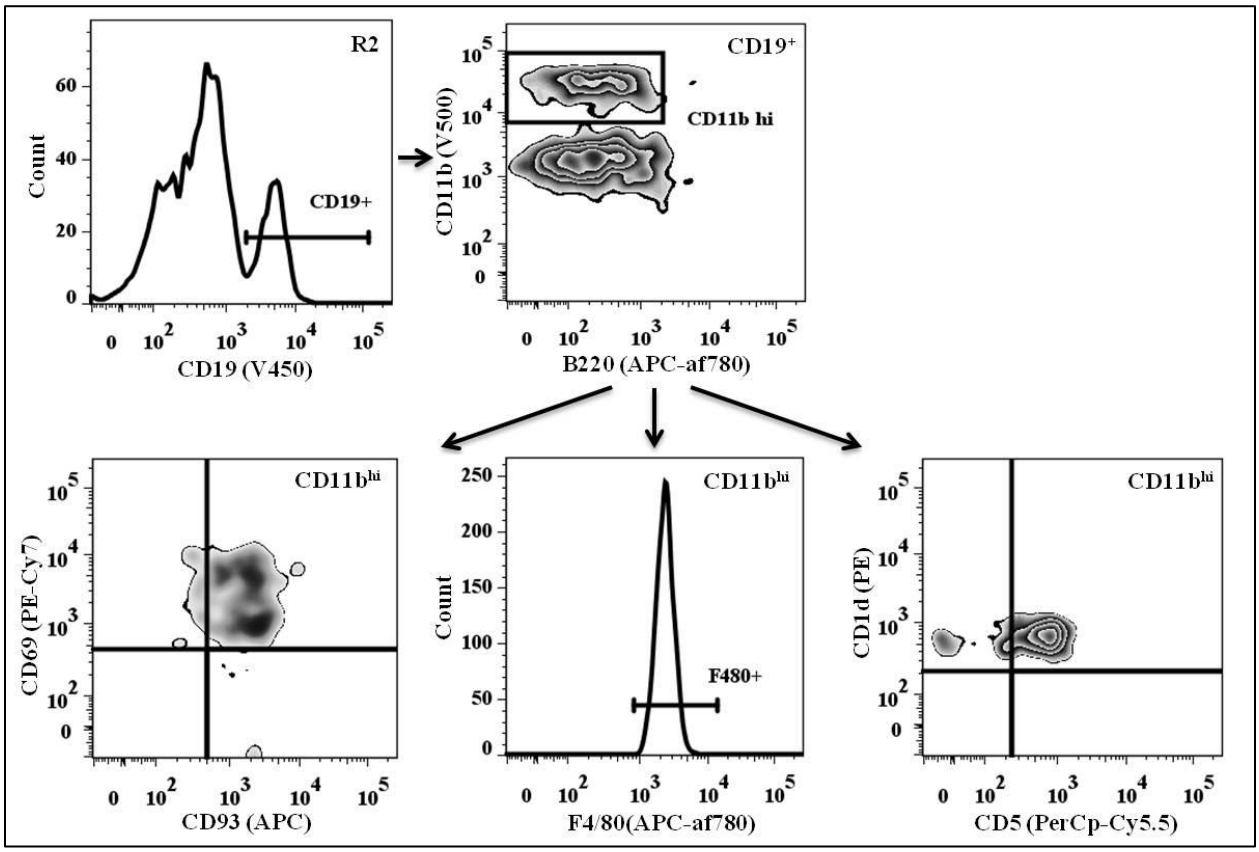

Figure 3.5. PSF contains an undefined population of leukocytes with macrophage, B cell and progenitor markers. Found within the R2 gate, they are referred to as preBoMs (pre-B or –macrophage cells) due to $CD19^+CD11b^{hi}F480^+CD93^+CD69^+CD1d^+CD5^+$ phenotype. This subset was not found in WAT.

Progenitor/Stem Populations

We also examined the prevalence of stem and progenitor cells as they may contribute to microenvironmental signaling and tissue-specific responses to energy. Additionally, they may be

recruited and educated to participate in tissue repair and re-organization and may contribute to various disease states. Figure 3.6a provides an overview of some notable progenitor markers present on $CD45^-$ cells within pmWAT and omWAT. RpWAT did not contain a sufficient SVF content for analysis of both immune and progenitor populations in this tissue.

CD34, CD73, CD105, Sca1, CD31, and Flk1 were all differentially expressed in pmWAT and omWAT ($p<0.05$) (Figure 3.6a). Of note, $CD45^-CD105^+CD73^+$ mesenchymal stem cells (MSCs)[27] were a more prominent percentage of the SVF in omWAT ($p<0.0001$), while $CD45^-Sca1^+CD34^+$ adipocyte precursor cells (APCs)[28] and $CD45^-CD105^+CD31^+Sca1^+CD117^+$ endothelial progenitor cells (EPCs)[29] were a higher percentage in pmWAT (both $p<0.0001$). However, based on total cell numbers, pmWAT contained a greater number of all three subsets due to the higher proportion of $CD45^-$ cells within the SVF (61.9% versus 24.5% respectively, $p<0.001$) (Figure 3.6b). Thus, stem and progenitor populations may also contribute to depot-specific differences between intra-abdominal adipose tissues.

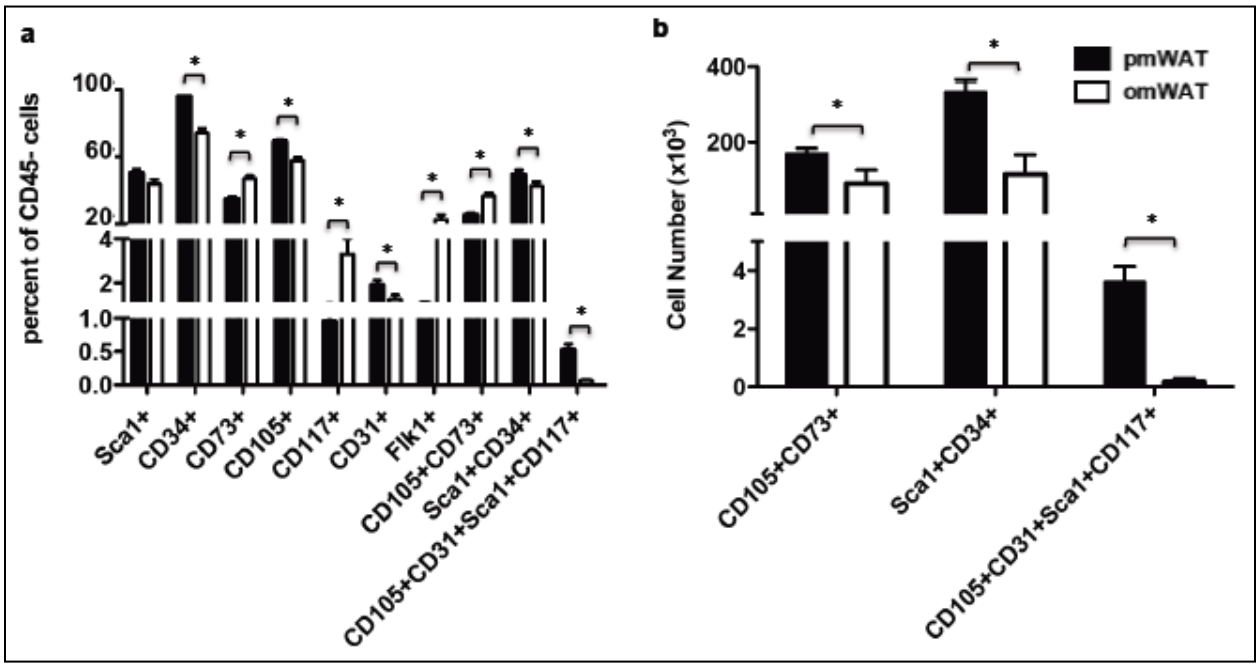

Figure 3.6. Intra-abdominal fat depots display unique progenitor subsets. **(a)** Percentage of CD45 negative cells that are positive for markers shown. **(b)** Total number of SVF cells positive for selected markers in pmWAT and omWAT.

Fat depot specific mRNA expression profile

qRT-PCR was performed to more extensively characterize the overall adipose tissue signaling milieu in these unique microenvironments. It is important to note that expression patterns represent the tissue as a whole (except in PSF), and thus are reflective of both adipocytes and SVF. A panel of inflammatory mediators, angiogenesis-associated molecules, adipokines and lipolysis-associated enzymes were used to provide an overview of genes that may contribute to depot-specific differences.

RpWAT and pmWAT exhibited highly similar mRNA expression profiles (Figure 3.7, Table 2), potentially due to the prevalence of adipocytes and $CD45^-$ cells. In contrast, a significant ($p<0.05$) upregulation of cytokines (*Il-1b*, *Il-2*, *Il-10*) and chemokines (*Ccl2*, Ccl5, *Ccl7*, *Ccl19*, *Cxcl1*, *Cxcl2*, *Cxcl10*, *Cxcl13*) was observed in omWAT. While this may be due in part to the large resident leukocyte population, it may also be required for active recruitment and continual maintenance of high leukocyte numbers. OmWAT also expressed significantly higher levels of *Apoe*, and lower levels of *Adipoq*, *Agt*, and *Lpl* as compared to pmWAT and rpWAT, indicating differences in lipid homeostasis regulation. Additionally, omWAT displayed increased *Hif1a* expression, which may be the result of chronic hypoxia[11]. However, this was not associated with a concomitant increase in *Vegfa*, perhaps because *Vegfa* was already highly expressed.

PSF, which was comprised almost exclusively of $CD45^+$-leukocytes, exhibited an mRNA expression profile similar to omWAT, denoted by decreased expression of *Tnfa* and *Il5*, and increased expression of *Ccl5, Cxcl1, Cxcl2, Cxcl13*, and *Tgfb* as compared to pmWAT. However, PSF expression of *Csf1, Ifng, Rorc, Il4, Ccl4, Ccl7, Ccl21, Cxcl12, Vegfa, C3*, and *Nos3* were significantly lower than all fat depots. Additionally, *Il2, Il10, Ccl19*, and *Cxcl10* were significantly higher($p<0.05$) in omWAT, but were significantly lower($p<0.05$) in PSF, as compared to pmWAT. As anticipated, of the three fat depots PSF was most similar to omWAT, which acts as its filtration system. However, as PSF is composed of primarily leukocytes, the cellular components and interactions among cell types in the two microenvironments are very different, resulting in unique expression profiles.

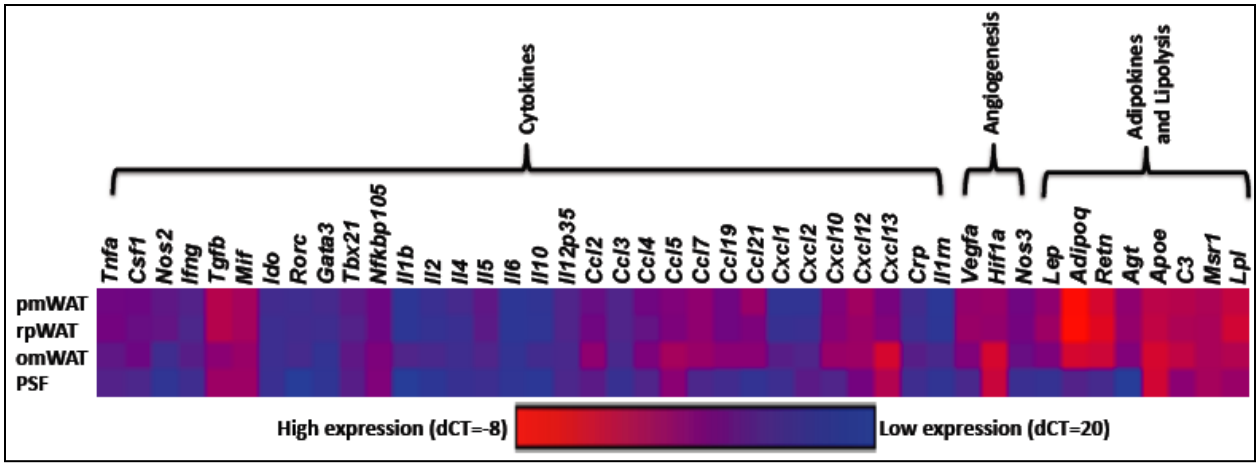

Figure 3.7. Gene expression analysis of intra-abdominal fat depots. Expressed as dCT, normalized to L-19.

DISCUSSION

Adipose tissue is a highly active and functionally diverse endocrine organ that has been associated with various metabolic disorders and certain cancers[1, 5, 6], especially in the case of V-WAT. However, the exact contribution of individual V-WAT depots to physiologic and pathologic functions is poorly understood. Here, we characterized SVF composition and homeostatic gene expression profiles of three intra-abdominal fat pads to determine depot-specific differences, as this may critically impact their functionality. This study highlights the unique immune profile of intra-abdominal fat depots and supports our hypothesis that they may each have distinct roles in biological functions and disease pathogenesis and thus should be evaluated independently.

In agreement with the previous designation of pmWAT and rpWAT as non-visceral intra-abdominal fat pads, the initial compositional profile of leukocytes based on lymphocyte (R1) versus monocyte/granulocyte (R2) fractions revealed an identical 1:2 ratio, while omWAT and PSF displayed a ratio of 3:2. This indicates that lymphocytes are the predominant leukocyte population in omWAT and PSF, while the monocytes/granulocyte fraction is dominant in pmWAT and rpWAT. However, upon further evaluation, high numbers of B1-cells were found within the R2 gate of rpWAT. Although the R1:R2 ratios of pmWAT and rpWAT are very similar, when expressed as a proportion of total T- and B-cells, the immune cell composition of rpWAT more closely resembles that of omWAT and PSF. This was

unexpected as the omWAT is considered "true" V-WAT while rpWAT has been described as a non-visceral intra-peritoneal fat pad.

B1-lymphocytes play an important role in immunosurveillance in the peritoneal cavity and are considered "innate-like" B-cells, possessing pattern recognition receptors to conserved bacterial and viral epitopes[30]. In naïve animals, there is a constant flux of B1-cells between omWAT and the PSF. However, their presence in other intra-abdominal fat pads has not been reported. Unexpectedly, we found a large proportion of B1-cells in rpWAT, comparable to PSF and higher than omWAT. Additionally, rpWAT expressed higher levels of *Il5*, a stimulator of B-cell growth and immunoglobulin secretion[31], than omWAT. In concordance with FACS data, qRT-PCR indicated constitutively high expression of *Cxcl13*, a chemoattractant for B1-cells[32], in all four microenvironments. Together, this suggests that the rpWAT may serve a yet undefined function in peritoneal B-cell immunomodulation.

An unexpected finding during the course of this study was the appearance of $CD19^{+}F4/80^{+}B220^{lo}CD11b^{hi}CD1d^{+}CD5^{+}D93^{+}CD69^{+}$ cells, which we have named PreBoMs based on their expression of B-cell-, macrophage- and progenitor-specific markers. It is unclear if this population represents the IL-10-producing regulatory (recently reported in spleen and PSF)[33, 34] or age-associated B-cells (reported in spleen only)[35], since the expression of F4/80 has not been reported in either cell type. Further analysis is needed to determine whether this PreBoM population is indeed a novel B-cell-like subset within the peritoneal cavity.

The $CD45^{-}$ component of the SVF includes fibroblasts, endothelial cells, and stem and progenitor populations. Adipose-associated stem and progenitor cells have been implicated in various biological processes and pathological conditions[36, 37]. While not comprehensive, our analysis highlights significant depot-specific stem/progenitor populations present in pmWAT and omWAT. The higher numbers of MSCs, APCs, and EPCs in pmWAT suggest that it may be a more abundant source of recruitable stem/progenitor cells. Similar to fat depot-specific leukocyte trafficking, unique signaling milieus may account for differences in progenitor populations. More in-depth depot-specific analyses are warranted to

determine the local and systemic implications of these populations in individual fat depots, particularly in the context of human disease states.

In summary, our results support the hypothesis that intra-abdominal fat pads represent distinct signaling microenvironments, each serving as its own "mini-organ"[38]. In agreement with previous reports indicating important functional differences between true visceral and non-visceral intra-abdominal fat pads in various metabolic disorders, we have found distinct differences in the SVF even within these subgroups. Our comparison of SVF composition, as well as overall gene expression of pmWAT, rpWAT, and omWAT, indicate that intra-abdominal fat depots cannot be used interchangeably. Hence, the comprehensive characterization of these immunomodulatory microenvironments provides the foundation for the design of future studies investigating depot-specific impacts on peritoneal homeostasis and chronic diseases. These findings support a new paradigm for the manner in which intra-abdominal fat should be studied.

DISCLOSURE

The authors declare no conflict of interest.

ACKNOWLEDGEMENTS

Special thanks to Melissa Makris for her help with FACS experimental design and analysis.

SUPPLEMENTARY MATERIAL

Leukocyte Characterization (% of CD45+, +/- SE)					
	Markers	**pmWAT**	**rpWAT**	**omWAT**	**PSF**
% $CD45^+$ (of viable)		**38.1 (3.6)**	**38.1 (2.5)**	**75.4 (1.2)**	**99.1 (0.3)**
% lymphocytes		**29.0 (3.1)**	**29.1 (3.0)**	**53.0 (8.3)**	**62.0 (1.1)**
% mono/granulocytes (R2)		**62.2 (3.0)**	**61.1 (3.5)**	**39.3 (8.3)**	**34.7 (3.1)**
R1					
B cells	**$CD19^+$**	**12.9 (1.8)**	**43.4 (2.2)**	**35.5 (1.5)**	**46.5 (1.2)**
B1	**$CD19^+CD11b^+B220^{lo/+}$**	**11.5 (1.7)**	**40.0 (2.1)**	**25.0 (1.1)**	**38.1 (1.2)**
B2	**$CD19^+CD11b^-B220^{lo/+}$**	**0.9 (0.2)**	**2.2 (0.4)**	**7.1 (0.9)**	**4.9 (0.8)**
T cells	**$CD3^+$**	**8.2 (0.8)**	**7.3 (0.8)**	**21.5 (1.7)**	**4.3 (0.4)**
T_H	**$CD3^+CD4^+$**	**4.6 (0.8)**	**3.7 (0.6)**	**12.8 (1.8)**	**3.1 (0.2)**
T_C	**$CD3^+CD8^+$**	**1.2 (0.1)**	**1.2 (0.2)**	**3.9 (0.5)**	**0.7 (0.1)**
NKT	**$CD3^+NK1.1^+$**	**0.9 (0.1)**	**0.7 (0.1)**	**0.6 (0.1)**	**0.3 (0.1)**
T_{REG}	**$CD3^+CD4^+CD25^+$**	**0.8 (0.3)**	**1.5 (0.4)**	**2.5 (0.2)**	**1.6 (0.2)**
$CD3^+CD4^-CD8^-NK1.1^-$		**2.4 (0.2)**	**2.3 (0.4)**	**4.5 (0.4)**	**0.4 (0.1)**
Myeloid precursors	**$CD3^-B220^-NK1.1^-CD11b^{hi}$**	**5.1 (0.6)**	**5.2 (0.4)**	**4.8 (0.3)**	**2.0 (0.1)**
mNK	**$NK1.1^+CD11b^+CD3^-$**	**3.4 (0.3)**	**3.0 (0.3)**	**1.4 (0.2)**	**1.3 (0.1)**
preNK	**$NK1.1^+CD11b^-CD3^-$**	**0.9 (0.1)**	**0.5 (0.1)**	**0.6 (0.1)**	**0.1 (0.04)**
DCs(I)	**$CD11c^+CD11b^{lo/+}$**	**6.7 (0.4)**	**8.3 (0.5)**	**7.6 (0.7)**	**4.6 (0.4)**
R2					
DCs (II)	**$CD11b^{+/lo}CD11c^+F4/80^-$**	**3.7 (1.5)**	**11.3 (6.4)**	**11.5 (4.0)**	**3.8 (1.5)**
LPMs	**$CD11b^+F4/80^+$**	**3.6 (0.6)**	**3.1 (0.5)**	**1.1 (0.2)**	**21.0 (1.4)**
SPMs	**$CD11b^+F4/80^{lo}$**	**41.6 (2.1)**	**22.9 (1.2)**	**11.1 (1.2)**	**2.9 (1.1)**
Monocytes (I)	**$CD11b^+F4/80^-$**	**1.4 (0.6)**	**10.2 (3.8)**	**4.0 (1.7)**	**0.2 (0.1)**
Monocytes (II)	**$CD11b^{lo}F4/80^-$**	**1.4 (1.1)**	**4.4 (1.4)**	**6.1 (2.4)**	**5.0 (2.2)**
PMNs	**$CD11b^+Ly6G^+Ly6C^+$**	**0.4 (0.1)**	**0.8 (0.1)**	**0.04 (0.03)**	**0**
PreBoMs	**$CD19^+CD11b^{hi}B220^{lo}F480^+CD93^+CD69^+$**	**0**	**0**	**0**	**0.7 (0.1)**

Supplementary Table S3.1 FACS analysis of intra-abdominal fat depots. PmWAT, rpWAT, omWAT and PSF.

Gene	rpWAT	omWAT	PSF
Tnfa	0.50 (0.67)	-3.84 (0.39)*	-9.17 (1.70)*
Csf1	-1.04 (0.52)	-0.90 (0.47)	-11.84 (2.05)*
Nos2	1.14 (0.65)	-17.74 (4.02)*	-134.99 (30.80)*
Ifng	-1.55 (1.24)	0.26 (0.68)	-7.76 (1.712)*
Tgfb	-1.27 (.14)	-23.33 (1.26)*	-7.84 (0.99)*
Mif	0.01 (0.62)	-2.25 (0.22)*	-1.07 (0.77)
Ido	-0.71 (1.01)	-1.61 (0.25)	-1.02 (0.76)
Rorc	1.38 (1.94)	1.66 (0.90)	-17.99 (0.50)*
Gata3	-1.69 (0.81)	-8.80 (2.92)*	-13.99 (2.46)*
Tbx21	-1.10 (0.93)	1.39 (0.65)	-0.84 (1.02)
NFkB	-0.31 (0.74)	3.02 (0.24)*	4.62 (1.02)*
Il1b	0.20 (1.12)	114.42 (78.18)*	9.57 (7.71)
Il2	-1.80 (1.57)	6.36 (1.49)*	-6.19 (2.18)*
Il4	-6.31 (4.47)	-1.57 (0.72)	-6.10 (1.81)*
Il5	-0.84 (0.85)	-3.38 (0.59)*	-24.54 (7.77)*
Il6	-0.55 (0.69)	1.86 (0.70)	0.85 (0.85)
Il10	-1.00 (0.54)	9.62 (1.73)*	-2.58 (0.62)*
Il12a	0.50 (0.66)	-1.88 (0.25)	-0.31 (0.88)
Ccl2	2.29 (1.53)	67.59 (33.34)*	-2.80 (1.64)
Ccl3	-0.85 (0.81)	-1.82 (0.67)	14.30 (5.41)*
Ccl4	-2.44 (0.50)	2.39 (0.35)	-14.10 (4.18)*
Ccl5	-1.00 (0.50)	11.65 (2.08)*	2.73 (1.08)*
Ccl7	0.52 (0.97)	1.86 (2.0)*	-214.80 (112.99)*
Ccl19	-0.47 (0.80)	5.76 (0.90)*	-42.96 (10.35)*
Ccl21	-10.27 (5.81)*	-3.46 (1.60)	-4387.09 (1360.31)*
Cxcl1	2.95 (0.56)	54.61 (20.49)*	5.52 (2.07)*
Cxcl2	3.36 (0.90)	32.22 (15.48)*	96.50 (37.33)*
Cxcl10	-0.089 (0.87)	4.72 (0.86)*	-46.87 (12.43)*
Cxcl12	-2.32 (0.42)*	-0.98 (0.51)	-21.79 (3.19)*
Cxcl13	2.06 (1.08)	488.67 (56.84)*	67.45 (19.31)*
Crp	-2.18 (1.69)	22.73 (13.83)*	4.03 (1.77)
Prom1	0.51 (0.77)	-0.15 (1.10)	-17.06 (4.83)
IL1rn	1.27 (2.10)	50.39 (24.96)*	3.31 (0.99)
Vegfa	1.05 (0.53)	-1.64 (1.62)	-255.32 (31.63)*
Hif1a	-0.89 (0.51)	74.87 (10.38)*	33.99 (5.56)*
Nos3	1.25 (0.60)	-2.25 (0.52)	-112.30 (40.96)*
Lep	3.65 (1.19)	-4.62 (2.16)	-1233.93 (376.92)*
Adipoq	1.78 (0.24)	-31.56 (5.28)*	-287768.13 (57680.49)*
Retn	2.25 (0.20)*	-2.08 (0.45)	-28554.69 (8773.49)*
Agt	1.29 (0.13)	-3.14 (0.77)*	-31365.74 (0.00)*
Apoe	1.50 (0.26)	5.64 (0.46)*	5.55 (1.63)*
C3	-1.75 (0.85)	2.49 (0.38)	-17.65 (5.20)*
Msr1	-1.32 (0.14)	-0.99 (0.46)	-1.43 (0.67)
Lpl	2.21 (0.25)*	-3.76 (1.10)	-22.46 (0.74)

Supplementary Table S3.2 Gene expression analysis of intra-abdominal fat depots. Data are presented as fold changes compared to pmWAT (± standard error of the mean), *p<0.05

REFERENCES

1. Caspar-Bauguil S, Cousin B, Galinier A, Segafredo C, Nibbelink M, Andre M*, et al.* Adipose tissues as an ancestral immune organ: site-specific change in obesity. *FEBS letters* 2005, **579**(17)**:** 3487-3492.
2. Park HT, Lee ES, Cheon YP, Lee DR, Yang KS, Kim YT*, et al.* The relationship between fat depot-specific preadipocyte differentiation and metabolic syndrome in obese women. *Clinical endocrinology* 2012, **76**(1)**:** 59-66.
3. Baglioni S, Cantini G, Poli G, Francalanci M, Squecco R, Di Franco A*, et al.* Functional differences in visceral and subcutaneous fat pads originate from differences in the adipose stem cell. *PloS one* 2012, **7**(5)**:** e36569.
4. Linder K, Arner P, Flores-Morales A, Tollet-Egnell P, Norstedt G. Differentially expressed genes in visceral or subcutaneous adipose tissue of obese men and women. *Journal of lipid research* 2004, **45**(1)**:** 148-154.
5. Montague CT, Prins JB, Sanders L, Zhang J, Sewter CP, Digby J*, et al.* Depot-related gene expression in human subcutaneous and omental adipocytes. *Diabetes* 1998, **47**(9)**:** 1384-1391.
6. Lee MJ, Wu Y, Fried SK. Adipose tissue heterogeneity: Implication of depot differences in adipose tissue for obesity complications. *Molecular aspects of medicine* 2012.
7. Foster MT, Shi H, Softic S, Kohli R, Seeley RJ, Woods SC. Transplantation of non-visceral fat to the visceral cavity improves glucose tolerance in mice: investigation of hepatic lipids and insulin sensitivity. *Diabetologia* 2011, **54**(11)**:** 2890-2899.
8. Wueest S, Yang X, Liu J, Schoenle EJ, Konrad D. Inverse regulation of basal lipolysis in perigonadal and mesenteric fat depots in mice. *American journal of physiology Endocrinology and metabolism* 2012, **302**(1)**:** E153-160.
9. Bjorntorp P. "Portal" adipose tissue as a generator of risk factors for cardiovascular disease and diabetes. *Arteriosclerosis* 1990, **10**(4)**:** 493-496.
10. Foster MT, Shi H, Seeley RJ, Woods SC. Transplantation or removal of intra-abdominal adipose tissue prevents age-induced glucose insensitivity. *Physiology & behavior* 2010, **101**(2)**:** 282-288.
11. Gerber SA, Rybalko VY, Bigelow CE, Lugade AA, Foster TH, Frelinger JG*, et al.* Preferential attachment of peritoneal tumor metastases to omental immune aggregates and possible role of a unique vascular microenvironment in metastatic survival and growth. *The American journal of pathology* 2006, **169**(5)**:** 1739-1752.
12. Berberich S, Dahne S, Schippers A, Peters T, Muller W, Kremmer E*, et al.* Differential molecular and anatomical basis for B cell migration into the peritoneal cavity and omental milky spots. *J Immunol* 2008, **180**(4)**:** 2196-2203.
13. Yu G, Wu X, Kilroy G, Halvorsen YD, Gimble JM, Floyd ZE. Isolation of murine adipose-derived stem cells. *Methods in molecular biology* 2011, **702:** 29-36.
14. Schmittgen TD, Livak KJ. Analyzing real-time PCR data by the comparative C(T) method. *Nature protocols* 2008, **3**(6)**:** 1101-1108.
15. Kwon EY, Shin SK, Cho YY, Jung UJ, Kim E, Park T*, et al.* Time-course microarrays reveal early activation of the immune transcriptome and adipokine dysregulation leads to fibrosis in visceral adipose depots during diet-induced obesity. *BMC genomics* 2012, **13:** 450.
16. Brake DK, Smith EO, Mersmann H, Smith CW, Robker RL. ICAM-1 expression in adipose tissue: effects of diet-induced obesity in mice. *American journal of physiology Cell physiology* 2006, **291**(6)**:** C1232-1239.
17. Kawanishi N, Yano H, Yokogawa Y, Suzuki K. Exercise training inhibits inflammation in adipose tissue via both suppression of macrophage infiltration and acceleration of phenotypic switching

from M1 to M2 macrophages in high-fat-diet-induced obese mice. *Exercise immunology review* 2010, **16:** 105-118.
18. Lumeng CN, DelProposto JB, Westcott DJ, Saltiel AR. Phenotypic switching of adipose tissue macrophages with obesity is generated by spatiotemporal differences in macrophage subtypes. *Diabetes* 2008, **57**(12)**:** 3239-3246.
19. Ray A, Dittel BN. Isolation of mouse peritoneal cavity cells. *Journal of visualized experiments : JoVE* 2010(35).
20. Sandoval P, Loureiro J, Gonzalez-Mateo G, Perez-Lozano ML, Maldonado-Rodriguez A, Sanchez-Tomero JA*, et al.* PPAR-gamma agonist rosiglitazone protects peritoneal membrane from dialysis fluid-induced damage. *Laboratory investigation; a journal of technical methods and pathology* 2010, **90**(10)**:** 1517-1532.
21. Rangel-Moreno J, Moyron-Quiroz JE, Carragher DM, Kusser K, Hartson L, Moquin A*, et al.* Omental milky spots develop in the absence of lymphoid tissue-inducer cells and support B and T cell responses to peritoneal antigens. *Immunity* 2009, **30**(5)**:** 731-743.
22. Yu J, Wei M, Mao H, Zhang J, Hughes T, Mitsui T*, et al.* CD94 defines phenotypically and functionally distinct mouse NK cell subsets. *J Immunol* 2009, **183**(8)**:** 4968-4974.
23. Smyth MJ, Cretney E, Kelly JM, Westwood JA, Street SE, Yagita H*, et al.* Activation of NK cell cytotoxicity. *Molecular immunology* 2005, **42**(4)**:** 501-510.
24. Ghosn EE, Cassado AA, Govoni GR, Fukuhara T, Yang Y, Monack DM*, et al.* Two physically, functionally, and developmentally distinct peritoneal macrophage subsets. *Proceedings of the National Academy of Sciences of the United States of America* 2010, **107**(6)**:** 2568-2573.
25. Rubtsova K, Marrack P, Rubtsov AV. Age-associated B cells: are they the key to understanding why autoimmune diseases are more prevalent in women? *Expert review of clinical immunology* 2012, **8**(1)**:** 5-7.
26. Yanaba K, Bouaziz JD, Haas KM, Poe JC, Fujimoto M, Tedder TF. A regulatory B cell subset with a unique CD1dhiCD5+ phenotype controls T cell-dependent inflammatory responses. *Immunity* 2008, **28**(5)**:** 639-650.
27. Dromard C, Bourin P, Andre M, De Barros S, Casteilla L, Planat-Benard V. Human adipose derived stroma/stem cells grow in serum-free medium as floating spheres. *Experimental cell research* 2011, **317**(6)**:** 770-780.
28. Macotela Y, Emanuelli B, Mori MA, Gesta S, Schulz TJ, Tseng YH*, et al.* Intrinsic differences in adipocyte precursor cells from different white fat depots. *Diabetes* 2012, **61**(7)**:** 1691-1699.
29. Fang S, Wei J, Pentinmikko N, Leinonen H, Salven P. Generation of functional blood vessels from a single c-kit+ adult vascular endothelial stem cell. *PLoS biology* 2012, **10**(10)**:** e1001407.
30. Montecino-Rodriguez E, Dorshkind K. New perspectives in B-1 B cell development and function. *Trends in immunology* 2006, **27**(9)**:** 428-433.
31. Horikawa K, Takatsu K. Interleukin-5 regulates genes involved in B-cell terminal maturation. *Immunology* 2006, **118**(4)**:** 497-508.
32. Ansel KM, Harris RB, Cyster JG. CXCL13 is required for B1 cell homing, natural antibody production, and body cavity immunity. *Immunity* 2002, **16**(1)**:** 67-76.
33. Poe JC, Smith SH, Haas KM, Yanaba K, Tsubata T, Matsushita T*, et al.* Amplified B lymphocyte CD40 signaling drives regulatory B10 cell expansion in mice. *PloS one* 2011, **6**(7)**:** e22464.
34. Matsushita T, Tedder TF. Identifying regulatory B cells (B10 cells) that produce IL-10 in mice. *Methods in molecular biology* 2011, **677:** 99-111.
35. Rubtsov AV, Rubtsova K, Fischer A, Meehan RT, Gillis JZ, Kappler JW*, et al.* Toll-like receptor 7 (TLR7)-driven accumulation of a novel CD11c(+) B-cell population is important for the development of autoimmunity. *Blood* 2011, **118**(5)**:** 1305-1315.

36. Christensen LH, Riise E, Bang L, Zhang C, Lund K. Isoallergen variations contribute to the overall complexity of effector cell degranulation: effect mediated through differentiated IgE affinity. *Journal of immunology* 2010, **184**(9)**:** 4966-4972.
37. Kidd S, Spaeth E, Watson K, Burks J, Lu H, Klopp A*, et al.* Origins of the tumor microenvironment: quantitative assessment of adipose-derived and bone marrow-derived stroma. *PloS one* 2012, **7**(2)**:** e30563.
38. Tchkonia T, Lenburg M, Thomou T, Giorgadze N, Frampton G, Pirtskhalava T*, et al.* Identification of depot-specific human fat cell progenitors through distinct expression profiles and developmental gene patterns. *American journal of physiology Endocrinology and metabolism* 2007, **292**(1)**:** E298-307.

CHAPTER 4.

Parity-Associated Protection Against Ovarian Cancer Metastasis in the Omental Fat Band

Courtney A. Cohen[1], Amanda A. Shea[2], C. Lynn Heffron[1], Eva M. Schmelz[2], Paul C. Roberts[1]

1. Department of Biomedical Sciences and Pathobiology, Virginia Polytechnic Institute and State University, Blacksburg, VA, United States

2. Department of Human Nutrition, Foods and Exercise, Virginia Polytechnic Institute and State University, Blacksburg, VA, United States

ABSTRACT

Ovarian cancer is an insidious and aggressive disease, typically undiscovered prior to metastasis due to its asymptomatic nature. However, epidemiological studies indicate that child-bearing (parity) is associated with decreased ovarian cancer risk. The molecular mechanisms responsible for this phenomenon are not understood. The omental fat band (OFB) is the primary site of ovarian metastasis in the peritoneal cavity. Characterized as a secondary lymphoid organ, it serves as a filtration system for the peritoneal serous fluid (PSF) and is capable of mounting both innate and adaptive immune responses during peritoneal immunosurveillance. We have used fluorescence-activated cell sorting (FACS) analysis and quantitative realtime PCR (qRT-PCR) to determine that parity is associated with an altered immune profile in the OFB, characterized by a reduction in monocytic subsets and B1-B cells as well as expression of their respective chemoattractants. We find that parity results in reduced tumor burden following intraperitoneal implantation compared to nulliparous animals, and that delayed tumor development is associated with a reduction in tumor-associated neutrophils (TANs) and macrophages (TAMs) recruited to the OFB (and PSF). These findings define a naturally occurring microenvironmental state in the OFB that is refractory to rapid metastatic tumor growth, and could provide insights into strategies for modulating or disrupting the pro-tumorigenic cascade that develops after cancer cell seeding.

INTRODUCTION

Ovarian cancer is the deadliest gynecological malignancy, responsible for 140,000 deaths in women annually worldwide[1, 2]. Additionally, it has one of the highest death-to-incidence ratios in the US due to late detection, a high degree of tumor heterogeneity and a high rate of disease recurrence[3, 4, 5].

During metastasis, ovarian cancer cells exfoliate from the primary tumor and disseminate throughout the peritoneal cavity in the serous fluid [6, 7]. The omental fat band (OFB) is the predominant site of peritoneal metastasis, with omental tumors observed in 80% of all women with serous ovarian carcinomas[5]. The OFB is considered a secondary lymphoid organ and contributes to immunosurveillance of the peritoneal cavity. It is composed of fatty tissue interspersed with immune cell aggregates or "milky spots"[8, 9], which consist of leukocytes, stem and progenitor cells, fibroblasts and endothelial cells[10] that are collectively referred to as the stromal vascular fraction (SVF). These milky spots also contain hypoxic regions that induce constant production of VEGF and other pro-angiogenic factors[9, 11]. It has been hypothesized that the inherent pro-angiogenic status of the OFB in the homeostatic state represents a pre-metastatic niche that can be harnessed to aid in tumor development. Disseminated tumor cells adhere to these milky spots within hours [12, 13] and promote a pro-tumorigenic microenvironment and subsequent tumor growth[6, 9, 13, 14]. While cancer cell-mesothelial cell interactions that impact cancer cell adherence have been the subject of investigation [15], the complex and dynamic interactions between metastatic cancer cells and resident leukocytes within this immunologically relevant microenvironment have not been well characterized.

Ovarian cancer is a disease of older women: more than 87% of women diagnosed with ovarian cancer are older than 55 years of age[16], and older women are more likely to be diagnosed with a later stage of the disease[17]; reducing their 5-year survival to less than 30%[16]. Risk factors associated with ovarian cancer include endometriosis, pelvic inflammatory disease and certain infertility treatments[18]. Conversely, oral contraceptives, some surgical procedures (e.g., tubal ligation, hysterectomy), lactation and parity are associated with a significantly decreased risk of ovarian cancer. Women who undergo an

early (<20 years old) full-term pregnancy have a significantly reduced lifetime risk of breast and ovarian cancer[19, 20, 21]. Additionally, the relative risk is inversely correlated to an increased number of offspring[22]. However, little is known about the persistent molecular and cellular changes that modulate ovarian cancer risk as a result of child-bearing.

We have reported that the homeostatic immune microenvironment of the OFB significantly differs from that of other intraperitoneal fat tissue with a distinct leukocyte profile, as well as a robust cytokine signaling network[23]. The impact of age or parity on this immune microenvironment is not known. However, this may have critical implications for the generation of a metastatic niche that determines successful tumor adherence and outgrowth within the peritoneal cavity. Given the importance of the OFB as a primary metastatic site, in the present study we comparatively characterized the stromal vascular fraction (SVF) and the respective gene expression profiles of OFBs from young adult nulliparous, mature adult nulliparous and mature parous mice in response to aggressive ovarian cancer cell seeding. The objective was to identify any age- and/or parity-specific cellularity changes inherent to the OFB that may shed light on parity-associated protection against cancer metastasis. In the present study, parity positively correlated with reduced peritoneal tumor burden. This was associated with distinct parity-associated changes to the pre-existing immune microenvironment within the OFB that may have provided protection. A more comprehensive understanding of the dynamic cellular interactions that occur during metastatic colonization and outgrowth is critical for the development of improved treatment strategies that effectively target the tumor microenvironment at the time of disease discovery. These insights may ultimately lead to novel strategies that re-polarize the immune microenvironment of the OFB in a manner that reflects a naturally occurring microenvironment refractory to cancer growth.

METHODS AND PROCEDURES

Cell Lines

The mouse ovarian surface epithelial (MOSE) cell model utilized in this study was developed from C57BL/6 mice and characterized previously [24, 25]. Tumorigenic MOSE cells were passaged once in

vivo by intraperitoneal (i.p.) injection into C57BL/6 mice and re-collected via peritoneal lavage after a 4-week incubation period to select for a more aggressive phenotype. These MOSE cells were then transduced with firefly luciferase (MOSE-L_{FFLv}) lentiviral particles (GeneCopoeia) as described[26] to facilitate live in vivo imaging of cancer cell outgrowth. The characteristics of MOSE-L_{FFLv} will be reported elsewhere. MOSE-L_{FFLv} cells were routinely maintained in high glucose DMEM (Invitrogen, Carlsbad, CA), supplemented with 4% fetal bovine serum (Hyclone, Logan UT), 100mg/ml penicillin and streptomycin and 1μg/ml puromycin (lentiviral particles utilize a puromycin resistance marker for selection of transduced cells).

Animals

Female C57BL/6 mice (Harlan Laboratories) were housed five per cage in a controlled environment (12 hour light/dark cycle at 21°C) with free access to water and food (18% protein rodent chow, Teklad Diets). Young adult nulliparous mice at 5 months of age (21g average body weight), mature adult nulliparous mice at 11 months of age (30g average body weight) and mature parous mice at 12 months of age (31g average body weight) were sacrificed by CO_2 asphyxiation. Mouse studies were conducted in accordance with the guidelines approved by the Virginia Tech Institutional Animal Care and Usage Committee.

MOSE-L_{FFLv} Injection

Preliminary dosage studies were performed to empiricallydetermine the appropriate cell number and time for tumor development and verify reproducibility. These studies determined that $1x10^4$ MOSE-L_{FFLv} cells injected i.p. cause fatal disease after 3 weeks of incubation, in contrast to the progenitor MOSE-L cells that require the injection of $1x10^6$ cells and approximately 12 weeks of incubation. The endpoint was determined when mice lost or gained weight, exhibited ruffled fur, a hunched appearance and had palpable ascites, indicative of late-stage fatal disease. Based on these results, all studies were performed using $1x10^4$ MOSE-L_{FFLv} cells, with a 21 day incubation time. Prior to injection, MOSE-L_{FFLv} cells were resuspended in 300μL sterile calcium- and magnesium-deficient phosphate buffered saline

($PBS^{-/-}$). Young adult nulliparous and mature parous mice (n=10 per group) were injected i.p. with either $1x10^4$ MOSE-L_{FFLv} cells or $PBS^{-/-}$ and sacrificed at 21 days post-injection.

Peritoneal Cancer Index (PCI)

In order to quantify relative tumor burden at the time of sacrifice, the PCI was determined as described previously, with minor modifications[27, 28]. The original PCI was adapted to apply to tumor size and region in mice, "quadrant areas" were modified to represent distinct organs and their mesentery in order to obtain more specific information regarding tumor cell dissemination and seeding. Specific regions evaluated included peritoneal cavity lining, ovaries, lesser omentum, greater omentum (OFB), diaphragm, liver, stomach, pancreas, spleen, kidney, small intestine, small intestine mesentery, large intestine, and large intestine mesentery. Tumor size was scored as **(0)**: no visible tumor, **(1):** < 1mm; **(2):** 1-3mm; **(3):** >3mm or solid mass. The maximum PCI score was 42, reflecting maximal size and 14 designated areas. Relative PCI scores were further validated by qRT-PCR analysis of FFL expression within the OFB employed as a tumor cell reporter gene.

Tissue and peritoneal serous fluid harvest

The OFB was harvested from each mouse, weighed, rinsed with $PBS^{-/-}$, and processed for FACS or placed into RNAlater (Qiagen) and stored at -80°C. Resident peritoneal cavity cells were collected via peritoneal lavage with 5ml of $PBS^{-/-}$. The effluent was centrifuged, subjected to erythrocyte lysis (155mM NH_4Cl, 10mM $KHCO_3$, 0.1mM EDTA), and further processed as described below.

Tissue Digestion

SVFs were isolated by digesting individual OFBs (n=4-6) in GKN-buffer containing 1.8mg/ml Type IV collagenase, 10% FBS, and 0.1mg/ml DNase as previously described[23]. Following digest at 37°C for 45 min, cells were passed through a 40μm cell strainer, and erythrocytes were lysed (see above).

FACS Analysis

Single cell suspensions derived from OFB and PSF were washed in flow buffer (2% BSA in $PBS^{-/-}$), blocked with Fc block (BD Biosciences) for 10 minutes at 4°C, rinsed and incubated with fluorochrome-labeled antibody combinations (available upon request) for 20 min at 4°C. Fluorochrome-labeled

antibodies specific for mouse CD45, CD11b, CD11c, F4/80, Ly6C, CD4, CD44, CD62L, B220, CD19, NK1.1, and Ly6G were obtained from eBioscience (San Diego, CA). CD3, and CD8 antibodies were obtained from BD Biosciences (San Jose, CA). Prior to analysis, cells were washed twice and resuspended in $PBS^{-/-}$ with propidium iodide for dead cell exclusion. FACS was performed on a FACSAria (BD Biosciences) and data was analyzed using Flowjo (TreeStar) software.

Quantitative real-time PCR (qRT-PCR)

Individual OFB were homogenized in Qiazol (Qiagen) and RNA was purified using an RNeasy Lipid Tissue Kit (Qiagen), according to manufacturer's instructions. RNA concentration was determined using a NanoDrop1000 spectrophotometer.RNA (n=4-6) was subjected to the iScript cDNA synthesis system (Biorad) according to manufacturer's protocol. qRT-PCR was performed with 12.5ng cDNA per sample using gene-specific SYBR Green primers (primer sequences are available upon request) designed with Beacon Design software. SensiMix SYBR and Fluorescein mastermix (Quantace) was used in a 15μL reaction volume. qRT-PCR was performed for 42 cycles at 95°C for 15 sec, 60°C for 15 sec, and 72°C for 15 sec, preceded by a 10 min incubation at 95°C on the iQ5 (Biorad). Melt curves were performed to ensure fidelity of the PCR product. The housekeeping gene was L19 and the ddCt method[29] was used to determine fold differences.

Statistical Analysis

Data are expressed as mean ± standard error of mean (SEM). FACS and qRT-PCR data were analyzed using a one-way ANOVA coupled with a Tukey Post-hoc test in SigmaPlot (Systat Software). Differences were considered statistically significant at $p<0.05$.

RESULTS

Epidemiological studies have reported increased ovarian cancer incidence in older women but a protective effect associated with parity[22]. Here, we postulated that parity may induce changes in the OFB that result in a pre-existing immune microenvironment that is protective against cancer metastasis.

Identification of a "protective signature" may provide important insights towards the development of targeted treatment strategies for metastatic ovarian cancer. In order to distinguish parity-associated changes from age-associated changes in the OFB, we chose three sets of mice: five-month old nulliparous young adults, twelve-month old mature parous adults and nulliparous mature adult mice. The comparison of these groups allowed us to differentiate between age- and parity-related changes in the peritoneal and OFB microenvironments.

OFB size and cellularity

As expected, the size of the OFB increased significantly with age between 5m and 11m nulliparous mice, coinciding with the overall age-associated weight gain (14.4g ± 1.5 and 28.2g ± 2.2, $p<0.01$). OFB weight also increased significantly with parity (51.8mg ± 4.3, $p<0.01$) (Figure 4.1A), although the average body weight between these aged matched groups was the same (29.8g ± 0.8 vs 31.7g ± 0.7). The SVF count within the OFB was significantly elevated as a function of both age and parity, increasing to over 8-fold in mature parous mice ($p<0.01$, Figure 4.1B). This indicates that parity induces a change in stromal vascular cell influx or proliferation and does not simply represent an increase in overall adiposity in the OFB. The proportion of $CD45^+$ leukocytes represented approximately 50% of the SVF in both young and mature nulliparous mice but represented >95% of the SVF in parous mice ($p<0.01$, Figure 4.1C). It is possible that this represents a loss or a differentiation of previously described resident stem/progenitor populations in the OFB with parity[23]. This would agree with previous reports of increased differentiation signaling in the parous mammary gland[30]. In order to make an initial assessment of how age and parity may impact the OFB transcriptome we evaluated the expression of a select set of immune-related genes using qRT-PCR on whole tissue samples. As shown, there are both age-and parity-associated differences in the expression of a number of important cytokines and chemokines in the homeostatic state (Figure 4.1D). In mature nulliparous animals, there is increased expression of a number of molecules chemotactic for monocytes (CCL1,CCL4 and CCL7, $p<0.05$) as compared to young nulliparous mice. TGFβ, an important regulator of tumor cell invasion and metastasis, is significantly upregulated in older mice, regardless of parity status ($p<0.01$). Parity-specific changes include a

significant downregulation of neutrophil chemoattractants (CXCL1, CXCL2, $p<0.05$), as well as several macrophage alternate activation-related genes characteristic of a tumor-associated phenotype (Arg1, M6pr, $p<0.05$). This indicates that inherent changes that occur as a result of aging and child-bearing affect the signaling microenvironment in the OFB. These signaling changes may explain the different proportions of leukocyte populations found residing with this tissue, which could in turn affect susceptibility to ovarian cancer metastasis.

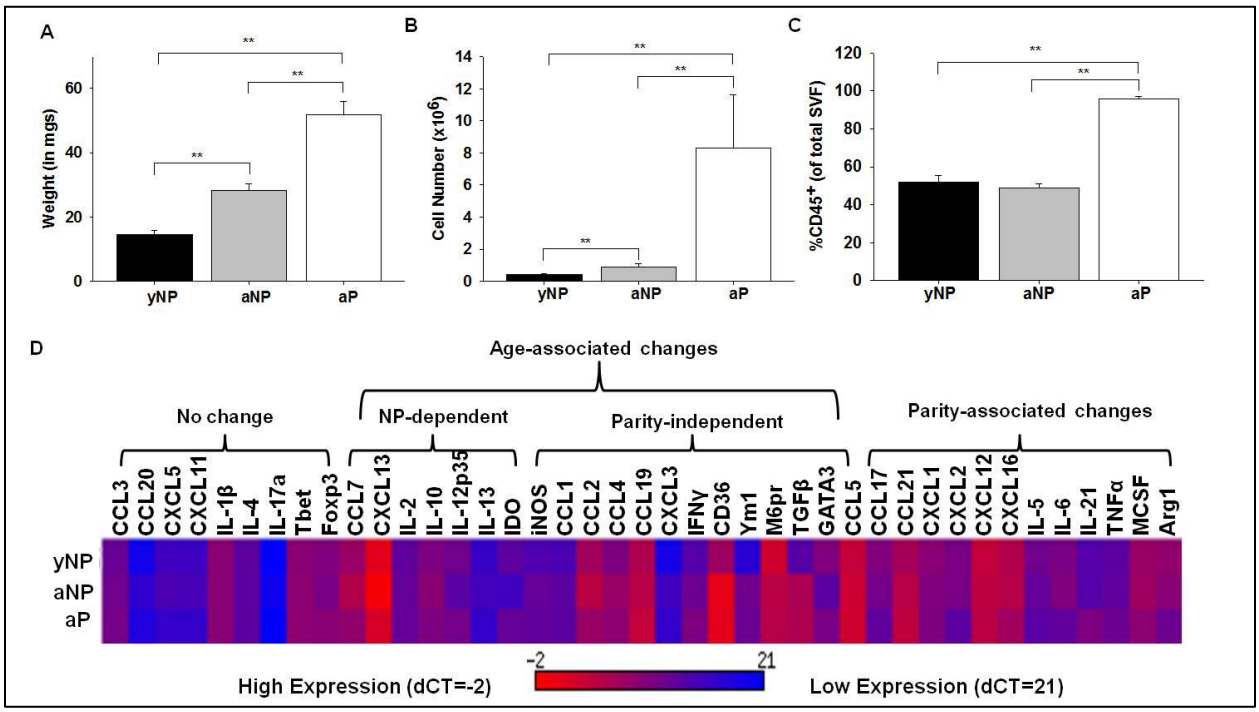

Figure 4.1. The OFB displays parity-associated differences in the SVF. Young adult nulliparous (yNP), mature adult nulliparous (aNP) and adult parous mice (aP) mice. **A)** Whole tissue OFB weight. **B)** Number of cells in the SVF isolated from digested OFB. **C)** $CD45^+$ population in OFB SVF. **D)** Gene expression profile of OFB.

OFB SVF Characterization

The SVF of individual OFBs were further characterized via FACS analysis to identify age- and parity-specific differences in immune cell composition. Viable cells (propidium iodide exclusion) were separated into $CD45^+$ leukocytes and $CD45^-$ stromal constituents. $CD45^+$ cells were subsequently separated into R1 (lymphocyte) and R2 (monocyte/granulocyte) gates based on forward/side scatter (Figure 4.2A), and leukocyte subsets were identified based on well-defined surface markers. The $CD45^+$

subsets associated with the OFB in nulliparous mice were comparable, irrespective of age. However, the immune cell composition of the parous OFB was strikingly different, supporting the hypothesis that parity does in fact lead to establishment of a unique omental microenvironment that may be inherently protective. Specifically, in the OFB of nulliparous mice the lymphocyte to monocyte/granulocyte (R1:R2) ratios were approximately 6:4 independent of age, whereas lymphocytes represented almost 90% of the $CD45^+$ cells isolated from the parous OFB (Figure 4.2B). This trend was mirrored in the peritoneal serous fluid (PSF), with an increase observed in the proportion of lymphocytes to monocytes/granulocytes in parous mice as compared to mature nulliparous mice of approximately 20% ($p<0.05$, Supplementary Table S4.1).

The parity-associated increase in lymphocytes was reflected across numerous subsets including $CD3^+$($p<0.01$) and $CD19^+$($p<0.05$) as well as $CD11c^+$($p<0.01$) cells with concomitant decreases detected in $F480^+$($p<0.01$) and $NK1.1^+$ ($p<0.01$) subsets compared to nulliparous mice (Figure 4.1C). Compared to their age-matched nulliparous counterparts, the OFB of parous mice also displayed significantly increased levels of $CD3^+CD4^+$, and significantly decreased $CD3^+CD8^+$ and $CD3^+CD4^-CD8^-$ cells ($p<0.05$, Figure 4.2D). Parity also caused a significant increase in the proportion of $CD3^+$ T cells and $CD19^+$ B cells in the PSF, with levels of NK cells and $CD11c^+$ cells unaffected ($p<0.05$, Supplementary Table S4.1).

There was a significant parity-associated shift in the subsets of $CD19^+$ B-lymphocytes residing in the OFB. $CD11b^+B220^{lo/+}$ B1 cells were the most prevalent subset of B cells in nulliparous mice, whereas in parous mice the $CD11b^-B220^{lo/+}$ B2-subset was dominant (Figure 4.2E). B1 cells are the predominant B cell type in the peritoneal cavity, and are considered a more "innate-like" population, with receptors for autoantibodies and conserved bacterial and viral epitopes[31]. This increase in B2 cells could indicate a more effective humoral response in the OFB of parous mice. However, it is important to note that while the relative proportion of B2 cells is higher in parous mice than in nulliparous mice, the SVF count was also 8-fold higher, indicative of a net increase in both B cell populations in parous mice.

Parity-associated changes were also evident within the macrophage subsets residing in the OFB, although these changes were not mirrored in the parous PSF. In the peritoneal serous fluid, macrophages are

typically subdivided into “large peritoneal macrophages” (LPMs), and “small peritoneal macrophages” (SPMs). LPMs can be distinguished via FACS based on forward/side scatter and relative CD11b and F480 surface staining. SPMs appear in the PSF as a result of LPS stimulation, and are derived from blood monocytes. The function of these populations in the OFB is undefined. Confirming previous reports, our study found that the PSF is comprised largely of LPMs in the homeostatic state, with SPMs representing only a minor fraction of the total macrophage composition[32]. This trend was not significantly altered by parity. In contrast, whereas the predominant macrophage population in the OFB of young and mature nulliparous mice was the $CD11b^{+}F480^{lo}$ population (SPMs), this population was significantly reduced in parous mice[32]. Further, the $CD11b^{+}F480^{+}$ population of macrophages (LPMs) was virtually undetectable in parous mice, although it represented approximately 8% of the R2 gate in both sets of nulliparous mice (Figure 4.2F) Finally, nulliparous mice had virtually indistinguishable immune cell profiles, indicating similar immunomodulatory microenvironments, unaffected by age at these timepoints.

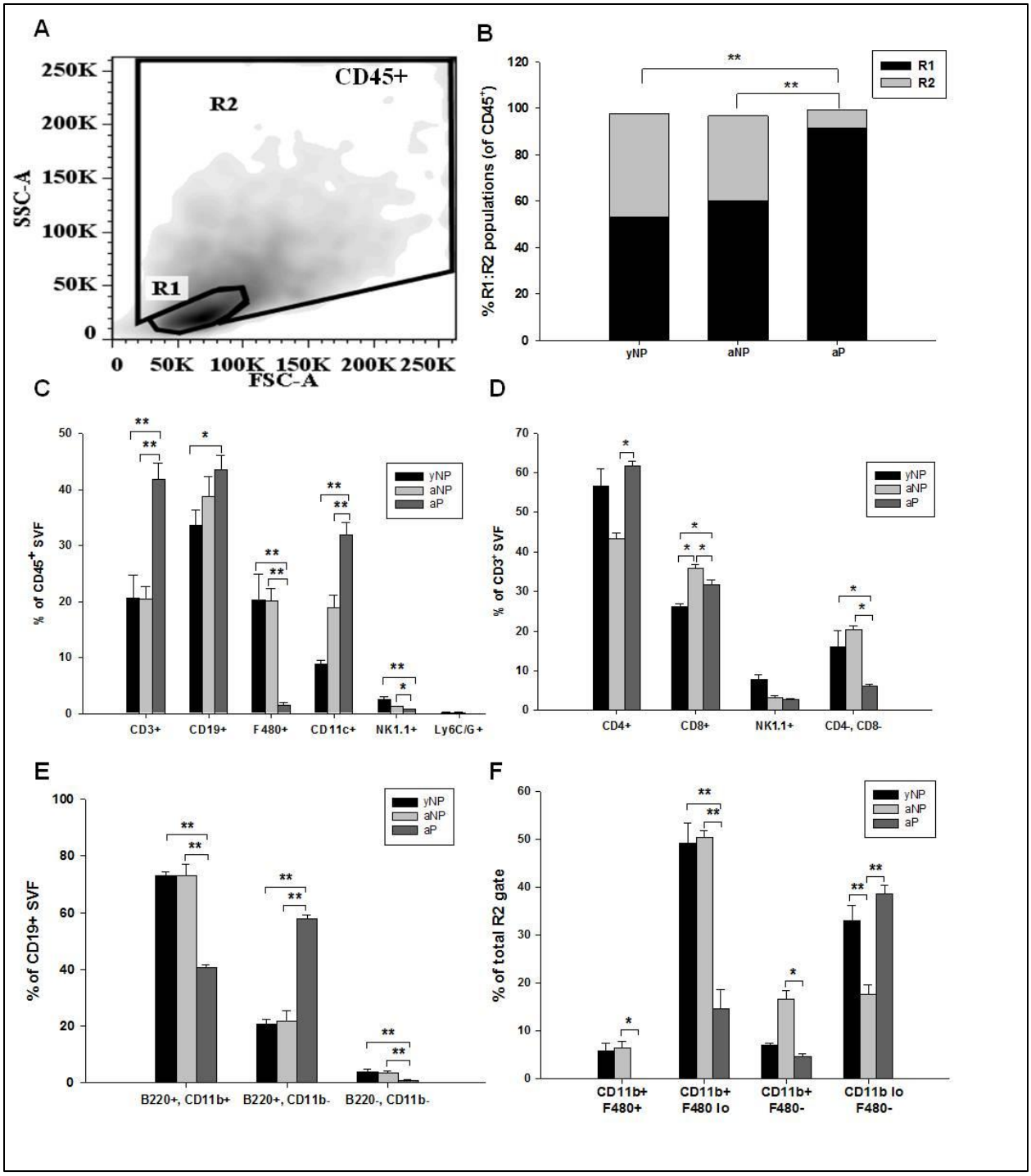

Figure 4.2. The OFB displays parity-associated differences in leukocyte populations. Young adult nulliparous (yNP), mature adult nulliparous (aNP) and mature parous mice (aP). **A)** $CD45^+$ leukocytes in the SVF of OFB were separated into regions R1 (lymphocytes) and R2 (monocytes/granulocytes) for further analysis. **B)** Distribution of R1:R2 populations in OFB. **C)** Overall immune cell populations in OFB. **D)** $CD3^+$ subsets within OFB. **E)** $CD19^+$ subsets within OFB. **F)** Monocyte/granulocyte subsets within OFB. *p<0.05, **p<0.01

Impact of parity on peritoneal tumor burden.

As parity has been implicated as a protective factor against ovarian and breast cancer, we next evaluated whether the parous microenvironment within the peritoneal cavity represents a niche that is truly refractory to disseminating ovarian cancer cells. To investigate this, we employed our previously described syngeneic murine ovarian cancer model[24] with minor modifications. Here we chose to use a highly aggressive variant of our MOSE-L cells (MOSE-L_{FFLv}) that results in widespread peritoneal outgrowth and ascites within 21 days of intraperitoneal implantation. These cells also express the firefly luciferase reporter gene that can be used as a gene tag for quantification of relative levels of tumor cells within tissues. At 21 days post intraperitoneal seeding of 1 x 10^4 MOSE-L_{FFLv} cells, nulliparous and parous mice were euthanized and the peritoneal cancer index (PCI) was assessed. Notably, parous mice had a significantly decreased tumor burden compared to nulliparous mice (Figure 4.3A; $p<0.01$). To confirm the OFB-specific tumor burden, we determined relative levels of the FFL reporter gene using qRT-PCR. As reflected in the PCI, FFL expression was five-fold higher in the OFB of nulliparous mice that received MOSE-L_{FFLv} cells as compared with parous mice ($p=0.059$; Figure 4.3B). The OFB from mock implanted mice ($PBS^{-/-}$ injection) were negative for FFL reporter gene expression (data not shown).

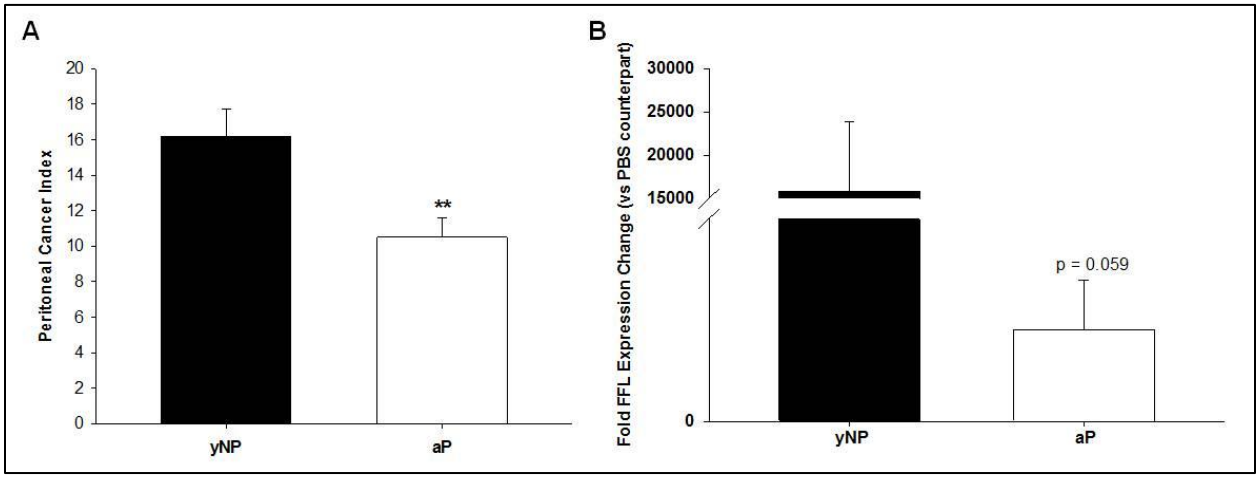

Figure 4.3. Parity reduces $MOSE_{FFL}$ tumor burden following intraperiteonal implantation. A**)** Peritoneal Cancer Index (PCI) (n =10). B**)** FFL expression in OFB of tumor-bearing mice compared to their PBS-injected counterparts.

Macroscopically, the OFB in nulliparous mice had been fully overtaken by fibrous tumor tissue and was virtually devoid of residual adipose tissue. Accordingly, the average weight of the OFB increased significantly in cancer-bearing nulliparous mice and 60% of mice had developed bloody ascites. In contrast, cancer-bearing parous mice presented with macroscopic individual tumor nodules throughout the OFB, but residual adipose tissue was still highly evident, and there was no evidence of ascites in these animals. The OFB weight did not change significantly between MOSE-L_{FFLv}- and vehicle-injected parous mice, confirming a significantly lower OFB tumor burden from that observed in nulliparous mice (Figure 4.4A). No organ-specific differences in tumor cell seeding were evident, parous mice simply had a reduced overall PCI.

The aggressive growth of MOSE-L_{FFLv} cells in nulliparous animals was coincident with a greater than 15-fold increase in the number of cells present within the SVF of the OFB (Figure 4.4B), albeit the proportion of $CD45^+$ leukocytes did not change (Figure 4.4C). This suggests that the tumor microenvironment was inducing a proliferation or influx of both leukocytes and $CD45^-$ stromal constituents. This trend was not observed in parous mice as the SVF cell counts did not vary significantly between MOSE-L_{FFLv} and control groups (Figure 4.4B,C). These results indicate that the OFB microenvironment of parous animals is inherently more resistant to either tumor outgrowth or to the recruitment of factors or cell types that are pro-tumorigenic.

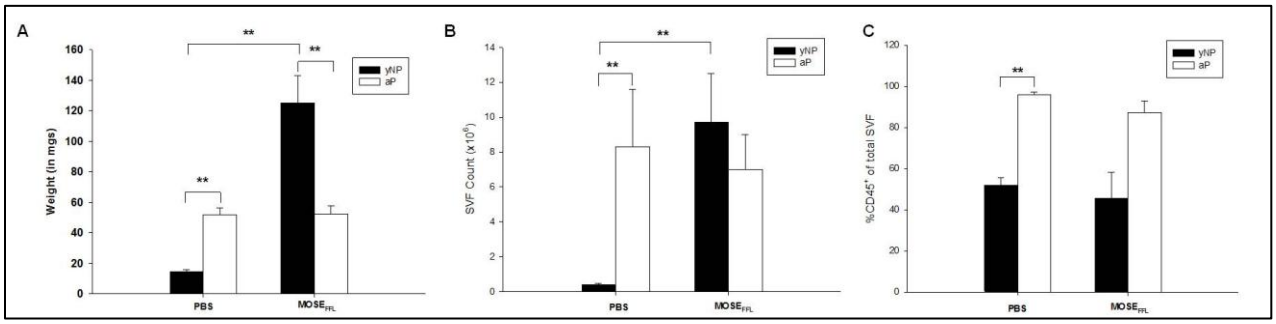

Figure 4.4. Parity reduces metastasis-associated influx of stromal cells to the OFB. Young adult nulliparous (yNP) and mature adult parous (aP) mice +/- MOSE-L_{FFLv} implantation. **A)** Whole tissue OFB weight. **B)** Number of SVF cells isolated from digested OFB. **C)** $CD45^+$ population in the OFB SVF.

OFB SVF Characterization with ovarian cancer

The OFBs of ovarian cancer-bearing animals were further characterized via FACS analysis in order to determine the impact of cancer cell seeding on leukocyte populations harbored within the OFB microenvironment. Irrespective of parity, there was a specific MOSE-L_{FFLv}- cancer cell associated change in the proportion of lymphocytes to monocyte/granulocytes (R1:R2) within the OFB. Specifically, a reduction in lymphocytes and a concomitant increase in monocyte/granulocytes within the $CD45^+$ leukocyte population was the trend in cancer-bearing OFBs (Figure 4.5A). This pattern was also evident in the PSF, with an increase in the proportion of monocytes/granulocytes in the OFB of both nulliparous (19% ± 11.0, p=0.21) and parous mice (15% ± 1.6, p<0.01) (Supplementary Table 4.2).

In nulliparous mice, this re-distribution of R1:R2 leukocytes was mirrored across all subsets with decreases noted in $CD3^+$, $CD19^+$, and $NK1.1^+$ cells, with slight concomitant increases in $F480^+$ and $CD11c^+$ cells. Interestingly, whereas levels of $CD4^+$ and $CD8^+$ subsets declined as a result of cancer, both double negative ($CD4^-CD8^-$)- and NK T cell subsets increased; although these trends did not reach significance in the OFB (Figure 4.5C). The former may represent a previously described immunosuppressive T cell population that inhibits immune responses by directly killing cytotoxic T cells and secreting TGFβ and IL-10[33]. Additionally, it may represent γδ T cells[33, 34, 35], but we are unable to speculate further as we did not evaluate TCR γδ expression in our study. No appreciable differences in the relative proportions of OFB associated B1 and B2 lymphocytes were noted in cancer-bearing nulliparous animals (Figure 4.5D). However in the PSF, the B1:B2 ratio increases from 3:1 in the homeostatic state to 5:1 as a consequence of MOSE-L_{FFLv} implantation (p<0.05, data not shown). As B1 cells act as the bridge between innate and adaptive immunity, producing low-affinity antibodies, this may be reflective of an ineffective immune reaction similar to human patients that present with anti-tumor antibodies that afford no disease protection. It is important to note that while the proportion of B1:B2 cells increases with cancer, the percentage of both B1 and B2 lymphocytes in the PSF leukocyte population actually decreases as a result of shifting R1:R2 ratios.

Following cancer cell administration, there was a significant and massive increase in the $CD11b^+Ly6C^+$ $Ly6G^+$ population (Figure 4.5B; p<0.001). We believe this to be the $CD11b^+Ly6C^+Ly6G^+$

tumor-associated neutrophil population (TANs) previously described by Fridlender et al[36, 37]. In conjunction with this increase, the $CD11b^{lo/+}F480^{-}$ monocyte subset levels significantly decreased as a result of cancer (Figure 4.5E). Hence the hallmark signature of nulliparous animals bearing cancer was the increase in TANs and loss of $CD11b^{lo/+}$F480- monocytes in the OFB. It is important to re-emphasize that while the proportion of some cell subsets did not change in the OFB microenvironment, net gain in cell populations was vastly increased as a result of cancer, evidenced by the large increase in overall SVF counts.

To complement our FACS analysis, we utilized qRT-PCR to more extensively characterize the overall signaling milieu of the OFB microenvironment as a consequence of peritoneal cancer dissemination. Expression patterns represent the tissue as a whole, and thus are reflective of adipocytes, the SVF, and cancer cells (in the MOSE-L_{FFLv} groups) embedded within the tissue. A panel of cytokines and chemokines was used to provide an overview of genes that may contribute to a pro-tumorigenic microenvironment (Supplementary Table S4.3). We found that expression of B cell chemoattractants (CXCL13, IL-5) were significantly downregulated, while monocyte-associated cytokines (CCL2, CCL20, iNOS, Arg1, Ym1) and neutrophil chemoattractants (CXCL1, CXCL3, CXCL5, CCL3) were significantly upregulated in nulliparous mice as a consequence of cancer (Figure 4.5F). These changes in the microenvironment transcriptome support the cellular changes found in the $CD45^{+}$ SVF, namely that there is a decrease in the proportion of B cells, and an approximately 100-fold increase in TANs in the OFB of cancer-bearing nulliparous mice.

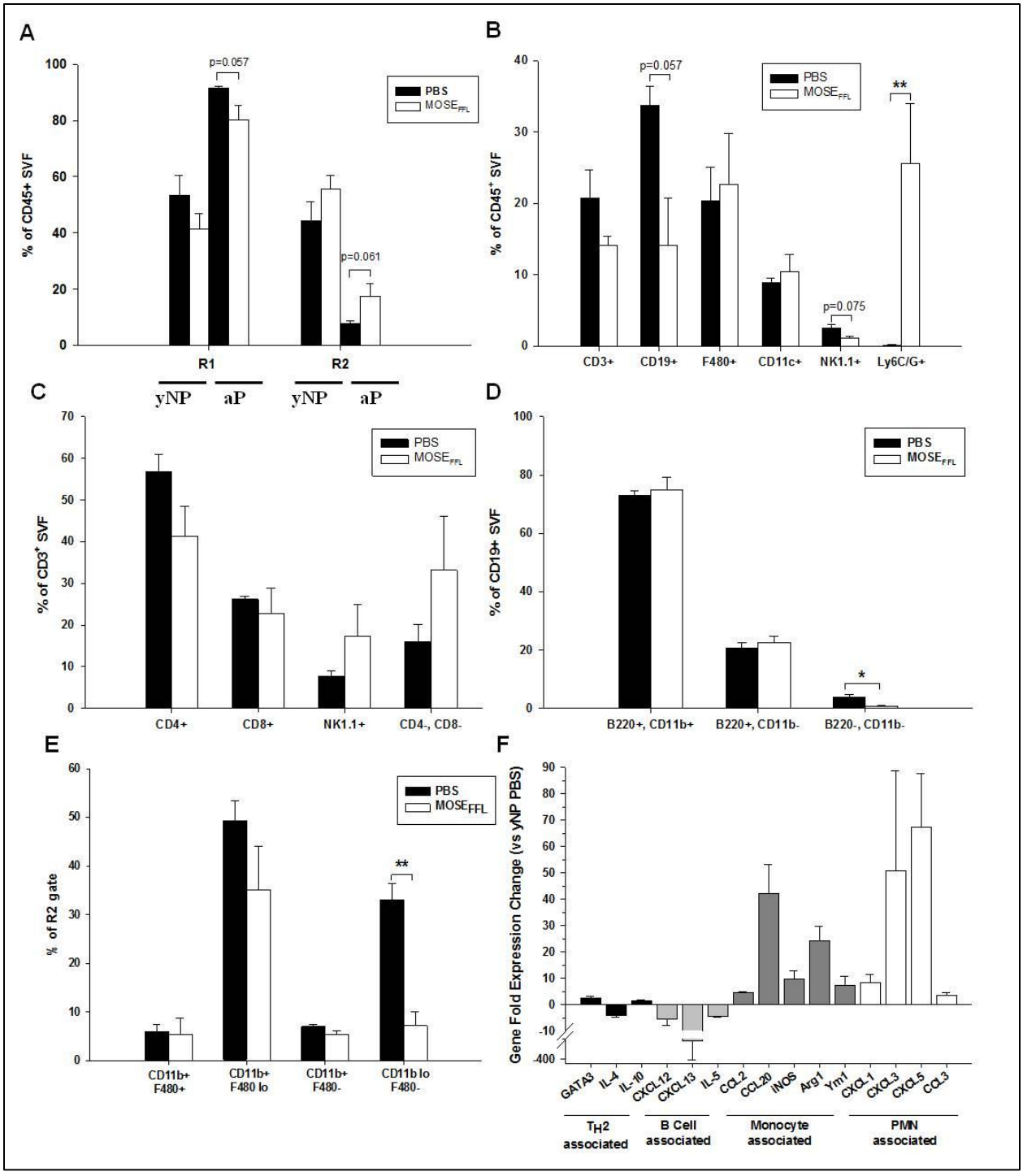

Figure 4.5. Ovarian cancer outgrowth causes macrophage and neutrophil influx in the OFB in nulliparous mice. Young adult nulliparous (yNP) mice +/- MOSE-L_{FFLv} cells. **A)** Distribution of R1:R2 leukocyte populations in yNP and aP OFB with MOSE-L_{FFLv}. **B)** Overall leukocyte population changes in OFB of yNP mice with MOSE-L_{FFLv} seeding. **C)** $CD3^+$ subset changes within OFB in yNP mice with MOSE-L_{FFLv} seeding. **D)** $CD19^+$ subset changes within OFB in yNP mice with MOSE-L_{FFLv} seeding. **E)** Monocyte/granulocyte subset changes within omentum in yNP mice with MOSE-L_{FFLv} seeding. **F)** Gene expression changes in yNP OFB with MOSE-L_{FFLv} seeding. All genes displayed were significantly changed from PBS control, * $p<0.05$. ** $p<0.01$

Interestingly, in contrast to nulliparous cancer-bearing animals, there was no significant net gain of $CD45^+$ cells in the OFB as a consequence of cancer in parous animals (Figure 4.4C), suggesting that recruitment signals may be compromised or dampened in the parous state. However, a similar shift in the leukocyte populations was detected in the parous omenta following cancer cell seeding, denoted by a slight decline in $CD3^+$ and $CD19^+$ cells and a slight increase in $F480^+$ and $CD11b^+Ly6C^+Ly6G^+$ cells (TANs) (Figure 4.6A). Notably, the influx of the TANs was reduced considerably, representing approximately 7% of the total $CD45^+$ population, compared to the 25% observed in nulliparous cancer-bearing animals (see also Figure 4.5C). This suggests that cancer mediated recruitment of TANs to the OFB may be compromised or dampened as a consequence of parity. In addition, a significant decline in $CD11b^{lo/+}F480^+$ monocytes was not observed in parous animals as a consequence of cancer seeding (Figure 4.6D), as determined in nulliparous mice. These levels were already significantly elevated in the homeostatic parous OFB and may serve an anti-tumorigenic function. The PSF also displayed an increase in TANs as a result of cancer cell dissemination ($p<0.01$, Supplementary Table 4.2), although this trend was also significantly reduced as compared to nulliparous mice ($p<0.05$). Additionally, the PSF in parous animals displayed a loss of LPMs, and an increase in SPMs with MOSE-L_{FFLv} dissemination. While the recruitment of SPMs into the PSF is indicative of an innate-like inflammatory response, in the case of parous animals this state may be able to override, at least transiently, the inherent immunosuppressive program elicited by the MOSE-L_{FFLv} cells.

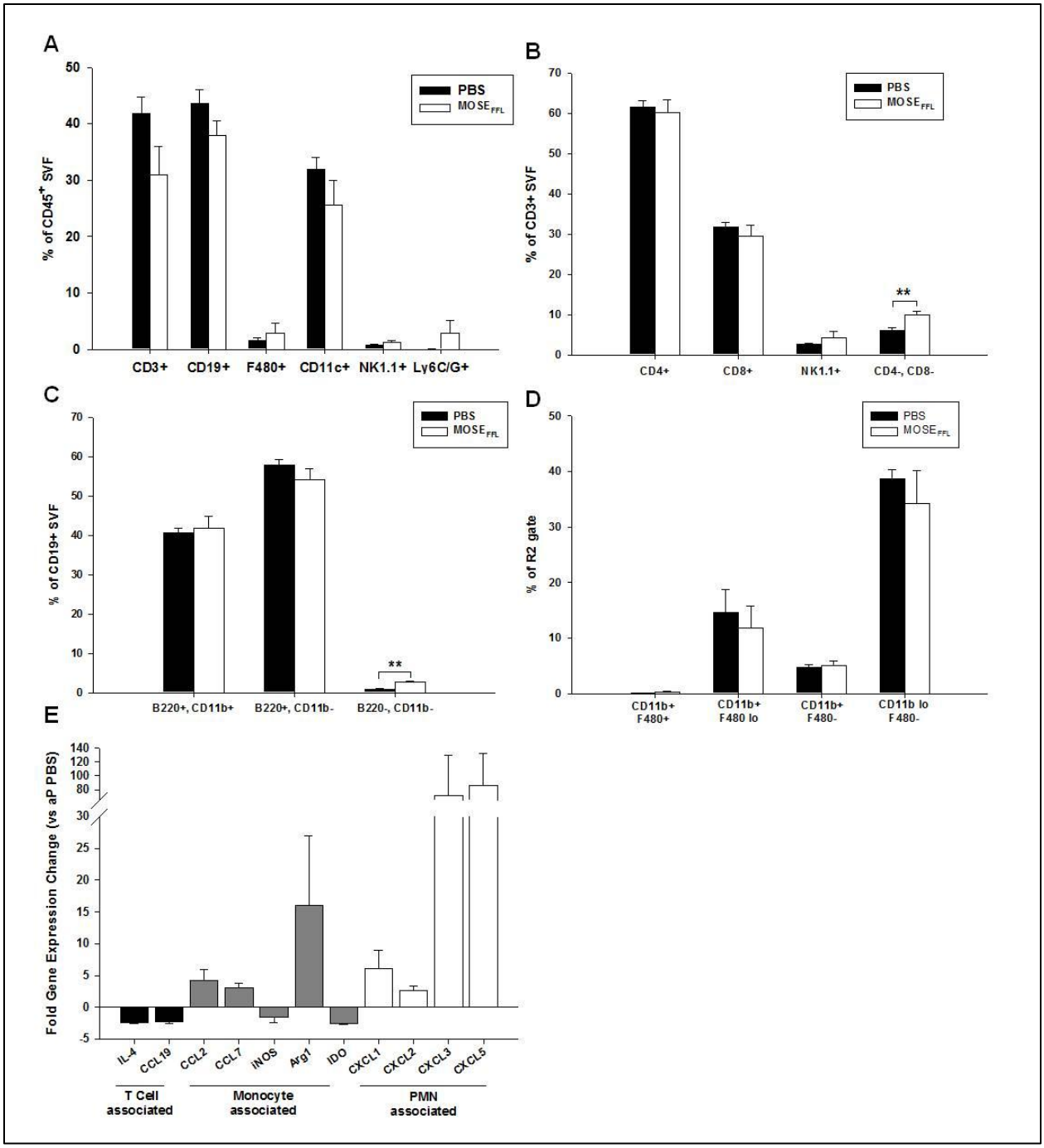

Figure 4.6. Parity reduces ovarian cancer outgrowth-associated influx of macrophages and neutrophils to the OFB. Mature adult parous (aP) mice +/- MOSE-L_{FFLv}. **A)** Overall leukocyte population changes in OFB of aP mice with MOSE-L_{FFLv}. **B)** $CD3^+$ subset changes within OFB in aP mice with MOSE-L_{FFLv}. **C)** $CD19^+$ subset changes within OFB in aP mice with MOSE-L_{FFLv}. **D)** Monocyte/granulocyte subset changes within OFB in aP mice with MOSE-L_{FFLv}. **E)** Gene expression changes in aP OFB with MOSE-L_{FFLv}. All genes displayed were significantly changed from PBS control, $p<0.05$. **$p<0.01$

It should also be noted that all lymphocyte subsets were maintained at high levels in the OFB of parous animals, irrespective of cancer. Sustained high levels of immune cells may help to maintain an activated state that is less conducive to cancer cell proliferation. It was noted that the B-lymphocyte subset distribution was shifted towards the B2 phenotype in parous animals (Figure 4.6C) which was the opposite trend to that observed in nulliparous animals (Figure 4.5D).

Comparative assessment of the gene expression profile (qRT-PCR) of omenta as a consequence of cancer revealed that several neutrophil chemoattractants were significantly upregulated in the OFB of cancer-bearing parous mice (Figure 4.6E). As these correlate with recruitment of TANs, we conclude that the parous microenvironment is somehow able to override the favorable protumorigenic niche that these cells help establish, such that tumor proliferation is reduced. Thus, the pre-existing parity-associated microenvironment may be naturally inclined to limit aggressive tumor growth. Understanding what defines the transient nature of this refractory state may provide novel insights to modulate and maintain this state in order to prevent recurrent disease.

DISCUSSION

Epidemiological studies indicate that parity reduces the risk of ovarian and breast cancer development. The molecular mechanisms behind the parity-related decrease in ovarian cancer incidence remain unclear but reports from breast cancer studies indicate a protective effect against primary tumor growth and cancer metastasis but not against neoplastic transformation [18, 20, 21, 30, 38]. It is possible that child-bearing results in a naturally occurring protective state that, if defined, could be harnessed and utilized in the treatment of ovarian cancer, preventing fatal metastatic outgrowth.

As a largely asymptomatic disease until the late stages, ovarian cancer is rarely detected prior to metastasis. The OFB is the primary metastatic site and is typically removed during surgical tumor debulking in an attempt to slow disease progression. However, as a secondary lymphoid organ, the OFB plays an important role in immunosurveillance in the peritoneal cavity; its removal results in impaired anti-bacterial responses in the abdomen, and an increased risk of sepsis after surgery[39].

In the present study, we compared the immune profiles of the OFB as a function of age and parity to begin characterization of a pre-existing immune niche that may be refractory to tumor growth. To this end, we determined the leukocyte composition and cytokine expression profiles of the OFB and PSF, both in the homeostatic state and following aggressive ovarian cancer cell implantation. In the homeostatic state, parity (but not age) resulted in a marked decrease in monocytic cell subsets and affiliated chemoattractants, and a shift to predominantly B2, as opposed to B1 B cells. After metastasis, parous mice exhibited a significantly reduced tumor burden as compared to nulliparous mice. In addition, the tumor microenvironment was characterized by an increase in TANs and TAMs, and an increase in B1 cells in nulliparous animals; a trend that was somewhat dampened in parous mice in conjunction with decreased tumor growth. Thus, we believe the parous OFB compositional profile is indicative of a pre-existing niche that is refractory to metastasis.

In order to more fully delineate the changes indicative of an inherently protective immune microenvironment, we evaluated a panel of immunoregulatory cytokines and chemokines in an attempt to determine an expression signature indicative of a protective state. This is schematically presented in Figure 4.7, to highlight the statistically significant gene expression changes associated with age, parity, cancer metastasis, or any combination therein (Figure 4.7, $p<0.05$; see Supplementary Table S4.3-4.6 for full list of genes evaluated). Hence we were able to determine age-related cytokine expression changes, irrespective of parity. We found a significantly increased expression of CXCL13 and IL-2 in the OFB of mature nulliparous mice, which is most likely indicative of reported age-related increases in milky spots dispersed throughout this tissue; CXCL13 is a B cell chemoattractant, and IL-2 induces the proliferation and activation of T cells, both important signaling molecules in secondary lymphoid organs. Parity (but not age) in the homeostatic state was associated with a significant decrease in a wide variety of chemoattractants for neutrophils (CXCL1, CXCL2; $p<0.05$) and monocytes (CCL2, MCSF $p<0.05$), as well as markers typically associated with an alternately activated, pro-tumorgenic phenotype (Arg1, M6pr, $p<0.05$). This data correlates well with the observed reduction of these cell types in the parous OFB based on FACS analysis, and may partially define the metastasis-resistant microenvironment. The

most conspicuous cancer-related finding was the significant increase in neutrophil chemoattractants, specifically CCL3, CXCL1, -2, -3 and -5 ($p<0.05$). Cancer-bearing mice, irrespective of parity, also had increased Arg1 expression, and young adult nulliparous mice had increased Ym1 expression, indicative of the presence of tumor-associated macrophages and a pro-tumorigenic microenvironment. This information could be valuable in the definition of the parous OFB as a naturally occurring protective microenvironment against ovarian cancer metastasis.

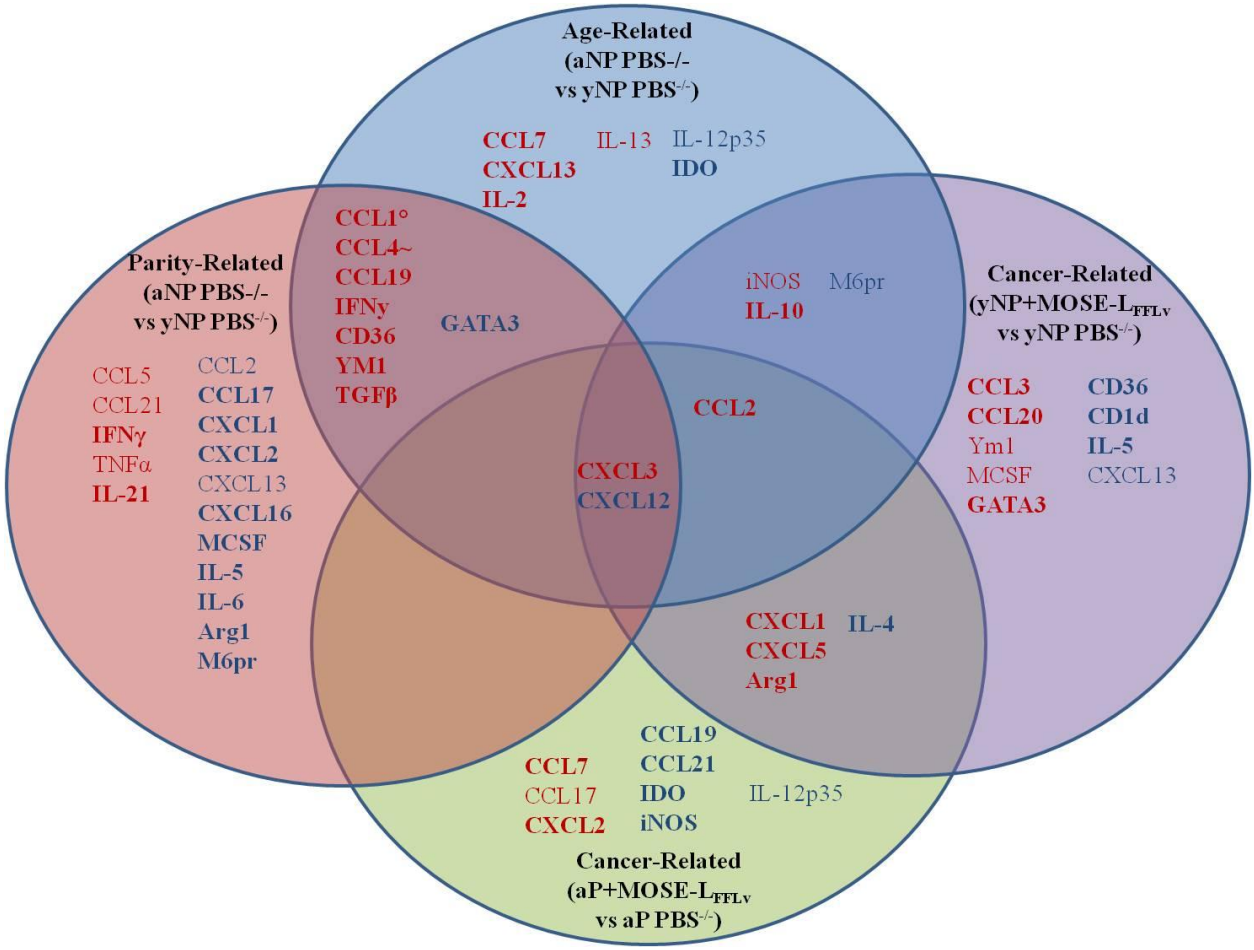

Figure 4.7. Gene expression changes in the OFB associated with age, parity, or cancer cell seeding. Genes in bold, $p<0.05$, genes in normal typeface $p=0.05$-0.08. Red indicates increased expression, blue indicates decreased expression.

Given the wealth of knowledge regarding the pro-tumorigenic nature of tumor-associated macrophages (TAMs)[40, 41], tumor-associated neutrophils (TANs)[42, 43], and myeloid-derived suppressor

cells (MDSCs)[44, 45], the cancer-related influx of these cell types is not surprising. Therefore we believe the decrease in these monocytic subsets in parous mice may partially define the pre-existing protective niche in the OFB. In other words, parity leads to a downregulation in the levels of cell subsets amenable to pro-tumorigenic polarization within the peritoneal cavity. A microenvironment that lacks these subsets, or is partially refractory to their recruitment following cancer cell seeding may slow the dynamics of cancer metastasis, resulting in delayed disease development, as we have shown.

The parous OFB was defined by an increased proportion of lymphocytes, both T and B cells. Tumor-infiltrating lymphocytes (TILs) have been correlated with improved prognosis and survival in a variety of cancer models, both mouse and human[46, 47, 48]. Therefore, we believe a net gain in lymphocytes may be another attribute of the protective parity signature in the OFB. While the effects of T cell populations in the tumor microenvironment have been well defined with the general trend being that an increase in tumor-associated T cells generally correlates with improved prognosis, the relationship between B cells and the pro-tumorigenic niche is not as well understood. In many murine studies the contribution of B cells to the tumor microenvironment has been largely overlooked; this is partially due to the effectiveness of $CD8^+$ T cell-mediated tumor cell killing when not suppressed by the tumor environment[49]. However, clinical studies, which typically extend over several years and are more indicative of the slowly developing pro-tumorigenic niche, have provided evidence of the importance of B cells in the tumor milieu[49]. Despite numerous reports alluding to anti-tumorigenic antibodies present in cancer patients there has been no real correlation between serum antibodies and improved prognosis. There is a much smaller, less cohesive collection describing tumor-infiltrating B cells (TIL-Bs) and their impacts on cancer progression[49, 50].

Recently, identification of a subset of $CD20^+$ tumor infiltrating B cells (TIL-Bs) that are strongly correlated with survival in ovarian cancer was reported. Here it was noted that the presence of $CD20^+$ cells together with $CD8^+$ T cells in the tumor microenvironment were associated with higher survival rates than the occurrence of either cell type alone, indicating a protective interaction[51]. Following IL-21 stimulation, TIL-Bs were able to produce granzyme B, which would be cytotoxic to tumors; and with

IFNα or TLR agonist stimulation, TIL-Bs directly kill tumor cells via TRAIL signaling[52, 53], indicating the active anti-tumorigenic role of these cells.

Killer B cells have also been described that produce apoptotic death-inducing ligands like Fas ligand (FasL, CD178), tumor necrosis factor-related apoptosis-inducing ligand (TRAIL) and programmed death ligands 1 and 2 (PD-L1, CD274 and PD-L2, CD273)[54]. However, the presence of these cells in the tumor microenvironment has actually been shown to inhibit protective immune responses, inducing apoptosis of cytolytic effector cells instead of malignant cells[54]. Regulatory B cells, which are characterized by the production of TGFβ and IL-10, also dampen immune responses, and have also been shown to inhibit protective immune responses against tumors[55]. These cells impair the priming of $CD8^+$ T cells, promoting a weak non-protective humoral response that is ineffective in tumor clearance. Hence, B cells are gaining widespread acceptance as key regulators and modulators or both pro- and anti-tumorigenic responses.

In our study, there was a shift in the B cell distribution from the nulliparous OFB which contained primarily B1 cells[23] to the predominantly B2 cells present in the parous OFB. B1 cells play an important role in immunosurveillance in the peritoneal cavity, and there is a constant flux between the PSF and the OFB. During infection, B1 cells generate large amounts of low-affinity IgM, IgA and IgG3, ensuring early protection[56]. B1 cells have been described as the precursors of tumor-promoting regulatory B cells[57]. Additionally, B1 cells themselves can express MUC18 (melanoma cell adhesion molecule) on their surface, and were found to bind to MUC18-expressing melanoma cells, enhancing melanoma metastasis in vivo through these MUC18/MUC18 interactions[58]. $CD5^+$ B1 cells also possess many of the above mentioned regulatory properties, including constitutive FasL and PD-L 2 expression and the ability to produce IL-10. If B1 cells are in fact the precursors to regulatory pro-tumorigenic cells in the OFB microenvironment, it stands to reason that a reduction in this cell subset in parous mice would contribute to a pre-existing protective niche that is refractory to metastatic growth. It is also interesting to speculate that while the B2 subset is predominant in the parous OFB in the homeostatic state, with cancer cell

seeding, the proportion of B1:B2 cells increases in both parous and nulliparous mice (data not shown). This supports the theory that B1 cells are polarized into a pro-tumorigenic population.

The effect of intratumoral B cells on disease progression is dependent on the timing of B cell infiltration. Thus, in established tumors, B cells seem to have a negative or suppressive effect, while early infiltration may elicit anti-tumorigenic responses[50]. With the recent renewed interest in and importance of tumor-infiltrating B cells, future studies utilizing additional functional markers are clearly warranted to determine the exact nature of the B cell subtypes within the parous omenta. However, it is interesting to speculate that the loss of "innate-like" B1 cells and influx of B2 cells in the OFB of parous mice reported here helps establish an anti-metastatic niche and represents another element of the protective parity signature.

We demonstrate here that parity was indeed associated with a significant reduction in peritoneal tumor burden following ovarian cancer cell implantation in the peritoneal cavity. The most significant population trend that we found in cancer-bearing mice was an increase in the proportion of infiltrating neutrophils to the OFB. These are highly similar to the TANs previously reported by Fridlender et al[37], and the reduced infiltration seen in parous mice represents another protective element of the parous microenvironment. TANs are a significant portion of the inflammatory infiltrate in a variety of tumor microenvironments and numerous cancer cell lines express neutrophil chemoattractants, highlighting their importance in supporting the tumor milieu[59, 60, 61, 62]. Additionally, depletion of TANs limits tumor metastasis, and neutrophil presence in tumors is correlated with poor prognosis in clinical settings[60, 63, 64]. The presence of TGFβ in the tumor microenvironment has been reported to be the driving factor in the polarization of neutrophils to a pro-tumorigenic (or "N2") type. We found that TGFβ expression is increased 100-fold in the OFB in both older nulliparous and parous animals. This age-related increase may play a crucial role in the association of increased ovarian cancer incidence in post-menopausal women. Decreased tumor burden in parous mice may be a result of decreased monocytic subsets present within the OFB, despite increased TGFβ expression.

Parity also resulted in an almost complete loss of $CD45^-$ progenitor populations present within the OFB. An important component in the tumor cellular milieu is the stromal contingent. These cells are recruited from adipose tissue and bone marrow in order to provide crucial growth factors, matrices, cytokines and nutrients in order to support rapid tumor growth[65, 66]. The loss of progenitor cells in the OFB may reflect another aspect of the "protective signature" associated with child-bearing, in that the scaffolding or accessory cells crucial to rapid tumor development are not initially available in situ. This may indicate a parity-associated differentiation or egress of $CD45^-$ progenitor populations within the OFB, in agreement with an increase in differentiation signals previously reported as part of a "parity signature" in mammary tissue[20, 21].

The OFB is not only important due to its role as a preferential site for ovarian cancer, but also because of its role in peritoneal immunosurveillance. Its removal results in subsequent impaired anti-bacterial responses in the abdomen, and an increased chance of sepsis following surgery[39]. Clearly, removal of this vital organ is not ideal, but it is generally regarded as necessary to help minimize recurrent disease. Thus, we believe it is critical to provide a comprehensive analysis of the molecular and cellular parity-induced changes, within this immunologically- and metastatically-relevant microenvironment. Further, we hypothesize that this information could define a "protected" state in the OFB, and provide insight into pathways that underlie this parity-associated protection. In turn, this parity-associated signature could provide a panel of molecular markers that could act as endpoints by which to evaluate the efficacy of immunotherapies designed to mimic this inherent protective state[20]. Here, we provide experimental data in support of epidemiological studies indicating that child-bearing provides inherent protection against ovarian cancer development, and we have defined specific immunological changes that occur in the primary metastatic niche as a result of this protective parous state. It is possible that this information could be used to re-polarize this active immune microenvironment towards an anti-tumorigenic manner in patients with late stage ovarian cancer. Future experiments should determine whether disease progression in parous mice is simply delayed as compared to nulliparous mice due to a different homeostatic immune profile, or progresses along a completely different pro-tumorigenic

mechanism. Finally, the efficacy of targeted manipulation of these cell subsets as a treatment modality for ovarian cancer metastasis is warranted.

SUPPLEMENTARY MATERIALS

Leukocyte Characterization (% of $CD45^+$ SVF, +/- SE)				
	Markers	**yNP PSF**	**aNP PSF**	**aP PSF**
% $CD45^+$ (of viable)		**98.3 (0.8)**	**99.3 (0.4)**	**99.9 (0.05)**
% lymphocytes		**55.2 (2.5)**	**66.4 (1.1)**	**84.8 (0.7)**
% mono/granulocytes (R2)		**44.0 (2.4)**	**30.4 (0.9)**	**14.9 (0.8)**
B cells	**$CD19^+$**	**64.7 (2.5)**	**73.9 (1.7)**	**80.6 (1.7)**
B1	**$CD19^+CD11b^+B220^{lo/+}$**	**46.3 (2.6)**	**58.4 (2.6)**	**32.5 (0.8)**
B2	**$CD19^+CD11b^-B220^{lo/+}$**	**15.8 (0.8)**	**13.9 (2.5)**	**47.3 (1.9)**
T cells	**$CD3^+$**	**6.3 (1.1)**	**5.2 (0.6)**	**9.6 (0.9)**
T_H	**$CD3^+CD4^+$**	**3.6 (0.5)**	**2.9 (0.4)**	**5.4 (0.7)**
T_C	**$CD3^+CD8^+$**	**2.0 (0.6)**	**1.8 (0.2)**	**3.5 (0.2)**
NKT	**$CD3^+NK1.1^+$**	**0.3 (0.2)**	**0.2 (0.08)**	**0.2 (0.01)**
T_{REG}	**$CD3^+CD4^+CD25^+$**	**0.1 (0.01)**	**0.9 (0.1)**	**0.7 (0.1)**
$CD3^+CD4^-CD8^-NK1.1^-$		**0.7 (0.1)**	**0.6 (0.04)**	**0.7 (0.05)**
mNK	**$NK1.1^+CD11b^+CD3^-$**	**0.3 (0.1)**	**0.7 (0.5)**	**0.2 (0.01)**
preNK	**$NK1.1^+CD11b^-CD3^-$**	**0.2 (0.03)**	**0.1 (0.05)**	**0.3 (0.02)**
R1 DCs	**$CD11c^+CD11b^{lo/+}$**	**1.7 (0.3)**	**5.2 (1.0)**	**5.8 (0.5)**
R2 DCs	**$CD11b^{+/lo}CD11c^+F4/80^-$**	**1.4 (0.4)**	**1.9 (0.3)**	**0.1 (0.01)**
LPMs	**$CD11b^+F4/80^+$**	**11.3 (1.4)**	**10.3 (1.1)**	**7.0 (1.0)**
SPMs	**$CD11b^+F4/80^{lo}$**	**2.4 (0.4)**	**5.4 (0.5)**	**1.0 (0.4)**
Monocytes	**$CD11b^+F4/80^-$**	**0.5 (0.1)**	**1.8 (0.3)**	**0.1 (0.04)**
Monocytes (2)	**$CD11b^{lo}F4/80^-$**	**13.1 (1.0)**	**12.2 (1.3)**	**4.5 (0.3)**
PMNs	**$CD11b^+Ly6G^+Ly6C^+$**	**0.07 (0.05)**	**0.02 (0.01)**	**0**
PreBoMs	**$CD19^+CD11b^{hi}B220^{lo}F480^+$ $CD93^+CD69^+$**	**0**	**0.2 (0.02)**	**0.1 (0.005)**

Supplementary Table S4.1. FACS analysis of age- and parity-associated changes in leukocyte composition in the PSF. Young adult nulliparous mice (yNP); mature adult nulliparous mice (aNP); mature adult parous mice (aP).

Leukocyte Characterization (% of $CD45^+$ SVF, +/- SE)					
		yNP mice		aP mice	
	Markers	$PBS^{-/-}$	MOSE-L_{FFLv}	$PBS^{-/-}$	MOSE-L_{FFLv}
% $CD45^+$ (of viable)		98.3 (0.8)	95.6 (1.7)	99.9 (0.05)	99.5 (0.2)
% lymphocytes		55.2 (2.5)	35.8 (11.0)	84.8 (0.7)	68.6 (1.6)
% mono/granulocytes (R2)		44.0 (2.4)	58.9 (9.5)	14.9 (0.8)	30.4 (1.6)
B cells	$CD19^+$	64.7 (2.5)	29.8 (12.3)	80.6 (1.7)	56.7 (7.4)
B1	$CD19^+CD11b^+B220^{lo/+}$	46.3 (2.6)	23.2 (9.0)	32.5 (0.8)	26.8 (9.3)
B2	$CD19^+CD11b^-B220^{lo/+}$	15.8 (0.8)	6.4 (3.2)	47.3 (1.9)	28.9 (8.3)
T cells	$CD3^+$	6.3 (1.1)	8.8 (2.6)	9.6 (0.9)	12.6 (2.3)
T_H	$CD3^+CD4^+$	3.6 (0.5)	5.4 (2.0)	5.4 (0.7)	8.2 (1.6)
T_C	$CD3^+CD8^+$	2.0 (0.6)	2.7 (0.6)	3.5 (0.2)	3.3 (0.7)
NKT	$CD3^+NK1.1^+$	0.3 (0.2)	0.3 (0.02)	0.2 (0.01)	0.1 (0.05)
T_{REG}	$CD3^+CD4^+CD25^+$	0.1 (0.01)	0.3 (0.2)	0.7 (0.1)	0.6 (0.2)
$CD3^+CD4^-CD8^-NK1.1^-$		0.7 (0.1)	0.5 (0.2)	0.7 (0.05)	1.0 (0.2)
mNK	$NK1.1^+CD11b^+CD3^-$	0.3 (0.1)	0.3 (0.1)	0.2 (0.01)	0.2 (0.02)
preNK	$NK1.1^+CD11b^-CD3^-$	0.2 (0.03)	0.1 (0.01)	0.3 (0.02)	0.2 (0.03)
R1 DCs	$CD11c^+CD11b^{lo/-}$	1.7 (0.3)	6.7 (2.3)	5.8 (0.5)	11.5 (1.5)
R2 DCs	$CD11b^{+/lo}CD11c^+F4/80^-$	1.4 (0.4)	1.6 (0.4)	0.1 (0.01)	0.5 (0.1)
LPMs	$CD11b^+F4/80^+$	11.3 (1.4)	15.4 (3.7)	7.0 (1.0)	1.0 (0.5)
SPMs	$CD11b^+F4/80^{lo}$	2.4 (0.4)	17.9 (5.3)	1.0 (0.4)	17.8 (1.6)
Monocytes	$CD11b^+F4/80^-$	0.5 (0.1)	0.4 (0.2)	0.1 (0.04)	0.5 (0.2)
Monocytes (2)	$CD11b^{lo}F4/80^-$	13.1 (1.0)	10.5 (1.0)	4.5 (0.3)	4.2 (1.5)
PMNs	$CD11b^+Ly6G^+Ly6C^+$	0.07 (0.05)	11.8 (4.4)	0	3.2 (2.7)
PreBoMs	$CD19^+CD11b^{hi}B220^{lo}F480^+$ $CD93^+CD69^+$	0	0	0.1 (0.005)	0.2 (0.08)

Supplementary Table S4.2. FACS analysis of cancer-associated changes in leukocyte composition in the PSF. Young adult nulliparous mice (yNP); mature adult parous mice (aP).

Gene Expression (Avg dCT ± SEM)			
Gene	**yNP PBS**	**aNP PBS**	**aP PBS**
CCL1	14.11 (.11)	12.47 (0.5)	12.68 (0.37)
CCL2	6.48 (0.2)	4.42 (0.2)	7.11 (0.2)
CCL3	11.32 (0.3)	10.79 (0.3)	10.42 (0.7)
CCL4	9.64 (0.2)	7.00 (0.2)	8.07 (0.6)
CCL5	3.50 (0.3)	2.82 (0.6)	2.57 (0.3)
CCL7	7.20 (0.3)	5.16 (0.2)	7.72 (0.1)
CCL17	9.42 (0.6)	10.29 (0.5)	12.07 (0.4)
CCL19	5.26 (0.2)	4.62 (0.1)	3.58 (0.3)
CCL20	19.02 (1.8)	16.58 (2.2)	17.80 (0.4)
CCL21	6.02 (1.0)	4.55 (0.7)	3.92 (0.1)
CXCL1	8.71 (0.2)	9.29 (0.2)	9.80 (0.2)
CXCL2	10.06 (0.2)	9.92 (0.2)	12.47 (0.2)
CXCL3	18.66 (1.4)	15.12 (0.8)	16.22 (0.3)
CXCL5	14.99 (0.7)	14.02 (0.2)	16.27 (0.4)
CXCL11	15.34 (0.1)	14.42 (0.4)	16.24 (0.5)
CXCL12	3.42 (0.1)	4.02 (0.2)	4.16 (0.1)
CXCL13	0.55 (0.3)	-1.08 (0.1)	1.75 (0.4)
CXCL16	5.13 (0.2)	4.73 (0.1)	6.48 (0.2)
CD36	6.70 (0.2)	0.24 (0.2)	0.85 (0.7)
IFNγ	13.25 (0.1)	11.25 (0.3)	9.75 (0.5)
Arg1	7.74 (0.6)	8.64 (0.2)	10.94 (0.4)
iNOS	13.71 (1.0)	11.79 (0.4)	12.03 (0.23)
IDO	12.72 (0.3)	15.15 (0.3)	11.72 (0.4)
GM-CSF	12.23 (0.2)	11.67 (0.3)	13.13 (0.5)
MCSF	7.28 (0.2)	6.98 (0.4)	8.31 (0.3)
M6pr	2.62 (0.1)	4.46 (0.8)	4.68 (0.3)
TGFβ	12.84 (0.7)	5.59 (0.3)	5.45 (0.2)
TNFα	12.42 (0.4)	12.11 (0.4)	11.28 (0.3)
Ym1	16.93 (0.4)	10.70 (0.3)	11.26 (1.1)
IL-1b	8.45 (0.7)	8.55 (0.7)	8.46 (0.6)
IL-2	12.33 (0.2)	11.68 (0.2)	11.99 (0.2)
IL-4	12.43 (0.3)	12.58 (0.8)	12.60 (0.2)
IL-5	10.62 (0.3)	11.76 (0.7)	13.02 (0.5)
IL-6	9.93 (0.2)	9.26 (0.2)	12.35 (0.2)
IL-10	9.74 (0.1)	8.70 (0.2)	9.65 (0.1)
IL-12p35	10.81 (0.5)	13.04 (0.7)	10.41 (0.2)
IL-13	15.93 (0.5)	14.59 (.04)	16.08 (0.3)
IL-17a	20.89 (1.89)	19.23 (1.5)	21.01 (1.0)
IL-21	13.39 (1.5)	13.12 (1.2)	9.84 (0.5)
Tbet	8.73 (0.1)	8.17 (0.2)	8.09 (0.4)
GATA3	9.16 (0.1)	12.51 (0.8)	10.20 (0.3)
Foxp3	9.40 (0.4)	10.02 (0.3)	8.72 (0.3)

SupplementaryTable S4.3. Gene expression analysis of age- and parity-associated changes in the OFB. Young adult nulliparous mice (yNP); mature adult nulliparous mice (aNP); mature adult parous mice (aP).

Fold Expression Change ± SEM (vs yNP PBS)		
Gene	**aNP PBS**	**aP PBS**
CCL1	4.25 (1.8)	3.0 (0.8)*
CCL2	4.28 (0.5)**	-1.52 (0.2)^
CCL3	1.52 (0.2)	2.64 (1.1)
CCL4	6.38 (0.6)**	3.83 (1.6)^
CCL5	1.74 (0.4)	2.03 (0.4)^
CCL7	4.26 (0.5)**	-1.42 (0.6)
CCL17	-1.65 (0.6)	-5.62 (1.8)*
CCL19	1.59 (0.2)*	3.33 (0.5)**
CCL20	38.7 (37.5)	2.64 (0.8)
CCL21	3.97 (1.2)	4.33 (0.4)^
CXCL1	-1.42 (0.3)	-2.04 (0.3)*
CXCL2	1.15 (0.2)	-5.20 (0.6)**
CXCL3	22.9 (15.1)^	5.71 (1.1)
CXCL5	2.01 (0.2)	-2.20 (0.7)
CXCL11	2.19 (0.6)	-1.61 (0.7)
CXCL12	-1.48 (0.1)*	-1.66 (0.1)**
CXCL13	3.12 (0.2)**	-2.03 (0.7)
CXCL16	1.32 (0.9)	-2.51 (0.3)**
CD36	91.0 (11.6)**	79.2 (31.8)**
IFNγ	4.42 (1.0)**	13.41 (4.0)**
Arg1	-1.82 (0.3)	-8.08 (2.01)**
iNOS	4.38 (1.2)^	3.32 (0.5)
IDO	-5.0 (1.1)**	2.30 (0.7)
GM-CSF	1.55 (0.4)	-1.62 (0.7)
MCSF	1.44 (0.4)	-1.93 (0.5)
M6pr	-2.77 (2.9)	-3.99 (0.9)**
TGFβ	162.8 (26.6)**	174.8 (30.2)**
TNFα	1.47 (0.4)	2.32 (0.4)^
Ym1	82.3 (16.9)**	130.8 (104.2)**
IL-1b	1.25 (0.3)	1.25 (0.5)
IL-2	1.61 (0.2)^	1.31 (0.2)
IL-4	1.66 (1.0)	-1.08 (0.2)
IL-5	-1.40 (1.4)	-4.49 (2.1)*
IL-6	1.66 (0.2)	-5.27 (0.6)**
IL-10	2.11 (0.2)**	1.10 (0.1)
IL-12p35	-3.04 (4.3)^	1.35 (0.1)
IL-13	2.87 (0.6)^	1.0 (0.2)
IL-17a	6.79 (3.3)	1.94 (1.4)
IL-21	2.02 (0.8)	13.7 (4.0)*
Tbet	1.54 (0.2)	1.75 (0.5)
GATA3	-7.6 (4.6)*	-1.95 (0.3)*
Foxp3	-1.47 (0.5)	1.71 (0.4)

Supplementary Table S4.4. Age- and parity-associated gene expression changes expressed as fold changes in the OFB. Young adult nulliparous mice (yNP); mature adult nulliparous mice (aNP); mature adult parous mice (aP).

*: $p<0.05$ **: $p<0.01$ ^: $p=0.08$-0.05

Gene Expression (Avg dCT ± SEM)		
Gene	**yNP FFL**	**aP FFL**
CCL1	13.53 (1.6)	13.15 (0.5)
CCL2	4.29 (0.2)	5.40 (0.5)
CCL3	9.62 (0.5)	10.85 (0.3)
CCL4	8.51 (0.6)	8.29 (0.2)
CCL5	5.46 (1.3)	3.15 (0.3)
CCL7	6.88 (0.6)	6.28 (0.4)
CCL17	9.80 (1.5)	10.85 (0.4)
CCL19	8.61 (2.0)	4.96 (0.4)
CCL20	13.72 (0.4)	17.39 (1.0)
CCL21	10.82 (2.3)	5.41 (0.3)
CXCL1	6.01 (0.8)	7.70 (0.6)
CXCL2	8.81 (0.9)	11.27 (0.4)
CXCL3	14.05 (1.3)	11.96 (1.1)
CXCL5	9.08 (0.5)	10.75 (0.9)
CXCL11	14.03 (1.2)	16.0 (0.5)
CXCL12	6.14 (0.6)	5.13 (0.4)
CXCL13	6.45 (2.6)	2.51 (0.7)
CXCL16	4.79 (0.3)	6.31 (0.3)
CD36	13.66 (1.2)	1.26 (0.7)
IFNγ	15.30 (1.4)	10.14 (0.4)
Arg1	3.20 (0.3)	8.01 (0.8)
iNOS	10.70 (0.7)	12.58 (0.1)
IDO	15.97 (1.8)	13.16 (0.3)
GM-CSF	13.92 (0.9)	13.25 (0.5)
MCSF	6.62 (0.2)	7.69 (0.3)
M6pr	4.33 (0.6)	4.74 (0.2)
TGFβ	12.10 (0.6)	5.86 (0.3)
TNFα	12.90 (1.0)	11.53 (0.4)
Ym1	14.51 (1.0)	11.05 (0.7)
IL-1b	8.05 (0.6)	8.85 (0.4)
IL-2	15.82 (1.9)	12.52 (0.4)
IL-4	14.47 (0.3)	14.02 (0.4)
IL-5	12.77 (0.1)	13.27 (0.4)
IL-6	10.85 (0.5)	11.95 (0.3)
IL-10	9.10 (0.1)	10.00 (0.4)
IL-12p35	12.38 (1.1)	11.49 (0.5)
IL-13	14.34 (2.0)	15.55 (0.2)
IL-17a	24.07 (0.9)	22.08 (0.3)
IL-21	14.93 (1.9)	10.80 (0.5)
Tbet	10.90 (1.4)	9.03 (0.3)
GATA3	7.82 (0.3)	10.08 (0.1)
Foxp3	10.70 (1.5)	9.60 (0.4)

Supplementary Table S4.5. Gene expression analysis of cancer-associated changes in the OFB. Young adult nulliparous mice (yNP); mature adult parous mice (aP).

Fold Expression Change ± SEM (vs PBS)		
Gene	**yNP FFL**	**aP FFL**
CCL1	4.93 (4.4)	-1.09 (0.2)
CCL2	4.61 (0.5)**	4.19 (1.7)*
CCL3	3.57 (1.0)*	-1.19 (1.0)
CCL4	2.67 (1.1)	-1.14 (10.3)
CCL5	-1.71 (3.5)	-1.34 (1.5)
CCL7	1.52 (0.7)	3.06 (0.7)
CCL17	2.26 (1.98)	2.61 (0.5)^
CCL19	-1.88 (13.5)	-2.32 (0.3)*
CCL20	42.23 (11.0)*	2.75 (1.4)
CCL21	-3.27 (53.9)	-2.55 (0.3)**
CXCL1	8.17 (3.2)*	6.05 (2.8)*
CXCL2	3.53 (2.2)	2.66 (0.7)*
CXCL3	50.73 (38.6)^	71.27 (58.1)*
CXCL5	67.3 (20.4)**	86.49 (45.9)**
CXCL11	4.84 (3.7)	1.42 (0.4)
CXCL12	-5.30 (2.6)*	-1.69 (1.1)^
CXCL13	-353.3 (48.9)^	-1.07 (0.6)
CXCL16	1.31 (0.2)	1.23 (0.3)
CD36	-61.12 (91.0)**	1.14 (0.4)
IFNy	-1.22 (4.6)	-1.17 (3.8)
Arg1	24.44 (5.5)**	15.99 (11.0)*
iNOS	9.62 (3.3)^	-1.45 (0.9)
IDO	-2.58 (16.7)	-2.54 (0.2)*
GM-CSF	-2.20 (2.5)	1.15 (0.4)
MCSF	1.6 (0.2)^	1.65 (0.3)
M6pr	-2.67 (1.3)^	-1.00 (1.6)
TGFβ	2.04 (0.9)	-1.25 (4.7)
TNFα	1.19 (0.8)	-1.04 (1.5)
Ym1	7.53 (3.5)^	1.84 (0.9)
IL-1b	1.58 (0.7)	-1.10 (0.1)
IL-2	-2.43 (13.8)	-1.23 (0.8)
IL-4	-4.0 (0.9)**	-2.42 (0.2)*
IL-5	-4.14 (0.4)**	1.01 (0.3)
IL-6	1.63 (0.6)	1.41 (0.2)
IL-10	1.56 (0.09)*	-1.12 (1.9)
IL-12p35	-1.72 (2.6)	-1.75 (0.5)
IL-13	6.23 (5.46)	1.48 (0.2)
IL-17a	-6.08 (5.1)	-1.92 (3.0)
IL-21	1.67 (1.6)	-1.68 (1.1)
Tbet	-1.76 (5.0)	-1.75 (0.6)
GATA3	2.63 (0.5)	1.10 (0.1)
Foxp3	1.08 (0.9)	-1.63 (1.9)

Supplementary Table S4.6. Cancer-associated gene expression changes in the OFB expressed as fold change. Young adult nulliparous mice (yNP); mature adult parous mice (aP).

*: $p<0.05$ **: $p<0.01$ ^: $p=0.08$-0.05

REFERENCES

1. Siegel R, Naishadham D, Jemal A. Cancer statistics, 2012. *CA: a cancer journal for clinicians* 2012, **62**(1)**:** 10-29.
2. Hunn J, Rodriguez GC. Ovarian cancer: etiology, risk factors, and epidemiology. *Clinical obstetrics and gynecology* 2012, **55**(1)**:** 3-23.
3. Benson JR, Jatoi I, Keisch M, Esteva FJ, Makris A, Jordan VC. Early breast cancer. *Lancet* 2009, **373**(9673)**:** 1463-1479.
4. Stone RL, Sood AK, Coleman RL. Collateral damage: toxic effects of targeted antiangiogenic therapies in ovarian cancer. *The lancet oncology* 2010, **11**(5)**:** 465-475.
5. Nieman KM, Kenny HA, Penicka CV, Ladanyi A, Buell-Gutbrod R, Zillhardt MR*, et al.* Adipocytes promote ovarian cancer metastasis and provide energy for rapid tumor growth. *Nature medicine* 2011, **17**(11)**:** 1498-1503.
6. Krishnan V, Stadick N, Clark R, Bainer R, Veneris JT, Khan S*, et al.* Using MKK4's metastasis suppressor function to identify and dissect cancer cell-microenvironment interactions during metastatic colonization. *Cancer metastasis reviews* 2012, **31**(3-4)**:** 605-613.
7. Kenny HA, Dogan S, Zillhardt M, A KM, Yamada SD, Krausz T*, et al.* Organotypic models of metastasis: A three-dimensional culture mimicking the human peritoneum and omentum for the study of the early steps of ovarian cancer metastasis. *Cancer treatment and research* 2009, **149:** 335-351.
8. Krist LF, Eestermans IL, Steenbergen JJ, Hoefsmit EC, Cuesta MA, Meyer S*, et al.* Cellular composition of milky spots in the human greater omentum: an immunochemical and ultrastructural study. *The Anatomical record* 1995, **241**(2)**:** 163-174.
9. Gerber SA, Rybalko VY, Bigelow CE, Lugade AA, Foster TH, Frelinger JG*, et al.* Preferential attachment of peritoneal tumor metastases to omental immune aggregates and possible role of a unique vascular microenvironment in metastatic survival and growth. *The American journal of pathology* 2006, **169**(5)**:** 1739-1752.
10. Park HT, Lee ES, Cheon YP, Lee DR, Yang KS, Kim YT*, et al.* The relationship between fat depot-specific preadipocyte differentiation and metabolic syndrome in obese women. *Clinical endocrinology* 2012, **76**(1)**:** 59-66.
11. Gray KS, Collins CM, Speck SH. Characterization of omental immune aggregates during establishment of a latent gammaherpesvirus infection. *PloS one* 2012, **7**(8)**:** e43196.
12. Krist LF, Kerremans M, Broekhuis-Fluitsma DM, Eestermans IL, Meyer S, Beelen RH. Milky spots in the greater omentum are predominant sites of local tumour cell proliferation and accumulation in the peritoneal cavity. *Cancer immunology, immunotherapy : CII* 1998, **47**(4)**:** 205-212.
13. Sorensen EW, Gerber SA, Sedlacek AL, Rybalko VY, Chan WM, Lord EM. Omental immune aggregates and tumor metastasis within the peritoneal cavity. *Immunologic research* 2009, **45**(2-3)**:** 185-194.
14. Collins D, Hogan AM, O'Shea D, Winter DC. The omentum: anatomical, metabolic, and surgical aspects. *Journal of gastrointestinal surgery : official journal of the Society for Surgery of the Alimentary Tract* 2009, **13**(6)**:** 1138-1146.
15. Khan S, Taylor JL, Rinker-Schaeffer CW. Disrupting ovarian cancer metastatic colonization: insights from metastasis suppressor studies. *Journal of oncology* 2010, **2010:** 286925.
16. Siegel R, DeSantis C, Virgo K, Stein K, Mariotto A, Smith T*, et al.* Cancer treatment and survivorship statistics, 2012. *CA: a cancer journal for clinicians* 2012, **62**(4)**:** 220-241.

17. Lim HY, Ju HY, Chung HY, Kim YS. Antitumor effects of a tumor cell vaccine expressing a membrane-bound form of the IL-12 p35 subunit. *Cancer biology & therapy* 2010, **10**(4)**:** 336-343.
18. Stewart LM, Holman CD, Aboagye-Sarfo P, Finn JC, Preen DB, Hart R. In vitro fertilization, endometriosis, nulliparity and ovarian cancer risk. *Gynecologic oncology* 2013, **128**(2)**:** 260-264.
19. Poole EM, Merritt MA, Jordan SJ, Yang HP, Hankinson SE, Park Y*, et al.* Hormonal and Reproductive Risk Factors for Epithelial Ovarian Cancer by Tumor Aggressiveness. *Cancer epidemiology, biomarkers & prevention : a publication of the American Association for Cancer Research, cosponsored by the American Society of Preventive Oncology* 2013.
20. D'Cruz CM, Moody SE, Master SR, Hartman JL, Keiper EA, Imielinski MB*, et al.* Persistent parity-induced changes in growth factors, TGF-beta3, and differentiation in the rodent mammary gland. *Molecular endocrinology* 2002, **16**(9)**:** 2034-2051.
21. Blakely CM, Stoddard AJ, Belka GK, Dugan KD, Notarfrancesco KL, Moody SE*, et al.* Hormone-induced protection against mammary tumorigenesis is conserved in multiple rat strains and identifies a core gene expression signature induced by pregnancy. *Cancer research* 2006, **66**(12)**:** 6421-6431.
22. Modugno F, Ness RB, Allen GO, Schildkraut JM, Davis FG, Goodman MT. Oral contraceptive use, reproductive history, and risk of epithelial ovarian cancer in women with and without endometriosis. *American journal of obstetrics and gynecology* 2004, **191**(3)**:** 733-740.
23. Cohen CA, Shea AA, Heffron CL, Schmelz EM, Roberts PC. Intra-Abdominal Fat Depots Represent Distinct Immunomodulatory Microenvironments: A Murine Model *PlosOne* 2013, **Accepted**
24. Roberts PC, Mottillo EP, Baxa AC, Heng HH, Doyon-Reale N, Gregoire L*, et al.* Sequential molecular and cellular events during neoplastic progression: a mouse syngeneic ovarian cancer model. *Neoplasia* 2005, **7**(10)**:** 944-956.
25. Creekmore AL, Silkworth WT, Cimini D, Jensen RV, Roberts PC, Schmelz EM. Changes in gene expression and cellular architecture in an ovarian cancer progression model. *PloS one* 2011, **6**(3)**:** e17676.
26. Swainson L, Mongellaz C, Adjali O, Vicente R, Taylor N. Lentiviral transduction of immune cells. *Methods in molecular biology* 2008, **415:** 301-320.
27. Carmignani CP, Sugarbaker PH. Synchronous extraperitoneal and intraperitoneal dissemination of appendix cancer. *European journal of surgical oncology : the journal of the European Society of Surgical Oncology and the British Association of Surgical Oncology* 2004, **30**(8)**:** 864-868.
28. Otto J, Jansen PL, Lucas S, Schumpelick V, Jansen M. Reduction of peritoneal carcinomatosis by intraperitoneal administration of phospholipids in rats. *BMC cancer* 2007, **7:** 104.
29. Schmittgen TD, Livak KJ. Analyzing real-time PCR data by the comparative C(T) method. *Nature protocols* 2008, **3**(6)**:** 1101-1108.
30. Tsubura A, Uehara N, Matsuoka Y, Yoshizawa K, Yuri T. Estrogen and progesterone treatment mimicking pregnancy for protection from breast cancer. *In vivo* 2008, **22**(2)**:** 191-201.
31. Montecino-Rodriguez E, Dorshkind K. New perspectives in B-1 B cell development and function. *Trends in immunology* 2006, **27**(9)**:** 428-433.
32. Ghosn EE, Cassado AA, Govoni GR, Fukuhara T, Yang Y, Monack DM*, et al.* Two physically, functionally, and developmentally distinct peritoneal macrophage subsets. *Proceedings of the National Academy of Sciences of the United States of America* 2010, **107**(6)**:** 2568-2573.
33. D'Acquisto F, Crompton T. CD3+CD4-CD8- (double negative) T cells: saviours or villains of the immune response? *Biochemical pharmacology* 2011, **82**(4)**:** 333-340.
34. Lu Y, Wang X, Yan W, Wang H, Wang M, Wu D*, et al.* Liver TCRgammadelta(+) CD3(+) CD4(-) CD8(-) T cells contribute to murine hepatitis virus strain 3-induced hepatic injury through a TNF-alpha-dependent pathway. *Molecular immunology* 2012, **52**(3-4)**:** 229-236.

35. Chen W, Ford MS, Young KJ, Zhang L. The role and mechanisms of double negative regulatory T cells in the suppression of immune responses. *Cellular & molecular immunology* 2004, **1**(5)**:** 328-335.
36. Fridlender ZG, Sun J, Kim S, Kapoor V, Cheng G, Ling L*, et al.* Polarization of tumor-associated neutrophil phenotype by TGF-beta: "N1" versus "N2" TAN. *Cancer cell* 2009, **16**(3)**:** 183-194.
37. Fridlender ZG, Sun J, Mishalian I, Singhal S, Cheng G, Kapoor V*, et al.* Transcriptomic analysis comparing tumor-associated neutrophils with granulocytic myeloid-derived suppressor cells and normal neutrophils. *PloS one* 2012, **7**(2)**:** e31524.
38. Merritt MA, De Pari M, Vitonis AF, Titus LJ, Cramer DW, Terry KL. Reproductive characteristics in relation to ovarian cancer risk by histologic pathways. *Human reproduction* 2013.
39. Van Vugt E, Van Rijthoven EA, Kamperdijk EW, Beelen RH. Omental milky spots in the local immune response in the peritoneal cavity of rats. *The Anatomical record* 1996, **244**(2)**:** 235-245.
40. Sica A, Schioppa T, Mantovani A, Allavena P. Tumour-associated macrophages are a distinct M2 polarised population promoting tumour progression: potential targets of anti-cancer therapy. *European journal of cancer* 2006, **42**(6)**:** 717-727.
41. Mantovani A, Schioppa T, Porta C, Allavena P, Sica A. Role of tumor-associated macrophages in tumor progression and invasion. *Cancer metastasis reviews* 2006, **25**(3)**:** 315-322.
42. Nozawa H, Chiu C, Hanahan D. Infiltrating neutrophils mediate the initial angiogenic switch in a mouse model of multistage carcinogenesis. *Proceedings of the National Academy of Sciences of the United States of America* 2006, **103**(33)**:** 12493-12498.
43. Piccard H, Muschel RJ, Opdenakker G. On the dual roles and polarized phenotypes of neutrophils in tumor development and progression. *Critical reviews in oncology/hematology* 2012, **82**(3)**:** 296-309.
44. Peranzoni E, Zilio S, Marigo I, Dolcetti L, Zanovello P, Mandruzzato S*, et al.* Myeloid-derived suppressor cell heterogeneity and subset definition. *Current opinion in immunology* 2010, **22**(2)**:** 238-244.
45. Dolcetti L, Peranzoni E, Ugel S, Marigo I, Fernandez Gomez A, Mesa C*, et al.* Hierarchy of immunosuppressive strength among myeloid-derived suppressor cell subsets is determined by GM-CSF. *European journal of immunology* 2010, **40**(1)**:** 22-35.
46. Pages F, Galon J, Dieu-Nosjean MC, Tartour E, Sautes-Fridman C, Fridman WH. Immune infiltration in human tumors: a prognostic factor that should not be ignored. *Oncogene* 2010, **29**(8)**:** 1093-1102.
47. Dunn GP, Bruce AT, Ikeda H, Old LJ, Schreiber RD. Cancer immunoediting: from immunosurveillance to tumor escape. *Nature immunology* 2002, **3**(11)**:** 991-998.
48. Zhang L, Conejo-Garcia JR, Katsaros D, Gimotty PA, Massobrio M, Regnani G*, et al.* Intratumoral T cells, recurrence, and survival in epithelial ovarian cancer. *The New England journal of medicine* 2003, **348**(3)**:** 203-213.
49. Nelson BH. CD20+ B cells: the other tumor-infiltrating lymphocytes. *Journal of immunology* 2010, **185**(9)**:** 4977-4982.
50. Spaner D, Bahlo A. B Lymphocytes in Cancer Immunology. In: Fowler JMaD (ed). *Experimental and Applied Immunotherapy*. Springer Science+Business Media, 2011.
51. Milne K, Kobel M, Kalloger SE, Barnes RO, Gao D, Gilks CB*, et al.* Systematic analysis of immune infiltrates in high-grade serous ovarian cancer reveals CD20, FoxP3 and TIA-1 as positive prognostic factors. *PloS one* 2009, **4**(7)**:** e6412.
52. Kemp TJ, Moore JM, Griffith TS. Human B cells express functional TRAIL/Apo-2 ligand after CpG-containing oligodeoxynucleotide stimulation. *Journal of immunology* 2004, **173**(2)**:** 892-899.

53. Hagn M, Schwesinger E, Ebel V, Sontheimer K, Maier J, Beyer T*, et al.* Human B cells secrete granzyme B when recognizing viral antigens in the context of the acute phase cytokine IL-21. *Journal of immunology* 2009, **183**(3)**:** 1838-1845.
54. Lundy SK. Killer B lymphocytes: the evidence and the potential. *Inflammation research : official journal of the European Histamine Research Society [et al]* 2009, **58**(7)**:** 345-357.
55. Inoue S, Leitner WW, Golding B, Scott D. Inhibitory effects of B cells on antitumor immunity. *Cancer research* 2006, **66**(15)**:** 7741-7747.
56. Hansell CA, Nibbs RJ. The odd couple: innate-like B cells and the chemokine scavenger D6. *Cell cycle* 2011, **10**(21)**:** 3619-3620.
57. Lund FE. Cytokine-producing B lymphocytes-key regulators of immunity. *Current opinion in immunology* 2008, **20**(3)**:** 332-338.
58. Staquicini FI, Tandle A, Libutti SK, Sun J, Zigler M, Bar-Eli M*, et al.* A subset of host B lymphocytes controls melanoma metastasis through a melanoma cell adhesion molecule/MUC18-dependent interaction: evidence from mice and humans. *Cancer research* 2008, **68**(20)**:** 8419-8428.
59. Eck M, Schmausser B, Scheller K, Brandlein S, Muller-Hermelink HK. Pleiotropic effects of CXC chemokines in gastric carcinoma: differences in CXCL8 and CXCL1 expression between diffuse and intestinal types of gastric carcinoma. *Clinical and experimental immunology* 2003, **134**(3)**:** 508-515.
60. Jensen HK, Donskov F, Marcussen N, Nordsmark M, Lundbeck F, von der Maase H. Presence of intratumoral neutrophils is an independent prognostic factor in localized renal cell carcinoma. *Journal of clinical oncology : official journal of the American Society of Clinical Oncology* 2009, **27**(28)**:** 4709-4717.
61. Wislez M, Rabbe N, Marchal J, Milleron B, Crestani B, Mayaud C*, et al.* Hepatocyte growth factor production by neutrophils infiltrating bronchioloalveolar subtype pulmonary adenocarcinoma: role in tumor progression and death. *Cancer research* 2003, **63**(6)**:** 1405-1412.
62. Ji H, Houghton AM, Mariani TJ, Perera S, Kim CB, Padera R*, et al.* K-ras activation generates an inflammatory response in lung tumors. *Oncogene* 2006, **25**(14)**:** 2105-2112.
63. Pekarek LA, Starr BA, Toledano AY, Schreiber H. Inhibition of tumor growth by elimination of granulocytes. *The Journal of experimental medicine* 1995, **181**(1)**:** 435-440.
64. Tazawa H, Okada F, Kobayashi T, Tada M, Mori Y, Une Y*, et al.* Infiltration of neutrophils is required for acquisition of metastatic phenotype of benign murine fibrosarcoma cells: implication of inflammation-associated carcinogenesis and tumor progression. *The American journal of pathology* 2003, **163**(6)**:** 2221-2232.
65. Ishii G, Sangai T, Oda T, Aoyagi Y, Hasebe T, Kanomata N*, et al.* Bone-marrow-derived myofibroblasts contribute to the cancer-induced stromal reaction. *Biochemical and biophysical research communications* 2003, **309**(1)**:** 232-240.
66. Kidd S, Spaeth E, Watson K, Burks J, Lu H, Klopp A*, et al.* Origins of the tumor microenvironment: quantitative assessment of adipose-derived and bone marrow-derived stroma. *PloS one* 2012, **7**(2)**:** e30563.

CHAPTER 5.

IL-12 Immunomodulation Reduces Peritoneal Outgrowth of Ovarian Cancer Cells

Courtney A. Cohen[1], Amanda A. Shea[2], C. Lynn Heffron[1], Eva M. Schmelz[2], Paul C. Roberts[1]

1. Department of Biomedical Sciences and Pathobiology, Virginia Polytechnic Institute and State University, Blacksburg, VA, United States

2. Department of Human Nutrition, Foods and Exercise, Virginia Polytechnic Institute and State University, Blacksburg, VA, United States

ABSTRACT

IL-12 plays an important role in the T_H1-type immune response and has also been described as a potent anti-tumorigenic therapeutic. While preclinical results were promising, systemic IL-12 was associated with a host of dangerous side effects in clinical trials. This galvanized the development of a new generation of targeted cancer therapeutic strategies including immune or accessory cells engineered to express secreted or membrane-bound IL-12 (mbIL-12). Ovarian cancer has one of the highest incidence-to-death ratios in neoplastic disease due to late detection and subsequent high prevalence of metastasis at the time of disease discovery. The omental fat band (OFB) is the well-known predominant site for ovarian cancer metastatic seeding, although it normally plays an immunoregulatory role in the peritoneal cavity as a secondary lymphoid organ. Using fluorescence-activated cell sorting (FACS) analysis we have illustrated the immune composition in the OFB after aggressive ovarian cancer cell seeding, characterized by an increase in tumor-associated neutrophils (TANs) and macrophages (TAMs). Further, by creating a mb-IL-12 expressing cell line variant, we demonstrated that localized IL-12 in the tumor microenvironment significantly delays disease development, with an over 200% extension in lifespan. Using quantitative realtime PCR (qRT-PCR), we found that mbIL-12 causes a reduction in the expression of neutrophil and macrophage chemoattractants (CXCL1, -2, -3 and CCL2, -7) early after intraperitoneal implantation (7 days). Decreased tumor burden also correlates with a significant reduction in TAN and TAM infiltration in the OFB at 3 weeks post-injection, indicating their importance in the progression of the pro-tumorigenic cascade. Vaccination with mbIL-12-expressing tumor cells did not offer protection against subsequent challenge, indicating the poor immunogenicity of these cells. This correlates with previous reports that IL-12 may be acting directly on macrophages, and may alter activation status. These findings demonstrate the efficacy of IL-12 expression directly at the immunological synapse in delaying metastatic outgrowth. If harnessed and re-mobilized to overcome tumor-affiliated immunosuppression, the immune microenvironment within the OFB could prove a powerful tool in metastatic disease treatment.

INTRODUCTION

Ovarian cancer has one of the highest incidence-to-death ratios in the world, in part due to a lack of early detection tools, its asymptomatic nature, and the high prevalence of metastasis at the time of discovery[1, 2, 3]. Metastasis occurs when ovarian cancer cells exfoliate from the primary tumor and disseminate throughout the peritoneal cavity, typically forming outgrowths on the omental fat band (OFB)[4, 5]. The OFB is composed of adipose tissue interspersed with immune cell aggregates ("milky spots") and is considered a secondary lymphoid organ because it plays an important role in immunosurveillance in the peritoneal cavity, capable of mounting innate and adaptive responses[6, 7, 8]. In women diagnosed with ovarian cancer, the OFB is typically removed during tumor debulking as a preventative measure, leaving women susceptible to peritoneal infections[7, 9]. Despite the normal protective immune function of the OFB, research indicates that cancer cells adhere to these milky spots and initiate an extremely effective signaling program resulting in the formation of a pro-tumorigenic microenvironment[10]. As the predominant site for ovarian cancer metastasis, and a secondary lymphoid organ with a diverse leukocyte population, the OFB provides a unique opportunity for targeted treatment strategies.

IL-12 is a potent immunomodulatory cytokine, and has been utilized in both laboratory and clinical settings as a cancer therapeutic[11, 12, 13]. IL-12 helps drive adaptive immune responses, polarizing naïve $CD4^+$ cells toward a T_H1 phenotype. The T_H1 response is generally protective against infection, and helps limit carcinogenesis[14]. It plays a crucial role in the induction of IFNγ secretion by T and NK cells, the differentiation of cytotoxic $CD8^+$ cells, and it increases the activity of NK cells[15, 16, 17, 18]. Additionally, it can reactivate and sustain tumor-specific memory $CD4^+$ T cells from a T_H2 to a protective T_H1 phenotype in the tumor microenvironment[19]. IL-12 has also been shown to have potent anti-angiogenic properties, as a result of IFNγ-induced production of IP-10 and Mig, indicating anti-tumorigenic activity through multiple pathways[20, 21, 22, 23, 24]. IL-12 has shown tumor regression or prevention in a wide variety of cancer models including ovarian, renal, gastrointestinal and mammary carcinomas, melanomas and

lymphomas; however the magnitude of outcome varies, most likely due to the variation of tumor type, cytokine dose and route of administration[14, 25, 26, 27, 28, 29].

Despite the wealth of promising pre-clinical results, initial clinical results using systemic IL-12 were relatively poor, and systemic IL-12 caused severe and dangerous side effects due to widespread diffusion to neighboring tissues[30, 31, 32, 33, 34]. Thus, more targeted approaches are under investigation and include intratumoral recombinant IL-12, local injection of virus engineered to secrete IL-12, as well as genetically modified tumor cell lines, DCs and fibroblasts expressing secretory or membrane-bound IL-12 (mbIL-12). These have shown varying degrees of success with tumor regression or prevention, linked to increased $CD8^+$ effector T and NK cell activity[21, 35, 36, 37, 38, 39, 40, 41, 42] For the treatment of ovarian cancer, IL-12-containing polymer delivery vehicles have been developed for i.p. injection. In preclinical studies, these reduced tumor growth and ascites accumulation, but their efficacy in Phase I clinical trials were disappointing, required repeat doses, and presented with side effects due to widespread dispersion in the peritoneal cavity[20, 43]. I.p. administration of recombinant IL-12 also yielded poor results[33]. Thus, a more controlled strategy is warranted.

We have previously shown that the OFB is a complex and diverse immune organ that undergoes polarizing events following the seeding of ovarian cancer cells, as well as parity-associated changes in the homeostatic state that provide a naturally metastasis-refractory microenvironment[44, 45] As the primary site for ovarian cancer metastasis, the OFB provides a unique opportunity to study the efficacy of immunomodulatory IL-12 treatment. Additionally, the OFB may provide an opportunity for the mobilization of the immune system towards an anti-tumorigenic state during peritoneal metastasis, if these interactions could be defined and selectively targeted.

In the present study, we comparatively characterized the OFB microenvironment as a consequence of time post-peritoneal implantation of benign, aggressive and highly aggressive ovarian cancer lines in a fully immune competent setting in order to gain insights into the recruitment factors that contribute to the establishment of the pro-tumorigenic state. Importantly, we evaluated whether presentation of IL-12 directly on the tumor cell surface was sufficient to disrupt the pro-tumorigenic

signaling cascade that develops following ovarian cancer metastasis to the OFB. Our results confirm that localized expression of membrane-bound IL-12 can reduce metastatic seeding and outgrowth of highly aggressive, metastatic ovarian cancer cells. We and others have previously shown that the metastatic microenvironment during aggressive tumor growth is characterized by an overwhelming increase in tumor-associated neutrophils and macrophages (TANs, TAMs) and increased chemotactic signaling for these leukocytes[46, 47, 48, 49]. Here, we determined that mbIL-12 mitigates recruitment of TANs and TAMs and interferes with rapid establishment of a pro-tumorigenic microenvironment within the peritoneal cavity. This work provides valuable insights into the kinetics of the pro-tumorigenic cascade, and highlights targets that could be disrupted for improved chemotherapeutics designed to target in a metastatic ovarian cancer.

METHODS AND PROCEDURES

Cell Lines

The mouse ovarian surface epithelial (MOSE) cell model utilized in this study was derived from C57BL/6 mice and characterized as previously described[50, 51]. In addition to benign MOSE-E (early) cells that are incapable of forming tumors in vivo, this study utilized an EGFP-expressing MOSE-L variant (MOSE-L_{EGFPv}) and a previously described FFL-expressing, MOSE-L variant (MOSE-L_{FFLv}) that was passaged once in vivo to increase aggressiveness[45]. MOSE-L_{FFLv} cells constitutively expressing a membrane-bound version of the murine IL-12 gene were established as described previously[52] Briefly, a murine single chain IL-12 p35p40 gene was amplified from pORF-mIL-12(p35p40) (Invivogen) and fused in frame to the transmembrane encoding region of the influenza HA gene. Following transfection of FFL cells with the mbIL-12/HA containing plasmid, stable G418-resistant subclones were established. (Sigma-Aldrich). Stable transfectants expressing IL-12 were screened by surface immunofluorescence staining using an anti-mouse IL-12p70 mAb (R&D Bio); the highest expressing subclone was expanded and designated MOSE-$L_{FFL/IL-12v}$. It was empirically determined in pilot studies that that $1x10^4$ MOSE-L_{FFLv}

cells injected i.p. results in fatal disease after 3 weeks incubation, in contrast to the parental MOSE-L cells (phenotypically identical to MOSE-L_{EGFPv} cells) which require a 1-5 x 10^6 cells and 12 weeks of incubation to present comparably. Cells were routinely maintained in high glucose DMEM (Invitrogen, Carlsbad, CA), supplemented with 4% fetal bovine serum (Hyclone, Logan UT), and 100mg/ml penicillin and streptomycin. FFL- and EGFP-expressing cells also receive 1µg/ml puromycin to maintain selection; IL-12/HA-expressing cells are propagated in both puromycin and G418 (1.4mg/ml) supplemented media as the IL-12 expression plasmid carries a geneticin resistance marker for selection.

Animals

12-week old female C57BL/6 mice (Harlan Laboratories) were housed five per cage in a controlled environment (12 hour light/dark cycle at 21°C) with free access to water and food (18% protein rodent chow, Teklad Diets). Mice were sacrificed by CO_2 asphyxiation; all animal work was performed in accordance with the guidelines approved by the Virginia Tech Institutional Animal Care and Usage Committee.

MOSE Cell Injections

Preliminary dosage studies were performed to determine the appropriate cell number and time for tumor development, and to verify tumor reproducibility for MOSE-L_{EGFPv} and MOSE-L_{FFLv} cell lines. Prior to injection, cells were resuspended in 300µL sterile calcium- and magnesium-deficient phosphate buffered saline ($PBS^{-/-}$). To determine the efficacy of membrane-bound IL-12 (mbIL-12), an initial proof-of-concept experiment was performed; mice (n=6) were injected i.p. with 2.5x10^6 MOSE-L_{FFLv} or MOSE-$L_{FFL/IL\text{-}12v}$ and sacrificed at MOSE-L_{FFL} cell endpoint (day 15 post-injection) to compare relative tumor burdens. The survival curve for MOSE-$L_{FFL/IL\text{-}12}$ cells was determined using an i.p. injection of 1x10^6 cells. Based on these combined preliminary study results, all subsequent studies were performed using 10^4 MOSE-L_{FFLv} and MOSE-$_{LFFL/IL\text{-}12v}$ cells, and 10^6 MOSE-L_{EGFPv} and MOSE-E (non-tumorigenic) cells. For challenge experiment, MOSE-L_{FFLv} and MOSE-$L_{FFL/IL\text{-}12v}$ cells were treated in-vitro with 50µg/ml Mitomycin C (MMC; $FFLv_{MMC}$, $FFL/IL\text{-}12v_{MMC}$) for 45 minutes at 37°C, as per manufacturer's instructions (Sigma-Aldrich) prior to injection. Mice (n=8) received $PBS^{-/-}$ (mock-injected), MOSE-

$L_{FFL/IL\text{-}12v}$, $FFLv_{MMC}$, or $FFL/IL\text{-}12v_{MMC}$ cells at $1x10^6$ cells i.p.. At week 5, n=3 mice per group were sacrificed to verify MMC treatment effectively halted tumor growth. Remaining mice (n=5 per group) received FFL challenge at $1x10^4$ i.p. at this time. For kinetics studies, mice (n=15) were sacrificed at 24 hours or 7 days post-injection with MOSE-L_{FFLv}, MOSE-$L_{FFL/IL\text{-}12v}$ or MOSE-L_{EGFPv}.

IVIS Imaging

Whole animal bioluminescence imaging was used to monitor tumor progression of FFL-expressing cancer cell lines. Briefly, mice were imaged using the IVIS100 Imaging System (Xenogen) and Living Image acquisition and analysis software (Caliper Life Sciences) as previously described[53]. Briefly, mice were injected with ketamine/xylazine i.p. (100mg/kg / 10mg/kg body weight), after which they were injected i.p. with 150mg/kg D-luciferin. Images were taken 5 minutes after second injection, exposure time was 1 minute.

Peritoneal Cancer Index (PCI)

Tumor burden at the time of sacrifice was determined as described previously, with minor modifications[54, 55] and is expressed as the peritoneal cancer index, PCI. The original PCI was adopted to apply to tumor size and region in mice. Previously described quadrant areas were modified to represent distinct organs and their mesentery to obtain more specific information regarding tumor cell dissemination and seeding. Specific regions included peritoneal cavity lining, ovaries, lesser omentum, greater omentum (OFB), diaphragm, liver, stomach, pancreas, spleen, kidney, small intestine, small intestine mesentery, large intestine, and large intestine mesentery (14 regions total). Tumor size score (**0-3**) from each region were determined macroscopically and denoted as **0**: no macroscopic tumor, **1**: < 1mm; **2**: 1-3mm ; or **3**: >3mm or solid tumor. The maximum composite PCI score was 42. Relative PCI scores were further verified by qRT-PCR analysis of FFL and EGFP expression within the OFB.

Tissue and peritoneal serous fluid harvest

The OFB was harvested from each mouse, weighed, rinsed with $PBS^{-/-}$, and processed for FACS or placed into RNAlater (Qiagen) and stored at -80°C. Resident peritoneal cavity cells were collected via

peritoneal lavage with 5ml of $PBS^{-/-}$. The effluent was centrifuged, subjected to erythrocyte lysis (155mM NH_4Cl, 10mM $KHCO_3$, 0.1mM EDTA), and further processed as described below.

Tissue Digestion

SVFs were isolated following digestion of individual OFBs in GKN-buffer containing 1.8mg/ml Type IV collagenase, 10% FBS, and 0.1mg/ml DNase as described previously[44]. After digestion at 37°C for 45 min, cells were passed through a 40µm cell strainer, subject to erythrocyte lysis and cells were pelleted by centrifugation and processed for FACS analysis.

FACS Analysis

Single cell suspensions derived from OFB and PSF were washed in flow buffer (2% BSA in $PBS^{-/-}$), blocked with Fc block (BD Biosciences) for 10 minutes at 4°C, rinsed and incubated with fluorochrome-labeled antibody combinations (available upon request) for 20 min at 4°C. Fluorochrome-labeled antibodies specific for mouse CD45, CD11b, CD11c, F4/80, Ly6C, CD4, CD44, CD62L, B220, CD19, NK1.1, and Ly6G were obtained from eBioscience (San Diego, CA). CD3, and CD8 antibodies were obtained from BD Biosciences (San Jose, CA). Prior to analysis, cells were washed twice and resuspended in $PBS^{-/-}$ with propidium iodide for dead cell exclusion. FACS was performed on a FACSAria (BD Biosciences) and data was analyzed using Flowjo (TreeStar) software.

Quantitative real-time PCR

Individual OFBs were homogenized in Qiazol (Qiagen) and RNA was purified using an RNeasy Lipid Tissue Kit (Qiagen), according to manufacturer's instructions. RNA concentration was determined using a NanoDrop1000 spectrophotometer. RNA was converted to cDNA using the iScript cDNA synthesis kit (Biorad) according to manufacturer's protocol. qRT-PCR was performed with 12.5ng cDNA per sample using gene-specific SYBR Green primers (primer sequences are available upon request) designed with Beacon Design software. SensiMix SYBR and Fluorescein mastermix (Quantace) was used in a 15µL reaction volume. qRT-PCR was performed for 42 cycles at 95°C for 15 sec, 60°C for 15 sec, and 72°C for 15 sec, preceded by a 10 min incubation at 95°C on the iQ5 (Biorad). Melt curves were

performed to ensure fidelity of the PCR amplicon. The housekeeping gene was L19 and the ddCt method[56] was used to determine fold differences.

Statistical Analysis

Data are expressed as mean ± standard error of mean (SEM). FACS and qRT-PCR data were analyzed using a one-way ANOVA coupled with a Tukey Post-hoc test in SigmaPlot (Systat Software). Differences were considered statistically significant at $p<0.05$.

RESULTS

Ovarian cancer is typically discovered in the later stages when metastasis has already occurred, preferentially seeding within the OFB. In a similar fashion, peritoneal implantation of $1x10^6$ MOSE-L_{EGFPv} cells led to their rapid localization to the OFB as early as 6 hours post-implantation (Figure 5.1A,B). Within 24 hours, cancer cell micro-implants have taken hold and are readily evident (Figure 5.1C,D). Likewise, using whole body bioluminescence imaging (BLI), we were able to monitor the progression of FFL-expressing MOSE-E (MOSE-E_{FFLv}, benign) and MOSE-L (MOSE-L_{FFLv}, highly aggressive) cells over time in live animals. Notably, MOSE-E_{FFLv} cells, which were readily detectable at 24 hours post-injection, were no longer detectable by day 8 suggesting that they are either cleared by innate defense mechanisms or are incapable of establishing a microenvironment conducive for their growth and survival. Conversely, MOSE-L_{FFLv} cells remained detectable at day 8 and continued to proliferate, eventually leading to widespread tumor outgrowth throughout the peritoneal cavity, consistent with their extremely aggressive phenotype (Figure 5.1E,F). It is noteworthy to mention that irrespective of tumorigenic potential all MOSE cells were able to localize to and accumulate initially within the OFB. Although the OFB is a secondary lymphoid organ, it is commonly repolarized into a pro-tumorigenic microenvironment during cancer cell metastasis, promoting disease progression. We reasoned that this dual functionality and diverse leukocyte component provides a unique opportunity for targeted anti-metastatic immunomodulatory treatments.

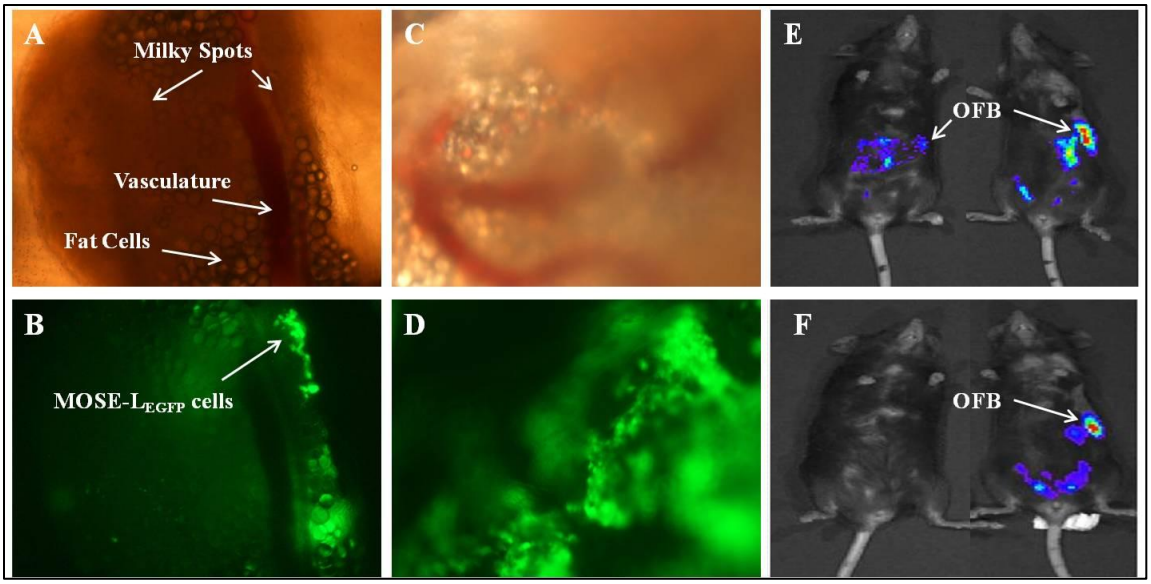

Figure 5.1. Ovarian cancer cells localize to the OFB within 6 hours of intraperitoneal implantation. **(A, B)** The OFB at 6 hours post-i.p. injection with 1x10^6 MOSE-L$_{EGFP}$ cells. **(C,D)** The OFB at 24 hours post-i.p. injection with MOSE-L$_{EGFP}$ cells. **(E)** IVIS imaging of MOSE-E$_{FFLv}$ and MOSE-L$_{FFLv}$ i.p. injected animals 24 hours post-injection. **(F)** IVIS imaging of MOSE-E$_{FFLv}$ and MOSE-L$_{FFLv}$ i.p. injected animals 8 days post-injection.

Due to its polarizing effects on both innate and adaptive immune cells and its demonstrated efficacy against ovarian and other cancer types[29], we postulated that highly localized IL-12 expression may be sufficient to shift the OFB towards an anti-tumorigenic state after cancer cell seeding. In order to circumvent the dangerous side effects affiliated with systemic or soluble IL-12 administration, we opted to express a membrane-bound version of the IL-12 protein directly on the surface of the highly aggressive MOSE-L$_{FFLv}$ cells. Thus, the effects of IL-12 should be restricted to direct interactions at the immunological synapse with cells that possess the IL-12 receptor (DCs, T cells, NK cells, monocytes, macrophages and B cells)[14, 57, 58, 59].

As depicted in Figure 5.2, we were able to generate an IL-12 expressing MOSE-L$_{FFLv}$ cell line that constitutively expresses membrane-bound IL-12 (mbIL-12) on the cell surface (Figure 5.2A,B). Importantly, expression of mbIL-12 did not alter the in vitro growth rate (Figure 5.2C) nor the colony forming capacity of the MOSE-L FFL cells, suggesting that the insertion of the IL-12 fusion gene did not adversely alter the proliferative or tumorigenic properties of the cell line. Importantly, we were also able

to use qRT-PCR method to verify the expression of EGFP in MOSE-L_{EGFPv} cells, IL-12 in MOSE-$L_{FFL/IL12v}$ cells, and FFL in both MOSE-L_{FFLv} and MOSE-$L_{FFL/IL-12v}$ lines (Figure 5.2D).

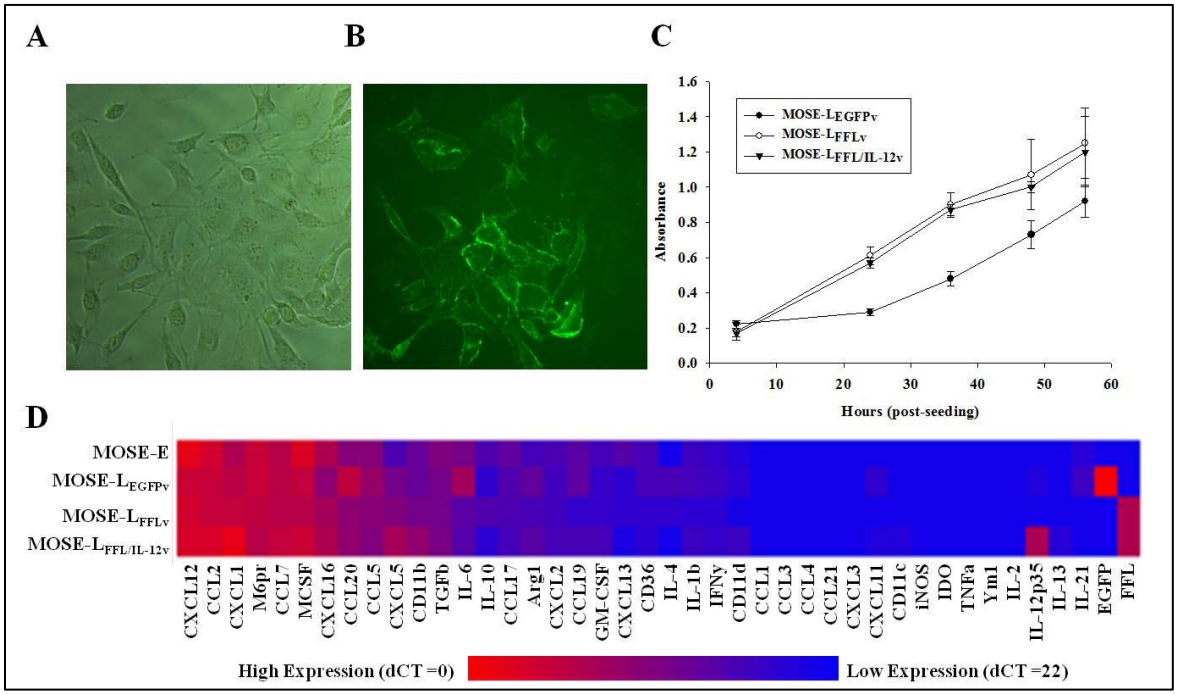

Figure 5.2. MOSE cell line phenotypic charactierization **(A,B)** Cell surface IL-12 staining of MOSE-$L_{FFL/IL-12v}$ **(C)** In vitro proliferation, MTT assay. **(D)** Gene expression of MOSE cell line variants.

Comparative qRT-PCR was also employed to determine whether MOSE cell lines with varying tumorigenic potential differentially expressed key cytokines and chemokines involved in the recruitment or activation of pro-tumorigenic cell types. It was also important to establish that the IL-12 gene insertion did not adversely alter the gene expression profile of these cells. Thus, a panel of 30 immune-related cytokines and chemokines were evaluated (Figure 5.2D) in order to determine factors that may alter the immune microenvironment and create a pro-tumorigenic niche. Interestingly, all MOSE cells irrespective of tumorigenic potential, express high levels of CXCL12, a chemokine that has been shown to recruit macrophages to breast tumors [60]. Cytokines involved in the recruitment and proliferation of monocytes (MCSF, CCL2, CCL7) were also highly expressed. The non-malignant MOSE-E cell line exhibited significantly decreased expression of neutrophil chemoattractants CXCL1 and CXCL5 compared to its

malignant counterparts. This is noteworthy because a reduction in the expression of these cytokines has been associated with a microenvironment that is refractory to peritoneal outgrowth in the OFB[45].

Impact of membrane-bound IL-12 on peritoneal tumor burden

As IL-12 has been implicated as a potent anti-tumorigenic immunomodulatory molecule, we were interested in evaluating its efficacy in a targeted fashion in an immune competent setting of ovarian cancer metastasis. Therefore, we utilized our previously described highly aggressive FFL-expressing cell line in conjunction with its mbIL-12 expressing counterpart to determine whether highly localized expression of IL-12 can significantly impact peritoneal seeding and outgrowth. Peritoneal implantation of a high dose of MOSE-L_{FFLv} ($2.5x10^6$ cells, i.p.) is highly lethal to C57BL/6 mice, with animals reaching established endpoints within 15 days. This corresponded with a high peritoneal cancer index (PCI) determined post-mortem. In contrast, animals receiving the same dose of MOSE-$L_{FFL/IL\text{-}12v}$ cells exhibited a significantly decreased tumor burden (Figure 5.3A, $p<0.01$). Of note, MOSE-$L_{FFL/IL\text{-}12v}$ cells resulted in significant lifespan extension as compared to MOSE-L_{FFLv} cells (1×10^4 i.p.), even when implanted at a 100-fold higher dosage (Figure 5.3b, $p<0.01$). It is important to highlight that while expression of mb-IL-12 did significantly extend lifespan, cancer was not completely eradicated, and animals had to eventually be sacrificed due to disease severity.

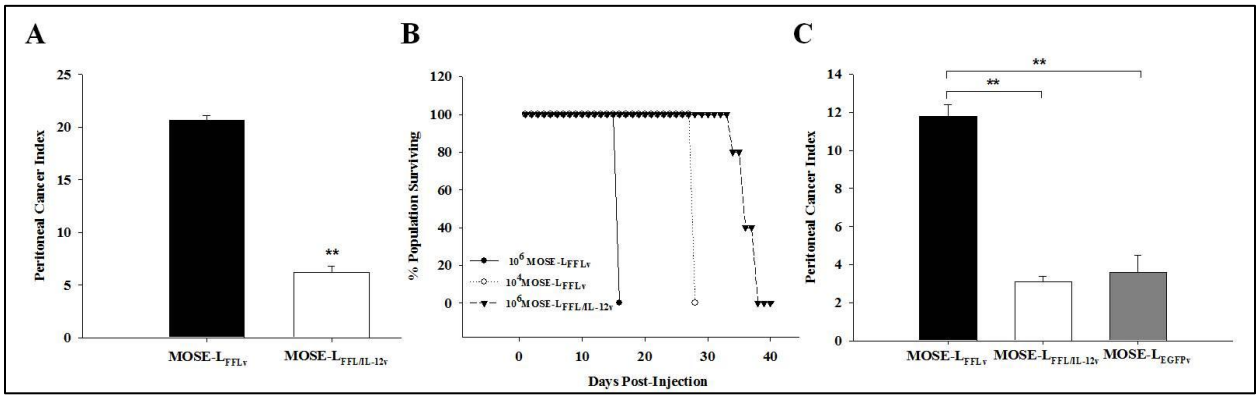

Figure 5.3. mbIL-12 reduces ovarian cancer cell tumorigenicity **(A)** PCI 15 days post-injection of $2.5x10^6$ cells i.p. (n=6) **(B)** Survival curve 10^6 MOSE-L_{FFLv}, 10^4 MOSE-L_{FFLv} and 10^6 MOSE-$L_{FFL/IL\text{-}12}$ cells. **(C)** PCI 3 weeks post-injection i.p. of $1.0x10^4$ MOSE-L_{FFLv}, $1x10^4$ MOSE-$L_{FFL/IL\text{-}12v}$ or $1x10^6$ MOSE-L_{EGFP} cells (n=15). ******: $p<0.01$.

Characterization of the OFB immune microenvironment as a consequence of tumor cell outgrowth

To gain insights into the mechanisms behind the increased survival of animals receiving the mbIL-12-expressing MOSE-$L_{FFL/IL\text{-}12v}$ cell line, we comparatively assessed the immune cell composition of the OFB, the primary metastatic seeding site, as a consequence of peritoneal tumor cell implantation. At 3 weeks post-implantation, animals administered MOSE-L_{FFLv}, MOSE-$L_{FFL/IL\text{-}12v}$, or MOSE-L_{EGFPv} cells were euthanized and the immune cell composition of the OFB and peritoneal serous fluid (PSF) were characterized by FACS analysis. MOSE-L_{EGFPv} cells have been previously characterized as a metastatic, but slowly developing disease model, necessitating the need for an increased dose of these cells to produce quantifiable tumor burden at the chosen timepoint. As noted, the MOSE-$L_{FFL/IL\text{-}12v}$ recipients again had a significantly reduced tumor burden compared to their non-IL-12-expressing counterparts ($p<0.01$). In fact, tumor burden was comparable to that of our more slowly-developing disease model which utilizes the MOSE-L_{EGFPv} cells administered at a 100-fold higher dosage of cells (1×10^6) (Figure 5.3c). Macroscopically, the OFB of MOSE-L_{FFLv} mice had been completely overtaken by tumor, with no detectable adipose tissue remaining. In contrast, MOSE-$L_{FFL/IL\text{-}12v}$ and MOSE-L_{EGFPv} mice had detectable tumor nodules in the OFB, but peritoneal tumor burden was significantly reduced.

FACS analysis of the immune cell composition of the OFB revealed several interesting differences with respect to the response elicited by the MOSE cell lines (Supplementary Table S5.1). In the MOSE-L_{FFLv} model, there was a significant shift in the proportion of lymphocytes (R1 gate) to monocytes/granulocytes (R2 gate) (Figure 5.4A, $p<0.01$). This shift was not evident in either MOSE-$L_{FFL/IL\text{-}12v}$ or MOSE-L_{EGFPv} mice, which maintained R1:R2 ratios comparable to mock-injected mice at this time point after implantation. This trend was mirrored in the PSF fluid with a significant difference observed for the MOSE-L_{FFLv} mice; the predominance of monocytes/granulocytes was even more marked (39.4% loss of lymphocytes, $p<0.01$; Supplementary Table S5.2).

In MOSE-L_{FFLv} mice, the redistribution of R1:R2 leukocytes was reflected across all immune cell subsets with decreases noted in $CD3^+$, $CD19^+$ and $NK1.1^+$ cells, and concomitant increases in $F480^+$ cells

(Figure 5.4 B-E, $p<0.01$). The leukocyte trend was somewhat different in the PSF, with the loss of lymphocytes reflected solely in the B cell, rather than both T and B cell populations ($p<0.01$; Supplementary Table S5.2). Additionally, while the presence of MOSE-L_{FFLv} cells in the PSF did not alter the proportion of large peritoneal macrophages (LPMs, the predominant PSF macrophage population in steady-state) it did significantly increase the proportion of small peritoneal macrophages (SPMs, previously reported to be indicative of inflammatory stimulation) as compared to mock-injected mice ($p<0.01$, Supplementary Table S5.2). This suggests that MOSE-L_{FFLv} cells are actively recruiting monocytes to the peritoneal cavity, where they are likely involved in maintaining a pro-tumorigenic, immunosuppressive state. Notably, there was also a massive increase in the $CD11b^{+}Ly6G^{+}Ly6C^{+}$ tumor-associated neutrophil (TAN) population in the OFB following MOSE-L_{FFLv} injection (Figure 5.4F, $p<0.01$). This pattern was also maintained in the PSF ($p<0.01$ Supplementary Table S5.2), indicating the importance of TANs and their recruitment in the rapid development of ovarian cancer cell metastasis in the peritoneal cavity.

In contrast, administration of MOSE-$L_{FFL/IL\text{-}12v}$ and MOSE-L_{EGFPv} cells resulted in a significantly increased proportion of $CD3^{+}$ T cells in the OFB as compared to mock-injected and MOSE-L_{FFLv} mice (Figure 5.4B, $p<0.01$). The proportions of $CD19^{+}$ B cells and $F480^{+}$ macrophages were not altered by the outgrowth of either MOSE-$L_{FFL/IL\text{-}12v}$ or MOSE-L_{EGFPv} cells in the OFB at the time of sacrifice (Figure 5.4C,D). While the proportion of NK 1.1^{+} cells decreased in the OFB as a result of MOSE-L_{EGFPv} cell outgrowth ($p<0.01$), this population was not reduced in the MOSE-$L_{FFL/IL\text{-}12v}$ model. It is possible that this is due to the known interactions of IL-12 on NK cell activation helping to maintain this population within the microenvironment. Interestingly, the TAN population was significantly increased as a consequence of MOSE-L_{EGFPv} growth in the OFB, albeit not to the extent caused by MOSE-L_{FFLv} cells. However, TANs were virtually absent from the MOSE-$L_{FFL/IL\text{-}12v}$ OFB microenvironment with levels mirroring that observed for the sham OFB (Figure 5.4F). This suggests that membrane-bound IL-12 may be negatively modulating the influx of TANs to the tumor microenvironment, which in turn is reflecting a less

conducive state for tumor outgrowth. The proportion of leukocyte populations in the PSF of MOSE-$L_{FFL/IL\text{-}12v}$ and MOSE-L_{GFPv} mice were not significantly altered as compared to mock-injected mice.

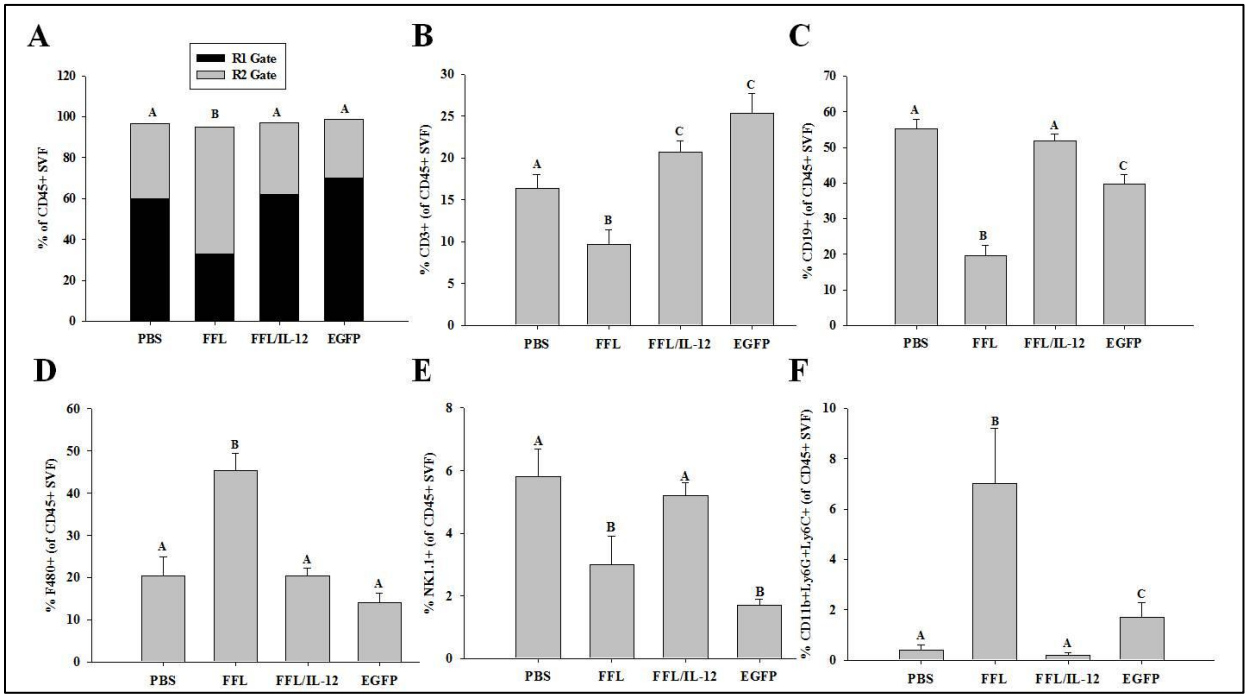

Figure 5.4. mbIL-12 reduces ovarian cancer outgrowth-associated influx of macrophages and neutrophils to the OFB. **(A)** Proportion of lymphocytes to monocytes/granulocytes (R1:R2) in total $CD45^+$ leukocyte fraction. **(B)** Proportion of $CD3^+$ T cells in total leukocytes. **(C)** Proportion of $CD19^+$ B cells in total leukocytes. **(D)** Proportion of $F480^+$ macrophages in total leukocytes. **(E)** Proportion of $NK1.1^+$ NK cells in total leukocytes. **(F)** Proportion of $CD11b^+Ly6G^+Ly6C^+$ tumor-associated neutrophils (TANs) in total leukocytes. Unlike letters indicate significance, $p<0.05$.

These cellularity changes as a consequence of tumor cell seeding and outgrowth were also supported by gene expression profiling of the OFB at the same time point. The mRNA expression of IL-2, a cytokine important for T cell proliferation was decreased 12-fold in the OFB of MOSE-L_{FFLv} mice as compared to controls ($p<0.01$, Supplementary Table S5.3). Additionally, CXCL13, a B cell chemoattractant was down-regulated 260-fold ($p<0.01$) and IL-12, important for T and NK cell activation, was down-regulated 21-fold in MOSE-L_{FFLv} mice as compared to controls. This was particularly interesting given the mitigating effect that mbIL-12 has on tumorigenicity. In addition, expression of monocyte and neutrophil chemoattractants (CXCL1, -2, -5) were significantly up-regulated in the OFB of MOSE-L_{FFLv} mice, compared to MOSE-$L_{FFL/IL\text{-}12}$ mice ($p<0.01$). Combined, this data

validates the role of IL-12 in modulating the balance between a protective and a pro-tumorigenic metastatic microenvironment. Of note, none of the microenvironmental gene expression changes described above were detected in the OFB of MOSE-$L_{FFL/IL-12v}$ mice, indicating their importance in aggressive disease development.

IL-12 expressing FFL cells retain their low immunogenicity and do not protect against tumor challenge

Given the preponderance of evidence describing the involvement of T and NK cells in the efficacy of IL-12 anti-tumorigenic treatment, we next designed a vaccination and challenge experiment to test whether the FFL cells were inherently poorly immunogenic and if membrane-bound IL-12 could increase their immunogenicity and elicit a protective anti-tumor immune response. Specifically, mitomycin C (MMC)-treated MOSE-L_{FFLv} and MOSE-$L_{FFL/IL-12v}$ cells ($FFLv_{MMC}$, $FFL/IL\text{-}12v_{MMC}$, respectively) were administered i.p. at $1x10^6$ to immune competent C57BL/6 female mice. At 5 weeks post-"inoculation" mice were challenged with $1x10^4$ highly aggressive MOSE-L_{FFLv} cells to determine whether pre-treatment with metabolically active, non-proliferating cancer cells, or cells expressing mbIL-12 were capable of overcoming immunosuppressive signals and eliciting a robust and protective anti-tumorigenic immune response. As shown in Figure 5.5, MOSE-L_{FFLv} tumor development was unaffected by pre-treatment with either of the MMC-treated cell lines ($FFLv_{MMC}$, $FFL/IL\text{-}12v_{MMC}$). It is important to note that the small subset (n=3) of mice that were sacrificed at time of MOSE cell challenge displayed no visible tumor development, validating the efficacy of MMC-treatment in the prevention of MOSE cell proliferation.

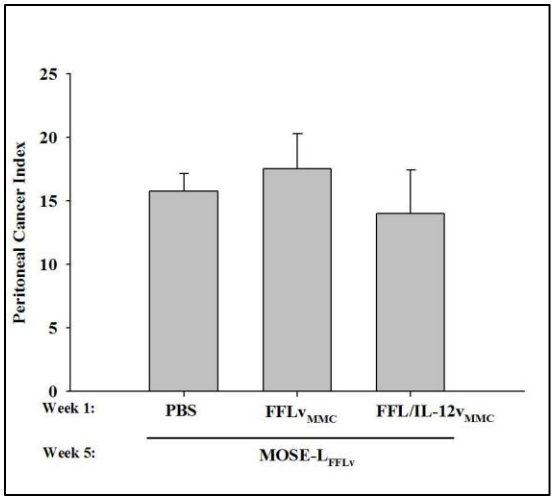

Figure 5.5. mbIL-12 does not provide protection against subsequent challenge. Peritoneal cancer index in mice (n=5) treated with $PBS^{-/-}$, $FFLv_{MMC}$ or $FFL/IL\text{-}12v_{MMC}$ at $1x10^6$ and challenged with MOSE-L_{FFLv} at $1x10^4$ at week 5.

Given the rapid and efficient ability of MOSE-L_{FFLv} cells to polarize the OFB microenvironment in a

pro-tumorigenic manner, we aimed to characterize the early events associated with this highly successful cascade. Thus, we performed a series of in vivo kinetic experiments, in which we administered MOSE cells of varying tumorigenic potential, including the highly aggressive MOSE-L_{FFLv} and its IL-12 expressing counterpart, the MOSE-$L_{FFL/IL\text{-}12v}$ cells. Here we hoped to elucidate some of the early differences (at 24 hours and 7 days post-implantation) in the OFB signaling microenvironment that may shed light on the nature of the IL-12 protective effect on tumor cell seeding and outgrowth. Unfortunately, at 24 hours post-implantation, a considerable influx of neutrophils and monocytes was observed in the OFB (Figure 5.6, Supplementary Table S5.4) and PSF (Supplementary Table S5.5) of all animals, including those receiving only a bolus of $PBS^{-/-}$. This appeared to be due to a transient injection insult and not by contamination with endotoxin as our PBS was certified endotoxin-free. A transient influx of phagocytic cells is common following i.p. injections, as shown[61, 62]. This influx did not allow us to definitively discern any differences as a consequence of a specific cell type that was implanted. By day 7, this reaction was receding, but this inflammatory response resulting from injury to the cavity prevented us from collecting any useful information regarding the initial MOSE-immune cell interactions via FACS analysis (Supplementary Table S5.6, S5.7). It is important to note that the possibility of vehicle contamination was ruled out by repeating this experiment with additional mice, and using an unopened bottle of sterile endotoxin-free $PBS^{-/-}$ from vendor. Bacterial contamination of cell lines was ruled out by streaking on agar plates; all cell lines were negative. Mice having a pre-existing infection was ruled out by sacrificing n=5 “untouched mice” housed in the same room as experimental animals and verifying the lack of these inflammatory cell populations.

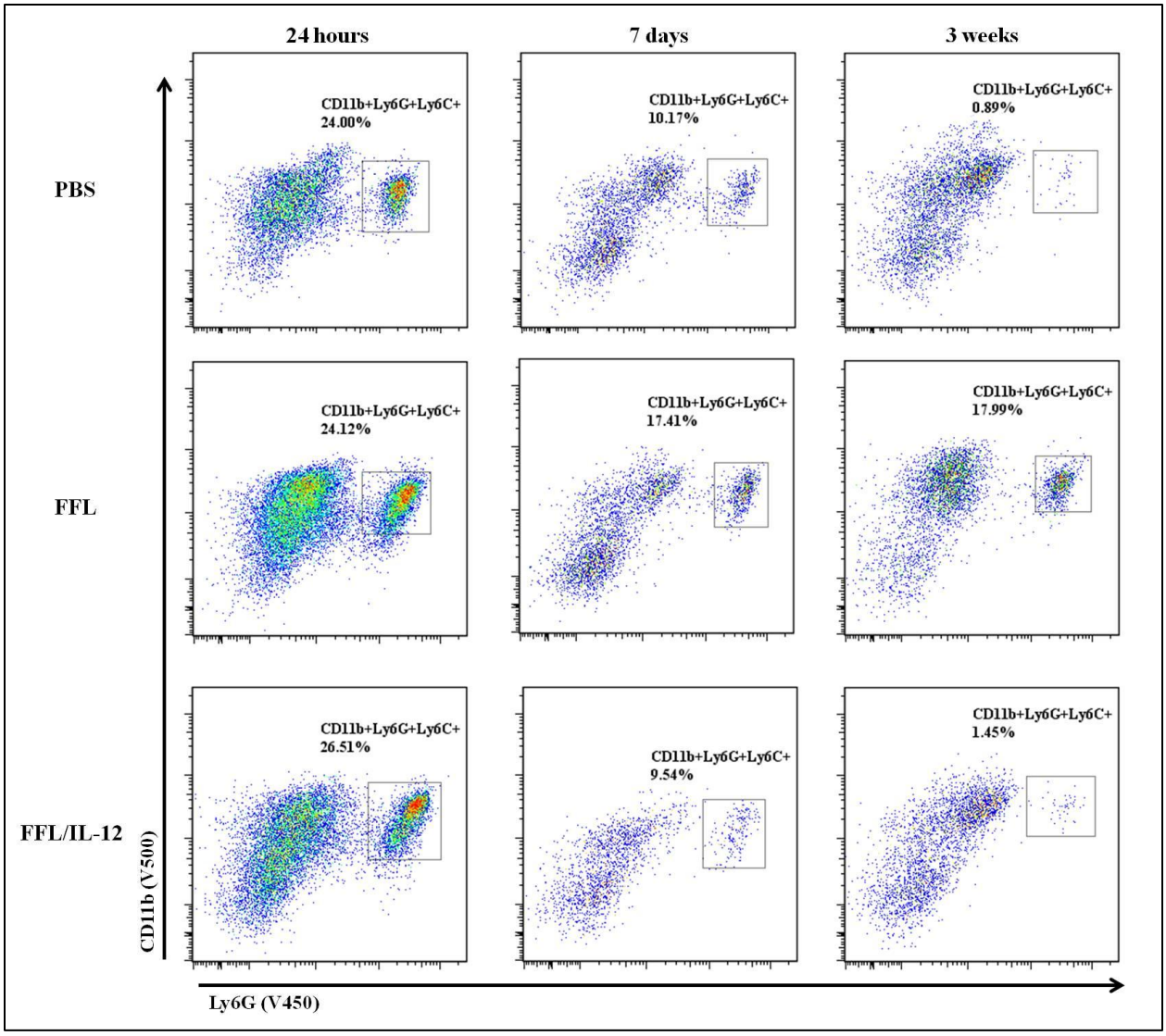

Figure 5.6. Intraperitoneal injection causes injury-related influx of inflammatory cells to the peritoneal cavity.

Although the residual inflammatory immune cells resulting from cavity-insult made changes in leukocyte populations difficult to discern 7 days post-MOSE cell injection, qRT-PCR analysis of the entire tissue did provide some interesting insights. In contrast to samples collected at 3 weeks post-injection in which all significant cytokine and chemokines expression changes occurred in the OFBs of MOSE-L_{FFLv} mice, at 7 days the most significant gene expression changes were taking place in the OFBs of MOSE-$L_{FFL/IL\text{-}12v}$ mice. At this timepoint a significant 2- to 3-fold decrease in the expression levels of several neutrophil chemokines (CXCL1, -2 and -3) was observed in the MOSE-$L_{FFL/IL\text{-}12}$ mice ($p<0.05$,

Supplementary Table S5.8). There was also a significant decrease in the levels of CCL2 and CCL7, important monocyte chemoattractants, and in VEGFa, an angiogenic factor ($p<0.05$). Together, these data suggest that the presence of IL-12 confined to the surface of the tumor cells helps establish a transiently refractory microenvironment that is less conducive for tumor cell outgrowth. Based on relative expression levels in the OFB, all MOSE lines experienced a regression at day 7, most likely due to an early but fleeting innate response, with successful outgrowth by 3 weeks post-implantation (Figure 5.7).

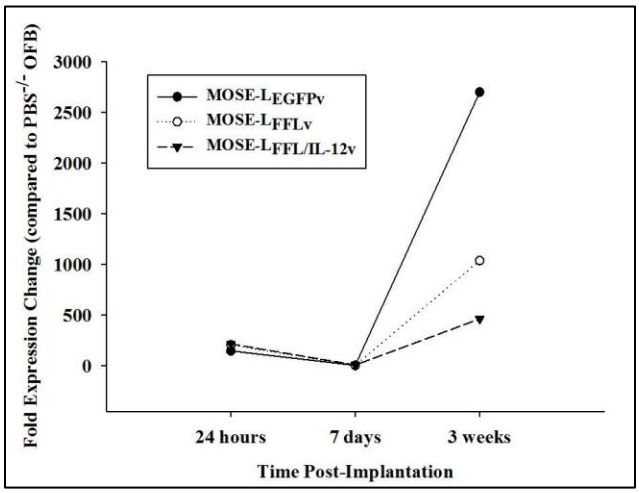

Figure 5.7. Ovarian cancer outgrowth in the OFB is non-linear. Expression of MOSE cell line gene tags (FFL and EGFP) at 24 hours, 7 days and 3 weeks post-implantation i.p.

DISCUSSION

IL-12 has been utilized in a wide variety of cancer models as a potent anti-tumorigenic therapeutic. However, clinical applications have been limited due to severe toxicity on healthy neighboring tissues associated with systemic IL-12. Ovarian cancer is typically diagnosed following disease metastasis, rendering intratumoral injections impossible and highlighting the need for a targeted therapeutic approach. The OFB is the primary site for ovarian cancer metastasis, and as a reservoir for peritoneal leukocytes offers a unique opportunity to evaluate immunomodulatory anti-metastatic therapies.

Here, we determined that the incorporation of membrane-bound IL-12 (mbIL-12) on the surface of aggressive ovarian cancer cells resulted in a significant reduction in peritoneal tumor burden after i.p. injection. Further, the reduction in disease severity correlated with a significant decrease in the expression

levels of key chemoattractants important in the recruitment of tumor associated neutrophils (TANs) and tumor-associated macrophages (TAMs), which were also present at significantly lower levels compared to the highly aggressive tumor microenvironment of the OFB. Vaccination with mitomycin c-treated cancer cells was not protective with or without mbIL-12, suggesting that MOSE cells are poorly immunogenic, and that the anti-tumorigenic activity of mbIL-12 in this model is unlikely to be due to generation of a robust adaptive immune response to the cancer cells. Notably, mbIL-12 resulted in a 200% lifespan extension in mice, which is extremely significant given the low 5-year survival rate and high rate of recurrent chemoresistant disease in ovarian cancer patients. While IL-12 mediated protection was significant, it was also transient and animals eventually experienced overwhelming disease. Together our data suggest that this mbIL-12 treatment method led to a significant, albeit transient, delay in the pro-tumorigenic cascade within the OFB due to dampened capacity in attracting pro-tumorigenic accessory cells.

A wealth of data has been gathered pertaining to the toxicity associated with systemic or soluble IL-12 administration, using a wide variety of cancer models[22, 29, 63, 64]. In clinical studies, intravenous and intraperitoneal administrations are considered deleterious to neighboring tissue, and side effects include fever, fatigue, nausea, vomiting, headache, pancytopoenia and hyperglycemia[65, 66]. Due to these systemic dosing restrictions, it is difficult to deliver therapeutically active dosages of IL-12 to solid tumor[67]. Improved targeting strategies such as liposome, alum and polymer-based delivery methods have resulted in significantly reduced toxic effects, but require repeated dosing to maintain therapeutic levels in situ [66]. Moreover, initial clinical results were underwhelming. IL-12 treatment in both solid tumors and hematological malignancies displayed an objective response rate between 0-11% when administered by itself or in combination with other therapies[14, 66]. The "objective response" refers to stable disease, as opposed to progressive disease. Regression was not achieved in these models. Preclinical and clinical studies evaluating the efficacy of direct intratumoral IL-12 injections have shown promising results but this method is inappropriate in patients with widespread metastatic disease such as ovarian cancer[25, 68, 69, 70].

IL-12 has also been used as an adjuvant to tumor antigen vaccines. When injected subcutaneously in conjunction with the melanoma gp100 antigen (highly expressed in stage III and IV melanoma) increased delayed-type hypersensitivity reactions were reported in 75% of patients, with a corresponding increase in peripheral levels of IFNγ levels[71]. However, efficacy declined when melanoma patients were administered IL-12 intravenouusly (i.v.) or vaccinated with different tumor antigens[72, 73] were not as significant when melanoma patients were treated with i.v. IL-12, or vaccinated with different tumor antigens. The latter studies suggest that the route of administration is key for tumor antigen vaccination efforts.

A wide variety of cells (tumor and accessory) have been engineered to produce secreted IL-12, inducing delayed tumor growth or protection against subsequent tumor challenge with varying degrees of success[36, 38, 74]. Engineered adenocarcinoma cells that secrete IL-12 in the tumor microenvironment can induce tumor cell rejection mediated by $CD8^+$ T cells, macrophage infiltration, vessel damage and necrosis[75]. Notably, co-administration of additional cytokines (IL-2, IL-18) or additional costimulatory molecules proved to be more effective overall in reducing tumor burden in this model than secreted IL-12 directly at the tumor site[76]. These differing results indicate the importance of evaluating tumor site-specific changes as a result of IL-12 expression. In other words, IL-12-mediated interactions may differ as a result of inherent differences in resident IL-12R-bearing populations within specific microenvironments.

There have been several examples of membrane-bound cytokines increasing the immunogenicity of tumor cells over and above the effects of secreted cytokines, ultimately leading to generation of robust anti-tumor immune responses[77, 78, 79]. The rationale for this strategy is that there is no free IL-12 release into the microenvironment, and presumably all interactions with IL-12 must be directly at the immunological synapse, reducing aberrant signaling events. MbIL-12 has been specifically tested in only a few different tumor types. In a model of colon carcinoma, Pan et al engineered CT26 cells to express either soluble or mIL-12, which were subsequently delivered by either the s.c. or i.v.(to mimic metastasis) route. Whereas i.v. administration of IL-12 secreting cells resulted in decreased lung metastasis; more marked reduction was demonstrated in mice receiving the mbIL-12 CT26 variant. Additionally, in the

membrane-bound form, 60% of mbIL-12 animals (n=5) were able to completely eliminate tumor, and remained tumor free 120 days post-implantation. MbIL-12 CT26 cells were protective against subsequent challenge with parental cells, highlighting that induction of potent long-term memory responses were achieved[21]. In a mbIL-12 expressing subcutaneous fibrosarcoma model, tumor formation was also significantly delayed and was associated with induction of tumor-specific CTL responses; although these were not sufficient to fully protect against challenge[41]. Together with our data, these studies highlight the efficacy of mbIL-12 as an effective targeting strategy in cancer therapeutics.

As noted, ovarian cancer is often diagnosed late, once the cancer has spread throughout the peritoneal cavity, which may influence the highly variable results obtained in preclinical and clinical testing of IL-12 for ovarian cancer. In a murine model, IL-12 was packaged in a polymer-DNA delivery system and injected i.p. These IL-12 polymer complexes were able to delay progression of disseminated tumor burden and inhibit ascites accumulation, but repeat injections were needed to maintain adequate local levels of cytokine[20]. When this model was carried into Phase I clinical trials, stable (as opposed to progressive) disease was noted in 6 out of 12 recurrent patients, although maximum survival was 19 months[43]. In a Phase II clinical trial using intraperitoneal recombinant human IL-12 injections, virtually no protection was offered, with the maximum result being stable disease in 2 out of 12 patients[33]. Both clinical studies were associated with side effects, including headaches, nausea, dizziness, fatigue, myalgia, fevers and grade 4 neutropenia. Thus, a more effective, controlled targeting approach needs to be considered for ovarian cancer or for peritoneal disease.

As described, IL-12 has been studied extensively in a variety of tumor types, and typically displays antitumor properties that are mediated by IFNγ secretion and several different effector cells, including $CD4^+$ and $CD8^+$ T cells, $CD3^+CD56^+$ NKT cells and NK cells[14, 29, 80, 81]. More recently, IL-12 has been found to profoundly inhibit tumor-induced Treg proliferation via IFNγ and IL-2 signaling[82]. This is crucial, given the immune suppression-dominated microenvironment present in advanced and aggressive tumors[83]. The mode of IL-12 administration has been shown to affect not only treatment efficacy but also the subtypes of tumor-infiltrating cells. For example, in a model of subcutaneous

mammary adenocarcinoma, local IL-12 administration in the tumor area resulted in significant infiltration of $CD8^+$ cells and NK cells; while systemic i.p. IL-12 injection resulted in additional infiltration of neutrophils and macrophages. In this model, systemic administration resulted in higher IFNγ production and tumor clearance[84], indicating the undervalued importance of IL-12 interactions with neutrophils and macrophages in disrupting the pro-tumorigenic cascade.

However, not all studies utilizing IL-12 have been correlated with positive results. In a clinical model of follicular B cell non-Hodgkin lytmphoma, administration of long-term IL-12 actually resulted in inferior protection, and elevated serum levels of IL-12 prior to treatment were associated with poor prognosis[66]. In fact, long-term IL-12 exposure in vitro caused T cells to lose their ability to produce IFNγ, suggesting IL-12-mediated immune impairment or exhaustion. T cell dysfunction in this case was associated with an upregulation in TIM-3 expression on T cells, and an increase in TIM-3 expressing TILs was found in this lymphoma model[66]. Clinical studies have also indicated an "adaptive" response to IL-12, in that the pharmacodynamics decrease significantly following the first dose of cytokine. Concurrently, IFNγ levels and frequency of circulating tumor-specific T cells decreased significantly[27, 85]. In our study, mbIL-12 delayed disease onset, but animals eventually reached established endpoints and had to be sacrificed due to overwhelming disease. Due to the transient nature of the observed response, we surmise that in our study the protective response elicited by mbIL-12 is dampened over time, allowing for the eventual shift towards pro-tumorigenic signals that are more conducive for tumor outgrowth. The lack of acquired protection to re-challenge also supports the hypothesis that mbIL-12 is acting locally to maintain a balance between anti- and pro-tumorigenic responses directly at the site of implantation, namely the OFB.

IL-12 has also been shown to circumvent or override the immune suppression inherent within many tumor microenvironments. Notably, IL-12 immunotherapy was effective at reactivating the anergic T cells present infiltrating non-small cell lung tumors, inducing their in situ proliferation, secretion of IFNγ and ability to kill cancer cells[86]. It is interesting to speculate that immunosuppressive mechanisms may differ between tumor microenvironments, with tumor cells able to establish site-specific pro-

tumorigenic niches depending on the pre-existing immune milieu. Alternatively, differences in efficacy may again be indicative of differences in dosage, administration route, animal model, handling, etc.

In addition to its immunomodulatory properties, IL-12 also acts as an anti-angiogenic molecule. In 1995, it was discovered that corneal neovascularization was inhibited by IL-12 in both immunocompetent and (albeit less so) in immunodeficient mice, suggesting an additional mode of action for IL-12 anti-tumorigenic properties[22]. IL-12 reduces the expression of matrix metalloproteinases required for neoangiogenesis[87]. Additionally, IFNγ induced by IL-12 signaling reduces the tumor cell production of VEGF, further downregulating angiogenic potential. NK cells play an important role in this pathway, as IL-12 signaling causes them to accumulate at sites of angiogenesis and become cytolytic for endothelial cells[88]. Further, an indirect byproduct of IL-12 signaling is the induction IFNγ inducible genes IP-10 and Mig [23, 24]. Intratumoral administration of Mig into subcutaneous Burkitt's tumors led to vascular damage and tumor necrosis, suggesting that IL-12 can also elicit bystander effects. While an in-depth look at IL-12 effects on angiogenesis in this model was beyond the scope of this study, this may partially explain the significant decrease in tumor burden displayed in mbIL-12 mice. Here the early angiogenic switch may be delayed or dysfunctional in the presence of mbIL-12 expressed on the tumor cells. As noted, this effect may not be sustainable for long periods of time, hence the transient and delayed nature of the response observed in our study.

TAMs are an important player in the tumor microenvironment, producing a slew of cytokines and chemokines conducive for tumor progression (ie CCL2, TGFβ). Monocytes and macrophages have an extremely plastic phenotype in that functional activities can be polarized to be inflammatory or anti-inflammatory, destructive or restorative[89, 90]. This plasticity is regulated by microenvironmental cytokines often resulting in functional profiles being subject to repeated alterations[91]. However, in the tumor microenvironment, macrophages are bathed in a constant immunosuppressive signaling milieu and thus display immunsuppressive and anti-inflammatory properties[89, 92, 93, 94]. Due to their highly plastic nature, these cells provide an important opportunity for immunotherapeutics. Given the importance of these cells

in this cascade, it is highly probable that IL-12 signaling alters their polarity to an anti-tumorigenic phenotype; albeit direct evidence of this was not confirmed in the present study.

While it is clear that effector lymphocytes can be targeted for immunomodulation by IL-12, only recently have monocytic subtypes likewise been evaluated for their antitumorigenic properties in response to IL-12 immunotherapy. In a subcutaneous model of Lewis lung carcinoma (3LLC), IL-12 containing microspheres significantly reduced the TAM expression of CCL2 and IL-10 within 90 minutes of treatment, although no description of effect on tumor burden was described[95]. Additionally, others have engineered $CD8^+$ T cells to secrete IL-12, resulting in a potent inflammatory state within the microenvironment that induced metastatic tumor regression[96]. However, contrary to most reports, IL-12 activity was not a result of T or NK cell stimulus. Instead, IL-12 was shown to directly reverse the immune escape mechanisms of MDSCs, DCs and TAMs present within the tumor microenvironment. With this reversal in the hardy immunosuppressive program, antigen processing and presentation were improved and $CD8^+$ effector T cells were activated. Additionally, there was a significant reduction in the $Ly6C^{hi}$ monocytic fraction in the tumor microenvironment[96]. These cells were previously described as the progenitor population to TAMs and TANs[97].

In our study, we characterized the composition of the metastatic tumor microenvironment present in the OFB. Specifically, we were able to demonstrate that the levels of infiltrating TANs and TAMs closely correlated with the disease state. Hence, the levels of OFB-associated TANs and TAMs were higher in animals presenting with highly aggressive disease than those in which disease progressed more slowly. The expression of mbIL-12 directly on the highly aggressive MOSE cell variant was sufficient to significantly delay tumor onset and the accumulation of TANs and TAMs was significantly reduced. As monocytic and neutrophil chemoattractant expression levels were also reduced as early as day 7 (Supp Mat), we believe that early mbIL-12 signaling is dampening their expression, possibly due to an early modulation of monocytic activation signals, as previously described[95]. Contrary to other animal models reports, we did not find evidence that CD8+ T cells or NK cells were involved in the protective effect of IL-12. However, we cannot definitively rule out whether IL-12 was activating local NK cells in a manner

that controlled the initial outgrowths, and this should be addressed in future studies. Instead, our results are in line with recent reports of IL-12 modulating monocytic subsets towards an anti-tumorigenic phenotype. In support of this, we found an mIL-12-associated decrease in the number of $Ly6C^{hi}$ monocytes present within the OFB following cancer cell seeding, indicating a decrease in TAN and TAM progenitor populations (data not shown). Our study indicates that the poorly immunogenic MOSE-L_{FFLv} cells are incredibly efficient in establishing a pro-tumorigenic niche within the OFB, and that highly localized expression of IL-12 is transiently able to ameliorate these effects, postponing the onset of severe disease. Future studies should help determine how IL-12 is dampening the recruitment of TANs and TAMs within the tumor microenvironment as well as define the activation status of local NK cells. While this study verifies the efficacy of IL-12 as a means to target peritoneal metastatic tumor development, more effective strategies to deliver and sustain mbIL-12 within the OFB need to be evaluated. Modifying cells within the OFB to express mbIL-12 may offer a means to prevent recurrent disease. However, for this to be effective, the OFB must be retained at the time of surgical debulking, contrary to current practice. Therefore, the OFB may present an effective target for immunomodulatory therapies designed to extend the life expectancy of ovarian cancer patients.

.

Supplementary Materials

Leukocyte Characterization (% of CD45+, +/- SEM)					
	Markers	**$PBS^{-/-}$ OFB**	**MOSE-L_{FFLv} OFB**	**MOSE-$L_{FFL/IL\text{-}12v}$ OFB**	**MOSE-L_{EGFPv} OFB**
% $CD45^+$ (of viable)		**81.7 (4.3)**	**58.1 (1.8)**	**78.6 (1.4)**	**87.1 (2.5)**
% lymphocytes		**60.1 (5.2)**	**32.8 (5.1)**	**62.0 (2.4)**	**70.1 (3.2)**
% mono/granulocytes (R2)		**36.3 (5.1)**	**62.0 (2.4)**	**34.9 (2.4)**	**28.7 (3.1)**
B cells	**$CD19^+$**	**55.2 (2.6)**	**19.7 (2.7)**	**51.8 (2.0)**	**39.7 (2.7)**
B1	**$CD19^+CD11b^+B220^{lo/+}$**	**24.0 (5.3)**	**5.9 (0.4)**	**23.4 (1.3)**	**29.6 (2.2)**
B2	**$CD19^+CD11b^-B220^{lo/+}$**	**22.4 (4.8)**	**12.3 (2.5)**	**19.2 (0.8)**	**8.5 (1.8)**
T cells	**$CD3^+$**	**16.4 (1.6)**	**9.7 (1.7)**	**20.7 (1.3)**	**25.3 (2.4)**
T_H	**$CD3^+CD4^+$**	**6.8 (1.3)**	**4.6 (1.0)**	**9.1 (1.0)**	**14.4 (1.9)**
T_C	**$CD3^+CD8^+$**	**3.2 (0.7)**	**2.0 (0.3)**	**5.4 (0.5)**	**8.0 (0.9)**
NKT	**$CD3^+NK1.1^+$**	**1.0 (0.2)**	**0.8 (0.4)**	**1.1 (0.1)**	**0.8 (0.1)**
T_{REG}	**$CD3^+CD4^+CD25^+$**	**0.07 (0.03)**	**0.07 (0.02)**	**0.1 (0.03)**	**0.9 (0.1)**
$CD3^+CD4^-CD8^-NK1.1^-$		**6.1 (0.5)**	**2.8 (0.4)**	**5.8 (0.3)**	**2.5 (0.2)**
NKs	**$NK1.1^+CD11b^+CD3^-$**	**5.8 (0.9)**	**3.0 (0.9)**	**5.2 (0.4)**	**1.7 (0.2)**
R1 DCs	**$CD11c^+CD11b^{lo/-}$**	**16.4 (1.6)**	**10.7 (2.1)**	**18.4 (1.3)**	**18.4 (2.0)**
R2 DCs	**$CD11b^{+/lo}CD11c^+F4/80^-$**	**3.4 (0.2)**	**3.1 (0.1)**	**3.6 (0.2)**	**5.1 (0.2)**
LPMs	**$CD11b^+F4/80^+$**	**2.6 (0.7)**	**9.8 (1.0)**	**2.4 (0.3)**	**3.2 (1.0)**
SPMs	**$CD11b^{+/lo}F4/80^{lo}$**	**17.7 (3.9)**	**35.5 (3.2)**	**18.0 (1.5)**	**10.8 (1.2)**
Monocytes	**$CD11b^+F4/80^-$**	**0.2 (0.1)**	**4.7 (1.4)**	**0.7 (0.1)**	**2.3 (0.3)**
Monocytes (2)	**$CD11b^{lo}F4/80^-$**	**4.2 (0.3)**	**3.0 (0.1)**	**4.9 (0.4)**	**9.0 (0.6)**
PMNs	**$CD11b^+Ly6G^+Ly6C^+$**	**0.4 (0.2)**	**7.0 (2.2)**	**0.2 (0.06)**	**1.7 (0.6)**
PreBoMs	**$CD19^+CD11b^{hi}B220^{lo}F480^+$ $CD93^+CD69^+$**	**0.7 (0.2)**	**0.4 (0.1)**	**0.5 (0.1)**	**0**

Supplementary Table S5.1. FACS analysis of leukocyte populations in the OFB 3 weeks post-injection.

Leukocyte Characterization (% of CD45+, +/- SEM)					
	Markers	**PBS$^{-/-}$ PSF**	**MOSE-L$_{FFLv}$ PSF**	**MOSE-L$_{FFL/IL-12v}$ PSF**	**MOSE-L$_{EGFPv}$ PSF**
% CD45$^+$ (of viable)		**99.9 (0.02)**	**86.8 (3.1)**	**99.9 (0.01)**	**99.2 (0.6)**
% lymphocytes		**56.1 (6.2)**	**16.7 (3.3)**	**52.6 (3.2)**	**62.9 (3.9)**
% mono/granulocytes (R2)		**43.8 (3.2)**	**79.1 (3.2)**	**47.7 (3.1)**	**36.2 (3.8)**
B cells	**CD19$^+$**	**54.8 (4.6)**	**14.5 (1.6)**	**46.3 (1.9)**	**60.4 (3.3)**
B1	**CD19$^+$CD11b$^+$B220$^{lo/+}$**	**23.4 (3.0)**	**6.2 (0.7)**	**21.0 (1.2)**	**46.4 (1.9)**
B2	**CD19$^+$CD11b$^-$B220$^{lo/-}$**	**24.6 (5.3)**	**7.5 (1.9)**	**18.4 (1.9)**	**13.5 (1.4)**
T cells	**CD3$^+$**	**5.8 (1.7)**	**4.4 (1.2)**	**6.9 (0.9)**	**6.6 (1.0)**
T$_H$	**CD3$^+$CD4$^+$**	**3.1 (0.8)**	**2.0 (0.6)**	**4.1 (0.5)**	**3.7 (0.5)**
T$_C$	**CD3$^+$CD8$^+$**	**1.8 (0.7)**	**1.7 (0.4)**	**1.9 (0.3)**	**2.3 (0.5)**
NKT	**CD3$^+$NK1.1$^+$**	**0.5 (0.3)**	**0.1 (0.05)**	**0.7 (0.5)**	**0.2 (0.04)**
T$_{REG}$	**CD3$^+$CD4$^+$CD25$^+$**	**0.04 (0.01)**	**0.05 (0.02)**	**0.1 (0.02)**	**0.4 (0.1)**
CD3$^+$CD4$^-$CD8$^-$NK1.1$^-$		**0.7 (0.2)**	**0.5 (0.2)**	**0.7 (0.1)**	**0.5 (0.1)**
NKs	**NK1.1$^+$CD11b$^+$CD3$^-$**	**14.5 (8.4)**	**0.6 (0.4)**	**7.9 (6.3)**	**0.4 (0.03)**
R1 DCs	**CD11c$^+$CD11b$^{lo/-}$**	**6.9 (1.0)**	**4.6 (0.6)**	**8.0 (0.6)**	**6.2 (0.9)**
R2 DCs	**CD11b$^{+/lo}$CD11c$^+$F4/80$^-$**	**1.2 (0.2)**	**2.7 (0.3)**	**1.4 (0.1)**	**1.5 (0.2)**
LPMs	**CD11b$^+$F4/80$^+$**	**23.8 (6.3)**	**25.9 (1.7)**	**26.1 (2.0)**	**18.5 (2.5)**
SPMs	**CD11b$^{+/lo}$F4/80^{lo}**	**7.9 (1.0)**	**34.6 (0.8)**	**11.3 (1.2)**	**3.7 (0.6)**
Monocytes	**CD11b$^+$F4/80$^-$**	**0.1 (0.04)**	**2.3 (0.8)**	**0.3 (0.1)**	**0.7 (0.1)**
Monocytes (2)	**CD11b^{lo}F4/80$^-$**	**4.3 (0.6)**	**9.1 (1.4)**	**7.0 (0.7)**	**10.4 (0.6)**
PMNs	**CD11b$^+$Ly6G$^+$Ly6C$^+$**	**0.1 (0.05)**	**7.4 (1.7)**	**0.07 (0.02)**	**0.7 (0.2)**
PreBoMs	**CD19$^+$CD11b^{hi}B220^{lo} F480$^+$CD93$^+$CD69$^+$**	**0.9 (0.3)**	**0.6 (0.1)**	**0.9 (0.1)**	**0**

Supplementary Table S5.2. FACS analysis of leukocyte populations in the PSF 3 weeks post-injection.

Gene Expression (Avg dCT ± SEM)				
Gene	**PBS**	**MOSE-L_{EGFPv}**	**MOSE-L_{FFLv}**	**MOSE-$L_{FFL/IL\text{-}12v}$**
Arg1	8.3 (1.0)		3.8 (0.6)	7.8 (0.7)
CCL1	14.2 (0.4)	13.2 (0.7)	16.3 90.9)	14.1 (0.6)
CCL2	4.5 (0.5)	5.5 (0.2)	3.7 (0.2)	3.9 (0.5)
CCL3	10.1 (0.5)		10.1 (0.2)	9.5 (0.5)
CCL5	4.0 (0.3)	4.3 (0.3)	7.3 (0.4)	3.4 (0.3)
CCL7	5.7 (0.5)		6.6 (0.3)	4.9 (0.5)
CD36	9.3 (0.4)		15.5 (0.7)	9.0 (0.3)
CXCL1	9.0 (0.6)	6.1 (1.0)	4.4 (0.3)	8.5 (0.8)
CXCL12	3.2 (0.1)		6.1 (0.1)	3.4 (0.2)
CXCL13	-0.73 (0.3)	0.3 (0.1)	7.9 (0.8)	-0.4 (0.3)
CXCL16	4.9 (0.3)		5.5 (0.5)	5.0 (0.2)
CXCL2	9.1 (0.7)	10.8 (0.7)	8.7 (0.7)	9.3 (0.8)
CXCL3	14.4 (1.5)	14.5 (3.5)	9.1 (0.6)	15.1 (1.0)
CXCL5	11.9 (0.7)	12.6 (1.3)	9.4 (0.2)	11.7 (0.5)
GM-CSF	11.7 (0.4)		14.0 (0.1)	11.9 (0.3)
HIF1a	5.2 (0.2)		4.5 (0.2)	5.1 (0.2)
IFNy	10.3 (1.3)	11.7 (1.2)	15.3 (1.7)	12.3 (1.2)
IL-10	8.3 (0.1)		8.6 (0.2)	7.7 (0.2)
IL-12p35	12.2 (0.2)	12.1 (0.8)	16.7 (0.3)	11.9 (0.3)
IL-13	13.5 (0.8)	13.8 (0.3)	15.3 (0.6)	13.8(0.5)
IL-1b	8.7 (0.5)		8.68 (0.3)	8.95 (0.3)
IL-2	11.4 (0.3)	13.8 (1.0)	14.9 (0.2)	11.6 (0.4)
IL-4	13.7 (0.3)	13.8 (1.0)	14.9 (0.2)	14.3 (0.4)
IL-6	9.9 (0.5)		10.6 (0.3)	10.2 (0.3)
iNOS	12.08 (0.2)		10.61 (0.2)	11.95 (0.5)
M6pr	4.2 (0.1)		5.6 (0.4)	4.3 (0.2)
MCSF	6.4 (0.2)		6.0 (0.2)	6.7 (0.2)
TGFb	12.5 (0.3)	4.6 (0.9)	13.0 (0.4)	13.2 (0.3)
TNFa	7.3 90.4)		10.3 (0.4)	7.5 (0.2)
VEGFa	4.9 (0.4)		3.7 (0.6)	5.3 (0.1)
Ym1	9.6 (0.9)		13.0 (0.7)	8.1 (0.9)

Supplementary Table S5.3. Gene expression analysis of the OFB 3 weeks post-injection. dCT calculated relative to L-19 (housekeeping gene) expression. NOTE: grayed out cells indicate that genes were not run due to sample restrictions.

Leukocyte Characterization (% of CD45+, +/- SEM)					
	Markers	**PBS$^{-/-}$ OFB**	**MOSE-L_{FFLv} OFB**	**MOSE-$L_{FFL/IL\text{-}12v}$ OFB**	**MOSE-L_{EGFPv} OFB**
% CD45$^+$ (of viable)		**82.9 (2.6)**	**88.2 (1.6)**	**87.2 (1.6)**	**87.8 (1.5)**
% lymphocytes		**34.9 (3.1)**	**29.7 (4.2)**	**29.7 (3.5)**	**37.5 (4.4)**
% mono/granulocytes (R2)		**63.6 (3.2)**	**69.1 (4.1)**	**68.8 (3.6)**	**61.4 (4.3)**
B cells	**CD19$^+$**	**17.4 (1.7)**	**13.7 (3.0)**	**24.5 (3.0)**	**22.3 (1.7)**
B1	**CD19$^+$CD11b$^+$B220$^{lo/+}$**	**7.4 (0.4)**	**6.1 (1.3)**	**9.1 (1.0)**	**8.9 (1.3)**
B2	**CD19$^+$CD11b$^-$B220$^{lo/+}$**	**9.3 (1.4)**	**5.8 (1.7)**	**11.8 (2.7)**	**9.6 (1.0)**
T cells	**CD3$^+$**	**7.6 (1.2)**	**6.9 (1.0)**	**7.3 (0.8)**	**10.0 (2.1)**
T_H	**CD3$^+$CD4$^+$**	**3.5 (0.6)**	**3.1 (0.7)**	**2.8 (0.6)**	**4.4 (1.4)**
T_C	**CD3$^+$CD8$^+$**	**1.0 (0.2)**	**0.8 (0.1)**	**1.0 (0.1)**	**1.4 (0.4)**
NKT	**CD3$^+$NK1.1$^+$**	**0.4 (0.02)**	**0.5 (0.1)**	**0.9 (0.1)**	**0.9 (0.2)**
T_{REG}	**CD3$^+$CD4$^+$CD25$^+$**	**0.1 (0.05)**	**0.2 (0.04)**	**0.1 (0.02)**	**0.1 (0.04)**
CD3$^+$CD4$^-$CD8$^-$NK1.1$^-$		**3.0 (0.5)**	**2.6 (0.3)**	**2.8 (0.3)**	**3.5 (0.5)**
mNK	**NK1.1$^+$CD11b$^+$CD3$^-$**	**2.4 (0.2)**	**2.0 (0.4)**	**2.2 (0.2)**	**2.4 (0.1)**
preNK	**NK1.1$^+$CD11b$^-$CD3$^-$**	**0.8 (0.04)**	**1.2 (0.03)**	**1.3 (0.1)**	**1.6 (0.2)**
R1 DCs	**CD11c$^+$CD11b$^{lo/-}$**	**7.7 (1.7)**	**5.6 (1.9)**	**4.0 (1.4)**	**6.8 (2.6)**
R2 DCs	**CD11b$^{+/lo}$CD11c$^+$F4/80$^-$**	**3.3 (0.8)**	**1.6 (0.8)**	**1.1 (0.6)**	**1.7 (0.9)**
LPMs	**CD11b$^+$F4/80$^+$**	**6.3 (0.7)**	**3.5 (0.7)**	**2.4 (0.4)**	**2.9 (0.3)**
SPMs	**CD11b$^{+/lo}$F4/80^{lo}**	**26.4 (1.2)**	**17.4 (2.4)**	**22.5 (3.6)**	**20.9 (1.0)**
Monocytes	**CD11b$^+$F4/80$^-$**	**1.0 (0.2)**	**4.4 (0.9)**	**4.0 (0.8)**	**4.6 (1.0)**
Monocytes (2)	**CD11b^{lo}F4/80$^-$**	**10.3 (0.8)**	**16.5 (2.9)**	**13.8 (1.9)**	**15.6 (1.9)**
PMNs	**CD11b$^+$Ly6G$^+$Ly6C$^+$**	**13.2 (1.9)**	**16.8 (2.5)**	**12.5 (2.2)**	**6.7 (1.0)**
PreBoMs	**CD19$^+$CD11b^{hi}B220^{lo} F480$^+$CD93$^+$CD69$^+$**	**0.5 (0.07)**	**0.2 (0.02)**	**0.2 (0.02)**	**0.2 (0.02)**

Supplementary Table S5.4. FACS analysis of leukocyte populations in the OFB 24 hours post-injection.

Leukocyte Characterization (% of CD45+, +/- SEM)					
	Markers	**PBS$^{-/-}$ PSF**	**MOSE-L$_{FFLv}$ PSF**	**MOSE-L$_{FFL/IL-12v}$ PSF**	**MOSE-L$_{EGFPv}$ PSF**
% CD45$^+$ (of viable)		**99.8 (0.1)**	**99.4 (0.2)**	**98.3 (1.0)**	**99.0 (0.8)**
% lymphocytes		**34.1 (2.7)**	**23.5 (3.9)**	**23.3 (3.4)**	**24.7 (3.4)**
% mono/granulocytes (R2)		**64.3 (2.6)**	**75.0 (3.8)**	**75.1 (3.4)**	**74.0 (3.5)**
B cells	**CD19$^+$**	**32.0 (1.9)**	**21.2 (3.5)**	**16.0 (1.7)**	**21.9 (3.5)**
B1	**CD19$^+$CD11b$^+$B220$^{lo/+}$**	**26.6 (1.6)**	**13.9 (3.1)**	**10.2 (1.0)**	**14.6 (2.5)**
B2	**CD19$^+$CD11b$^-$B220$^{lo/+}$**	**4.5 (1.8)**	**4.0 (1.1)**	**3.9 (1.1)**	**4.9 (0.7)**
T cells	**CD3$^+$**	**3.3 (0.5)**	**3.2 (0.4)**	**3.9 (0.3)**	**5.2 (0.8)**
T$_H$	**CD3$^+$CD4$^+$**	**2.0 (0.4)**	**2.2 (0.3)**	**2.6 (0.2)**	**3.5 (0.5)**
T$_C$	**CD3$^+$CD8$^+$**	**0.6 (0.1)**	**0.4 (0.1)**	**0.6 (0.1)**	**0.9 (0.2)**
NKT	**CD3$^+$NK1.1$^+$**	**0.5 (0.2)**	**0.2 (0.03)**	**0.2 (0.04)**	**0.2 (0.04)**
T$_{REG}$	**CD3$^+$CD4$^+$CD25$^+$**	**0.05 (0.02)**	**0.09 (0.04)**	**0.02 (0.01)**	**0.05 (0.01)**
CD3$^+$CD4$^-$CD8$^-$NK1.1$^-$		**0.7 (0.1)**	**0.4 (0.1)**	**0.6 (0.1)**	**0.7 (0.2)**
mNK	**NK1.1$^+$CD11b$^+$CD3$^-$**	**3.5 (1.5)**	**1.5 (0.3)**	**1.3 (0.1)**	**1.9 (0.2)**
preNK	**NK1.1$^+$CD11b$^-$CD3$^-$**	**0.2 (0.03)**	**0.8 (0.2)**	**0.7 (0.2)**	**0.8 (0.1)**
R1 DCs	**CD11c$^+$CD11b$^{lo/-}$**	**4.9 (1.2)**	**3.3 (0.8)**	**3.1 (0.9)**	**4.3 (1.3)**
R2 DCs	**CD11b$^{+/lo}$CD11c$^+$F4/80$^-$**	**1.4 (0.4)**	**0.4 (0.1)**	**0.3 (0.1)**	**0.7 (0.4)**
LPMs	**CD11b$^+$F4/80$^+$**	**13.1 (2.3)**	**5.3 (2.4)**	**4.0 (1.2)**	**5.6 (1.8)**
SPMs	**CD11b$^{+/lo}$F4/80^{lo}**	**26.4 (1.7)**	**27.7 (2.3)**	**32.1 (3.4)**	**28.5 (1.5)**
Monocytes	**CD11b$^+$F4/80$^-$**	**0.6 (0.1)**	**2.5 (0.7)**	**5.5 (1.5)**	**6.4 (1.4)**
Monocytes (2)	**CD11b^{lo}F4/80$^-$**	**17.4 (1.4)**	**25.9 (3.8)**	**21.6 (3.4)**	**28.1 (3.3)**
PMNs	**CD11b$^+$Ly6G$^+$Ly6C$^+$**	**4.7 (1.7)**	**8.8 (2.2)**	**10.0 (2.4)**	**5.3 (0.9)**
PreBoMs	**CD19$^+$CD11b^{hi}B220^{lo} F480$^+$CD93$^+$CD69$^+$**	**0.4 (0.04)**	**0.1 (0.02)**	**0.2 (0.08)**	**0.06 (0.01)**

Supplementary Table S5.5. FACS analysis of leukocyte populations in the PSF 24 hours post-injection.

Leukocyte Characterization (% of CD45+, +/- SEM)					
	Markers	**PBS$^{-/-}$ OFB**	**MOSE-L$_{FFLv}$ OFB**	**MOSE-L$_{FFL/IL-12v}$ OFB**	**MOSE-L$_{EGFPv}$ OFB**
% CD45$^+$ (of viable)		**76.2 (2.1)**	**80.1 (1.8)**	**80.1 (2.5)**	**88.4 (2.0)**
% lymphocytes		**63.1 (2.6)**	**61.2 (1.4)**	**63.8 (2.9)**	**64.8 (3.6)**
% mono/granulocytes (R2)		**31.7 (2.8)**	**32.6 (1.9)**	**33.6 (2.8)**	**32.9 (3.8)**
B cells	**CD19$^+$**	**34.5 (4.8)**	**35.4 (1.0)**	**30.2 (3.4)**	**31.1 (2.8)**
B1	**CD19$^+$CD11b$^+$B220$^{lo/+}$**	**16.5 (1.9)**	**15.6 (0.7)**	**12.9 (1.0)**	**17.5 (2.8)**
B2	**CD19$^+$CD11b$^-$B220$^{lo/+}$**	**12.1 (3.1)**	**11.9 (0.6)**	**12.4 (3.5)**	**9.5 (2.0)**
T cells	**CD3$^+$**	**9.4 (2.0)**	**7.9 (1.4)**	**10.5 (2.4)**	**8.2 (1.5)**
T$_H$	**CD3$^+$CD4$^+$**	**5.5 (1.1)**	**4.1 (1.4)**	**5.2 (1.0)**	**3.8 (0.6)**
T$_C$	**CD3$^+$CD8$^+$**	**3.1 (0.4)**	**2.7 (0.3)**	**3.8 (0.14)**	**2.2 (0.1)**
NKT	**CD3$^+$NK1.1$^+$**	**1.3 (0.2)**	**1.4 (0.1)**	**1.8 (0.2)**	**1.6 (0.4)**
T$_{REG}$	**CD3$^+$CD4$^+$CD25$^+$**	**0.1 (0.01)**	**0.1 (0.02)**	**0.07 (0.02)**	**0.3 (0.04)**
CD3$^+$CD4$^-$CD8$^-$NK1.1$^-$		**5.1 (0.4)**	**5.2 (0.3)**	**6.5 (0.3)**	**5.6 (0.5)**
mNK	**NK1.1$^+$CD11b$^+$CD3$^-$**	**3.5 (0.3)**	**4.3 (0.4)**	**5.3 (0.6)**	**4.8 (1.1)**
preNK	**NK1.1$^+$CD11b$^-$CD3$^-$**	**2.0 (0.2)**	**1.7 (0.1)**	**1.8 (0.2)**	**1.0 (0.2)**
R1 DCs	**CD11c$^+$CD11b$^{lo/-}$**	**17.8 (0.9)**	**15.4 (0.6)**	**16.9 (1.6)**	**22.3 (2.6)**
R2 DCs	**CD11b$^{+/lo}$CD11c$^+$F4/80$^-$**	**3.2 (0.5)**	**3.7 (0.5)**	**4.3 (1.0)**	**3.7 (0.5)**
LPMs	**CD11b$^+$F4/80$^+$**	**4.1 (0.7)**	**5.2 (0.9)**	**4.7 (0.9)**	**3.7 (0.9)**
SPMs	**CD11b$^{+/lo}$F4/80^{lo}**	**16.8 (2.3)**	**15.1 (1.2)**	**13.8 (2.3)**	**18.3 (1.8)**
Monocytes	**CD11b$^+$F4/80$^-$**	**1.3 (0.2)**	**1.1 (0.1)**	**0.9 (0.2)**	**2.6 (0.3)**
Monocytes (2)	**CD11b^{lo}F4/80$^-$**	**6.4 (0.7)**	**8.1 (1.0)**	**6.1 (0.8)**	**6.2 (1.0)**
PMNs	**CD11b$^+$Ly6G$^+$Ly6C$^+$**	**1.3 (0.5)**	**2.3 (1.0)**	**1.3 (1.0)**	**1.2 (0.3)**
PreBoMs	**CD19$^+$CD11b^{hi}B220^{lo} F480$^+$CD93$^+$CD69$^+$**	**0.07 (0.01)**	**0.2 (0.03)**	**0.1 (0.04)**	**0.1 (0.02)**

Supplementary Table S5.6. FACS analysis of leukocyte populations in the OFB 7 days post-injection.

Leukocyte Characterization (% of CD45+, +/- SEM)					
	Markers	**PBS$^{-/-}$ PSF**	**MOSE-L$_{FFLv}$ PSF**	**MOSE-L$_{FFL/IL\text{-}12v}$ PSF**	**MOSE-L$_{EGFPv}$ PSF**
% CD45$^+$ (of viable)		**99.7 (0.2)**	**99.8 (0.1)**	**99.8 (0.1)**	**99.9 (0.01)**
% lymphocytes		**55.7 (2.1)**	**55.6 (2.5)**	**50.4 (4.7)**	**39.7 (2.2)**
% mono/granulocytes (R2)		**44.1 (2.1)**	**44.6 (2.5)**	**49.2 (4.7)**	**59.8 (2.2)**
B cells	**CD19$^+$**	**45.2 (2.4)**	**43.9 (3.3)**	**35.4 (5.9)**	**29.3 (0.8)**
B1	**CD19$^+$CD11b$^+$B220$^{lo/+}$**	**31.5 (2.4)**	**30.2 (1.7)**	**21.8 (3.6)**	**20.3 (2.0)**
B2	**CD19$^+$CD11b$^-$B220$^{lo/+}$**	**9.3 (1.6)**	**11.7 (2.5)**	**10.8 (2.6)**	**7.0 (1.3)**
T cells	**CD3$^+$**	**6.9 (0.8)**	**5.7 (0.5)**	**5.7 (1.0)**	**6.1 (1.2)**
T$_H$	**CD3$^+$CD4$^+$**	**3.7 (0.4)**	**2.7 (0.3)**	**3.0 (0.5)**	**3.2 (0.6)**
T$_C$	**CD3$^+$CD8$^+$**	**1.7 (0.3)**	**1.7 (0.3)**	**1.4 (0.3)**	**1.4 (0.4)**
NKT	**CD3$^+$NK1.1$^+$**	**0.5 (0.2)**	**0.8 (0.4)**	**0.4 (0.1)**	**1.1 (0.5)**
T$_{REG}$	**CD3$^+$CD4$^+$CD25$^+$**	**0.1 (0.04)**	**0.06 (0.01)**	**0.05 (0.01)**	**0.1 (0.02)**
CD3$^+$CD4$^-$CD8$^-$NK1.1$^-$		**1.3 (0.2)**	**1.2 (0.1)**	**1.2 (0.2)**	**1.3 (0.3)**
mNK	**NK1.1$^+$CD11b$^+$CD3$^-$**	**1.9 (0.9)**	**5.8 (4.2)**	**3.0 (1.4)**	**2.7 (1.5)**
preNK	**NK1.1$^+$CD11b$^-$CD3$^-$**	**0.4 (0.03)**	**0.5 (0.1)**	**0.4 (0.07)**	**0.3 (0.05)**
R1 DCs	**CD11c$^+$CD11b$^{lo/-}$**	**8.4 (0.5)**	**7.0 (0.4)**	**8.3 (1.4)**	**7.8 (1.1)**
R2 DCs	**CD11b$^{+/lo}$CD11c$^+$F4/80$^-$**	**1.1 (0.1)**	**1.2 (0.1)**	**1.5 (0.2)**	**1.7 (0.3)**
LPMs	**CD11b$^+$F4/80$^+$**	**25.1 (1.8)**	**17.4 (1.7)**	**14.6 (1.8)**	**15.7 (2.3)**
SPMs	**CD11b$^{+/lo}$F4/80^{lo}**	**9.7 (1.1)**	**23.5 (1.7)**	**26.5 (4.5)**	**34.3 (3.1)**
Monocytes	**CD11b$^+$F4/80$^-$**	**0.5 (0.1)**	**0.5 (0.1)**	**0.6 (0.1)**	**1.3 (0.4)**
Monocytes (2)	**CD11b^{lo}F4/80$^-$**	**8.6 (0.5)**	**7.5 (0.4)**	**7.3 (0.6)**	**8.1 (1.2)**
PMNs	**CD11b$^+$Ly6G$^+$Ly6C$^+$**	**0.2 (0.05)**	**0.3 (0.1)**	**0.1 (0.06)**	**0.5 (0.3)**
PreBoMs	**CD19$^+$CD11b^{hi}B220^{lo} F480$^+$CD93$^+$CD69$^+$**	**0.2 (0.01)**	**0.3 (0.05)**	**0.3 (0.04)**	**0.3 (0.06)**

Supplementary Table S5.7. FACS analysis of leukocyte populations in the PSF 7 days post-injection.

Gene Expression (Avg dCT ± SEM)				
Gene	**PBS**	**MOSE-LEGFPv**	**MOSE-LFFLv**	**MOSE-LFFL/IL-12v**
Arg1	8.9 (0.6)	8.0 (0.4)	8.1 (0.4)	9.0 (0.3)
CCL1	14.8 (0.4)	13.5 (0.6)	15.3 (0.2)	15.2 (0.5)
CCL2	6.5 (0.4)	6.3 (0.3)	6.9 (0.3)	7.7 (0.2)
CCL3	11.5 (0.4)	11.3 (0.2)	11.5 90.1)	11.7 (0.2)
CCL5	4.3 (0.2)	3.9 (0.2)	4.4 (0.2)	4.0 (0.3)
CCL7	7.3 (0.3)	7.2 (0.3)	7.2 (0.3)	8.3 (0.1)
CXCL1	10.2 (0.3)	9.7 (0.3)	10.1 (0.2)	11.0 (0.2)
CXCL12	3.7 90.3)	4.1 90.1)	3.9 (0.2)	4.3 (0.1)
CXCL13	-1.4 (0.1)	0.1 (0.1)	-1.2 90.2)	-0.66 (0.3)
CXCL16	5.5 (0.1)	5.2 (0.1)	5.6 (0.1)	6.1 (0.1)
CXCL2	10.2 (0.4)	10.5 (0.2)	10.8 (0.1)	11.6 (0.5)
CXCL3	15.9 (1.1)	16.3 (0.3)	15.5 (0.5)	18.6 (0.3)
CXCL5	15.7 90.4)	15.0 (0.2)	15.8 (0.2)	16.6 (0.2)
GM-CSF	12.4 (0.1)	12.6 (0.3)	12.5 (0.2)	13.0 90.1)
HIF1a	5.4 90.2)	5.2 (0.1)	5.7 (0.1)	5.6 (0.2)
IFNy	9.1 (0.8)	10.6 (1.1)	10.1 (0.4)	11.6 (0.8)
IL-10	8.9 (0.3)	8.3 (0.3)	8.7 (0.2)	9.1 (0.1)
IL-12p35	12.6 90.2)	12.1 (0.3)	13.0 90.2)	12.7 (0.1)
IL-13	15.6 (0.3)	14.5 (0.6)	15.6 (0.8)	17.3 (0.4)
IL-1b	9.5 (0.3)	10.6 (0.4)	9.8 (0.1)	10.9 (0.5)
IL-2	13.0 (0.2)	12.0 (0.2)	12.8 (0.2)	12.9 (0.2)
IL-4	13.7 (0.3)	13.1 (0.2)	14.9 (0.3)	14.5 90.3)
IL-6	10.2 (0.4)	11.1 (0.2)	10.8 (0.1)	11.7 (0.2)
iNOS	13.4 (0.4)	13.2 (0.3)	13.6 (0.1)	14.2 (0.3)
M6pr	4.3 (0.3)	4.2 (0.1)	4.8 (0.1)	4.6 (0.1)
MCSF	6.8 (0.4)	6.8 (0.1)	7.5 (0.2)	7.7 (0.2)
TGFb	7.1 (0.4)	6.7 (0.2)	7.3 (0.1)	7.5 (0.1)
TNFa	9.0 (0.4)	8.6 (0.2)	9.1 (0.1)	9.1 (0.1)
VEGFa	6.0 (0.3)	5.8 (0.2)	6.7 (0.2)	6.7 (0.2)
Ym1	10.9 (0.8)	1.4 (0.6)	9.5 (0.5)	9.1 (0.7)

Supplementary Table S5.8. Gene expression analysis of the OFB 7 days post-injection. dCT calculated relative to L-19 (housekeeping gene) expression.

REFERENCES

1. Siegel R, DeSantis C, Virgo K, Stein K, Mariotto A, Smith T*, et al.* Cancer treatment and survivorship statistics, 2012. *CA: a cancer journal for clinicians* 2012, 62(4): 220-241.
2. Hunn J, Rodriguez GC. Ovarian cancer: etiology, risk factors, and epidemiology. *Clinical obstetrics and gynecology* 2012, 55(1): 3-23.
3. Benson JR, Jatoi I, Keisch M, Esteva FJ, Makris A, Jordan VC. Early breast cancer. *Lancet* 2009, 373(9673): 1463-1479.
4. Krishnan V, Stadick N, Clark R, Bainer R, Veneris JT, Khan S*, et al.* Using MKK4's metastasis suppressor function to identify and dissect cancer cell-microenvironment interactions during metastatic colonization. *Cancer metastasis reviews* 2012, 31(3-4): 605-613.
5. Gerber SA, Rybalko VY, Bigelow CE, Lugade AA, Foster TH, Frelinger JG*, et al.* Preferential attachment of peritoneal tumor metastases to omental immune aggregates and possible role of a unique vascular microenvironment in metastatic survival and growth. *The American journal of pathology* 2006, 169(5): 1739-1752.
6. Krist LF, Kerremans M, Broekhuis-Fluitsma DM, Eestermans IL, Meyer S, Beelen RH. Milky spots in the greater omentum are predominant sites of local tumour cell proliferation and accumulation in the peritoneal cavity. *Cancer immunology, immunotherapy : CII* 1998, 47(4): 205-212.
7. Gray KS, Collins CM, Speck SH. Characterization of omental immune aggregates during establishment of a latent gammaherpesvirus infection. *PloS one* 2012, 7(8): e43196.
8. Rangel-Moreno J, Moyron-Quiroz JE, Carragher DM, Kusser K, Hartson L, Moquin A*, et al.* Omental milky spots develop in the absence of lymphoid tissue-inducer cells and support B and T cell responses to peritoneal antigens. *Immunity* 2009, 30(5): 731-743.
9. Krist LF, Eestermans IL, Steenbergen JJ, Hoefsmit EC, Cuesta MA, Meyer S*, et al.* Cellular composition of milky spots in the human greater omentum: an immunochemical and ultrastructural study. *The Anatomical record* 1995, 241(2): 163-174.
10. Sorensen EW, Gerber SA, Sedlacek AL, Rybalko VY, Chan WM, Lord EM. Omental immune aggregates and tumor metastasis within the peritoneal cavity. *Immunologic research* 2009, 45(2-3): 185-194.
11. Bigda J, Mysliwska J, Dziadziuszko R, Bigda J, Mysliwski A, Hellmann A. Interleukin 12 augments natural killer-cell mediated cytotoxicity in hairy cell leukemia. *Leukemia & lymphoma* 1993, 10(1-2): 121-125.
12. Andrews JV, Schoof DD, Bertagnolli MM, Peoples GE, Goedegebuure PS, Eberlein TJ. Immunomodulatory effects of interleukin-12 on human tumor-infiltrating lymphocytes. *Journal of immunotherapy with emphasis on tumor immunology : official journal of the Society for Biological Therapy* 1993, 14(1): 1-10.
13. Zou JJ, Schoenhaut DS, Carvajal DM, Warrier RR, Presky DH, Gately MK*, et al.* Structure-function analysis of the p35 subunit of mouse interleukin 12. *The Journal of biological chemistry* 1995, 270(11): 5864-5871.
14. Del Vecchio M, Bajetta E, Canova S, Lotze MT, Wesa A, Parmiani G*, et al.* Interleukin-12: biological properties and clinical application. *Clinical cancer research : an official journal of the American Association for Cancer Research* 2007, 13(16): 4677-4685.
15. Curtsinger JM, Lins DC, Mescher MF. Signal 3 determines tolerance versus full activation of naive CD8 T cells: dissociating proliferation and development of effector function. *The Journal of experimental medicine* 2003, 197(9): 1141-1151.

16. Kalinski P, Hilkens CM, Wierenga EA, Kapsenberg ML. T-cell priming by type-1 and type-2 polarized dendritic cells: the concept of a third signal. *Immunology today* 1999, 20(12): 561-567.
17. Yoo JK, Cho JH, Lee SW, Sung YC. IL-12 provides proliferation and survival signals to murine CD4+ T cells through phosphatidylinositol 3-kinase/Akt signaling pathway. *Journal of immunology* 2002, 169(7): 3637-3643.
18. Trinchieri G. Interleukin-12 and the regulation of innate resistance and adaptive immunity. *Nature reviews Immunology* 2003, 3(2): 133-146.
19. Wesa A, Kalinski P, Kirkwood JM, Tatsumi T, Storkus WJ. Polarized type-1 dendritic cells (DC1) producing high levels of IL-12 family members rescue patient TH1-type antimelanoma CD4+ T cell responses in vitro. *Journal of immunotherapy* 2007, 30(1): 75-82.
20. Fewell JG, Matar MM, Rice JS, Brunhoeber E, Slobodkin G, Pence C*, et al.* Treatment of disseminated ovarian cancer using nonviral interleukin-12 gene therapy delivered intraperitoneally. *The journal of gene medicine* 2009, 11(8): 718-728.
21. Pan WY, Lo CH, Chen CC, Wu PY, Roffler SR, Shyue SK*, et al.* Cancer immunotherapy using a membrane-bound interleukin-12 with B7-1 transmembrane and cytoplasmic domains. *Molecular therapy : the journal of the American Society of Gene Therapy* 2012, 20(5): 927-937.
22. Voest EE, Kenyon BM, O'Reilly MS, Truitt G, D'Amato RJ, Folkman J. Inhibition of angiogenesis in vivo by interleukin 12. *Journal of the National Cancer Institute* 1995, 87(8): 581-586.
23. Sgadari C, Angiolillo AL, Tosato G. Inhibition of angiogenesis by interleukin-12 is mediated by the interferon-inducible protein 10. *Blood* 1996, 87(9): 3877-3882.
24. Kanegane C, Sgadari C, Kanegane H, Teruya-Feldstein J, Yao L, Gupta G*, et al.* Contribution of the CXC chemokines IP-10 and Mig to the antitumor effects of IL-12. *Journal of leukocyte biology* 1998, 64(3): 384-392.
25. Rook AH, Wood GS, Yoo EK, Elenitsas R, Kao DM, Sherman ML*, et al.* Interleukin-12 therapy of cutaneous T-cell lymphoma induces lesion regression and cytotoxic T-cell responses. *Blood* 1999, 94(3): 902-908.
26. Ansell SM, Geyer SM, Maurer MJ, Kurtin PJ, Micallef IN, Stella P*, et al.* Randomized phase II study of interleukin-12 in combination with rituximab in previously treated non-Hodgkin's lymphoma patients. *Clinical cancer research : an official journal of the American Association for Cancer Research* 2006, 12(20 Pt 1): 6056-6063.
27. Bajetta E, Del Vecchio M, Mortarini R, Nadeau R, Rakhit A, Rimassa L*, et al.* Pilot study of subcutaneous recombinant human interleukin 12 in metastatic melanoma. *Clinical cancer research : an official journal of the American Association for Cancer Research* 1998, 4(1): 75-85.
28. Motzer RJ, Rakhit A, Thompson JA, Nemunaitis J, Murphy BA, Ellerhorst J*, et al.* Randomized multicenter phase II trial of subcutaneous recombinant human interleukin-12 versus interferon-alpha 2a for patients with advanced renal cell carcinoma. *Journal of interferon & cytokine research : the official journal of the International Society for Interferon and Cytokine Research* 2001, 21(4): 257-263.
29. Colombo MP, Trinchieri G. Interleukin-12 in anti-tumor immunity and immunotherapy. *Cytokine & growth factor reviews* 2002, 13(2): 155-168.
30. Ferlazzo G, Pack M, Thomas D, Paludan C, Schmid D, Strowig T*, et al.* Distinct roles of IL-12 and IL-15 in human natural killer cell activation by dendritic cells from secondary lymphoid organs. *Proceedings of the National Academy of Sciences of the United States of America* 2004, 101(47): 16606-16611.
31. Atkins MB, Robertson MJ, Gordon M, Lotze MT, DeCoste M, DuBois JS*, et al.* Phase I evaluation of intravenous recombinant human interleukin 12 in patients with advanced

malignancies. *Clinical cancer research : an official journal of the American Association for Cancer Research* 1997, 3(3): 409-417.

32. Leonard JP, Sherman ML, Fisher GL, Buchanan LJ, Larsen G, Atkins MB*, et al.* Effects of single-dose interleukin-12 exposure on interleukin-12-associated toxicity and interferon-gamma production. *Blood* 1997, 90(7): 2541-2548.
33. Lenzi R, Edwards R, June C, Seiden MV, Garcia ME, Rosenblum M*, et al.* Phase II study of intraperitoneal recombinant interleukin-12 (rhIL-12) in patients with peritoneal carcinomatosis (residual disease < 1 cm) associated with ovarian cancer or primary peritoneal carcinoma. *Journal of translational medicine* 2007, 5: 66.
34. Lenzi R, Rosenblum M, Verschraegen C, Kudelka AP, Kavanagh JJ, Hicks ME*, et al.* Phase I study of intraperitoneal recombinant human interleukin 12 in patients with Mullerian carcinoma, gastrointestinal primary malignancies, and mesothelioma. *Clinical cancer research : an official journal of the American Association for Cancer Research* 2002, 8(12): 3686-3695.
35. van Herpen CM, Bussink J, van der Kogel AJ, Peeters WJ, van der Voort R, van Schijndel A*, et al.* Interleukin-12 has no effect on vascular density, perfusion, hypoxia and proliferation of an implanted human squamous cell carcinoma xenograft tumour despite up-regulation of ICAM-1. *Anticancer research* 2005, 25(2A): 1015-1021.
36. Tahara H, Zeh HJ, 3rd, Storkus WJ, Pappo I, Watkins SC, Gubler U*, et al.* Fibroblasts genetically engineered to secrete interleukin 12 can suppress tumor growth and induce antitumor immunity to a murine melanoma in vivo. *Cancer research* 1994, 54(1): 182-189.
37. Tahara H, Lotze MT, Robbins PD, Storkus WJ, Zitvogel L. IL-12 gene therapy using direct injection of tumors with genetically engineered autologous fibroblasts. *Human gene therapy* 1995, 6(12): 1607-1624.
38. Tahara H, Zitvogel L, Storkus WJ, Zeh HJ, 3rd, McKinney TG, Schreiber RD*, et al.* Effective eradication of established murine tumors with IL-12 gene therapy using a polycistronic retroviral vector. *Journal of immunology* 1995, 154(12): 6466-6474.
39. Nishioka Y, Hirao M, Robbins PD, Lotze MT, Tahara H. Induction of systemic and therapeutic antitumor immunity using intratumoral injection of dendritic cells genetically modified to express interleukin 12. *Cancer research* 1999, 59(16): 4035-4041.
40. Meko JB, Yim JH, Tsung K, Norton JA. High cytokine production and effective antitumor activity of a recombinant vaccinia virus encoding murine interleukin 12. *Cancer research* 1995, 55(21): 4765-4770.
41. Lim HY, Ju HY, Chung HY, Kim YS. Antitumor effects of a tumor cell vaccine expressing a membrane-bound form of the IL-12 p35 subunit. *Cancer biology & therapy* 2010, 10(4): 336-343.
42. Bramson JL, Hitt M, Addison CL, Muller WJ, Gauldie J, Graham FL. Direct intratumoral injection of an adenovirus expressing interleukin-12 induces regression and long-lasting immunity that is associated with highly localized expression of interleukin-12. *Human gene therapy* 1996, 7(16): 1995-2002.
43. Anwer K, Barnes MN, Fewell J, Lewis DH, Alvarez RD. Phase-I clinical trial of IL-12 plasmid/lipopolymer complexes for the treatment of recurrent ovarian cancer. *Gene therapy* 2010, 17(3): 360-369.
44. Cohen CA, Shea AA, Heffron CL, Schmelz EM, Roberts PC. Intra-Abdominal Fat Depots Represent Distinct Immunomodulatory Microenvironments: A Murine Model *PlosOne* 2013, Accepted
45. Cohen CA, Shea AA, Heffron CL, Schmelz EM, Roberts PC. Parity-Associated Protection Against Ovarian Cancer Metastasis in the Omental Fat Band. *in progress* 2013.

46. Gregory AD, Houghton AM. Tumor-associated neutrophils: new targets for cancer therapy. *Cancer research* 2011, 71(7): 2411-2416.
47. Fridlender ZG, Sun J, Kim S, Kapoor V, Cheng G, Ling L*, et al.* Polarization of tumor-associated neutrophil phenotype by TGF-beta: "N1" versus "N2" TAN. *Cancer cell* 2009, 16(3): 183-194.
48. Gordon S. Alternative activation of macrophages. *Nature reviews Immunology* 2003, 3(1): 23-35.
49. Sica A, Schioppa T, Mantovani A, Allavena P. Tumour-associated macrophages are a distinct M2 polarised population promoting tumour progression: potential targets of anti-cancer therapy. *European journal of cancer* 2006, 42(6): 717-727.
50. Roberts PC, Mottillo EP, Baxa AC, Heng HH, Doyon-Reale N, Gregoire L*, et al.* Sequential molecular and cellular events during neoplastic progression: a mouse syngeneic ovarian cancer model. *Neoplasia* 2005, 7(10): 944-956.
51. Creekmore AL, Silkworth WT, Cimini D, Jensen RV, Roberts PC, Schmelz EM. Changes in gene expression and cellular architecture in an ovarian cancer progression model. *PloS one* 2011, 6(3): e17676.
52. Khan T, Heffron CL, Roberts PC. Membrane-bound IL-12 and IL-23 serve as potent mucosal adjuvants on whole inactivated influenza vaccines. *J Interferon and Cytokine Res* 2013, accepted pending minor revisions.
53. Luker KE, Smith MC, Luker GD, Gammon ST, Piwnica-Worms H, Piwnica-Worms D. Kinetics of regulated protein-protein interactions revealed with firefly luciferase complementation imaging in cells and living animals. *Proceedings of the National Academy of Sciences of the United States of America* 2004, 101(33): 12288-12293.
54. Carmignani CP, Sugarbaker PH. Synchronous extraperitoneal and intraperitoneal dissemination of appendix cancer. *European journal of surgical oncology : the journal of the European Society of Surgical Oncology and the British Association of Surgical Oncology* 2004, 30(8): 864-868.
55. Otto J, Jansen PL, Lucas S, Schumpelick V, Jansen M. Reduction of peritoneal carcinomatosis by intraperitoneal administration of phospholipids in rats. *BMC cancer* 2007, 7: 104.
56. Schmittgen TD, Livak KJ. Analyzing real-time PCR data by the comparative C(T) method. *Nature protocols* 2008, 3(6): 1101-1108.
57. Grohmann U, Belladonna ML, Vacca C, Bianchi R, Fallarino F, Orabona C*, et al.* Positive regulatory role of IL-12 in macrophages and modulation by IFN-gamma. *Journal of immunology* 2001, 167(1): 221-227.
58. Airoldi I, Guglielmino R, Carra G, Corcione A, Gerosa F, Taborelli G*, et al.* The interleukin-12 and interleukin-12 receptor system in normal and transformed human B lymphocytes. *Haematologica* 2002, 87(4): 434-442.
59. Watford WT, Moriguchi M, Morinobu A, O'Shea JJ. The biology of IL-12: coordinating innate and adaptive immune responses. *Cytokine & growth factor reviews* 2003, 14(5): 361-368.
60. Welford AF, Biziato D, Coffelt SB, Nucera S, Fisher M, Pucci F*, et al.* TIE2-expressing macrophages limit the therapeutic efficacy of the vascular-disrupting agent combretastatin A4 phosphate in mice. *The Journal of clinical investigation* 2011, 121(5): 1969-1973.
61. Robitaille R, Dusseault J, Henley N, Desbiens K, Labrecque N, Halle JP. Inflammatory response to peritoneal implantation of alginate-poly-L-lysine microcapsules. *Biomaterials* 2005, 26(19): 4119-4127.
62. Vandenbossche GM, Bracke ME, Cuvelier CA, Bortier HE, Mareel MM, Remon JP. Host reaction against empty alginate-polylysine microcapsules. Influence of preparation procedure. *The Journal of pharmacy and pharmacology* 1993, 45(2): 115-120.

63. **Brunda MJ, Luistro L, Warrier RR, Wright RB, Hubbard BR, Murphy M*, et al.* Antitumor and antimetastatic activity of interleukin 12 against murine tumors. *The Journal of experimental medicine* 1993, 178(4): 1223-1230.**
64. **Weiss JM, Subleski JJ, Wigginton JM, Wiltrout RH. Immunotherapy of cancer by IL-12-based cytokine combinations. *Expert opinion on biological therapy* 2007, 7(11): 1705-1721.**
65. **Carreras J, Lopez-Guillermo A, Fox BC, Colomo L, Martinez A, Roncador G*, et al.* High numbers of tumor-infiltrating FOXP3-positive regulatory T cells are associated with improved overall survival in follicular lymphoma. *Blood* 2006, 108(9): 2957-2964.**
66. **Yang ZZ, Grote DM, Ziesmer SC, Niki T, Hirashima M, Novak AJ*, et al.* IL-12 upregulates TIM-3 expression and induces T cell exhaustion in patients with follicular B cell non-Hodgkin lymphoma. *The Journal of clinical investigation* 2012, 122(4): 1271-1282.**
67. **Kerkar SP, Muranski P, Kaiser A, Boni A, Sanchez-Perez L, Yu Z*, et al.* Tumor-specific CD8+ T cells expressing interleukin-12 eradicate established cancers in lymphodepleted hosts. *Cancer research* 2010, 70(17): 6725-6734.**
68. **van Herpen CM, van der Laak JA, de Vries IJ, van Krieken JH, de Wilde PC, Balvers MG*, et al.* Intratumoral recombinant human interleukin-12 administration in head and neck squamous cell carcinoma patients modifies locoregional lymph node architecture and induces natural killer cell infiltration in the primary tumor. *Clinical cancer research : an official journal of the American Association for Cancer Research* 2005, 11(5): 1899-1909.**
69. **Kilinc MO, Aulakh KS, Nair RE, Jones SA, Alard P, Kosiewicz MM*, et al.* Reversing tumor immune suppression with intratumoral IL-12: activation of tumor-associated T effector/memory cells, induction of T suppressor apoptosis, and infiltration of CD8+ T effectors. *Journal of immunology* 2006, 177(10): 6962-6973.**
70. **Zhao X, Bose A, Komita H, Taylor JL, Kawabe M, Chi N*, et al.* Intratumoral IL-12 gene therapy results in the crosspriming of Tc1 cells reactive against tumor-associated stromal antigens. *Molecular therapy : the journal of the American Society of Gene Therapy* 2011, 19(4): 805-814.**
71. **Lee P, Wang F, Kuniyoshi J, Rubio V, Stuges T, Groshen S*, et al.* Effects of interleukin-12 on the immune response to a multipeptide vaccine for resected metastatic melanoma. *Journal of clinical oncology : official journal of the American Society of Clinical Oncology* 2001, 19(18): 3836-3847.**
72. **Cebon J, Jager E, Shackleton MJ, Gibbs P, Davis ID, Hopkins W*, et al.* Two phase I studies of low dose recombinant human IL-12 with Melan-A and influenza peptides in subjects with advanced malignant melanoma. *Cancer immunity* 2003, 3: 7.**
73. **Peterson AC, Harlin H, Gajewski TF. Immunization with Melan-A peptide-pulsed peripheral blood mononuclear cells plus recombinant human interleukin-12 induces clinical activity and T-cell responses in advanced melanoma. *Journal of clinical oncology : official journal of the American Society of Clinical Oncology* 2003, 21(12): 2342-2348.**
74. **Coughlin CM, Salhany KE, Wysocka M, Aruga E, Kurzawa H, Chang AE*, et al.* Interleukin-12 and interleukin-18 synergistically induce murine tumor regression which involves inhibition of angiogenesis. *The Journal of clinical investigation* 1998, 101(6): 1441-1452.**
75. **Cavallo F, Signorelli P, Giovarelli M, Musiani P, Modesti A, Brunda MJ*, et al.* Antitumor efficacy of adenocarcinoma cells engineered to produce interleukin 12 (IL-12) or other cytokines compared with exogenous IL-12. *Journal of the National Cancer Institute* 1997, 89(14): 1049-1058.**
76. **Zitvogel L, Mayordomo JI, Tjandrawan T, DeLeo AB, Clarke MR, Lotze MT*, et al.* Therapy of murine tumors with tumor peptide-pulsed dendritic cells: dependence on T cells, B7 costimulation, and T helper cell 1-associated cytokines. *The Journal of experimental medicine* 1996, 183(1): 87-97.**

77. Zhang L, Kerkar SP, Yu Z, Zheng Z, Yang S, Restifo NP*, et al.* Improving adoptive T cell therapy by targeting and controlling IL-12 expression to the tumor environment. *Molecular therapy : the journal of the American Society of Gene Therapy* 2011, 19(4): 751-759.
78. Ling P, Gately MK, Gubler U, Stern AS, Lin P, Hollfelder K*, et al.* Human IL-12 p40 homodimer binds to the IL-12 receptor but does not mediate biologic activity. *Journal of immunology* 1995, 154(1): 116-127.
79. Jana M, Dasgupta S, Saha RN, Liu X, Pahan K. Induction of tumor necrosis factor-alpha (TNF-alpha) by interleukin-12 p40 monomer and homodimer in microglia and macrophages. *Journal of neurochemistry* 2003, 86(2): 519-528.
80. Broderick L, Yokota SJ, Reineke J, Mathiowitz E, Stewart CC, Barcos M*, et al.* Human CD4+ effector memory T cells persisting in the microenvironment of lung cancer xenografts are activated by local delivery of IL-12 to proliferate, produce IFN-gamma, and eradicate tumor cells. *Journal of immunology* 2005, 174(2): 898-906.
81. Kieper WC, Prlic M, Schmidt CS, Mescher MF, Jameson SC. Il-12 enhances CD8 T cell homeostatic expansion. *Journal of immunology* 2001, 166(9): 5515-5521.
82. Cao X, Leonard K, Collins LI, Cai SF, Mayer JC, Payton JE*, et al.* Interleukin 12 stimulates IFN-gamma-mediated inhibition of tumor-induced regulatory T-cell proliferation and enhances tumor clearance. *Cancer research* 2009, 69(22): 8700-8709.
83. Beyer M, Schultze JL. Regulatory T cells in cancer. *Blood* 2006, 108(3): 804-811.
84. Cavallo F, Di Carlo E, Butera M, Verrua R, Colombo MP, Musiani P*, et al.* Immune events associated with the cure of established tumors and spontaneous metastases by local and systemic interleukin 12. *Cancer research* 1999, 59(2): 414-421.
85. Mortarini R, Borri A, Tragni G, Bersani I, Vegetti C, Bajetta E*, et al.* Peripheral burst of tumor-specific cytotoxic T lymphocytes and infiltration of metastatic lesions by memory CD8+ T cells in melanoma patients receiving interleukin 12. *Cancer research* 2000, 60(13): 3559-3568.
86. Broderick L, Brooks SP, Takita H, Baer AN, Bernstein JM, Bankert RB. IL-12 reverses anergy to T cell receptor triggering in human lung tumor-associated memory T cells. *Clinical immunology* 2006, 118(2-3): 159-169.
87. Mitola S, Strasly M, Prato M, Ghia P, Bussolino F. IL-12 regulates an endothelial cell-lymphocyte network: effect on metalloproteinase-9 production. *Journal of immunology* 2003, 171(7): 3725-3733.
88. Yao L, Sgadari C, Furuke K, Bloom ET, Teruya-Feldstein J, Tosato G. Contribution of natural killer cells to inhibition of angiogenesis by interleukin-12. *Blood* 1999, 93(5): 1612-1621.
89. Stout RD, Suttles J. Functional plasticity of macrophages: reversible adaptation to changing microenvironments. *Journal of leukocyte biology* 2004, 76(3): 509-513.
90. Gordon S, Taylor PR. Monocyte and macrophage heterogeneity. *Nature reviews Immunology* 2005, 5(12): 953-964.
91. Stout RD, Jiang C, Matta B, Tietzel I, Watkins SK, Suttles J. Macrophages sequentially change their functional phenotype in response to changes in microenvironmental influences. *Journal of immunology* 2005, 175(1): 342-349.
92. Bronte V, Serafini P, Apolloni E, Zanovello P. Tumor-induced immune dysfunctions caused by myeloid suppressor cells. *Journal of immunotherapy* 2001, 24(6): 431-446.
93. Mullins DW, Burger CJ, Elgert KD. Tumor growth modulates macrophage nitric oxide production following paclitaxel administration. *International journal of immunopharmacology* 1998, 20(10): 537-551.
94. Elgert KD, Alleva DG, Mullins DW. Tumor-induced immune dysfunction: the macrophage connection. *Journal of leukocyte biology* 1998, 64(3): 275-290.

95. Watkins SK, Egilmez NK, Suttles J, Stout RD. IL-12 rapidly alters the functional profile of tumor-associated and tumor-infiltrating macrophages in vitro and in vivo. *Journal of immunology* 2007, 178(3): 1357-1362.

96. Kerkar SP, Goldszmid RS, Muranski P, Chinnasamy D, Yu Z, Reger RN*, et al.* IL-12 triggers a programmatic change in dysfunctional myeloid-derived cells within mouse tumors. *The Journal of clinical investigation* 2011, 121(12): 4746-4757.

97. Movahedi K, Laoui D, Gysemans C, Baeten M, Stange G, Van den Bossche J*, et al.* Different tumor microenvironments contain functionally distinct subsets of macrophages derived from Ly6C(high) monocytes. *Cancer research* 2010, 70(14): 5728-5739.

CHAPTER 6.

Conclusions

The face of cancer research is changing. In 2000, Hanahan and Weinberg published their iconic work introducing the "Hallmarks of Cancer". This work represented decades of compiled research, and has thus far been cited over 16,000 times. The phrase has become so symbolic of the diverse arena that encompasses cancer research that in March of 2013, a new open access online journal entitled Cancer Hallmarks released its first "volume", targeting multidisciplinary advances and significant discoveries relating to the hallmarks of cancer. In 2000, there were six identified hallmarks (sustaining proliferative signaling, evading growth suppressors, activating invasion and metastasis, enabling replicative immortality, and inducing angiogenesis and resisting cell death)[1]. These hallmarks reflect the interests of the time, and research attention was mainly focused on the intrinsic mechanisms by which cancer cells transform and progress. In 2011, Hanahan and Weinberg published again, identifying the "next generation" of cancer hallmarks. This work summarized the advances in knowledge gained over the last decade, incorporating two new hallmarks (deregulating cellular energetics and avoiding immune destruction), and two "enabling characteristics" (genome instability and tumor-promoting inflammation)[2]. Thus, research attention has evolved from internal mechanisms (oncogenes, for instance) to dynamic microenvironmental interactions[3, 4] between tumor cells and the surrounding stroma (leukocytes, endothelial cells, progenitors, etc) that are constantly shifting to aid the progression of a pro-tumorigenic cascade. Much emphasis has been given to this emerging idea of a complex and heterogenous signaling milieu between a host of cell types, inducing an intricate pro-tumorigenic microenvironment.

The immune system plays a paradoxical role in tumor progression. While capable of recognizing and eradicating tumors, in many scenarios immune cells can be hijacked to facilitate tumor survival and growth[5]. Research is ongoing to characterize different immune cell subsets that play a role in this pathogenesis[6, 7, 8, 9], and the mechanisms and kinetics behind their polarization.

This dissertation has focused on defining the immune compositional changes in the predominant site of ovarian cancer metastasis, the omental fat band (OFB). Previous work has demonstrated that ovarian cancer is a disease typically diagnosed post-metastasis, and that disseminated tumor cells in the peritoneal cavity preferentially adhere and form outgrowths at the OFB[10]. In fact, tumor cells seem to home directly to "milky spots", or immune cell aggregates in the OFB, indicating an early cancer cell-leukocyte interaction that facilitates continued outgrowth. Due to its role as a secondary lymphoid organ, and subsequent ability to mount effective innate and adaptive responses, we believe that the OFB could be harnessed in an immunomodulatory manner and redirected to discourage tumor growth or survival in the peritoneal cavity.

However, other peritoneal fat pads have also been shown to contribute to a variety of disease states, mainly through secreted signals and recruitable stromal cells. Additionally, there seems to be some conflicting information in the literature regarding identification and applicability of various fat depots, particularly in the context of visceral fat, which (in contrast to subcutaneous fat) is associated with cardiovascular disease, insulin dysregulation and certain cancers[11, 12, 13]. Therefore, we first characterized the OFB in the homeostatic state, and evaluated inherent differences between alternate intra-abdominal fat depots (parametrial and retroperitoneal). In keeping with our hypothesis, we found that fat pads represent distinct immunomodulatory microenvironments, and should be evaluated independently in regard to physiological processes and disease. Importantly, the parametrial fat pad, which is the most often used representative of "visceral fat", had a distinct immune compositional profile, indicating a divergent role in intraperitoneal pathogeneses. Further, the parametrial fat pad doesn't exist in humans, suggesting that this depot may be an inappropriate model for studying the contributions of intra-abdominal fat to human disease. Consistent with its role as an immunomodulator in the peritoneal cavity, the OFB has a diverse and unique immune profile that may be uniquely suited to immunotherapeutic manipulation. Therefore, the overall goal of this dissertation was to define the immune compositional profile of the OFB, and how this was affected by age (the median age in ovarian cancer is 60+) and parity (correlated with decreased ovarian cancer in epidemiological studies). Additionally, we hypothesized that inherent changes in these

states would affect the success of the pro-tumorigenic cascade and that, if defined, could be harnessed and redirected to discourage metastasis in the peritoneal cavity.

Although ovarian cancer is considered an aggressive and hard-to-treat disease due to its asymptomatic nature and high incidence of metastasis, parity (child-bearing) has been correlated with protection in epidemiological studies. The mechanisms behind protection are largely unknown, although in breast cancer there are indications that parity is associated with increased differentiation of stromal cells in the mammary tissue, and that these effects are refractory to metastasis but not initial transformation. Therefore, we utilized the OFB as the primary site of ovarian cancer metastasis to determine inherent changes in the homeostatic state that may be part of the "protective signature" affiliated with parity. We determined that child-bearing was in fact protective against metastatic tumor growth following intraperitoneal implantation and we characterized the hallmark of a metastatic microenvironment as containing high levels of tumor-associated neutrophils (TANs) and macrophages (TAMs), as well as a predominant B1 B cell phenotype. Additionally we determined that the parous protective signature was correlated with a decreased incidence of neutrophils, macrophages and B1s in the homeostatic state, and decreased expression of chemokines for these pro-tumorigenic immune cell subsets following cancer cell injection. This parous signature provides valuable insight into a naturally-occurring microenvironment that is refractory to ovarian cancer cell metastasis, elucidating potential targets for therapeutics.

As the above studies validated our hypothesis that parity-associated protection against ovarian cancer metastasis is associated with resident and/or infiltrating leukocyte populations in the OFB , we sought to evaluate the efficacy of IL-12, a potent anti-tumorigenic cytokine, when delivered directly to the metastatic microenvironment. As a promising cancer therapeutic associated with severe side effects during clinical trials, IL-12 has prompted a wealth of research regarding targeted delivery systems to avoid systemic distribution[14, 15, 16]. As a disease rarely discovered prior to metastasis, and with a specified site of primary metastatic development that doubles as an active immune organ, ovarian cancer is an excellent candidate for targeted immunotherapeutic strategies. Thus, we engineered a membrane-bound

IL-12 expressing MOSE cell variant and evaluated comparative tumor burden and immune profiles within the OFB and PSF following implantation. Localized delivery of mbIL-12 did reduce tumor burden, extending lifespan by over 200%. This is particularly significant given the low 5-year survival rate in ovarian cancer patients. Delayed disease was associated with an early reduction (7 days post-injection) in chemoattractants specific for the pro-tumorigenic immune populations mentioned above (TAMs, TANs). Although vaccination with mbIL-12 expressing tumor cells was not protective against subsequent tumor challenge, there was a significant reduction in pro-tumorigenic immune populations, indicating that IL-12 interferes with their recruitment to the tumor microenvironment. Overall, we demonstrate that mbIL-12 resulted in delayed disease progression, and hypothesize that localization of this potent immunotherapeutic to the tumor microenvironment reduced the efficiency with which cancer cells are able to generate an overwhelming pro-tumorigenic niche.

Thus, we believe that the formation of the pro-tumorigenic niche occurs in a cascading fashion, with the initial influx of pro-tumorigenic cells as a result of cancer cell seeding inducing an autocrine loop -type accumulation of overwhelming immunosuppression and pro-metastatic signaling. These findings suggest that the initiation and potentiation of the pro-tumorigenic cascade is a dynamic and complex process. By defining the immune compositional profile of the OFB, changes induced as a result of parity, and the associated delay in the formation of the tumor microenvironment, we have added to the broader field of cancer immunology and ovarian cancer metastasis. Further, we illustrate the importance of specific leukocyte populations at the tumor site to facilitate rapid tumor growth. We have additionally demonstrated the feasibility of altering the kinetics of the tumor microenvironment using an immunomodulatory treatment strategy. The targeted nature of the membrane-bound cytokine makes this delivery method ideal for a metastatic model in which local administration at a tumor site is not practical. This work also suggests that the OFB may prove particularly amenable to immunomodulatory interventions, and if maintained following tumor debulking, could prove a valuable tool in restoring customary immune function. Traditional cancer treatments target different facets of the original six Hallmarks, such as alkylating agents or antimetabolites that target quickly dividing DNA, or anti-VEGF

drugs to target angiogenesis. This research is consistent with more modern combinatorial approaches that target accessory cells in the tumor milieu. Thus, we believe that an improved comprehension of the site-specific, constantly evolving cross-talk within the diverse tumor microenvironment is crucial to overcoming ovarian cancer.

REFERENCES

1. Hanahan D, Weinberg RA. The hallmarks of cancer. *Cell* 2000, **100**(1)**:** 57-70.
2. Hanahan D, Weinberg RA. Hallmarks of cancer: the next generation. *Cell* 2011, **144**(5)**:** 646-674.
3. Pietras K, Ostman A. Hallmarks of cancer: interactions with the tumor stroma. *Experimental cell research* 2010, **316**(8)**:** 1324-1331.
4. Floor SL, Dumont JE, Maenhaut C, Raspe E. Hallmarks of cancer: of all cancer cells, all the time? *Trends in molecular medicine* 2012, **18**(9)**:** 509-515.
5. de Visser KE, Eichten A, Coussens LM. Paradoxical roles of the immune system during cancer development. *Nature reviews Cancer* 2006, **6**(1)**:** 24-37.
6. Hagemann T, Wilson J, Burke F, Kulbe H, Li NF, Pluddemann A*, et al.* Ovarian cancer cells polarize macrophages toward a tumor-associated phenotype. *J Immunol* 2006, **176**(8)**:** 5023-5032.
7. Gordon S, Martinez FO. Alternative activation of macrophages: mechanism and functions. *Immunity* 2010, **32**(5)**:** 593-604.
8. Fridlender ZG, Sun J, Kim S, Kapoor V, Cheng G, Ling L*, et al.* Polarization of tumor-associated neutrophil phenotype by TGF-beta: "N1" versus "N2" TAN. *Cancer cell* 2009, **16**(3)**:** 183-194.
9. Ostrand-Rosenberg S, Sinha P. Myeloid-derived suppressor cells: linking inflammation and cancer. *Journal of immunology* 2009, **182**(8)**:** 4499-4506.
10. Gerber SA, Rybalko VY, Bigelow CE, Lugade AA, Foster TH, Frelinger JG*, et al.* Preferential attachment of peritoneal tumor metastases to omental immune aggregates and possible role of a unique vascular microenvironment in metastatic survival and growth. *The American journal of pathology* 2006, **169**(5)**:** 1739-1752.
11. Klopp AH, Zhang Y, Solley T, Amaya-Manzanares F, Marini F, Andreeff M*, et al.* Omental adipose tissue-derived stromal cells promote vascularization and growth of endometrial tumors. *Clinical cancer research : an official journal of the American Association for Cancer Research* 2012, **18**(3)**:** 771-782.
12. Kidd S, Spaeth E, Watson K, Burks J, Lu H, Klopp A*, et al.* Origins of the tumor microenvironment: quantitative assessment of adipose-derived and bone marrow-derived stroma. *PloS one* 2012, **7**(2)**:** e30563.
13. Foster MT, Shi H, Softic S, Kohli R, Seeley RJ, Woods SC. Transplantation of non-visceral fat to the visceral cavity improves glucose tolerance in mice: investigation of hepatic lipids and insulin sensitivity. *Diabetologia* 2011, **54**(11)**:** 2890-2899.
14. Fewell JG, Matar MM, Rice JS, Brunhoeber E, Slobodkin G, Pence C*, et al.* Treatment of disseminated ovarian cancer using nonviral interleukin-12 gene therapy delivered intraperitoneally. *The journal of gene medicine* 2009, **11**(8)**:** 718-728.
15. Tahara H, Lotze MT, Robbins PD, Storkus WJ, Zitvogel L. IL-12 gene therapy using direct injection of tumors with genetically engineered autologous fibroblasts. *Human gene therapy* 1995, **6**(12)**:** 1607-1624.
16. Colombo MP, Trinchieri G. Interleukin-12 in anti-tumor immunity and immunotherapy. *Cytokine & growth factor reviews* 2002, **13**(2)**:** 155-168.

Appendix A-The MOSE Model

Many different models have been developed over the years to evaluate ovarian cancer. Problems arise from the differences in ovarian cancer subtypes, and the inability of researchers to induce carcinogenesis genetically due to a lack of a specific promoter for the ovaries[1].

While mice do undergo an estrus cycle with distinct stages, they do not in fact develop spontaneous ovarian cancer.[2] However, more than 80% of ovarian cancers are thought to arise from the ovarian surface epithelium, and thus sygeneic murine ovarian epithelial tumor models have been developed. Briefly, mouse surface epithelial (MOSE) cells are removed from the ovary and cultured in vitro. In 2000, Roby et al first demonstrated that MOSE cells can spontaneously transform with repeated passages, increasing tumorigenicity[3]. This discovery led to the seminal work in the Roberts/Schmelz labs described previously[4], that resulted in the MOSE cell line that we utilize throughout this study. Our MOSE model displays a progressively more aggressive phenotype, consistent with the stages of human ovarian cancer. The evolving phenotype of the MOSE cell line is described in Figure A1. Notably, as cells progress they lose contact inhibition and cobblestone morphology, and gain the ability to undergo anchorage independent growth and invade a collagen plug. Importantly, many of the traits that characterize the transformation of human surface epithelium, such as alterations in the actin cytoskeleton, cellular adhesion proteins, as well as downregulation of E-cadherin to promote the epithelial-to-mesenchymal transition typical of metastasis, are described in our MOSE model[4].

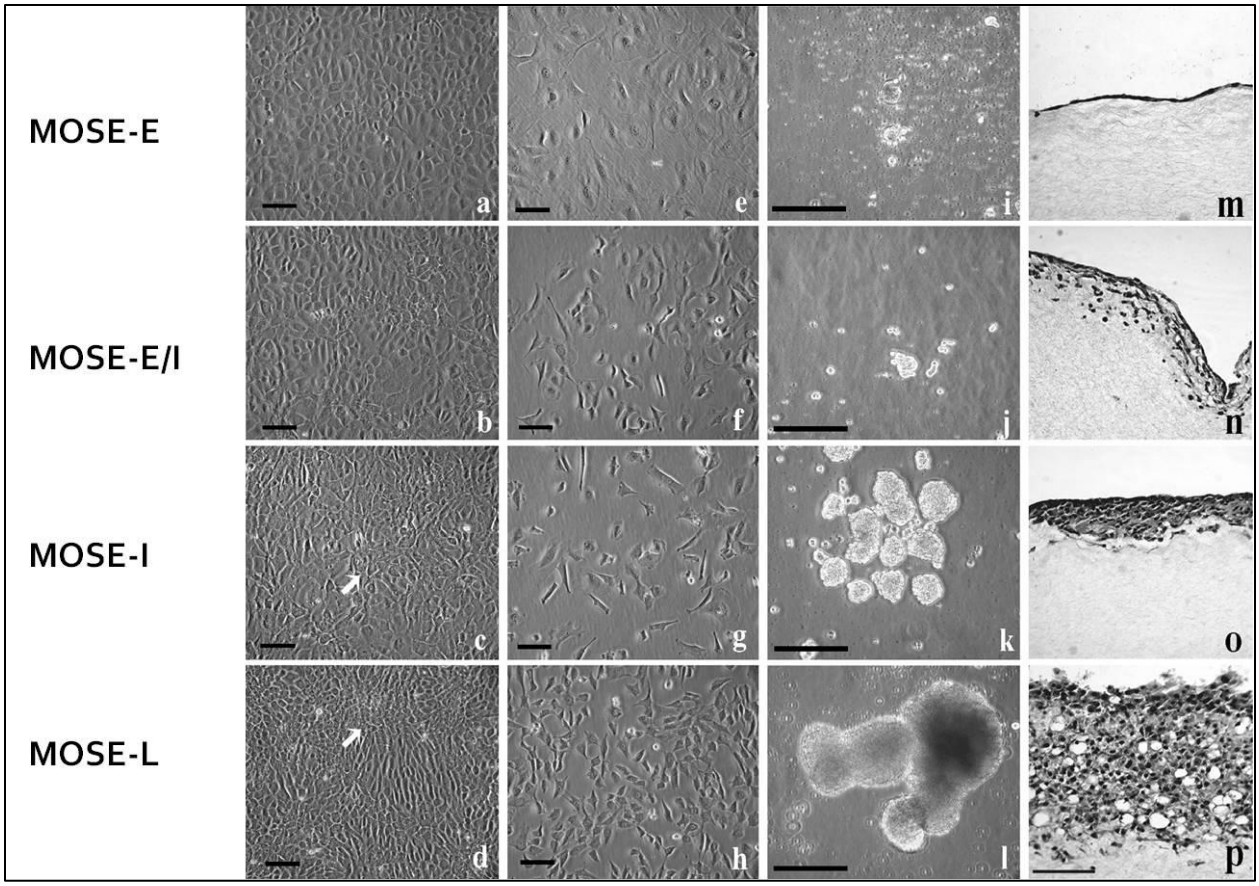

Figure A1. The MOSE model. Cellular morphology of MOSE transitional cell lines in primary culture at confluent (a – d) and subconfluent (e – h) cell densities. Multicellular spheroids were cultivated for 7 days (i – l). Organotypic collagen raft cultures were cultivated for 14 days (m– p).

1. Fong MY, Kakar SS. Ovarian cancer mouse models: a summary of current models and their limitations. *Journal of ovarian research* 2009, **2**(1)**:** 12.
2. Nunez-Cruz S, Connolly DC, Scholler N. An orthotopic model of serous ovarian cancer in immunocompetent mice for in vivo tumor imaging and monitoring of tumor immune responses. *Journal of visualized experiments : JoVE* 2010(45).
3. Roby KF, Taylor CC, Sweetwood JP, Cheng Y, Pace JL, Tawfik O*, et al.* Development of a syngeneic mouse model for events related to ovarian cancer. *Carcinogenesis* 2000, **21**(4)**:** 585-591.
4. Roberts PC, Mottillo EP, Baxa AC, Heng HH, Doyon-Reale N, Gregoire L*, et al.* Sequential molecular and cellular events during neoplastic progression: a mouse syngeneic ovarian cancer model. *Neoplasia* 2005, **7**(10)**:** 944-956.